The Dissertation Committee for Sylvia Nordfjord certifies that this is the approved version of the following dissertation:

Late Quaternary geologic history of New Jersey middle and outer continental shelf

Committee:

James A. Austin, Jr., Supervisor

John A. Goff

William E. Galloway

William Fisher

Ron Steel

Christopher Sommerfield

Late Quaternary geologic history of New Jersey middle and outer continental shelf

by

Sylvia Nordfjord, B.S.

Dissertation

Presented to the Faculty of the Graduate School of

The University of Texas at Austin

in Partial Fulfillment

of the Requirements

for the Degree of

Doctor of Philosophy

The University of Texas at Austin

December 2005

Dedication

For my kids,

Alexander and Karolina,

and my husband,

Alejandro

Acknowledgements

It quickly becomes apparent that one cannot complete a research project of this magnitude without the generosity of many people. First, I would like to thank my supervisor Dr. Jamie Austin and my advisor Dr. John Goff for all their help and guidance and for the opportunity to do this work. I have enjoyed being part of their research group. Their mentoring has allowed me to evolve from a student to a colleague, by always having respect and confidence in my abilities. But most of all, they have always infused a level of excitement and fun in the work that I have done. I would like to express my deepest thanks to my advisors Jamie and John for their patient reading and re-reading of the critical chapters of this dissertation, and for many hours of stimulating discussion. I would also like to thank my committee and other co-fellow researcher: Dr. Chris Sommerfield, Dr. Bill Galloway, Dr. Bill Fisher and Dr. Ron Steel, Dr. Sean Gulick, Dr. Craig Fulthorpe, for their thought-provoking conversations and sharing of ideas during my study. I would like to thank ONR for supporting my graduate research, and for the financial support provided through Ewing/Worzel and BP fellowships and several awards (DOSECC, Chevron and Endowed Presidential Scholarships). Thanks are also due to the crew of R/V *Endeavor, Cape Henlopen* and *Knorr*, who battled perilous seas in the name of science and Steffen Saustrup who help me with the processing of the chirp data. I would not have completed this degree without the unfaltering support and care of my

Late Quaternary geologic history of New Jersey middle and outer continental shelf

Publication No._____

Sylvia Nordfjord, PhD

The University of Texas at Austin, 2005

Supervisor: James A. Austin, Jr.

Analysis of high-resolution (1-4 kHz) seismic chirp profiles of the New Jersey mid-outer continental shelf, coupled with sediment samples, reveal the stratigraphic architecture resulting from the last glacio-eustatic cycle: dendritic (fluvial?) channel systems truncated by a transgressive ravinement. Quantitative geomorphologic analysis of these systems provides estimates of paleo-hydrologic parameters needed to link channel morphology to the hydrodynamic setting when these systems were active. These channels were presumably fluvial systems developed on a subaerial shelf during the Last Glacial Maximum (LGM), ~22-20 ka. During ensuing Holocene sea-level rise, these fluvial channels became estuarine/tidal, before erosion and final burial. Mean tidal paleo-flow estimates for these systems with flow velocities of 1.0-1.5 m/s and shear stresses sufficient to initiate transport of grains 2-8 mm in diameter (i.e., coarse sand and fine gravel) as bed-load, are consistent with modern tidal creeks of the same dimensions. However, paleo-flow estimates, assuming a fluvial environment with velocities of 1.1-2.0 m/s, and retrodicted fluvial discharge and boundary shear stresses would have been sufficient to transport particles up to ~15 mm in diameter (i.e., gravel) as bed-load. We

suggest that either the fluvial drainages never reached equilibrium during high-discharge flows, perhaps due to melt-water pulses following the LGM, or that tidal influences have modified the original fluvial geometry. Imaged and sampled channel-fills reveal a retrogradational shift of four sedimentary facies, in ascending order: 1) fluvial lags, SF1, 2) estuarine mixed sand and muds, SF2, (3) estuary central bay muds, SF3, and 4) redistributed estuary mouth sands, SF4. Three intra-fill transgressive surfaces, B1-3, interpreted as bay flooding surface, intermediate flooding surface and tidal ravinement, respectively, are also either wholly or partly preserved. My study demonstrates that wave- and tide-dominated facies can coexist within channel fills. These fill units are truncated by a morphologic irregular, transgressive wave ravinement surface, the T-horizon, which, in turn, is overlain by Holocene marine sand deposits. A ~10 m bathymetric rise in T forms both the mid-shelf scarp and the base of a smaller Holocene wedge. The modern seafloor of the New Jersey shelf experiences post-transgressive erosion, which is variously expressed.

Table of Contents

List of Tables

List of Figures

Chapter 1: Introduction

High-resolution seismic studies have been performed off the coast of New Jersey in order to study the latest Quaternary history of sedimentation. Much of this work has been conducted as a part of the Office of Naval Research's STRATAFORM (Nittrouer and Kravitz, 1995) and Geoclutter initiatives. STRATAFORM (STRATA FORmation on continental Margins) was a multi-year, collaborative, multidisciplinary study of the formation and preservation of continental margin stratigraphy. Geoclutter, a follow-on to STRATAFORM, specifically investigated systematic casual relationships between geologic phenomena and discrete acoustic signals (geoclutter). Dense coverage of data has been essential for Geoclutter, and provides a tremendous opportunity for stratigraphic investigations. In particular, shallowly buried fluvial channel systems and their fill, identified in several earlier studies (Davies at al., 1992; Austin et al., 1996; Austin et al., 2000; Duncan et al., 2000; Sheridan et al., 2000), can be mapped in greater detail and diversity of scales, because the Geoclutter program has collected seismic data at greater density over a larger area and at higher resolution than previous efforts.

This introduction describes the motivation for this study, the statement of the problem, geological settings, data and methods, and an expanded section on seismic and sequence stratigraphic concepts that were useful. Chapters 2, 3 and 4 comprise interpretations of latest Quaternary stratigraphy and seafloor morphology across the New Jersey shelf from ~40 m water depth to the shelf edge at ~150 m water depth (Figure 1.1). Chapter 2 (published as Nordfjord et al., 2005) describes the physical dimensions and shapes of shallowly-buried channels imaged beneath the middle and outer New Jersey

1
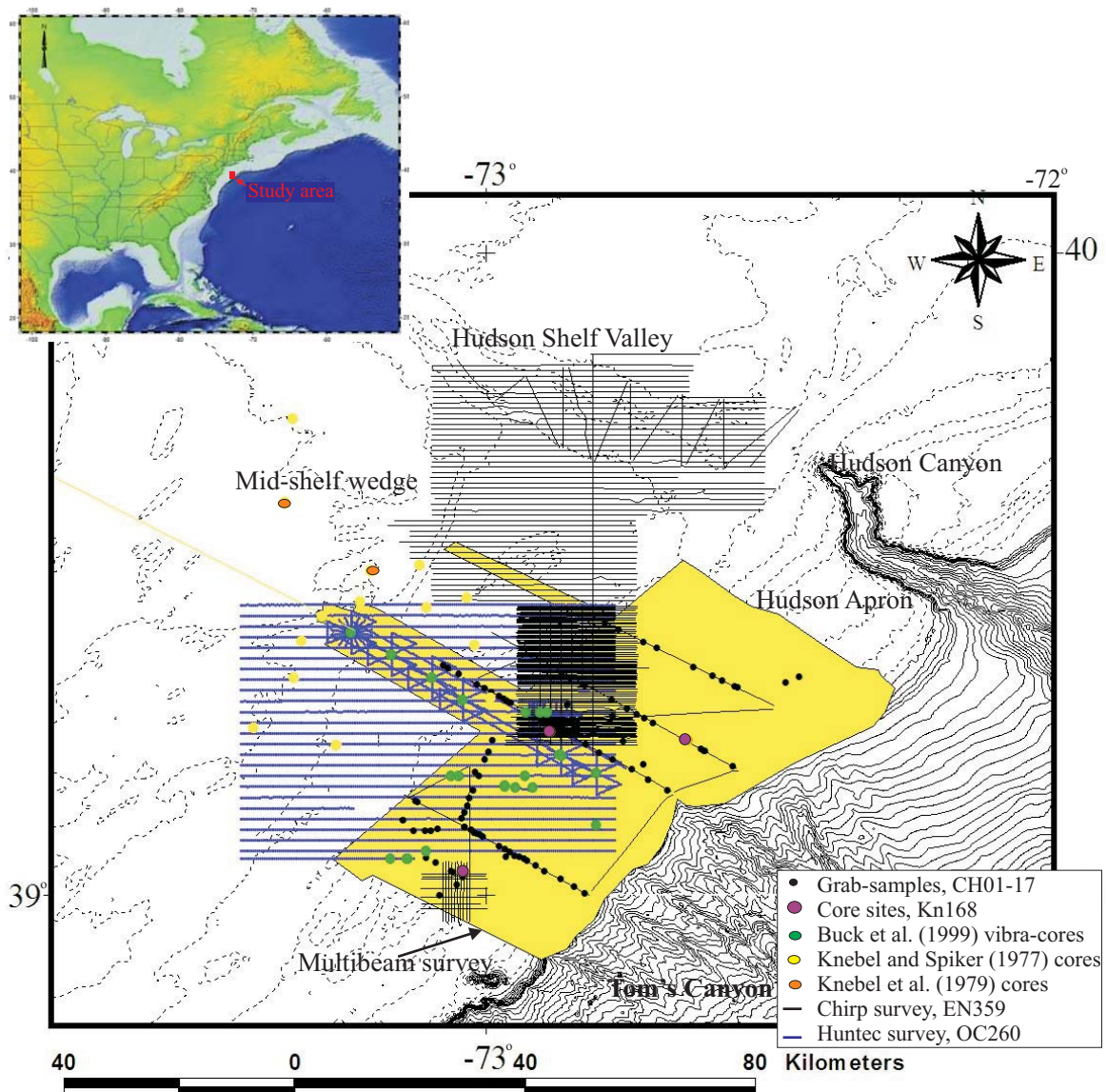
Figure 1.1: Location of 2D deep-towed chirp sonar and Huntec track lines collected in 2001 aboard R/V *Endeavor* (EN359) and in 1993 aboard R/V *Oceanus* (Cruise 260), superimposed on NOAA's bathymetry of the New Jersey middle and outer continental shelf. Grab samples, vibra-cores, AHC-800 cores and multibeam survey area are also marked. Inset shows the study area in a more regional perspective.

2

shelf in order to estimate the hydrographic regimes associated with the paleoenvironments prevailing when these now shallowly buried channels were active. I measure parameters associated with the geomorphology of these channel systems, in order to investigate their paleo-flow characteristics. Chapter 3 (Nordfjord et al., in revision) discusses shallow stratigraphy of these seismically mapped, extensive, shallowly buried, dendritic drainage systems. Based on superposition and geometries of seismic facies, I recognize a fluvial lag facies, estuarine coastal plain deposits, muddy central basin sediments and estuary mouth complex sedimentary facies, including tidal inlets, washovers and tidal deltas. Chapter 4 (Nordfjord et al., in prep.) uses the complete suite of ultra-high resolution chirp reflection data (1-4 kHz), swath bathymetry, grab samples and short cores (Figure 1.1) to elucidate shallow stratigraphy and seafloor morphology on the mid-outer shelf (~40 m to ~120 m water depth). This analysis has been done to assess the role and record of erosion and deposition associated with the Holocene transgression.

STUDY MOTIVATION

Since its introduction in the 1970s, sequence stratigraphy has become a standard tool in both academic and the oil industry geoscience. The majority of research in sequence stratigraphy has been accomplished either with low-resolution seismic data (e.g., Vail et al., 1977a, b) or in outcrops of Mesozoic rocks (e.g., Van Wagoner, 1988). Detailed climate and sea-level data and precise dating are not available for those types of records. Studies of late Quaternary depositional systems can help modify sequence stratigraphic models and add details that would not otherwise be included. One of the goals of this work is to determine the depositional history of sediments from the last

eustatic cycle on the New Jersey continental shelf and to examine any implications the area may have for sequence stratigraphic models. Interpretations of stratigraphic architecture are guided by sequence stratigraphic principles and observations of terrigenous clastic depositional systems in modern and ancient analogs (Vail et al., 1977a, b, c; Nummedal and Swift, 1987; Galloway, 1989; Van Wagoner et al., 1990; Posamentier and Allen, 1993; Galloway and Hobday, 1996). Bounding surfaces and reflection terminations are defined using seismic stratigraphic methods originally defined by Mitchum et al. (1977a, b). A variety of published literature has been used for sea-level and climate information (Dillon and Oldale, 1978; Broecker et al., 1989; Barber et al., 1999; Lambeck and Chappell, 2001).

One major advantage of using Quaternary stratigraphy to test stratigraphic models is the abundant evidence of glacio-eustatic change independent of inferences based solely on sequence stratigraphy. The magnitude and timing of the most recent sea level cycle (ca. 120 ka to Present) are now fairly well established globally (Figure 1.2) from numerous independent proxies (Imbrie et al., 1982; Fairbanks, 1989; Dansgaard et al., 1989). Records of foraminiferal $\delta^{18}O$ data from deep-sea cores are proxy records of global ice volume and sea level during the Pleistocene and Holocene. Given the assumed tectonic stability of the New Jersey margin during this cycle, various researchers have used the global curve to place some chronological and paleobathymetric constraints on the latest Quaternary stratigraphy of the New Jersey margin (Milliman, 1990; Davies et al., 1992; Austin et al., 1996; Davies and Austin, 1997; Carey et al., 1998, Buck et al, 1999; Goff et al., 1999; Duncan et al., 2000; Sheridan et al., 2000; Gulick et al., 2005; Nordfjord et al., 2005). In addition, the Quaternary section is relatively thin and shallow on the New Jersey shelf, which allows the use of seismic methods capable of resolving features on a much finer scale (<1m) than is possible with conventional seismic data

4
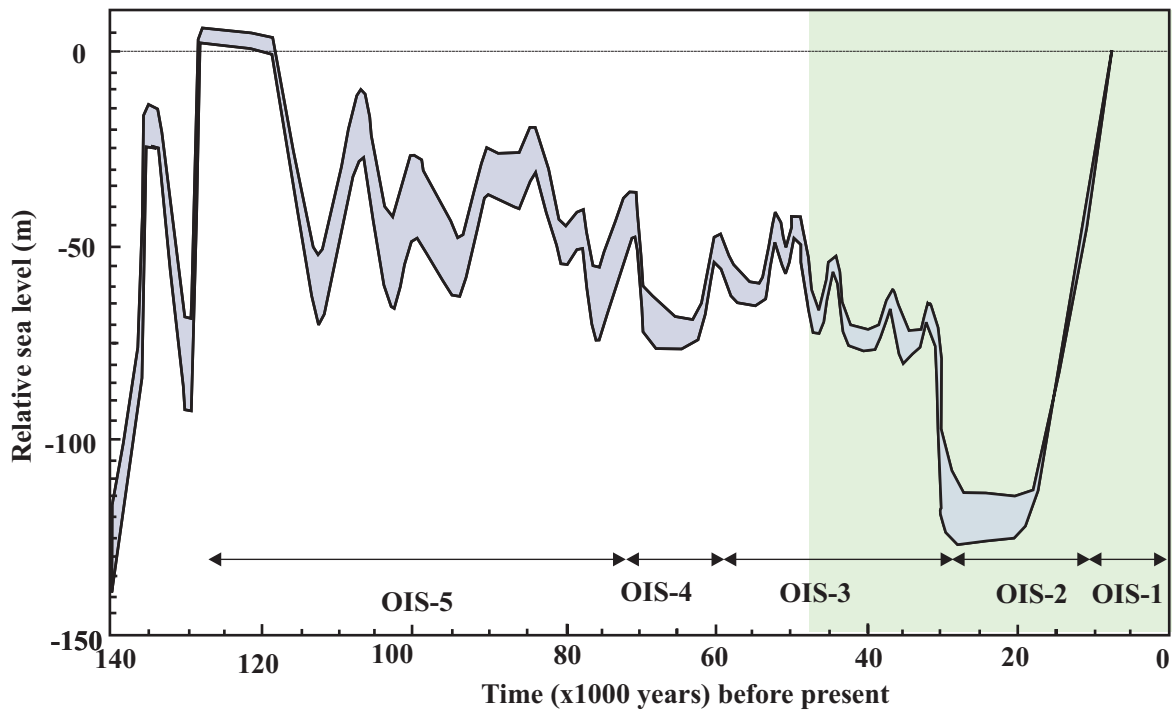
Figure 1.2: Lambeck and Chappell (2001)'s sea-level curve. The last 40 kyr has been the focus of this study, which constitutes Oxygen Isotope Stage (OIS) 1, 2 and 3. Green shaded area shows the time interval in focus for this dissertation.

(Carey et al., 1998). Sediment supply, which is in large part a function of climatic controls, and eustasy together control how depositional systems form (Posamentier and Allen, 1993; Etheridge et al., 1998). To understand in detail the role played by sea-level fluctuations and sediment input on the stratigraphic evolution of portions of a passive basin margin, it is necessary to examine the transgressive to regressive sedimentary deposits beneath the shelf. High-frequency glacio-eustatic sea level cycles have been shown to be responsible for repeated migration of nearshore depositional environments from the inner to outer shelf and back again (Tesson at al., 2000). The STRATAFORM initiative has addressed the challenge of understanding the impact of sediment fluxes across margins by using a "nested" investigative approach (Figure 1.1), with precisely navigated high-resolution 2D and some 3D seismic surveys (at various frequencies) integrated with carefully planned coring programs at two contrasting continental margins, the passive New Jersey margin and the tectonically active Eel River basin.

STATEMENT OF THE PROBLEM

The Quaternary sediments of the Atlantic shelf and coastal zone are represented by lithofacies that developed in response to repeating depositional and erosional regimes controlled by sea-level fluctuations (Riggs and Belknap, 1988). The resulting stratigraphic record can be incomplete (Hine and Snyder, 1985; Belknap and Kraft, 1981; Demarest and Kraft, 1987), which is largely the result of multiple erosional transgressions (Fischer, 1961; Swift, 1968), non-deposition and erosion during lowstands during the Quaternary. Marine transgressions and regressions produce fluvial erosion unconformities and ravinement unconformities (or diastems) that, in areas subject to high frequency sea-level fluctuations (such as the Quaternary strata of the New Jersey shelf), can lead to large parts of stratigraphic time being represented by unconformable surfaces.

6

Those unconformities that result from subaerial exposure during glacial stages (i.e., fluvial erosion unconformities) can represent large time periods on these updip margins of oceanic basins, compared to their distal basinal correlative surfaces. The depositional hiatuses represented by these surfaces may be expected to decrease in a basinward direction. The principal characteristic of the Quaternary Period is the high-frequency nature of sea-level oscillations (44 in the past 2.48 million years, with an average periodicity of 100 kyr), which has had a direct impact on the stratigraphic signatures in both terrestrial and marine sedimentary records (Beard et al., 1982; Morrison, 1991). The principal result of high-frequency glacio-eustasy has been the preservation of an incomplete and complex Quaternary stratigraphy along the U. S. Atlantic continental margin.

The morphology of unconformities within the stratigraphic section can be used to predict formative mechanisms or controlling geologic processes, and constrain depositional settings for the intervening sediments (Galloway and Hobday, 1996, p. 274-77; Thorne and Swift, 1991). Since erosional surfaces can record as much time as the intervening sediments in any given stratigraphic section, their identification and characterization (e.g., whether ravinement or fluvial erosion) is crucial to an understanding of the actual preserved record, particularly at the temporal and spatial scales of Quaternary events. The delineation of sequence and sequence boundary geometries, the numbers and types of unconformities, and the types of fill between these surfaces, will permit reconstruction of paleoenvironments and paleogeography for the Quaternary section. This framework is necessary to build an accurate integrated stratigraphic model for this part of New Jersey's shelf.

The aim of my dissertation research is to investigate the latest Pleistocene-Holocene sedimentary record of the mid-outer continental shelf of New Jersey using

deep-towed chirp sonar images, coupled with lithological and chronostratigraphic control from available sediment cores. From these data, I delineate the stratigraphic architecture in three dimensions, determine the physical properties of the shallow (<30 m deep) sediments from core data, and then tie these pieces of information together. In particular, I focus on an extensive, shallowly buried fluvial channel system, the channel fill material, and overlying transgressive deposits. I then infer the sequence of depositional and erosional processes that have accompanied the most recent episode of eustatic change (Nordfjord et al., 2005; Nordfjord et al., in revision; Nordfjord et al., in prep.).

In this investigation, seismic reflection terminations and configurations are interpreted as stratification patterns, and seismic analysis is used to interpret environmental setting and lithofacies. Seismic facies units are mapped as three-dimensional seismic units composed of groups of reflections whose parameters (configuration, amplitude, continuity, frequency) differ from those of adjacent facies units. They are interpreted in terms of the depositional environments, the energy of the depositing medium, and the potential lithologic content of the strata generating the seismic facies reflection pattern (Mitchum et al., 1977b).

GEOLOGICAL SETTING

The Mid-Atlantic Bight, including the New Jersey margin, lies south of the terminal moraine of the Laurentide ice sheet on Long Island (Figure 1.1). This part of the U.S. continental margin consists of a broad (120-150 km) and gently sloping (<0.001°) shelf (Figure 1.1), with a mixed energy hydrodynamic regime that includes a tidal range of 1-2 m, mean significant wave height of ~1 m (Duane et al., 1972), and generally southwestward-directed currents (Butman et al., 1979). This hydrodynamic regime means that periglacial conditions have prevailed in a storm-dominated environment since LGM

~22 ka. Periglacial effects of glacial advance and retreat have affected sediment supply and fluvial drainage patterns on this margin. At maximum lowstand, the edge of the Laurentide ice sheet presumably occupied the position of mapped terminal moraines located along Long Island (Figure 1.1). The current New Jersey shoreline was then separated from the ice front by ~150 km of subaerially exposed continental shelf (Duncan et al., 2000). The shelf break is located at water depths between 100-150 m and several scarps, often assumed to be paleo-shorelines, have been mapped on the shelf (Veatch and Smith, 1939; Emery and Uchupi, 1972; Dillon and Oldale, 1978; Swift et al., 1980). The Hudson Apron (Figure 1.1) is a seaward bulge in the margin, and numerous submarine canyons incise the modern slope and outer most shelf (Pratson and Ryan, 1994).

The U.S. Atlantic margin is a mature passive margin, with well-developed, large-scale river drainages that have persisted for most of the late Cenozoic (Ashley and Sheridan, 1994). The Hudson and Delaware River systems are examples that penetrate deep into the Appalachian hinterland. Beneath the shelf, the valley fills of these major rivers are sedimentologically complex, because of the enormous scale of incision of their valleys into the exposed continental shelf (Swift et al., 1980; Ashley and Sheridan, 1994). In addition, cycles of exposure and burial associated with glacial activity have resulted in complex three-dimensional patterns of sedimentary structures across the margin (Evans et al., 2000).

Sediment input onto the New Jersey margin has been limited since the last major period of deglaciation (Swift, 1983a, b; Milliman et al., 1990; Swift and Thorne, 1991; Poag, 1992). The modern New Jersey margin is sediment starved; most fluvial input is trapped in river-mouth estuaries (Hudson, Delaware) or lagoons (behind barrier islands). The shelf surface is a layer of sand formed by shoreline retreat during the Holocene sea-level rise (Goff et al., 1999). However, below the relict surface is a rich record of late

Quaternary sedimentation that is >15 m thick (Davies and Austin, 1997). The Quaternary and Tertiary strata in the upper ~100 m contain clinoform features and other evidence of margin aggradation and progradation (Nittrouer and Kravitz, 1996).

Isostatic adjustment to the weight of the late Wisconsinan ice sheet is a source of differential crustal movement. Isostatic models generally predict substantial effects at distances of hundreds of kilometers from the ice sheet (Dillon and Oldale, 1978; Peltier, 1998). However, late Quaternary sediment loading, compaction and thermal subsidence are considered to be minimal on the outer part of this divergent margin, and are, therefore, considered to have negligible impact on the shallow deposits studied. Subsidence rates and sediment supply are low relative to rates of eustasy, and as a result sequences are thin, fragmented and complex. Local effects, such as shifting river drainage and glacial isostasy, can significantly influence sequence preservation (Davies and Austin, 1997; Carey et al., 1998).

DATA

My dissertation work will be based on ultra-high resolution deep-towed chirp seismic data, and some ground truth provided by coring. The seismic data consist of nearly 4300 km of ultra high-resolution profiles data collected aboard the R/V *Endeavor* during cruise leg EN359 in August, 2001 (Figure 1.1). The chirp system is well suited for imaging the shallow, complex Quaternary stratigraphy of the New Jersey shelf. The source emits swept-frequency signals (multiple pings/s) of 1-4 kHz and 1-15 kHz, and the data have vertical resolution of ~30 cm and penetrate <30 m. These data have significantly better ability to resolve the shallow stratigraphy in a high-resolution manner than the conventional seismic acquition methods that use lower-frequency sources (e.g., 10- 60 Hz). The "chirp method" limits geometrical spreading by keeping the source close

to the sea-floor while acquiring the seismic data. The chirp survey covers a total area of roughly 50 x 80 km, located on the middle and outer shelf between the 40 m isobath and the shelf break at ~130 m, ~90 km from the modern coastline (Figure 1.1). The survey area and track line density were chosen to enable robust imaging and evaluation of candidate geoclutter targets, primarily the outcrop of the prominent R-reflection and the buried channels. Accurate ship positions were obtained by differential global positioning system (DGPS). Because the chirp system was deep-towed, ghost reflections do not interfere with reflections of geological interest.

   Seismic data collection was divided into four areas (Figure 1.1):

• Area 1 consists of ~100 E-W profiles of ~14 km length, with line spacing of 200 m to 400 m, and seven N-S crossing lines. Within the same area, a 2x2 km "pseudo 3D box" (~33 m profile spacing) was also acquired. The area covered by Area 1 includes two separate dendritic, shallowly buried valley systems trending in a northeast-southwest direction.

• Area 2, of great interest for the acoustic modelers because of well resolved geoclutter targets, consisted of ~20 N-S seismic profiles with a spacing of 200 m, and seven E-W crossing lines. A number of fluvial channels also occur in this area.

• Area 3 profiles provided regional coverage to the shelf edge, as well as ties to recent grab samples and geotechnical measurements.

• Area 4 provided regional coverage northward to the Hudson mid-shelf valley, and consists of ~50 E-W profiles with a line spacing of half a nautical mile (~900 m), as well as a number of NW-SE, NE-SW and N-S lines, particularly crossing the buried channel.

The Geoclutter survey area overlaps several preexisting, lower-frequency seismic reflection surveys, Huntec boomer 2D and 3D seismic surveys, and surficial and shallow

sediment samples (i.e., grab samples, vibracores, piston cores; Figure 1.1). The seafloor within the area of interest has also been surveyed with multibeam bathymetry and sidescan backscatter as part of the STRATAFORM program (Goff at al., 1999) (Figure 1.1). The high-resolution bathymetry of the mid- and outer shelf exhibits relict oblique ridges, flow-parallel swales floored with elongate ribbons, erosion pits and transverse dunes, which are all evidence of seafloor sculpting by SW-directed currents on the shelf (Goff et al., 1999; Goff et al., 2005).

Coring has provided ground truth for the nested geophysical profiles and added chronostratigraphic data from the sediment samples already collected for STRATAFORM and GEOCLUTTER (Austin et al., 1996; Buck et al., 1999; Duncan et al., 2000; Alexander et al., 2003). Sediment cores collected by DOSECC AHC-800 rotary drilling system September/October 2002 aboard *R/V Knorr* provided correlations for seismic facies interpretations, material for chronostratigraphical analysis and physical properties measurements. In addition, ~100 seafloor sediment samples, velocity measurements and some hydraulically dampened gravity cores were collected in the area during the summer of 2001 on board R/V *Cape Henlopen* (Figure 1.1). These data provided physical property information (e.g., density, compressional velocity, grain-size distribution, resistivity) from precisely located samples at the sediment/water interface. Integration of the high-resolution seismic data, bathymetry and backscatter maps (collected with Simrad EM1000 multibeam system mounted on the CHS *Creed*) with the physical property data from both the seafloor samples and long-cores improved earlier interpretations of seafloor morphology and lithology. These data also enhanced my understanding of the seismic facies typical for this periglacial shelfal environment.

METHODOLOGY

Seismic interpretation

The first parts of my dissertation, Chapters 2 and 3, focus on interpreting seismic profiles from Area 1, with particular attention to the extensive, shallowly buried dendritic drainage systems found there. The evolution of the valley-fill of these systems provides information about the stratigraphic and geologic history during the last glacial-eustatic cycle. In Chapter 4, I investigate the Holocene transgressive record, which constitutes the transgressive ravinement surface and the surficial sand sheet deposited following the ravinement.

My analysis of the New Jersey chirp data provides an improved understanding of the high-resolution shelf sedimentary record. Major differences in seismic character between stratified and chaotic reflection patterns are observed within the strata, both between seismic sequences, and laterally within individual sequences. These character differences suggest spatial and temporal changes in key parameters, such as rate of sediment input and sedimentary processes, which in turn have important implications for understanding the geological history of the region. Thus, I can relate sedimentary facies patterns to sequence stratigraphy.

My seismic time-to-depth conversions are based on the assumption that the acoustic velocities of water and very shallow, water-filled sediments are similar (1750 m/s; Tesson et al., 2000; Goff et al., 2004). Seismic reflection character is dominantly controlled by the scale of sedimentary structures within the deposit, the nature of the bounding surfaces, and the lateral and stratigraphic variability that creates impedance contrasts. Direct observations of acoustic features and properties that are indicative of lithofacies are rarely possible with conventional seismic data, because the correlation of

conventional seismic records with outcrop or well-log data involves a huge jump in scale. However, by using ultra high-resolution seismic reflection data correlated with targeted, accurately positioned core information, a better prediction of lithofacies distribution can be achieved (Nichol et al., 1996; Foyle and Oertel, 1997; Carey et al., 1998; Tesson et al., 2000; Liu et al., 2002; Yoo et al., 2002; Lericolais et al., 2003; Posamentier and Kolla, 2003; Reynaud et al., 2003; Anderson and Fillon, 2004; FitzGerald et al., 2004; Lobo et al., 2004; Nordfjord et al., in revision). Schlumberger's Geoquest IESX software, available at UTIG, allows for interpreting seismic profiles and mapping horizons.

Analysis of stratal reflection terminations (erosional truncation, onlap, downlap; Figure 1.3) and of reflections configurations (i.e., acoustic facies), allows identification of small-scale seismic units and their boundaries. These general concepts of seismic stratigraphy can be applied to my high-resolution data. However, linking architecture to process cannot always be done in the same way as with interpretation of low-resolution seismic data, because of the difference of scales of observation. For instance, autocyclic processes such as lobe switching or bedform migration will have greater effect at the high-resolution scale (Rabineau et al., 1998).

Superposition of stratigraphic elements and bathymetric features are used for interpreting geological history. Crosscutting relationships among stratigraphic elements provide the relative timing of events, and the morphologies of the features provide clues to the processes by which they are formed (Hernandez-Molina et al., 1994; Bartek and Wellner, 1995; Genesous and Tesson, 1996; Yoo and Park, 1997; Rabineau et al., 1998; Blum and Tornquist, 2000; Tesson et al., 2000; Anderson and Fillon, 2004).

14

UPPER BOUNDARY

Truncation

Toplap

Apparent truncation

Onlap
(coastal)

Fault
truncation

Downlap

Onlap
(marine)

Downlap

LOWER BOUNDARY
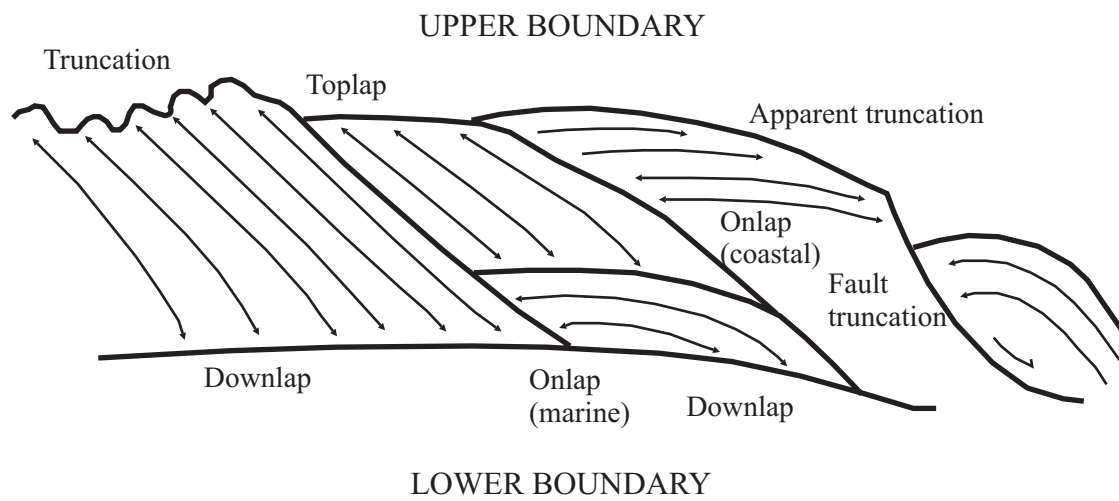
Figure 1.3:   Types of reflection terminations (Emery and Myers, 1996).

Ground truth from core data

Ground truth provided by the coring data constrains processes and events interpreted from the chirp data (Austin et al., 1996). Sediment cores were collected in 2002 deployed from the Woods Hole Oceanographic Institution research vessel R/V *Knorr* supported by ONR, using the DOSECC AHC-800 (Active Heave Compensation drilling to 800 m) drilling system. The AHC-800 is a modification of DOSECC's GLAD800 lake drilling system for ocean conditions. An important early task was to propose potential drillsites, based on interpretation of the chirp data. Targeted core data provide paleoenvironmental, paleobathymetric and chronostratigraphic constraints. Physical properties (density, porosity, velocity) were also obtained by multisensor track logging, which facilitated the correlation of the seismic data with the lithology and paleoenvironments of the upper ~30 m of the sediment column. I examined the relationships among sediment geoacoustic properties and direct comparison of down-core variations of these properties with corresponding high-resolution profiles. The aims were to characterize the variability of geoacoustic properties in these sediments, to relate the nature of geoacoustic properties to the character and origin of reflectors on high-resolution seismic profiles, and to place both geoacoustic property variability and the origin/physical significance of reflectors into the context of spatial and temporal variations of environmental processes. Delineation of seismo-stratigraphic boundary characteristics could be greatly facilitated by physical properties studies of sediment cores that penetrate strata of interest (e.g., Sommerfield et al., 2002). These data were analyzed in cooperation with Dr. Chris Sommerfield at College of Marine Studies, University of Delaware, and Dr. Clark Alexander at Skidaway Institute of Oceanography, Savannah, Georgia.

BENEFITS AND IMPACTS

My dissertation research evaluates the evolution and preservation of shallow stratigraphy on the New Jersey passive margin. Results can be extrapolated to understand high-frequency sequence development on other continental margins. I seek to improve my understanding of shelf stratigraphic responses to sea level change through examination of stratigraphy developing during the Quaternary, when, at least off New Jersey, rates of eustatic change greatly exceeded those of sediment supply and subsidence.

Benefits of creating a high-frequency stratigraphic framework include the ability to predict ancient and future geologic environments and related climatic fluctuations, as well as to constrain the effects of base level change on stratal evolution. The scales and temporal/spatial resolution of these geophysical data are appropriate for investigating crosscutting relationships that conventional bathymetry maps and lower-frequency seismic reflection profiles cannot resolve. By groundtruthing the available seismic stratigraphy, I also unravel the complex depositional history of the New Jersey continental margin, and provide new insights on relationships between stratal properties and subbottom reflectors.

Studies such as this, of variable, small-scale features typical of Quaternary coastal and shelfal environments, require an interdisciplinary approach using precisely located, high-resolution 2D (and ideally 3D) seismic surveys integrated with a carefully planned coring program. This integrated approach can resolve many ambiguities and considerably "sharpen" the picture (Davies et al., 1992). This is particularly crucial in glacial and periglacial geological environments, which exhibit rapid and complex horizontal and vertical variations in stratigraphic characteristics (Anderson and Molina, 1989; Hambry, 1994). This work extends the technological limits of my ability to observe seafloor

17

geomorphology and shallow stratigraphy. In the form of densely-sampled, high-resolution geophysical profiles and maps, satellite-navigated samples, and computer-aided models, we have new "glasses" that help us observe and measure what we previously had to infer. By mapping the distribution and trends of distinct, shallowly buried dendritic drainage systems, and then by sampling them systematically, I should be able to discern the complicated patterns of fluvial and marginal marine sedimentation that represent the shelf's response to Quaternary sea level fluctuations of varying frequency.

Insights gained from studying stratigraphic and geomorphic responses to base level fluctuations are valuable as a part of a larger effort to understand the effects of sea level variation on siliciclastic, sediment-starved continental margins like the U.S. east coast. The larger effort, to understand sea level variations in a global context by integrating studies worldwide (Hernandez-Molina et al., 1994; Nichol et al., 1994; Sejrup et al., 1994; Bartek and Wellner, 1995; Miller et al., 1995; Genesous and Tesson, 1996; Davies and Austin, 1997; Foyle and Oertel, 1997; Yoo and Park, 1997; Rabineau et al., 1998; Carey et al., 1998; Duncan et al., 2000; Tesson et al., 2000; Liu et al., 2002; Yoo et al., 2002; Posamentier, 2002; Lericolais et al., 2003; Posamentier and Kolla, 2003; Reynaud et al., 2003; Anderson and Fillon, 2004; FitzGerald et al., 2004; Lobo et al., 2004; Nordfjord et al., in revision), will enable eventual calibration of the global-eustatic curve. Obtaining the best possible chronostratigraphic control of the Quaternary portion of the stratigraphic record constitutes a step toward correlating modern processes with process-based features inferred from the preserved geologic record. This type of study is essential for demonstrating how the generalized sequence stratigraphic model can be fitted to the specific characteristics of a given shelf, enabling a model to be generated for realistic predictions of the distribution of source and reservoir rocks (Carey et al., 1998).

18

OVERVIEW OF PERTINENT SEISMIC AND SEQUENCE STRATIGRAPHIC CONCEPTS

Seismic stratigraphy, and its more recent outgrowth, sequence stratigraphy, serve as predictive tools to identify, correlate and impose chronostratigraphic order on the depositional record (Payton, 1977; Vail, 1987; Posamentier and Vail, 1988; Van Wagoner et al., 1988, 1990; Boyd et al., 1989; Galloway, 1989; Miall, 1991, 1992; Mitchum and Van Wagoner, 1991; Posamentier et al., 1992: Weimer, 1992; Posamentier and Weimer, 1993). The methodology relies on the premise that marine transgressions and regressions induce landward and basinward migrations of the coastline that alter sediment accommodation space. Transgressions and regressions induce development of marine and fluvial unconformities whose recognition is fundamental to sequence stratigraphic interpretation. Variations in accommodation space, coupled with sediment supply variability and basin margin physiography, primarily determine the three-dimensional geometries and facies components of the sediment volumes (depositional sequences; Figure 1.4) that accumulate. The methodology serves as a fundamental tool in the chronostratigraphic reconstruction of any marine basin setting, but is particularly well-suited for passive-margin basins.

Swift et al. (1991) and Thorne and Swift (1991) developed a regime-based, semi-quantitative model of continental margin sedimentation in which they questioned the finer details of the Vail et al. (1977a) and Galloway (1989) models. They described geometric systems tracts that are definable on the basis of geometry, which contrasts with the Vail model where system tracts are defined principally on the basis of lithology. Thorne and Swift (1991b) also pointed out the significance of pre-ravinement back-step (back-barrier) wedge deposits (Figure 1.5), not considered by the Vail model, that become important components of the transgressive system tract as developed on barrier and (or) embayed coastlines. The back-step wedge geometric system tract consists of two

19
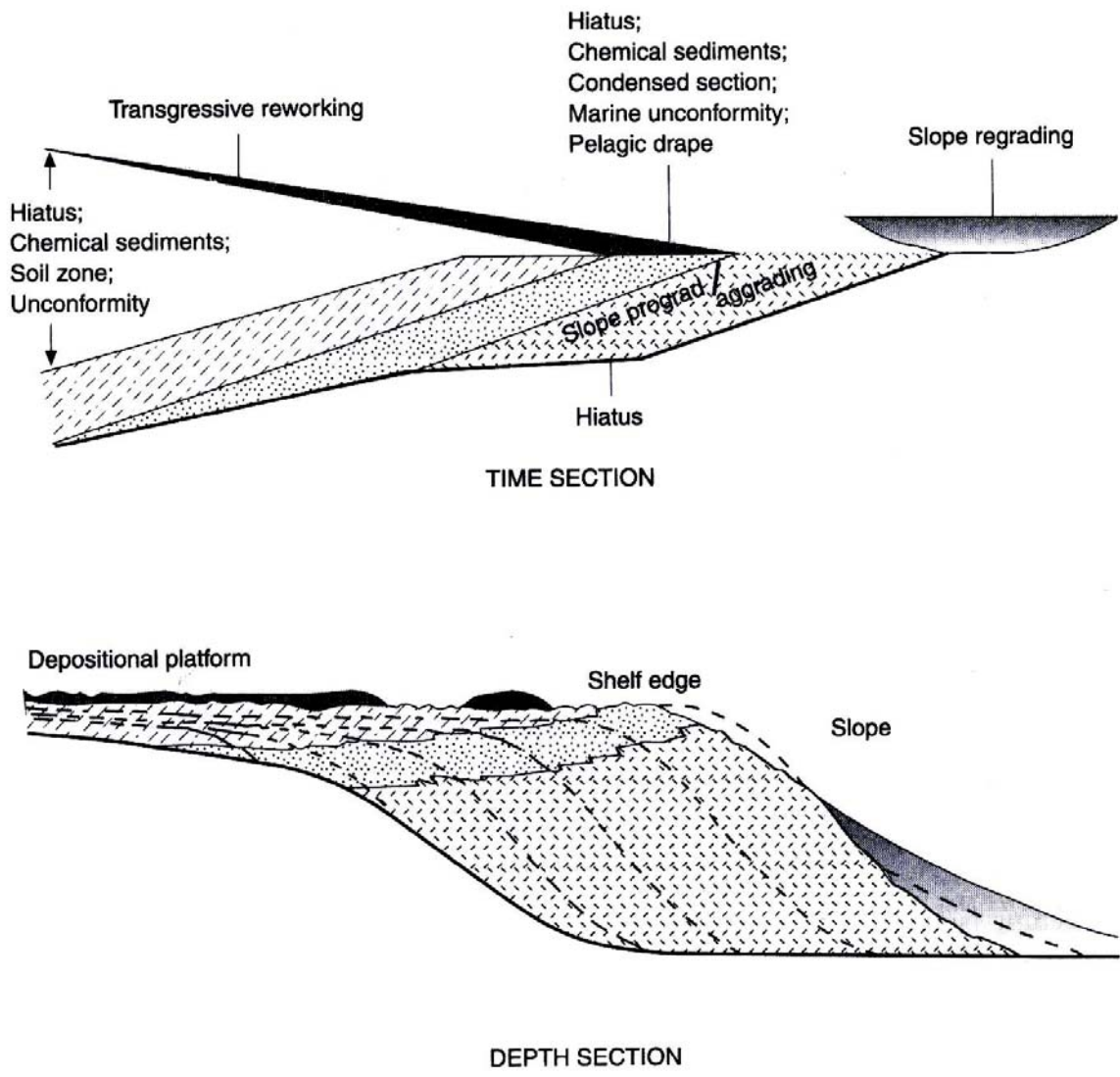
Figure 1.4: A genetic stratigraphic sequence, after Galloway (1989).

generalized depositional systems, the back-barrier (estuarine) wedge and the back-step shelf wedge (Figure 1.5), which are separated from each other by the transgressive ravinement (Thorne and Swift, 1991). These back-step wedge deposits are observable on high-resolution seismic records of Quaternary marine deposits.

The Thorne and Swift (1991) regime model describes sequence architecture as being controlled by "geohistorical" variables. Using these variables, sequence architecture can be interpreted in terms of regime conditions, and in terms of the directions and rates of regime-condition change. The variables are identified as the rate and direction of sea-level change (R), sediment input rate (Q), sediment grain-size (M) and the rate of sediment transport (D). The product of Q and M is the regime expression for effective sediment supply, while the product of R and D is the regime expression for effective accommodation potential (Thorne and Swift, 1991). These variables were used to describe an accommodation to supply ratio, ¥, where ¥ is approximated by the ratio of RD to QM, and can be applied to several scales of continental margin sedimentation; the application of this regime ratio to the inner shelf is pertinent to this study. Where ¥>1, the regime is said to be R-dependent and accommodation-dominated, autochthonous sedimentation dominates, and rivers at the coastal zone function as estuaries. Where ¥<1, the shelf regime is said to be Q-dependent and supply-dominated, allochtonous sedimentation dominates and rivers at the coastal zone function as deltas (Swift and Thorne, 1991a; Thorne and Swift, 1991). Generally, regressive shelves are characterized by values of ¥ less than unity, while transgressive shelves possess ¥ greater than unity.

On seismic records, two types of surfaces are imaged; unconformities or erosional surfaces (fluvial, ravinement, maximum-flooding and local-diastem types) and stratal (or depositional) surfaces (Figure 1.6). Fluvial erosion surfaces, created by fluvial entrenchment and subaerial weathering, develop at time scales of 10^4 to 10^5 years or

21
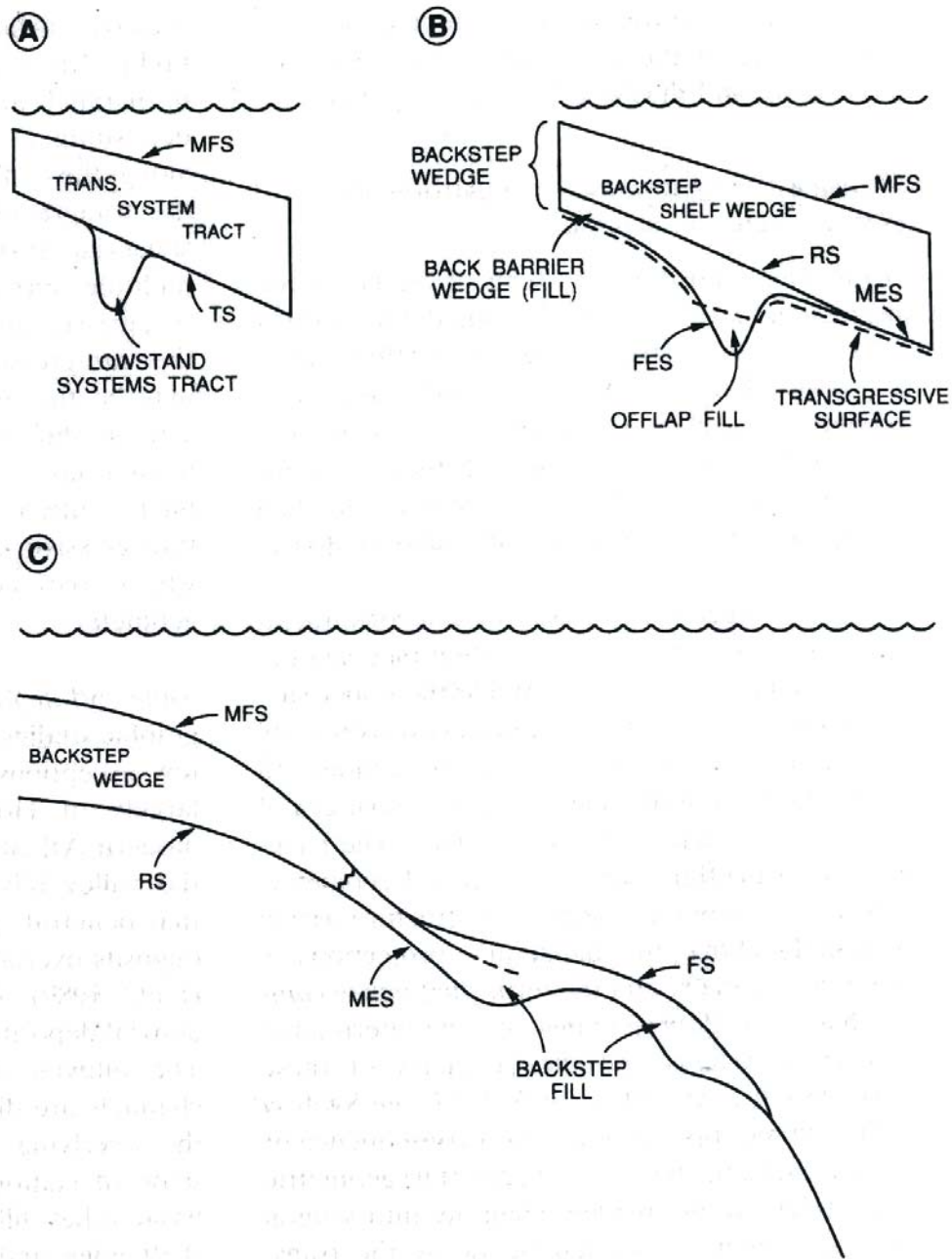
Figure 1.5: Schematic illustration of surfaces bounding and within the back-step wedge (fill) systems tract. (A) Vail (1987) model. TS= transgressive ravinement; MFS= marine flooding surface. (B) Swift and Thorne (1991) model showing distinct transgressive and ravinement surfaces. RS= ravinement surface; MES= marine erosion surface. Transgressive surface is dashed. (C) Two generations of offshore back-step fill. Second generation accumulates as maximum erosion surface begins to form on back-step wedge (Swift and Thorne, 1991a).

22

more, and may thus be termed unconformities in both a classical sense (Gary and McCafee, 1974), and in the context of sequence stratigraphy (Nummedal and Swift, 1987; Vail, 1987; Van Wagoner et al., 1987, 1988). On continental margins, fluvial erosion surfaces are generated principally during sea-level fall (Figure 1.6), lowstand, and the early part of sea-level rise.

The transgressive ravinement surface, because it is a marine unconformity, is considered a diastem, representing a much smaller interval of time (Demarest and Kraft, 1987; Nummedal and Swift, 1987). It does not represent a regional boundary between time-stratigraphic units (as is the case for the fluvial erosion unconformity), unless it forms the sequence boundary by removing the underlying fluvial erosion surface. During the Quaternary, ravinements have been created principally during marine transgression of the continental shelf accompanying glacio-eustatic rise (Figures 1.7 and 1.8), but they can also form during regressions. Ravinements are associated with hiatuses on the order of 10^1 to 10^3 years duration in the Quaternary record, and are referred to as diastems rather than unconformities. At shorter temporal scales (10^0 to 10^2 years), erosional surfaces created by laterally migrating tidal inlet thalwegs, and deflation zones between shoreface and shelf sand ridges, are also referred to as diastems (e.g., the tidal scour diastem and the channel-base diastem; Nummedal and Swift, 1987; Swift et al., 1991).

Fluvial and ravinement unconformities and maximum flooding surfaces (MFS, Figure 1.5) develop in response to changes in relative sea-level (Figure 1.6), and their recognition is critical to the identification and description of depositional sequences and their internal components (system tracts and parasequences; Figure 1.6). The seismic stratigraphic method, using the Vail methodology, relies on the identification of fluvial unconformities (and correlative conformities) to subdivide the stratigraphic record into unconformity-bounded depositional sequences. Depositional sequences are further

23

shelf delta,
aggradation & progradation

downlap

rise fall rise

hemipelagic and pelagic sedimentation

1. **Highstand systems tract:** low rate progradation and aggradation
(base level rise at the shoreline and normal regression)

fluvial erosion or bypass

shelf-edge
delta with offlap

rise fall rise

regressive
slope onlap surface

2. **Falling stage systems tract:** high rate progradation and offlap
(base level fall at the shoreline and forced regression)

slope fans and slumps
basin floor fans

fluvial onlap

shelf-edge
delta with topset

rise fall rise

3. **Lowstand systems tract:** low rate progradation and aggradation
(base level rise at the shoreline and normal regression)

fluvial onlap

coastal onlap

rise fall rise

estuary

marine onlap
(slope apron)

4. **Transgressive systems tract:** retrogradation and aggradation
(base level rise at the shoreline and transgression)

subaerial unconformity	maximum regressive surface
correlative conformity	maximum flooding surface
basal surface of forced regression	within-trend normal regressive surface
ravinement surface	lateral shifts of facies

Figure 1.6:   Regional architecture of depositional systems, systems tracts and
stratigraphic surfaces. System tracts are defined by stratal stacking
patterns and bounding surfaces, with an inferred timing relative to the
sea-level curve (Catuneanu, 2002).

24

subdivided into system tracts, parasequences and seismic facies units (Vail et al., 1977; Vail, 1987; Van Wagoner et al., 1988).

Depositional sequences are stratigraphic units consisting of genetically-related generally conformable, strata, bounded above and below by unconformities or correlative conformity surfaces (Mitchum et al., 1977, Part 2, Part 6; Posamentier and Vail, 1988; Van Wagoner et al., 1988). They are deposited between sea-level fall inflection points on the eustatic curve. The classic depositional sequence is a third order sequence (Vail, 1987; Swift et al., 1991; Posamentier and Weimer, 1993). The base and the top of the sequence are defined by fluvial erosion surfaces, or by correlative conformities in the basinward direction. Within the sequence, a transgressive ravinement is located above, and is separated from, the fluvial unconformity, while higher in the sequence, a maximum flooding surface is developed (Figure 1.6). Kidwell (1993) has noted that such classic sequences tend to develop under conditions of "moderate" subsidence (10^1-10^2 cm/10^3 yr). In low-subsidence settings ($<10^1$ cm/10^3 yr), the sequence is thinner and may be bounded by ravinement surfaces rather than fluvial unconformities. These upper and lower ravinement sequence boundaries may remove the maximum flooding and fluvial unconformity surfaces, respectively, so that the sequence may record only transgressive (post-ravinement) deposition. However, subsidence rate alone does not determine sequence geometry; equally critical are the sea-level change rate, the frequency of sea-level change, sediment supply, and basin margin physiography and how these three factors interact with subsidence rate.

High-resolution, shallow-penetration reflection seismic profile data from coastal and shelf settings are well suited to seismic stratigraphic analysis of glacio-eustatically controlled Quaternary depositional sequences that are commonly developed and accessible in these settings. Such data are becoming increasingly important in the

25

stratigraphic analysis of cyclic transgressive and regressive sequences found on continental margins (Beard et al., 1982; Kindinger, 1988; Posamentier et al., 1992; Allen and Posamentier, 1993). Because of the higher resolution (~0.1 m) obtained in such reflection seismic profiling, reflectors inferred to be stratal surfaces are more likely to agree closely with the time-equivalence assumption. High-resolution seismic data may therefore be used to resolve stratigraphic units at the (thick) bed, formation or allo-formation scale.

Quaternary-aged fluvial erosion surfaces, observed beneath the Atlantic inner continental shelf, have been incised during periods of lowered sea-levels associated with glacial maxima (Figure 1.6). Fluvial erosion surfaces may begin incising the coastal plain/shelf surface as sea-level starts to fall, and continue incising until grade is achieved or until sea-level rises again and induces deposition on top of the unconformity. Models by Schumm (1993) indicate that fluvial valleys may either alter sinuosity, incise or aggrade on inner shelf areas during sea-level fall. They also have the capability to compensate for drop in base-level by changing their hydraulic radii or channel roughness (the R and n terms in the Manning Equation; Rouse, 1946). Thorne and Swift (1991) have described the degree of development of a fluvial erosion surface during sea-level fall as being controlled by variability in the regime ratio, ¥. They indicate that inter-regional development of the fluvial erosion surface during sea-level fall occurs only when the accommodation/supply ratio, ¥, decreases.

Stream aggradation or incision is governed by the relative gradients of the coastal plain and inner shelf and by sediment supply (Schumm, 1993). Basinward retreat of the shoreline results in the expansion of established drainage basins and the creation of new, smaller drainage basins on the emerging shelf surface as fluvial systems develop and

26

respond to the drop in base-level (Schumm, 1993). Basin margin physiography can also be important, in that it can control the development and location of incised valleys.

The relief developed on the subaerial unconformity (fluvial erosion surface) is related to drainage basin size, slope of emerging subaerial landscape, regional geology, time available for fluvial incision and the magnitude of sea-level fall (Demarest and Leatherman, 1985; Van Wagoner et al., 1990). The hiatus associated with the fluvial erosion surface generally decreases in a basinward direction, where the surface ultimately becomes a conformable surface.

The concept of the ravinement surface was first defined by Stamp (1921), and described further by Swift (1968; Figure 1.8B). The ravinement was perceived to have resulted from erosional retreat of the shoreface during marine transgression (Figures 1.7 and 1.8). The principal causal force in landward shoreface migration and ravinement generation is the action of breaking waves, associated littoral currents, and wind-driven and tidal currents on the shoreface. The ravinement may therefore be thought of as a "wave ravinement" in the sense of Allen and Posamentier (1993), in that it is cut principally by erosion induced by wave-driven currents, with a lesser input from tidal currents. The transgressive ravinement surface forms at the base of the shoreface during marine transgression (Fischer, 1961; Swift, 1968; Swift and Thorne, 1991a). It represents the retreat path left by the landward-migrating shoreface, a process that occurs when the accommodation:supply ratio, ¥, is greater than unity, and the rate of change of ¥ is positive.

On barrier coastlines, lagoonal deposition landward of, and stratigraphically beneath, the ravinement may be contemporaneous with inner shelf sedimentation above the ravinement (the "transgressive marine sand sheet" of Swift, 1968; Figure 1.8). The ravinement surface represents the first significant marine flooding event across the shelf,
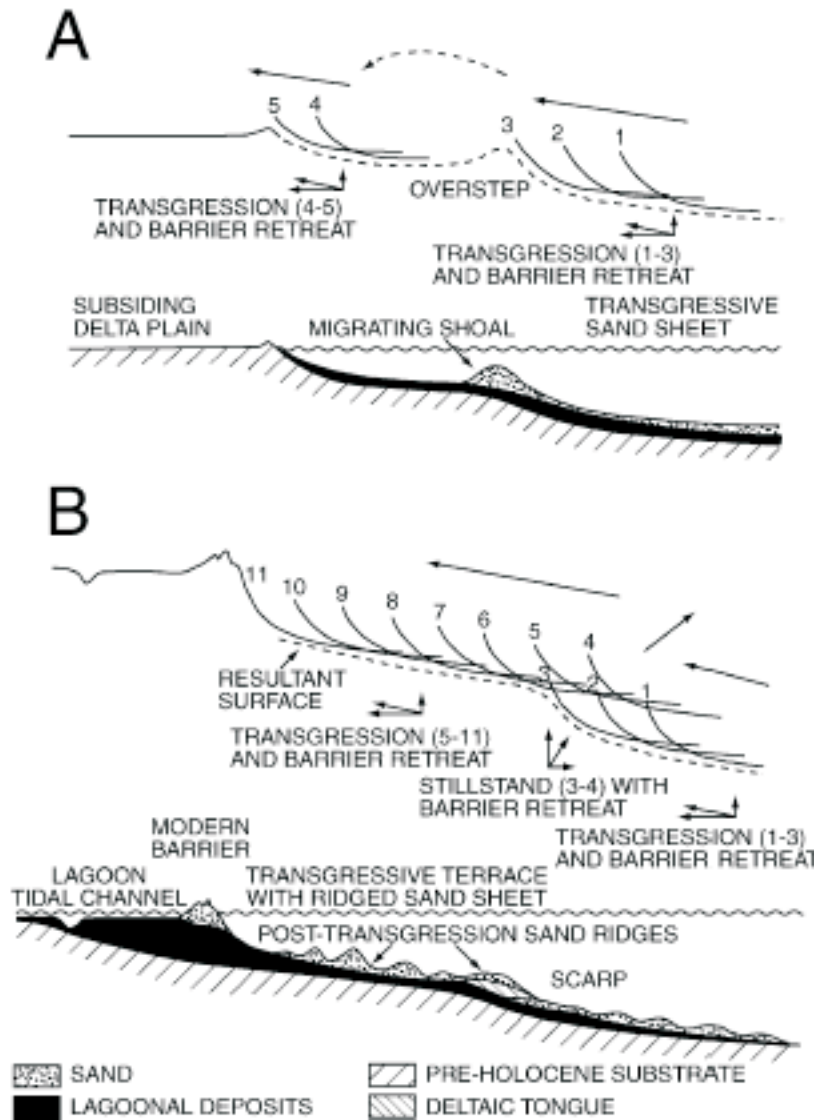
Figure 1.7: (A) Diagram showing successive shoreface profiles in the case of barrier overstep (Swift, 1975). (B) Diagram illustrating the shoreface profile at various positions during shoreface retreat interrupted by a progradation episode. The thick wedge of back-barrier (lagoonal) sediments below the ravinement surface and the site of sand above the ravinement surface accumulate during upward accretion and little horizontal retreat (Swift, 1975).

28

CONTINUOUS TRANSGRESSION
(steady rate of relative sea-level rise)

A Barrier retreat
(Johnson, 1919; Sanders and Kumar, 1975)

LAND   SEA
retrograded barrier
wRs
HT2
LT2 wRs   HT1
2   LT1

barrier
HT1
LT1
1

B Shoreface erosion; shoreface retreat
(Bruun, 1962; Swift, 1968)

shoreline   sea-level rise
3   SL3
2   SL2
1   SL1
projected   erosion
wRs   increasing
ravinement wRs3   accommodation
diastem   wRs2   3
onlap wedge of transgressive wRs1   2
shelf sediments   1

C Healing phase
(Posamentier and Allen, 1993)

backstepping
barrier beaches
transgressive lag
"healing phase"
deposits

peat
marine mud
older deposits
shoreface/barrier sand
transgressive lagoonal sediments (mud)
wave ravinement surface (wRs)

HT/LT = high tide; low tide   SL = sea level

Figure 1.8:   Schematic inner-shelf to shoreface profiles illustrating stratigraphic response to continuous transgression. (A) Barrier retreat is caused by wave erosion (ravinement) during relative sea-level rise in environments where barrier-lagoon systems are present. (B) Similarly, shoreface erosion or shoreface retreat assumes an adjustment profile of the shoreface during transgression in accordance with the Bruun rule. (C) Healing phase deposits form when sediment eroded during ravinement is transported beyond the shelf edge.

29

and defines the base of the transgressive marine section (Van Wagoner et al., 1988), or the base of the back-step shelf wedge (Thorne and Swift, 1991; Figure 1.5). On barrier coastlines, the ravinement is underlain by transgressive paralic deposits that rest directly on the antecedent fluvial unconformity (Figure 1.9; Demarest et al., 1981; Belknap and Kraft, 1985). These are the back-barrier wedge deposits that make up the lower component of the back-step wedge geometric system tract (Thorne and Swift, 1991).

In estuary mouth regions, strong tidal currents may scour the seabed and create a variable-relief erosional or ravinement surface (Demarest and Kraft, 1987), within the baymouth area that migrates landward in response to sea-level rise (Figures 1.10 and 1.11). This transgressive erosional surface has been referred to as the "tidal ravinement" by Allen and Posamentier (1993), to distinguish it from a wave ravinement that is created in an oceanic shoreface setting. The surface develops in a bay mouth setting, where tidal currents dominate over wave orbital currents; however, in wave-dominated estuaries, wave forcing may also be important. The tidal ravinement may be expected to have a more restricted occurrence in the coast-parallel direction due to its direct association with evolving estuaries. The relief developed on a tidal ravinement surface will generally be greater that that associated with a wave ravinement, particularly in strike-oriented sections. Relief will be dependent on tidal regime (e.g., microtidal versus macrotidal), estuarine tidal prism, estuary mouth width (Figure 1.10), littoral sediment supply and also on wave climate. Conceptually, the surface is created by a migrating tidal-scour trench at the estuary mouth (Figure 1.10), such as the Chesapeake Channel within the modern Chesapeake Bay mouth. Lateral and landward migration of the scour trench permits the tidal ravinement surface to be downlapped and onlapped by estuary-mouth sands shed off adjacent shoals and estuary-margin spits. The downlapping characteristic, in particular, helps distinguish the tidal ravinement surface from the wave ravinement surface.

30
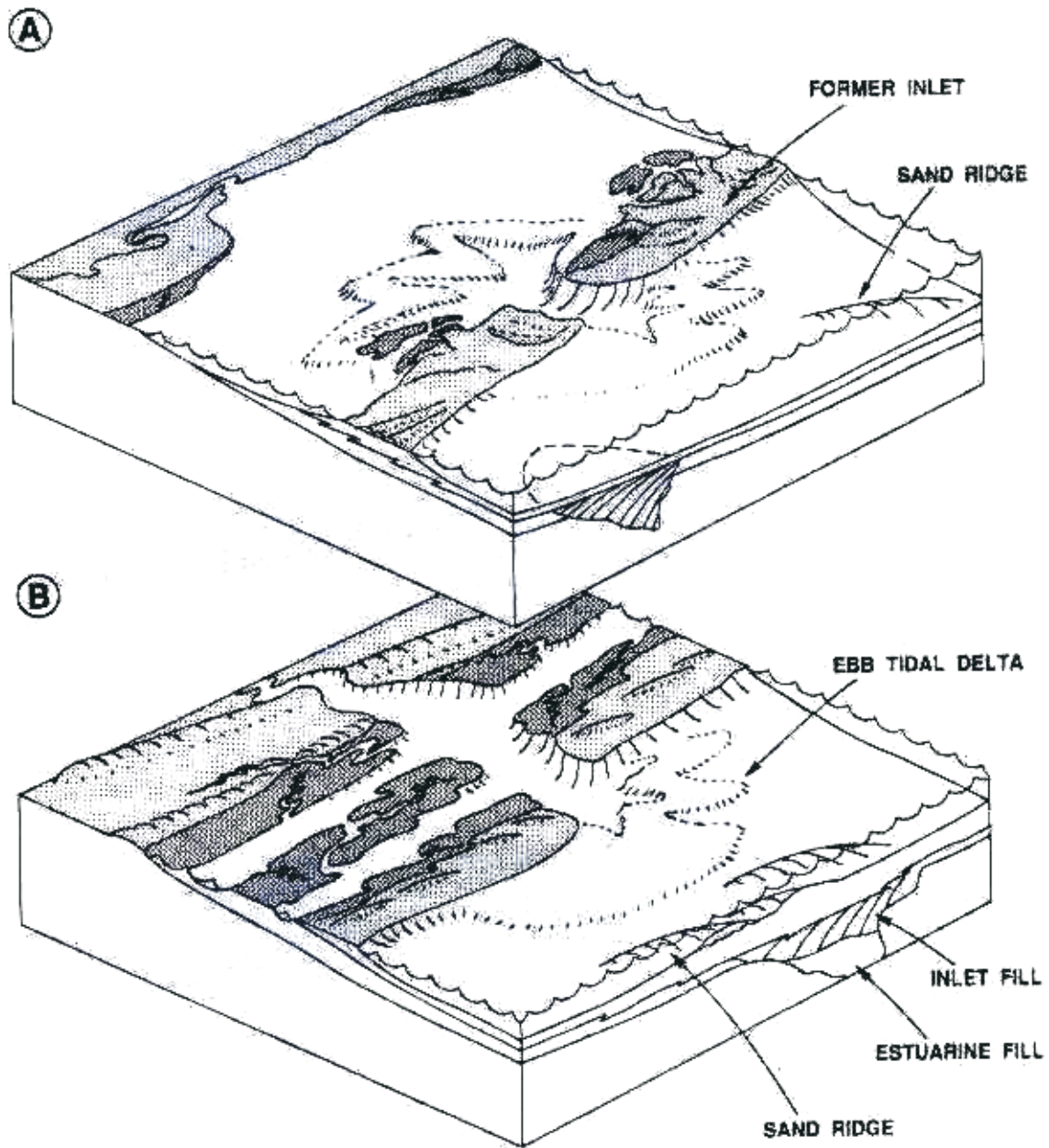
Figure 1.9: Classes of continuous barrier retreat. (A) Marsh-lagoon mode of barrier retreat. (B) Open lagoon mode of barrier retreat (Based on Oertel, 1987; Emery and Myers, 1996)

The tidal ravinement will move landward with continued transgression as the estuary mouth moves landward. Because of its association with tidal scouring, the tidal ravinement may be expected to occur at greater depths than the coeval wave ravinement located at the shoreface. Within a complete transgressive paleo-valley fill succession, therefore, the tidal ravinement will be overlain by the wave ravinement, and will merge with or be truncated by the latter on paleo-estuary flanks. On barrier coastlines with small embayments (tidal inlets), an analogous tidal ravinement surface develops at tidal inlets where it has been referred to as the tidal inlet diastem by Swift et al. (1991). This analogous surface is created within the tidal inlet throat by periodically-reversing tidal currents (which may be reinforced by the wave regime) that may attain velocities of 2 m/s (6.5 km/hr).

Within transgressive paleo-valley fill successions on the updip areas of basin margins, the three transgressive surfaces described above (the sequence-bounding fluvial unconformity, tidal ravinement and wave ravinement) may potentially be preserved in vertical succession (Figures 1.10 and 1.11). Within the lower part of the incised-valley fill, a fourth transgressive, or flooding, surface may be preserved. This surface marks the boundary between fluvial deposits and overlying transgressive estuarine deposits (Figure 1.10). The subjacent fluvial deposits are expected to be transgressive in origin (having backfilled the paleo-valley during transgression). However, fluvial deposits may also have accumulated during sea-level fall due to alluvial aggradation (Figures 1.10 and 1.11), as suggested by Allen and Posamentier (1993) for fluvial deposits in the lower parts of the Gironde estuary fill succession. This estuarine transgressive surface, also referred to as a tidal flooding surface (Allen and Posamentier, 1993), or a bay ravinement diastem (Nummedal and Swift, 1987), represents the retreat path of a landward migrating bayline within a paleo-estuary in response to transgression (Posamentier et al., 1988).
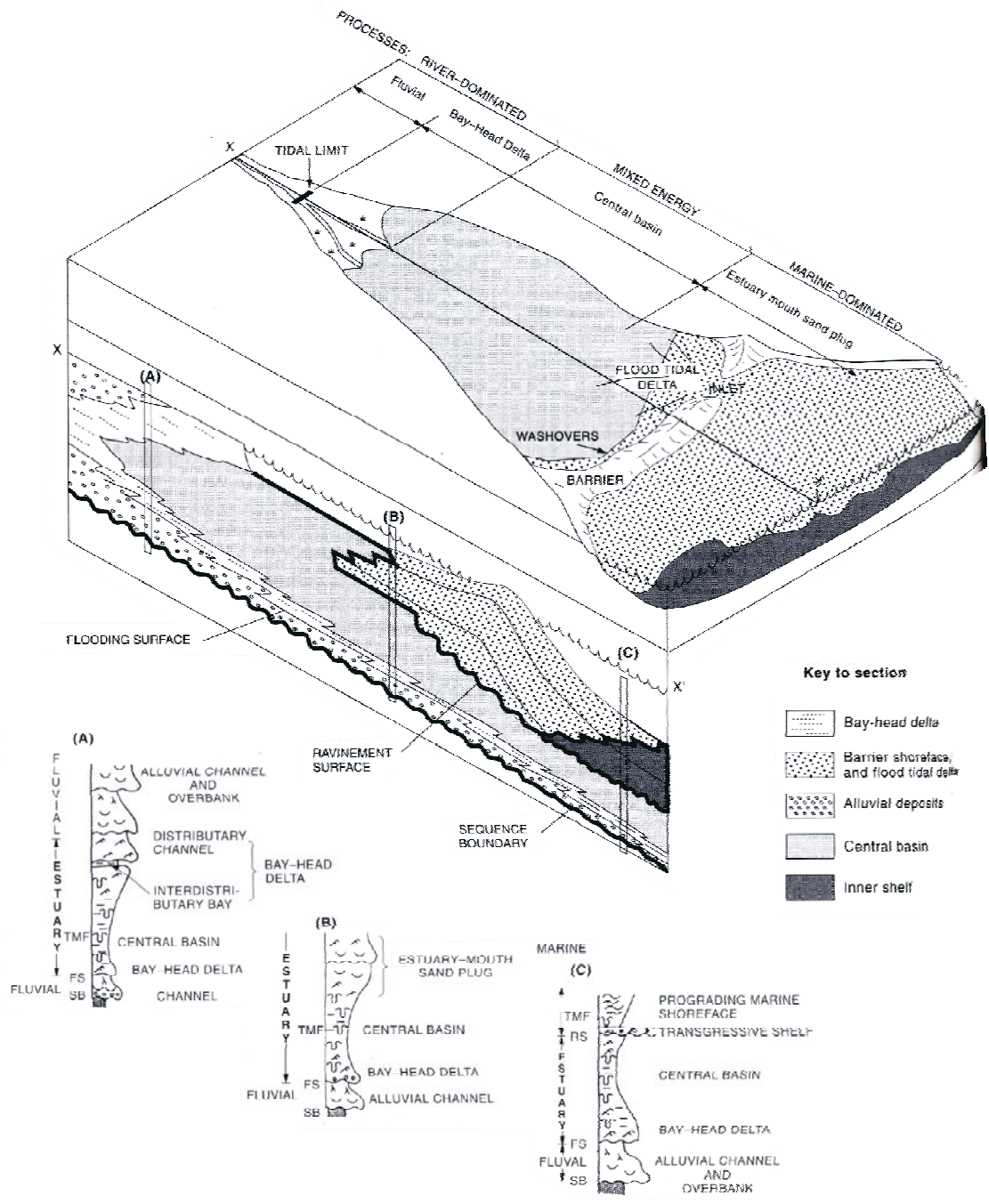
Figure 1.10: Wave-dominated estuary (after Dalrymple et al., 1992). TMF, time of maximum flooding; RS, ravinement surface; SB, sequence boundary; FS, flooding surface
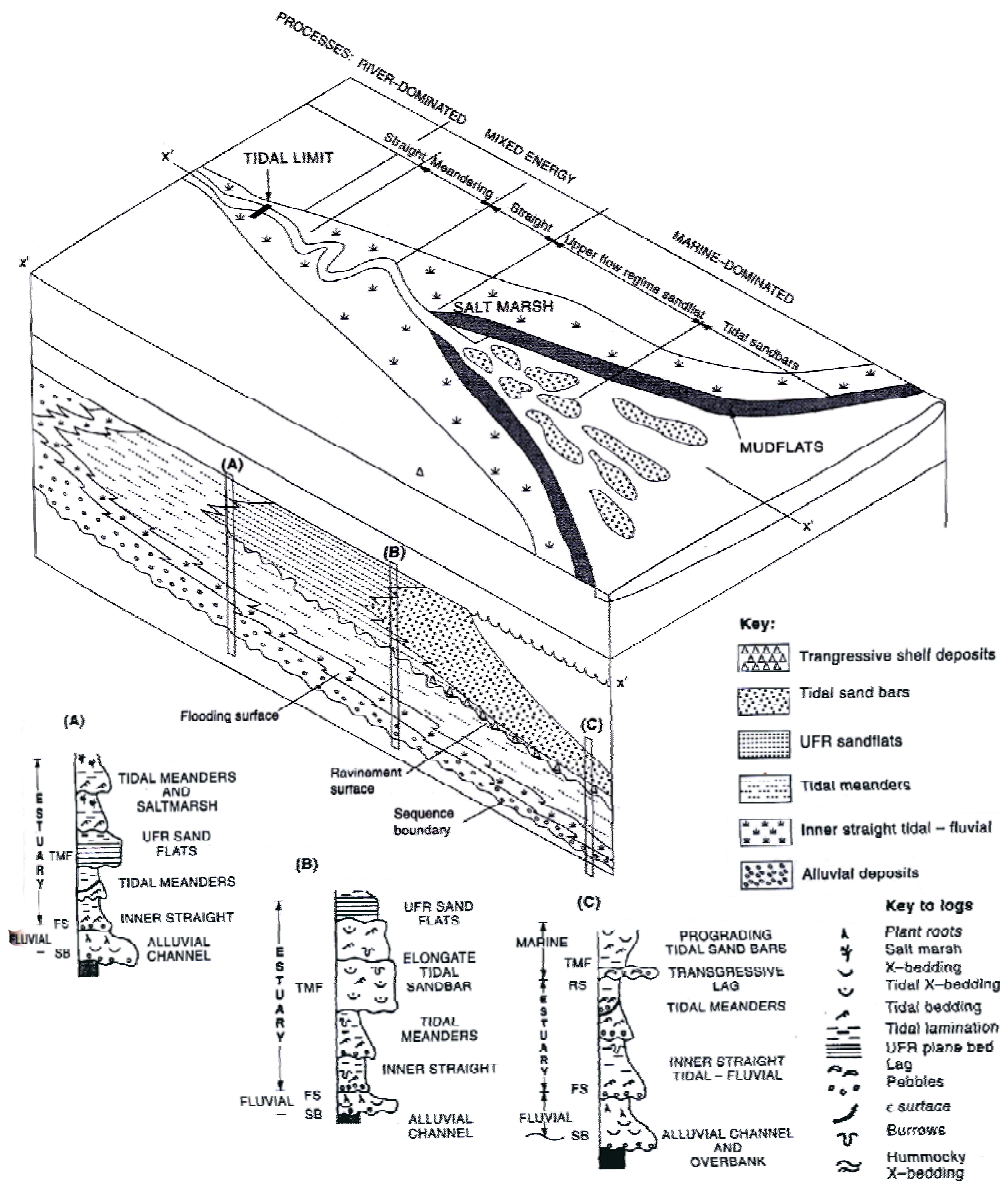
Figure 1.11: Tide-dominated estuary (after Dalrymple et al., 1992). TMF, time of maximum flooding; RS, ravinement surface; SB, sequence boundary; FS, flooding surface; UFR, upper flow regime

The estuarine transgressive surface (Figures 1.10 and 1.11) is the estuarine equivalent of the oceanic shoreface ravinement that develops on high-energy, open, oceanic coasts (Figures 1.7 and 1.8). It separates submerged alluvial plain strata from overlying transgressive estuarine deposits (Figures 1.10 and 1.11). Where alluvial plain strata did not accumulate, or were subsequently removed by the erosional estuarine transgressive surface, the latter merges with the fluvially-incised sequence boundary.

The landward-migrating bayline separates a shrinking alluvial plain from an expanding estuarine plain during transgression. It has been defined as the demarcation line between fluvial and paralic or delta plain environments (Figures 1.10 and 1.11; Posamentier et al., 1988; Miall, 1991), and as the point of onlap of bay or estuarine facies onto underlying fluvial facies (Anderson et al., 1992; Allen and Posamentier, 1993). Posamentier and Vail (1988), Posamentier et al. (1988) and Anderson et al. (1992) suggest that the bayline marks the base-level encroachment into a flooding paleo-valley during transgression. The trailing estuarine transgressive surface is significant because it delineates the boundary between fluvial and estuarine or bay depositional environments, and marks the first major paralic-marine flooding event into an evolving paleo-valley fill sequence.

The maximum flooding, or downlap, surface (MFS) separates the highstand deposits of the upper part of a depositional sequence from transgressive deposits beneath (Figure 1.6); it can potentially define the lower sequence boundary in low-subsidence, low sediment supply, high-energy shelf settings, as it marks the change from transgressive systems tract to highstand system tract depositional conditions (Vail, 1987). In the Thorne and Swift (1991) regime model, the maximum flooding surface is ideally an isochronous boundary that marks a change of regime from one where ¥ is greater than unity (transgressive system tract) to one where ¥ is less than unity (highstand system

tract). The surface thus indicates the start of a phase of basin-margin development where accommodation, or the rate of change of accommodation, has been exceeded by sediment supply.

The MFS is also the surface used to define the boundaries of genetic stratigraphic sequences in the Galloway model (Figure 1.4; Galloway, 1989). The maximum flooding surface begins to develop once the transgressive shoreline has reached its maximum landward position. However, the hiatus associated with the maximum flooding surface increases in a basinward direction (Thorne and Swift, 1991). Transgressive (retrogradational) strata beneath the maximum flooding surface are overlain by aggradational to progradational strata that occur above the maximum flooding surface, and, on the updip margins of a basin, may be equated with prograding strand plain and prograding shoreface depositional environments (Figure 1.6). These highstand deposits have a low preservation potential (Thorne and Swift, 1991) on low sediment supply basin margins, due to later erosion by fluvial and transgressive ravinement unconformities.

The term "transgressive surface" may apply to a number of erosional surfaces (Figure 1.5), depending on geographic location and the completeness of the overlying depositional sequence. When more than one transgressive erosional surface is preserved in vertical section, the lowermost surface overlain by back-stepping parasequences is treated as the transgressive surface (Thorne and Swift, 1991). The transgressive surface is thus defined by the fluvial erosion surface when the back-step wedge geometric system tract is well-developed. However, the fluvial erosion surface may be truncated by the transgressive ravinement on the shelf, in which case the ravinement surface serves as the transgressive surface. If so, then the back-barrier wedge depositional system is absent from the sequence (Thorne and Swift, 1991).

On embayed coastlines, the transgressive surface can be any one of four erosional surfaces (in areas landward of the oceanic coastline). Within estuaries (Figures 1.10 and 1.11), the transgressive surface may be marked by the fluvial erosion surface, the bay ravinement (estuarine transgressive surface), or by the tidal ravinement surface, if upper- to middle-estuary deposits are not preserved. Just seaward of the estuary mouth, the wave ravinement is developed; the wave ravinement may ultimately truncate the underlying estuarine transgressive surface and tidal ravinement surface, and thereby serve as the transgressive surface and the basal unconformity to the highstand sequence. On barrier coasts, the transgressive surface is represented by the fluvial erosion surface behind the barrier island chain, and is overlain by back-barrier wedge deposits. On the seaward side of the barrier islands, the transgressive surface is marked by the ravinement surface, and ultimately by the distal-correlative marine erosion surface, or by the fluvial erosion surface, if it has not been truncated. Minor diastems, such as the inlet channel-base diastem, may locally serve as the transgressive surface where they truncate the fluvial erosion surface at inlet throats.

This high-resolution reflection-seismic study will focus on the updip, usually thin, portions of transgressive and lowstand system tracts. It is expected that component depositional systems, and possibly the seismic equivalents of lithofacies, will be detectable on the seismic data.

On basin margin settings, the base of a sequence, whether defined by a fluvial erosion surface or by a ravinement unconformity, is marked by back-stepping transgressive coastal or marine deposits of the transgressive systems tract. These deposits onlap the lower sequence boundary in the landward direction. The upper part of a sequence, represented by the upper transgressive systems tract and the highstand systems tract (back-step wedge geometric systems tract and offlap wedge geometric systems tract,

respectively) may be missing, depending on the degree of incision by the overlying sequence boundary. The preservation potential of highstand systems tract deposits may generally be expected to be poor because erosion during subsequent regression and transgressions. To identify depositional sequence boundaries, patterns of onlap, downlap (both types of base lap), toplap and truncation, will be used to describe reflector termination patterns at the boundaries. The first three relationships are associated with non-depositional hiatuses, while latter is associated with a variable-duration erosional hiatus (Mitchum et al., 1977b; Vail, 1987; Van Wagoner et al., 1987).

Chapter 2: Seismic geomorphology of buried channel systems on the New Jersey outer shelf: Assessing past environmental conditions

INTRODUCTION

The study of coastal plain fluvial and marginal marine system dynamics and the responses of these systems to external controls over different temporal scales are important for the reconstruction of past sea-level fluctuations from sedimentary strata. The geomorphology of buried, incised valley systems on continental shelves provides a broader understanding of the variables affecting deposition, erosion and preservation of shelfal strata. Regime variables that influence the stratigraphic record of a mature, passive margin include sediment supply from the adjacent continent, millennial sea-level fluctuations, and climatic changes as a result of glacial waxing and waning.

Outcrop studies of incised valley systems from Book Cliff, Utah (Van Wagoner et al., 1990) and from the Viking Formation, Alberta (Posamentier and Allen, 1993) documented complex evolution of valley incision and fill in response to relative changes in base level. Studies like these have given rise to the sequence stratigraphic term 'incised valley system', defined as a *"fluvially-eroded, elongate topographic low that is typically larger than a single channel form, and is characterized by an abrupt seaward shift of depositional facies across a regionally mappable sequence boundary at its base. The fill typically begins to accumulate during the next base-level rise, and may contain deposits of the following highstand and subsequent sea-level cycles"* (Zaitlin at al., 1994, p. 47). Van Wagoner et al. (1990) reported such a basinward shift in facies from Book Cliff, where shallow marine to non-marine strata were deposited above mid- to outer-shelf mudstones at the bases of incised valleys. Posamentier and Allen (1993) interpreted incised-valley fill within the Viking Formation as predominantly estuarine. They believed

that the surface at the base of the fill was a combined result of erosion by fluvial processes and subsequent modification by tidal currents.

Incised valley systems shallowly buried on continental shelves can be investigated at outcrop scale offshore using very high resolution seismic acquisition techniques. With sufficient geophysical coverage, channels buried in continental shelf sediment sections can be mapped, enabling us to extrapolate geometries and facies of channel fills to a greater area than is generally possible by means of outcrop studies. Generally, offshore studies are focused on the evolution of sedimentary sequences during the most recent sea-level cycle. Examples include continental shelf investigations off the U.S. east coast (Knebel et al., 1979; Belknap and Kraft, 1985; Davies et al., 1992; Ashley and Sheridan, 1994; Foyle and Oertel, 1997), in the Gulf of Mexico (Galloway, 1981; Suter and Berryhill, 1985; Anderson et al., 1996), the Yellow Sea (Bartek and Wellner, 1995; Warren and Bartek, 2002), and off the mouth of the Rhone River (Gensous and Tesson, 1996). Investigated buried incised valleys range widely in size, from hundreds of meters wide and <10m deep, to several kilometers wide and tens of meters deep (Dalrymple et al., 1994).

Shelf incisions resembling river channels are mappable stratal surfaces that record the existence and migration of depositional environments on continental margins (Galloway and Sylvia, 2002). The sequences comprising incised valley fills generally represent sediments deposited in a range of environments, from fluvial and estuarine to fully marine (Nichols and Biggs, 1985; Nichols et al., 1991; Shanley and McCabe, 1992; Zaitlin et al., 1994; Buck et al., 1999).

Because these buried channels represent paleo-drainages, my objective is to link these features with one or more hydraulic paleoenviroments. In this paper, I integrate classic geomorphologic principles developed for fluvial and estuarine systems with

interpretations of extremely high quality seismic images of the latest Quaternary stratigraphic record on the outer continental shelf off New Jersey. This wide (>150 km), gently sloping (~0.06°), mature passive continental margin (Figure 2.1) is excellent for this type of investigation, due to its minimal subsidence and quiescent tectonic setting (Swift and Field, 1981). Because latest Quaternary sediment supply to the shelf is virtually nonexistent, eustacy is the prevalent force driving sedimentation and erosion.

I seek to understand the genesis and evolution of widely observed, shallowly buried incised valley systems long recognized beneath this continental shelf. The primary data set consists of a dense grid of 1-4 kHz, deep-towed chirp seismic data collected over ~600 km^2 (Figure 2.1). First, I measure dimensional and spatial variables from interpreted images of buried channel horizons, then analyze those data within a quantitative geomorphology context in order to understand the observed seismic stratigraphic architecture. I use current understanding of marginal marine and fluvial systems, specifically medium-sized streams in lowland plains (Dury, 1976) and tidal creeks (Friedrichs, 1995), to infer past hydrologic conditions. Next, I measure mean and maximum depth, channel width, cross-sectional area, width-to-depth ratios, channel slope and sinuosity. Finally, I relate dimensions, shapes, trends and inferred paleo-flow properties of the buried channels with modern analogs. My analysis allows us to infer latest Quaternary environments and formative processes of these outer shelf, buried incised valleys when they were active systems.

I seek to build on a long tradition of reconstructing past hydrologic conditions from geologic evidence. Quantitative geomorphologic investigations of modern streams (e.g., Leopold and Maddock, 1953; Schumm, 1968; Dury, 1976; Williams, 1978; Dury, 1985; Hey and Thorne, 1986) have compiled suites of measurements of channel width, depth, velocity, cross-sectional area and discharge, *en route* to establishing empirical
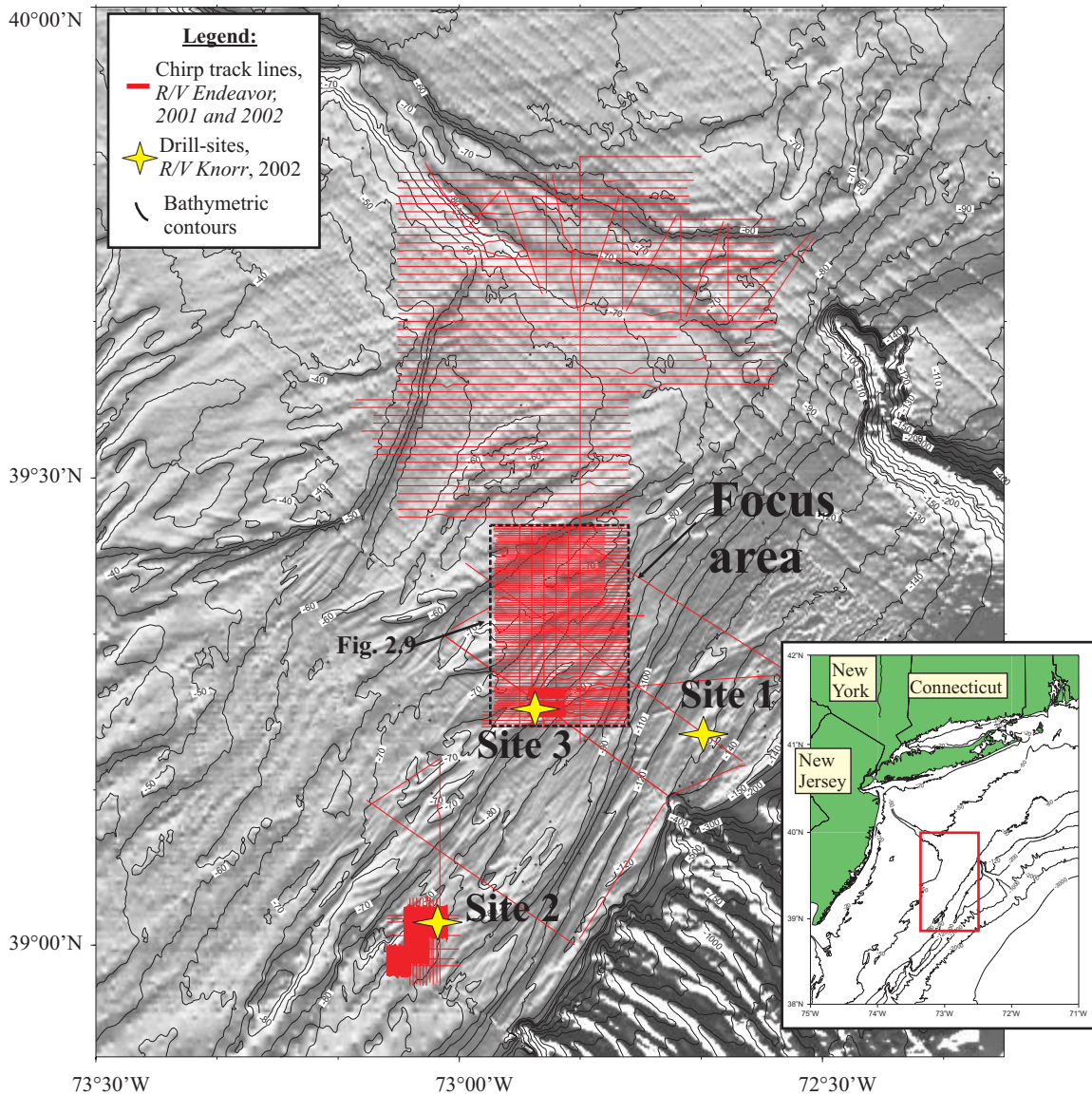
Figure 2.1:   Location of deep-towed chirp sonar track lines collected in 2001 and
2002 aboard R/V Endeavor (EN359 and EN370), superimposed on
NOAA's bathymetry merged with STRATAFORM swath mapping (Goff
et al., 1999) of the New Jersey middle and outer continental shelf. Box
shows focus area. 1-3 are boreholes.

42

relationships among hydraulic variables for a range of stream environments. For example, Friedrichs (1995) surveyed the literature on estuaries to find 242 channel sections in 26 separate tidal systems, and noted that channel cross-sectional area (in m^2) is nearly equivalent to peak (spring) tidal discharge (in m^3/s). Based on channel cross-sectional measurements, he then proposed a procedure for predicting peak discharges throughout a tidal network. Gallagher (2002) employed hydraulic equations derived empirically for modern rivers to estimate latest Pleistocene proglacial meltwater discharges through a paleo-channel on the Celtic Sea continental shelf. Combined with paleo-flow dimensions, such sediment transport capabilities can yield paleo-flow estimates *en route* to deducing paleoenvironmental conditions necessary for transporting sediments in buried channels (Gallagher, 2002).

GEOLOGIC SETTING

The New Jersey continental shelf is part of a tectonically quiescent, wide (>150 km) passive margin (Figure 2.1). Latest Quaternary depositional sequences are at most tens of meters thick, a result of low subsidence and sediment supply rates during this period (Milliman and Emery, 1968). The last ~50 kyrs of stratigraphy can thus be imaged using shallow penetration, very-high resolution seismic reflection techniques. Such surveys have been performed on the outer New Jersey shelf with 3.5 kHz, Huntec boomer and most recently by deep-towed chirp sonar; some of these have been integrated with coring programs (Knebel and Spiker, 1977; Davies and Austin, 1997). In addition, multibeam bathymetry/backscatter data have been acquired and calibrated using ~100 seafloor grab samples (Goff et al., 1999; Goff et al., 2004). All of these data have improved my understanding of the latest Quaternary evolution of this region.

43

The principal observed seismic stratigraphic horizons and interpreted sequences have been summarized by Duncan et al. (2000). They include the "R" horizon, outer shelf wedge, the "Channels" horizon, related channel fills, the "T" horizon and the post-T sand-sheet (Figure 2.2). Regional reflector "R" was originally interpreted by McClennen (1973) to be a subaerial exposure surface cut during the last regression and lowstand (Milliman et al., 1990; Sheridan et al., 2000). Based on 1-3.5 kHz Huntec deep-towed boomer seismic profiles, Duncan et al. (2000) re-interpreted "R" as a combined subaerial and marine unconformity that formed earlier, during the last regression on a sediment-starved shelf. "R" off New Jersey was then overlain by a muddy, marine outer shelf wedge deposited ca. 46.5-28.9 ka; this wedge was emplaced during the LGM (Figure 2.2).

Davies et al. (1992) identified and mapped the "Channels" horizon as an incision surface eroding both the outer shelf wedge and "R" (Figure 2.2). These shallowly buried incisions were mapped with regional deep-towed Huntec profiles, including limited 3-D coverage, which verified their dendritic, fluvial geometry (Austin et al., 1996; Duncan et al., 2000). Vibracore samples from a fill located within the flank of one channel at ~76 m water depth encountered alternations between inner-to-middle shelf and inner-shelf to marginal-marine benthic foraminifera faunal assemblages, implying at least three subtle (<10 m?) base-level fluctuations within that channel as it filled (Lagoe et al., 1997; Buck et al., 1999). An AMS ^{14}C age of 12,300 ± 450 yrs was derived from this fill (Buck et al., 1999), consistent with Davies et al. (1992) original hypothesis that these channels were incised during the LGM (ca. 25-15.7 ka) and subsequently filled during the Holocene transgression. Duncan et al. (2000) also identified a variable-amplitude seismic reflector truncating "Channels" which they named "T". The "T" horizon is generally sub-parallel to the seafloor, caps channel fills, and forms the base of a widespread surficial sand unit
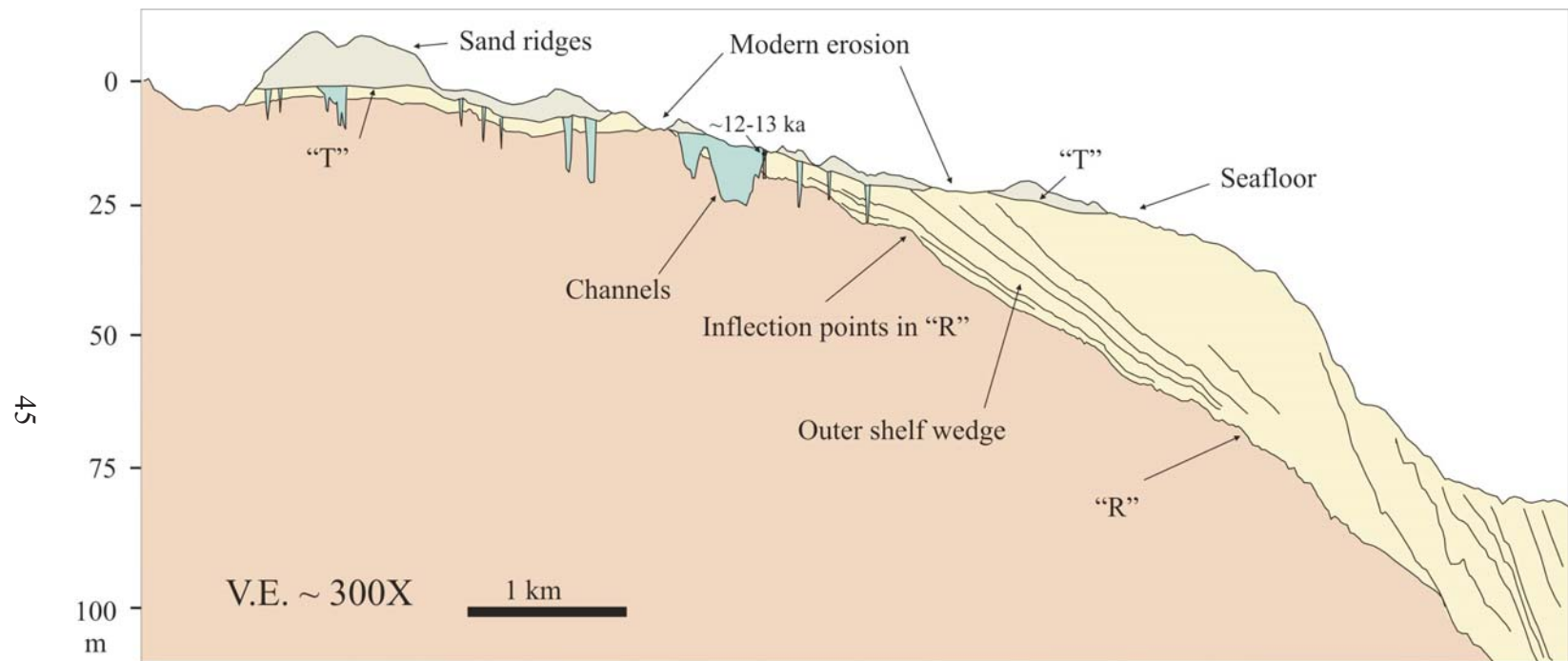
Figure 2.2:   Schematic cross-section showing late Quaternary stratigraphic of the New Jersey shelf (from Duncan et al., 2000). Age refers to backfilling of channels (Lagoe et al., 1997; Buck et al., 1999).

(Goff et al., 1999; Figure 2.2). Duncan et al. (2000) interpreted "T" as a transgressive ravinement surface, the result of shoreface erosion during the Holocene transgression.

Using swath maps, Goff et al. (1999, 2004) investigated the morphology of the seafloor on the outer New Jersey shelf since the last transgression. These include clusters of relict, oblique-to-flow sand ridges, ribbon-floored swales and erosion pits. They have concluded that modern erosion has significantly modified the shallow subsurface stratigraphic record (Figure 2.2).

METHODOLOGY

Data

This study is based primarily on seismic horizons interpreted using ~4300 km of deep-towed chirp seismic data collected aboard the R/V *Endeavor* in 2001 (cruise EN359) and 2002 (cruise EN370) (Figure 2.1). This chirp system is well-suited for imaging the shallow, complex latest Quaternary stratigraphy of the New Jersey shelf. The source emits swept-frequency signals (multiple pings/s) of 1-4 kHz and 1-15 kHz. The data provide vertical resolution of ~10 cm, horizontal resolution of ~2 m and image as deeply as 30 m sub-seafloor. My focus area has a profile track spacing of typically 200 m over ~600 km^2. These data resolve shallow stratigraphy much better than previously used surface-towed sources and receivers, often characterized by frequencies <100 Hz. Chirp processing steps included application of time varying gain to compensate for spherical divergence, smoothing the seafloor at 75-trace intervals, predictive deconvolution, application of a 1-3.5 kHz bandpass filter, zeroing returns prior to the seafloor arrival to remove multiples, and shifting each trace to the correct seafloor arrival time relative to the sea-surface. The 1-4 kHz data were also corrected for tidal fluctuations. A multiple

46

reflection off the bottom of the towfish, where both the source and receiver are located, creates a consistent artifact within each imaged section, but does not seriously impede interpretation.

To calibrate the chirp profiles, a limited number of sediment cores were collected aboard R/V *Knorr* (cruise KN168) in 2002 at three sites (Figure 2.1), using a heave-compensated version of a lake drilling system. These are the longest, highest-quality cores collected from this part of the margin and represent a unique set of samples to provide temporal, stratigraphic and environmental context for the seismic stratigraphic interpretation.

Interpretation methodology

Seismic mapping of observed incisions

Seismic mapping involved the following: (A) Observations of stratal reflection terminations (truncation, onlap) and of reflection configurations (i.e., acoustic facies) allowed us to identify meter-scale seismic units and their boundaries, e.g.., lenticular bodies interpreted as filled channels (Figure 2.3). Three-dimensional descriptions of the geometries of observed incisions, including vertical and lateral changes in seismic facies, interconnectedness, trend and dimensions, represent the main focus of this investigation. (B) Interpretation of shallowly buried channel systems was conducted with Geoquest® software. I recognized flanks of drainage systems as inclined surfaces that truncated underlying strata. I mapped basal surfaces as the generally consistent seismic transition from a transparent facies below to a chaotic facies above. (C) I used superposition of stratigraphic elements and bathymetric features where appropriate to interpret geological

47
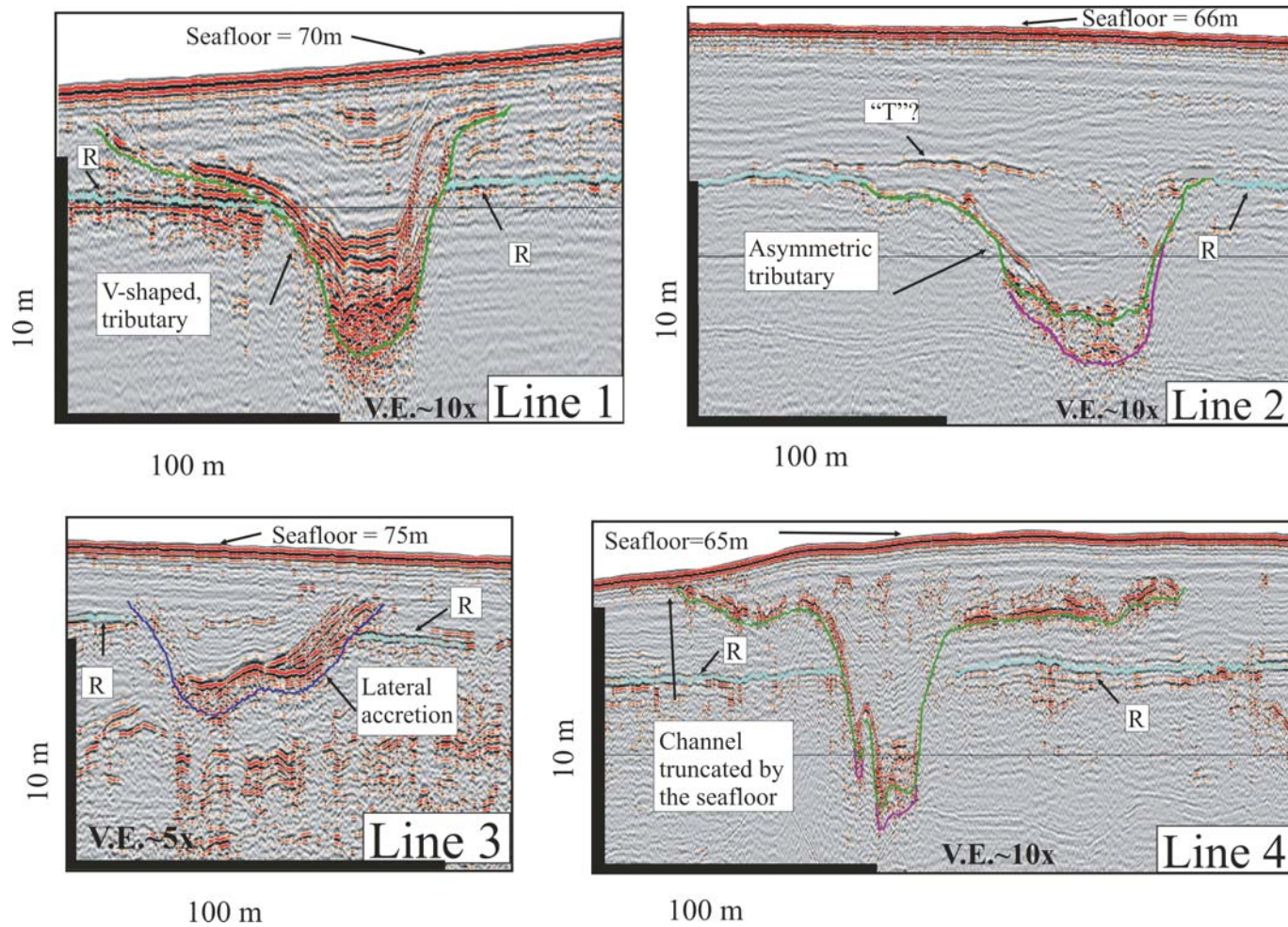
Figure 2.3:   Seismic cross-section of tributary channels from deep-towed chirp seismic profiles. Location in Figure 2.9.

48

Seafloor = 72m

R

10 m

Continuous, laminated seismic facies

Box-shaped, trunk channel- typical high w/d ratio

V.E.~10x Line 5

100 m

Seafloor = 70m

10 m

T?

Tributary merging with the main/trunk channel

Chaotic seismic facies- channel lag?

Trunk/main channel

Transparent seismic facies - fine-grain sediments?

V.E.~10x Line 6

100 m
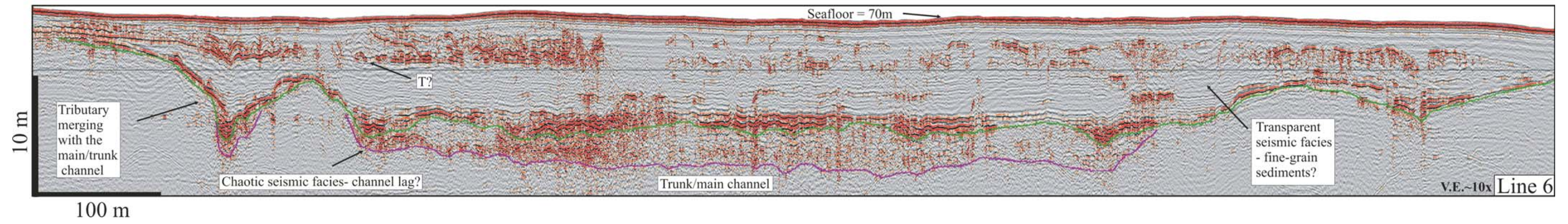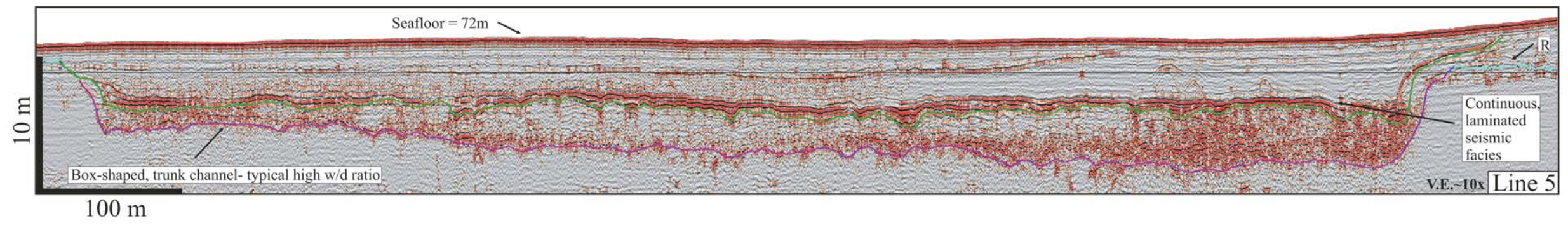
history. Observed crosscutting relationships among stratigraphic elements provided the relative timing of events, and the geometries of mapped features provided clues to the processes by which they are formed.

Interpolating mapped channels in space

Interpolation is required to infer 3-D stratigraphic architecture from 2-D seismic profiles. Unfortunately, standard interpolation techniques (Goff and Nordfjord, 2004) fail to maintain continuity along the traces of channel systems between profiles, and provide no means to define channel edges; both properties are critical for along-stream definition of morphologic parameters, such as width, depth and area. Goff and Nordfjord (2004) have developed a channel interpolation technique that relies on prior definition of a channel trace, easily defined by eye when track spacing is smaller than channel widths. The trace of each channel segment is used to define a coordinate system, with the "x"-axis representing distance along the channel trace and the "y"-axis distance perpendicular to the trace. Interpreted channel horizon points are transformed into this system; channel curvature is largely removed, edges are easily identified and channel continuity can be enforced by preferential interpolation in the along-channel direction. After interpolation within this coordinate system and clipping beyond channel edges, interpolated values are transformed back into a geographic reference frame. Where channels intersect, interpolations are merged by selecting the maximum depth. Figure 2.4 displays the interpreted channel system before and after interpolation.
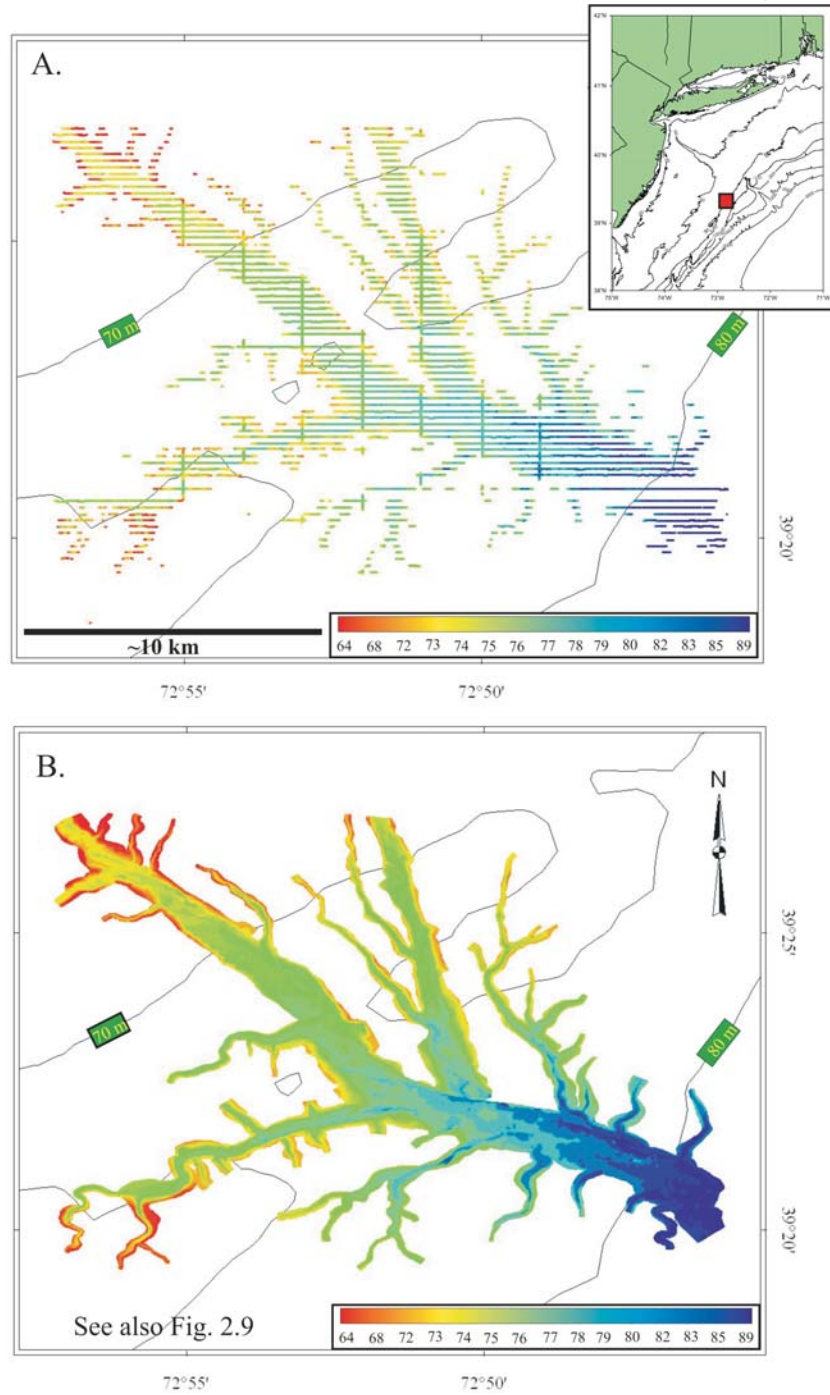
Figure 2.4: Maps of shallowly buried, dendritic drainage systems on the New Jersey outer shelf before (A) and after (B) interpolation (see also Goff and Nordfjord, 2005).

51

Quantitative geomorphologic analyses of mapped drainage systems

Morphometric analysis of paleo-channels can provide estimates of parameters needed to link channel morphology to paleo-hydrology, so-called discharge "retrodiction" (Rotnicki, 1983). This method involves applying empirically derived hydraulic equations for modern rivers and estuaries to estimate former discharges on the basis of preserved paleo-channel geometry, assuming uniformitarianism. The method sheds light on the channel-shaping discharge, which has physical limits in both fluvial and marginal marine environments, as well as sediment-transport potential (Baker, 1974; Costa, 1983; Williams, 1983).

I derive paleo-hydraulic variables from the morphology of observed and interpolated drainage networks on the New Jersey outer shelf (Figure 2.4). Cross-sections were measured perpendicular to each channel path at intervals of 5 m. Measured parameters included width, mean- and maximum depth, slope gradient, meander length, and path length (Figure 2.5). I also computed aspect (width/depth) ratios and cross-sectional areas (Figure 2.4) as a function of downstream distance. Channel sinuosity was computed from the following relationship: arc wavelength (λ) / meander length (L) (Leopold et al., 1964) (Figure 2.6).

The stratigraphy of drainage networks mapped on the New Jersey shelf suggests that they could be either fluvial or estuarine in origin. Therefore, I have looked to hydraulic geometry for additional paleoenvironmental constraints. For example, whereas bank-full discharge in rivers scales with watershed area upstream of a given channel cross-section (Knighton, 1998, and references therein), tidal discharge in estuaries scales instead with tidal-prism volume (Jarrett, 1976). Accordingly, channel-shaping discharge in rivers is the bank-full flood, whereas in coastal inlets and estuaries it is the peak spring

52
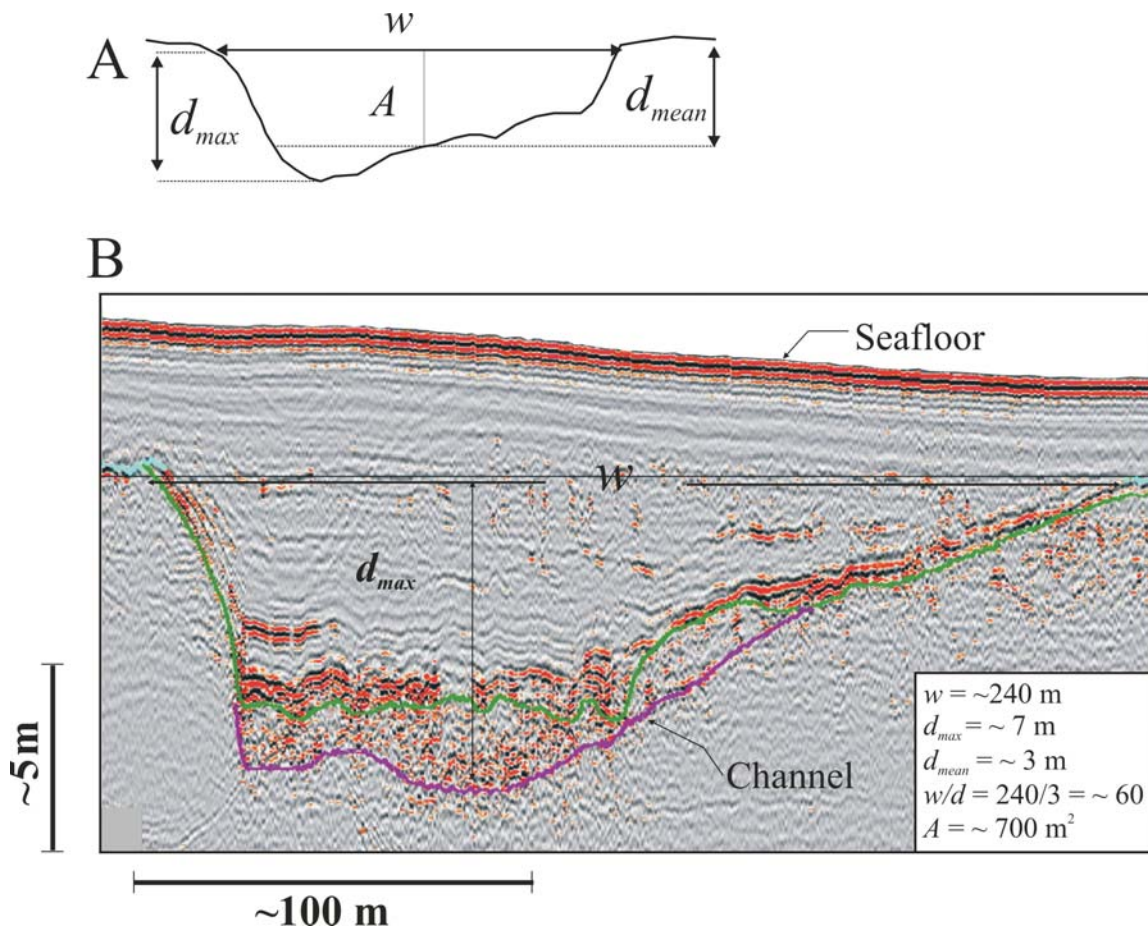
Figure 2.5: The geometry of a typical drainage cross-section and attendant hydraulic geometry relations. (A) Sketch showing relevant hydraulic parameters for this study, modified from Leopold et al. (1964). (B) Representative chirp profile of New Jersey outer shelf shallowly buried channels. Parameters are w = width, dmean = mean depth, dmax = maximum depth and A = cross-sectional area. Mean depth is cross-sectional area divided by channel width. See Figure 2.9 for location of seismic profile.

53

tide. In my analysis, I have considered both fluvial and estuarine origins as possible explanations for the hydraulic geometry of the buried channels on the New Jersey shelf; I therefore make comparisons with modern analogs developed for both marginal marine systems (Friedrichs, 1995; Rinaldo et al., 1999) and for medium-sized, mid-latitude streams (Dury, 1976; 1985; Figure 2.7).

I have estimated paleo-discharge for the presumed tidal systems on the basis of the power-law equation:

$$Q = A^{\alpha},$$
(1)

where Q is water discharge, A is cross-sectional area (Friedrichs, 1995). I have used a mean value of $\alpha = 0.96$ (Friedrichs, 1995) in my computations of paleo-discharge, after measuring channel cross-sectional areas (Figure 2.7). This exponent value is based on previous studies of worldwide modern tidal channels (Table 1 in Friedrichs, 1995).

I have used the following empirical equation from Dury (1976) for fluvial systems to calculate paleo-discharge:

$$Q = 0.83 A^{1.09},$$
(2)

Unlike other hydraulic equations (*e.g.,* Williams, 1978), Eq.(2) does not require knowing water-surface slope, which in the case of paleo-channels can only be loosely estimated from regional topographic grade. From computed paleo-discharges, I have obtained mean flow velocity from the continuity equation:
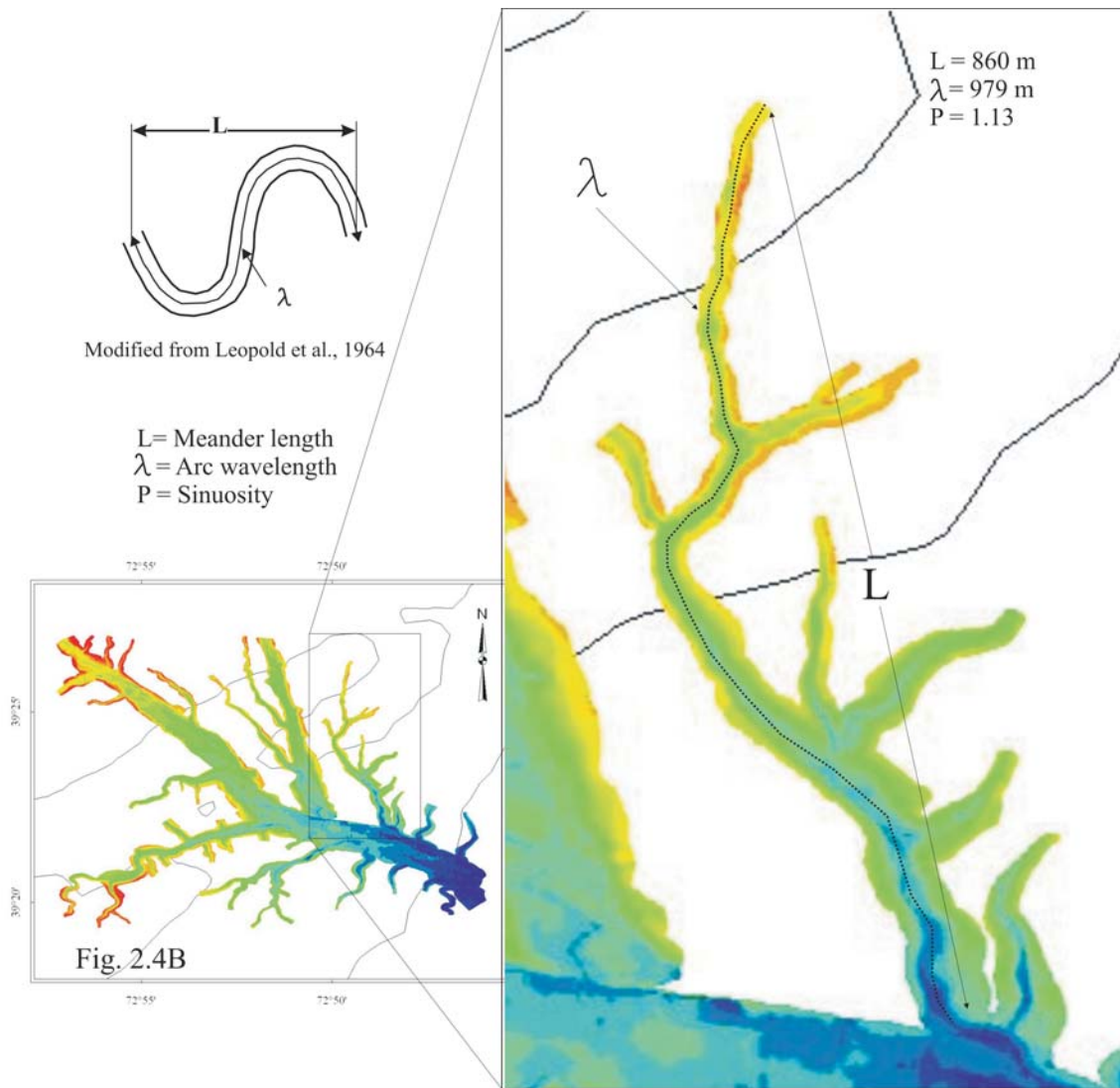
Figure 2.6: Channel pattern properties that were included in the morphometric analysis. Sinuosity is an important classification factor, which can facilitate the correlation of paleo-drainages with modern analogs.

Range of	min	max
width, see Fig. 2.5	< 100 m	> 1800 m
depth, see Fig.2.5	1 m	~25 m
straight length *	500 m	14 000 m
path length **	500 m	15 000 m
cross-sectional area	100 m2	> 4000 m2
gradient (degrees)	0.0001	0.01
width/depth ratios	35	> 500
sinuosity, see Fig. 2.6	1.01	1.2

* Straight length - distance of a straight line from the "head"
to end, see Fig. 2.6
** Path length- distance of thalweg within mapped channel,
see Fig. 2.6

Table 2.1:   Hydraulic parameter ranges of New Jersey mapped channels

$$Q = A v, \tag{3}$$

where v is mean velocity. I then estimated boundary shear stress for comparison with Shields' (1936) entrainment function, constraining the size of sediments that could be transported in the paleo-channel.

For both fluvial and marginal marine channels, I have used a quadratic stress law to estimate boundary shear stress, τ (Sternberg, 1972):

$$\tau = C_d \rho_f v^2, \tag{4}$$

where C_d is drag coefficient, ρ_f is fluid density (here $\rho_f = 1$ g/cm^3). I have used a generally accepted value of $C_d = 0.0025$, assuming that the computed value of v is representative ~100 cm above the bed and for fully rough, turbulent flow (Sternberg, 1972). Accordingly, the estimated boundary stress is, in all likelihood, a maximum approximation. I then compare these values to a modified Shield's curve (in Miller, et al., 1977) to find the maximum grain-size that the New Jersey system was able to transport.

River classification

The Rosgen (1994) classification system emphasized hydraulic parameters to define river systems (Figure 2.8). Based on parameters such as aspect ratios, sinuosity and channel gradient, Rosgen divided identified rivers into categories (Figure 2.8). His system primarily applies to rivers in equilibrium. That may not be true for the observed
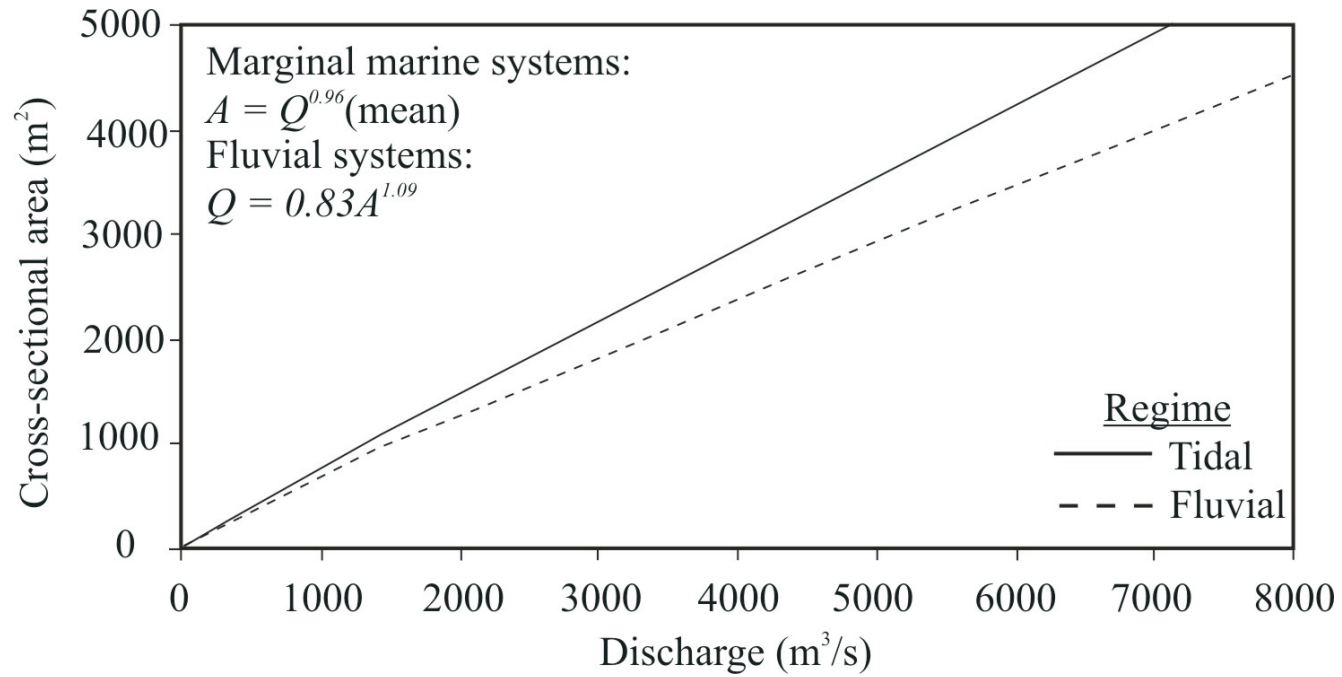
Figure 2.7: Curve displaying the best-fit relations for the regime equations (Friedrichs, 1995; Dury, 1976) utilized for this study.

New Jersey shelf system. However, measured and computed hydraulic variables of the interpreted shelf channel system can be directly compared with the morphological characteristics in Rosgen's (1994) classification. I compare aspect ratio, sinuosity and slope with his categories in order to infer paleo-drainage type for the New Jersey system.

ANALYSIS

Incised valley morphologies

My densely spaced, high resolution seismic profiles allow us to resolve subsurface channels in greater detail and over a wider range of spatial scales than previous imaging efforts on the New Jersey outer continental shelf (Figure 2.3). My mapping confirms that complex dendritic drainages are shallowly buried (generally <5 m) beneath the outer shelf (Davies et al., 1992; Davies and Austin, 1997; Buck et al., 1999; Duncan et al., 2000). I have mapped two extensive drainage systems within the 600 km^2 area in 70-90 m water depths (Figures 2.1, 2.4 and 2.9). Principal drainage axes for both drainages are oriented NW-SE, roughly perpendicular to regional bathymetric contours. Both systems exhibit a convergent branching pattern with cross-sectional areas that generally increase seaward, to a width of ~2 km for the northern drainage and ~1 km for the southern drainage. These channels exhibit ~25 m of elevation change over a distance of ~15 km (Figure 2.9), a seaward dip of 0.002˚.

These dendritic drainages are generally characterized by tributaries that join larger streams at acute angles (<90) (Knighton, 1998). The average junction angle of the main channel-major tributary intersections is ~60˚, ranging from 88˚ to ~25˚ (Figure 2.9). Both systems are composed of at least fourth-order channel segments, according to the Horton (1945) stream ordering scheme (Figure 2.9). However, I have examined that scheme and

60

	Aa+ >10%	A 4-10%	B 2-4%	C <2%	D <4%	DA <0.5%	E <2%	F <2%	G 2-4%
Dominant slope range									
Flood-prone area – – – – Bankfull stage ———									
Cross-section									
Plan View									
Stream Types	Aa+	A	B	C	D	DA	E	F	G
SIN.	< 1.2		> 1.2	> 1.4	< 1.1	1.1-1.6	> 1.5	> 1.4	> 1.2
W/D	< 12		> 12	> 12	> 40	< 40	< 12	> 12	< 12
SLOPE (degrees)	.04-.099		.02-.039	< .02	< .02	< .005	< .02	< .02	.02-.039
	Straight		Low sinuosity	Meandering	Braided	Anasto-mosed	Stable Meandering	Entrenched Meandering	Gullies
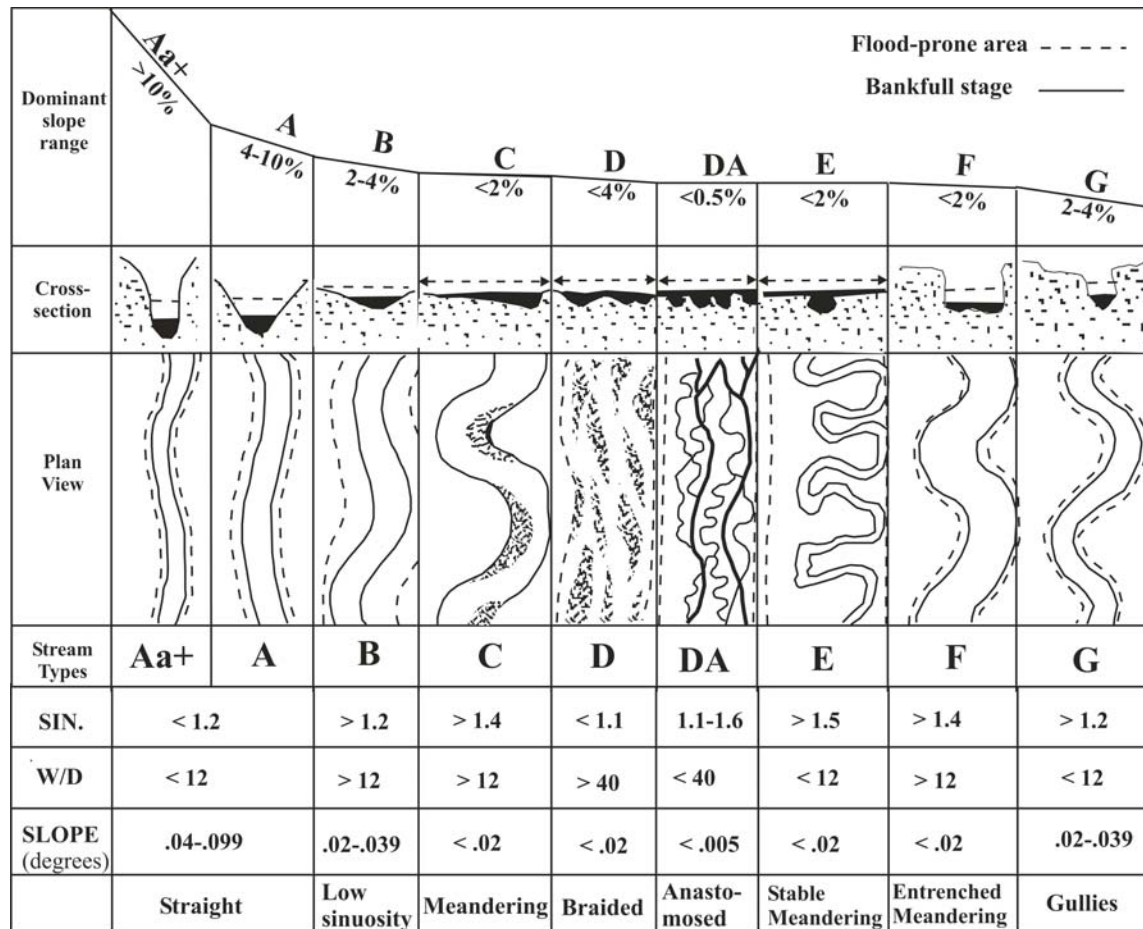
Figure 2.8: Classification of rivers, after Rosgen (1994), based on the morphological characteristics of river channels. The number of active channels, entrenchment, width-to-depth (aspect) ratio, sinuosity, channel slope and nature of bed material are the characteristics used to classify a river segment. The Rosgen system classifies only river reaches (a straight portion of the river) and not entire river systems. The characteristics of the mapped New Jersey channels are consistent with Type D/braided rivers.

find it inappropriate for the New Jersey systems, because the observed channels do not always bifurcate into equally significant channel branches (e.g., see deeper part of main channel in the northern system, Figure 2.9), and thus cannot be assigned the same order number.

The mapped dendritic systems differ in channel shapes, sizes, and the nature of channel-fill sediment compositions. Channel shapes have generally lenticular cross-sections. However, depth of basal scour and the extent of lateral accretion vary considerably, resulting in a broad spectrum of channel shapes, even within the same channel segment (Figure 2.10). Widths (w) range from hundreds of meters to kilometers and depths (d_{max}) range from a few meters to tens of meters. Generally, trunk (main) channels have box–like cross-sections, whereas tributary channels have V-shaped cross-sections (Figure 2.3). Cross-sections also range from symmetric to asymmetric; symmetrical, box-shaped geometries represent larger channels. Smaller channels are more triangular in cross section, with a less distinct, chaotic basal fill (Figure 2.10).

The "Channels" horizon is discontinuous, existing obviously only where channels themselves exist. On the 1-15 kHz chirp data, I could generally map the basal incision (Figure 2.11), a boundary identified based on a consistent contrast between a chaotic seismic facies above and more transparent response below. Within and between channel-fill parasequences, differences between stratified and chaotic reflection patterns are observed often. Figure 2.10 illustrates downstream and cross-sectional changes of seismic facies within a portion of the southern drainage.

Channel flanks are often steep (>50˚) and thus difficult to image, complicating the interpretation of channel geomorphology. Where observed, flanks are often a composite
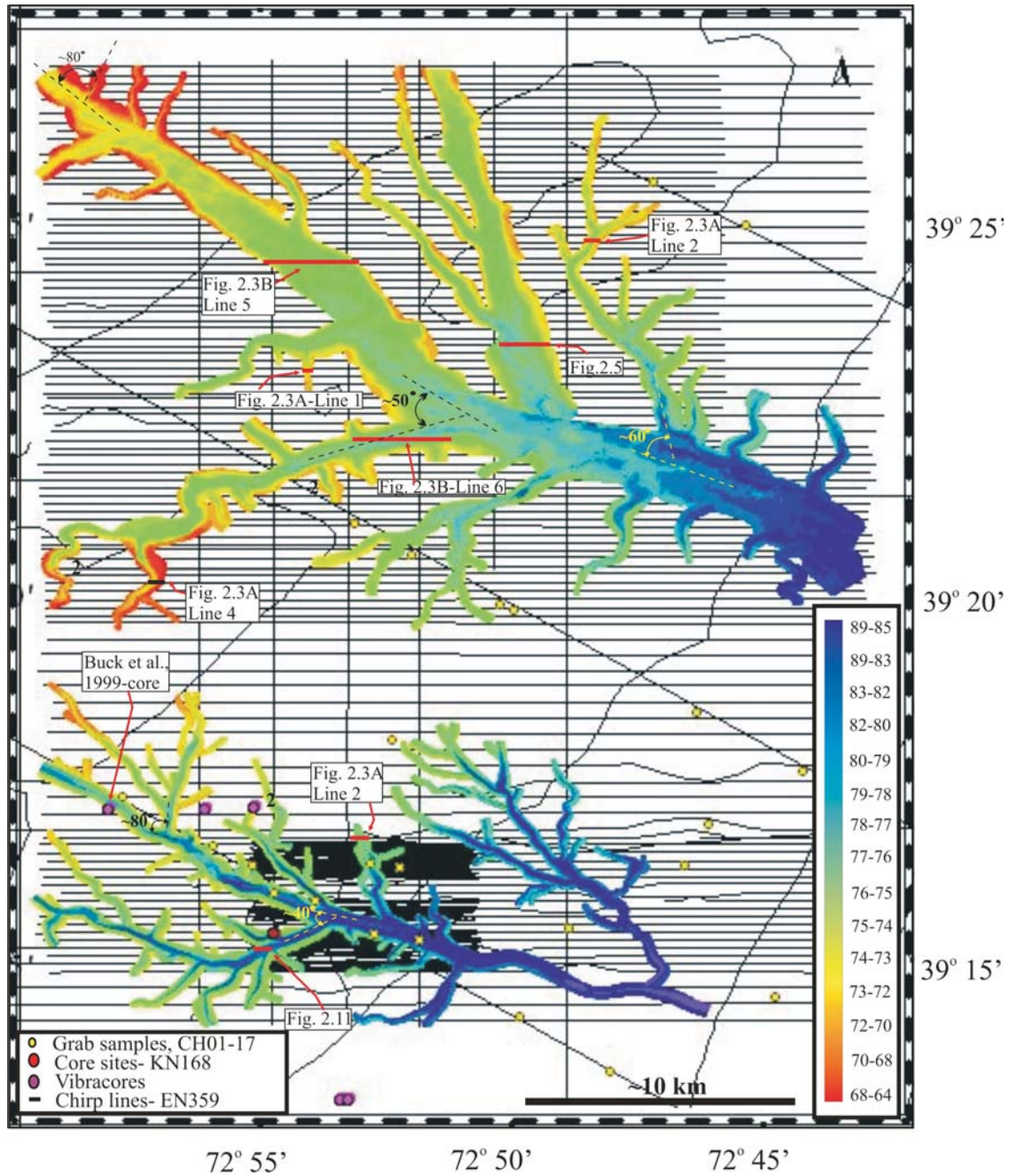
Figure 2.9: Two interpolated, shallowly-buried drainage systems mapped beneath the outer New Jersey continental shelf (see Figure 2.1 for location of focus area). These drainages exhibit dendritic patterns. Example tributary junction angles, which average ~60°, are shown. Red-highlighted lines indicate seismic profiles shown in Figure 2.3. Depth of channels in meters below sea level, based on a velocity of 1500 m/s.
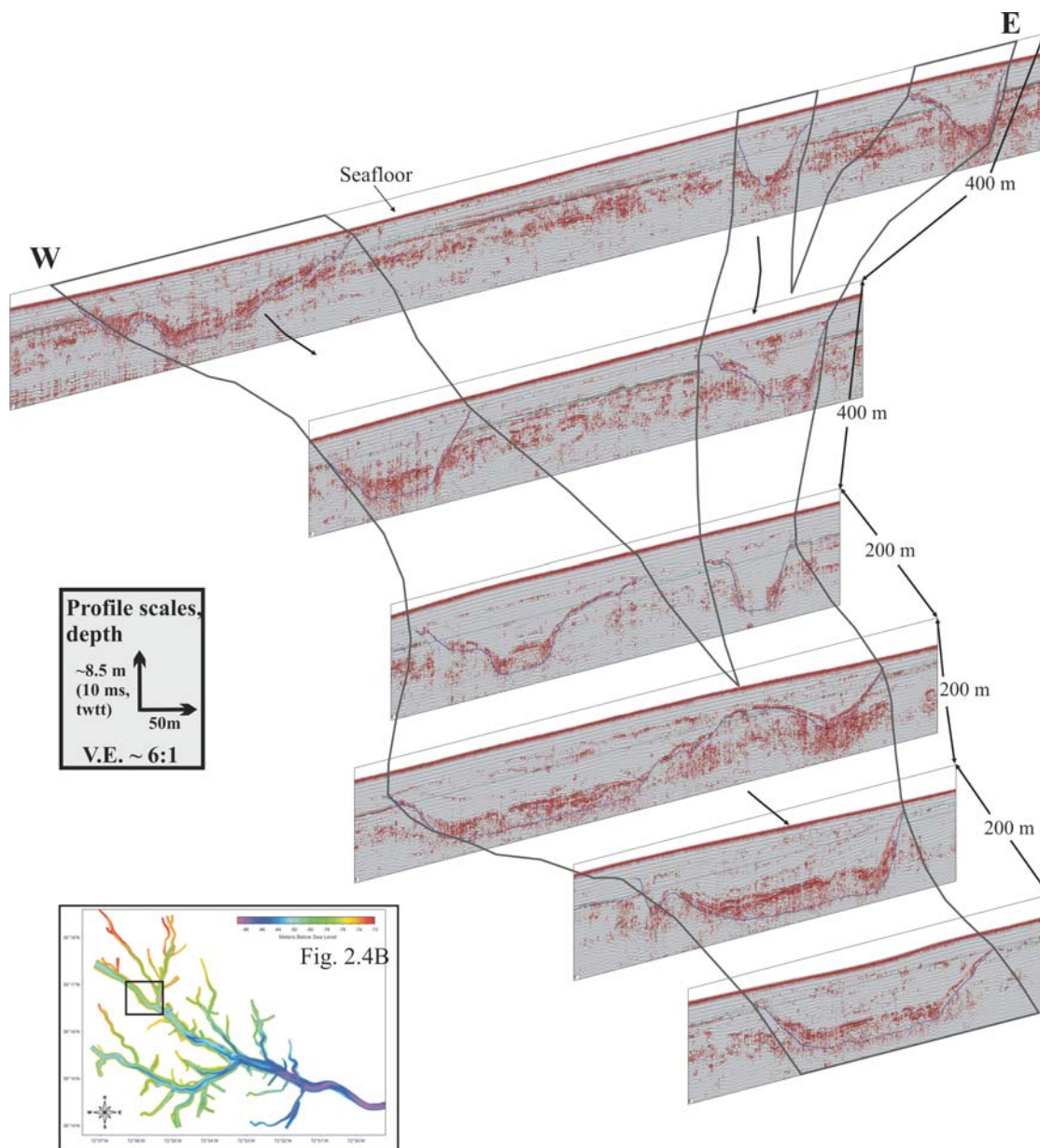
Figure 2.10: Fence diagram illustrating downstream trends of a portion of the southern channel system in the focus area (see Fig. 2.1). Width and depth clearly change over distances of hundreds of meters. Both flat-lying and chaotic reflections are imaged within channel fills. Channel-fills are often capped by the transgressive sand sheet.

surface; repetitive cut-and-fill can be observed. Older surfaces (incisions??) either pinch out along flanks or are more usually truncated by younger surfaces (Figure 2.11).

Channel-fill units are often capped with a thin sediment veneer. "T" truncates "Channels" and channel-fills, while forming the base of a surficial sand sheet that extends across much of the shelf and overlies these drainages (Goff et al., 1999; Duncan et al., 2000) (Figures 2.3 and 2.11). Such truncation prevents, in some cases, accurate estimations of channel widths and depths (see Figure 2.5).

Channel dimensions and paleo-flow estimates

Table 2.1 displays the range in hydraulic parameters calculated for the buried channels analyzed in this study. Histograms (Figure 2.12) show the distribution of hydraulic parameters, and demonstrate the dominance of smaller channels. The mapped channels widen and deepen seaward (Figure 2.9). Lower width/depth ratios generally correspond to smaller, v-shaped tributaries (lines 1-4, Figure 2.3), whereas higher width/depth ratios generally correspond to the larger, box-shaped trunk channels (lines 5-6, Figure 2.3).

Next, I correlated these morphological characteristics with channel types in the Rosgen (1994) classification scheme (Figure 2.8). Low sinuosities and gradients linked with high width/depth ratios typical of New Jersey channels are consistent with a D-type river, classified as a "braided" drainage system. However, I suspect that the original fluvial channels incising the New Jersey shelf were modified through transgressive erosion and deposition. High width/depth ratios (>50) are also characteristic of tidal systems; for example, width/depth ratios for the modern tidal Delaware River and estuary are 50–250 and 250–2500, respectively (Walsh, 2004).
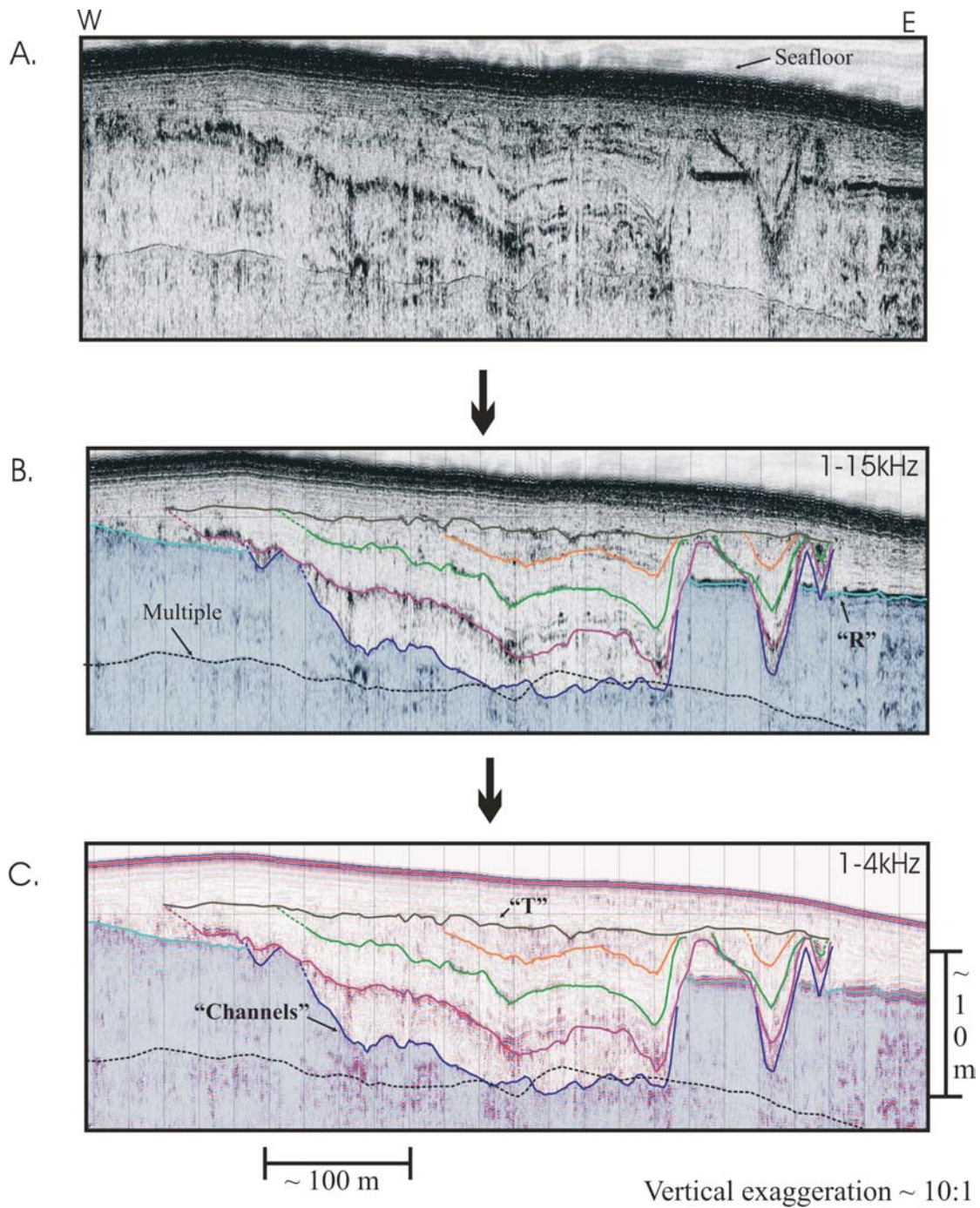
Figure 2.11: (A) Uninterpreted chirp profile at 1-15kHz, showing both basal surface and internal surfaces within channel fill. (B) Seismic horizon interpretation superimposed over the channel cross section shown in (A). (C) Seismic display of the same section as in (A) and (B), but acquired at 1-4 kHz. Profile is located in Figure 2.9.
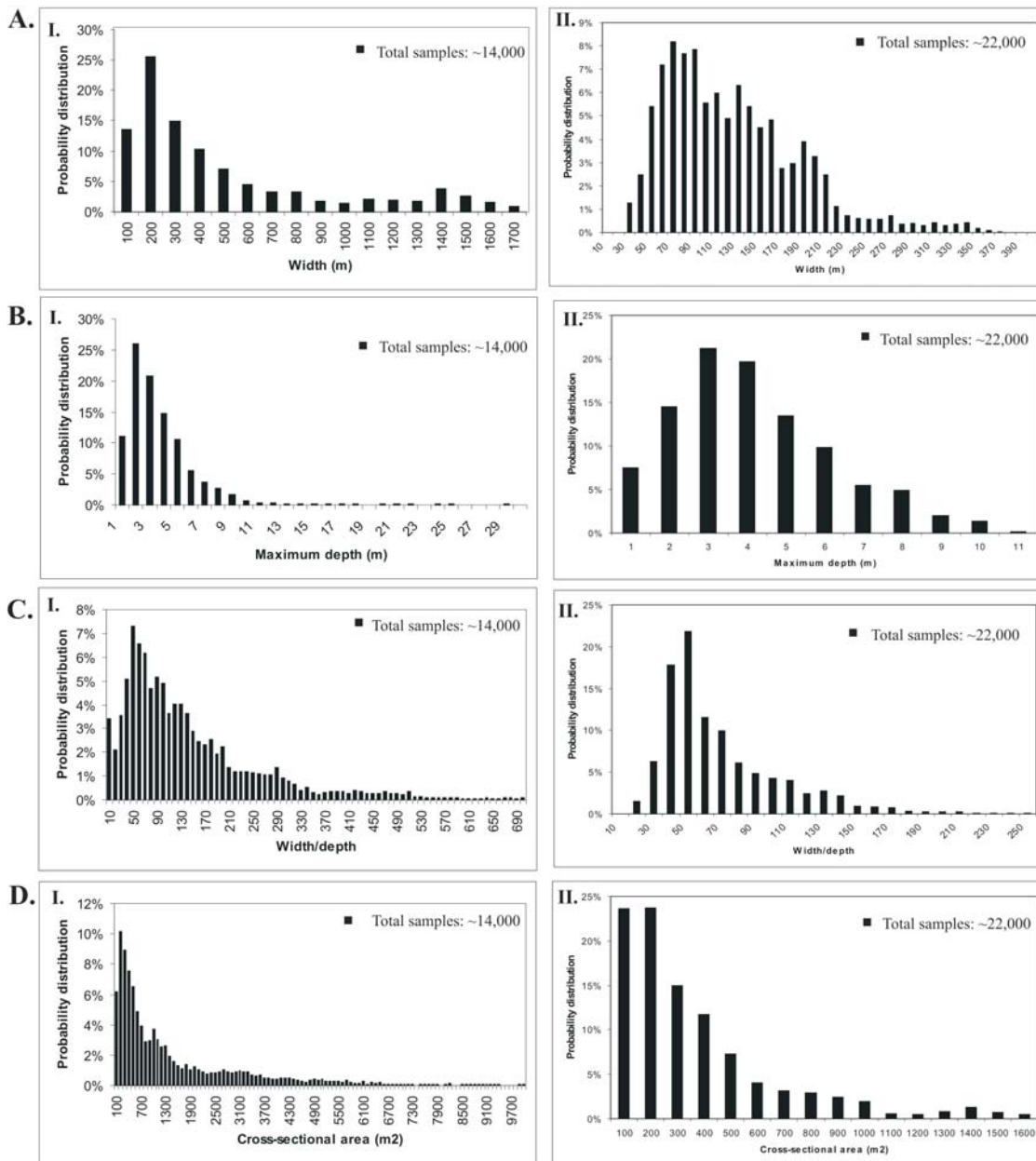
Figure 2.12: Histogram distributions of measured New Jersey buried channel dimensions for the northern network (I) and southern network (II) (Figure 2.9), including (A) width (m), (B) maximum depth (m), (C)width/depth ratios and (D) cross-sectional area (m^2) (See Figure 2.5 for criteria for parameters). Smaller channels dominate the distributions. Parameter values with the highest probabilities of occurrence are: 100-200 m channel widths, 3-5 m maximum depths, < 5000 m^2 area and width/depth ratios of 60-70.

On the basis of channel cross-sectional areas, and available hydraulic equations described above for marginal marine systems, maximum paleo-tidal discharges would have been from 120 to >5600 m^3/s, with corresponding channel-mean velocities of 1.0-1.5 m/s (Table 2.2). Maximum fluvial discharges would have ranged from 125 to >7000 m^3/s, with velocities of ~1.0-2.0 m/s (Table 2.2).

Bed shear stresses estimated from Eq. (4) for marginal marine systems range from 20 to 56 dynes/cm^2 (1 dynes/cm^2 = 0.1 Pascal), and for fluvial systems from 25 to 100 dynes/cm^2. These estimated stresses are sufficient to initiate transport of grains 2-8 mm in diameter (i.e., very coarse sand and fine gravel) as bedload, and finer-grained sediment in suspension. Retrodicted fluvial discharge and boundary shear stresses would have been sufficient to transport particles up to ~15 mm in diameter (gravel) as bedload.

DISCUSSION

Basic attributes of the New Jersey outer shelf channels

Development of dendritic drainage systems

Unconsolidated sediments of Coastal Plain alluvium are well suited for development of dendritic drainage systems: channels can form quickly in response to sea-level fall, and tributary systems can develop in a preferred downslope/seaward orientation without structural influence. Three lines of evidence indicate that the seismically observed channels were first formed by fluvial incision. First, they cut in many cases deeply into older Pleistocene units, below the "R" horizon. Coring beneath "R" sampled coarse, consolidated sands that would presumably be highly resistant to such erosion, implying significant energy. Second, the chaotic seismic facies commonly present at the

67

Paleo-hydraulic property	Tidal drainage systems	Fluvial drainage systems
Mean Discharge	120-5600 m^3/s	125-7000 m^3/s
Mean velocity	1.0-1.5 m/s	1.0-2.0 m/s
Boundary shear stress	20-56 dynes/cm^2	25-100 dynes/cm^2
Grain Size Diameter	2-8 mm	< 15 mm

Table 2.2:   Paleoflow estimates of our mapped New Jersey channels

base of channel fills is likely to represent gravel lags. My interpretation is supported by recent grab samples in the vicinity (Goff et al., 2005), which sampled rounded gravels >5 cm in diameter from what appears seismically to be the base of a recently eroded channel-fill. Third, the dendritic nature of these drainages is indicative of surface runoff and subaerial processes (e.g., Howard, 1971).

Previous modeling (Horton, 1945; Howard, 1971; Pelletier, 2003) has shown that the inclination of the surface upon which drainages develop significantly influences the texture of them, expressed as drainage density (total channel length/drainage area). Changes in relief of the Coastal Plain prior to channel entrenchment on the New Jersey shelf probably resulted in the subtle observed differences in channel lengths, junction angles of tributaries and sinuosities of the two mapped drainages (Figure 2.9). I have plotted gradients of mapped channels against their sinuosities; this relationship shows a general trend of decreasing maximum sinuosity with increasing gradient (Figure 2.13). Such a trend is consistent with previous studies. Schumm (1963), for example, established that channel sinuosity is dependent on river gradient.

Stream junction angles are another important morphologic property of drainage systems (Abrahams, 1984). These angles have been shown previously to be related to gradient relationships at tributary junctions, where steeper topography normally yields larger angles (Horton, 1945; Howard, 1971). For example, Howard (1971) has explained that if a tributary approaches the main stream at too small an angle, then flow in the tributary will be diverted toward the main stream in the vicinity of the junction by necessary erosion and aggradation. Plots of tributary junction angles from the New Jersey subsurface channels (see Figure 2.9) display some trends for such angles versus both gradient and channel length (Figure 2.14). Tributaries merging at >65˚ angles are shorter than ~5 km, while channel branches with >0.004˚ channel gradients are all correlated with
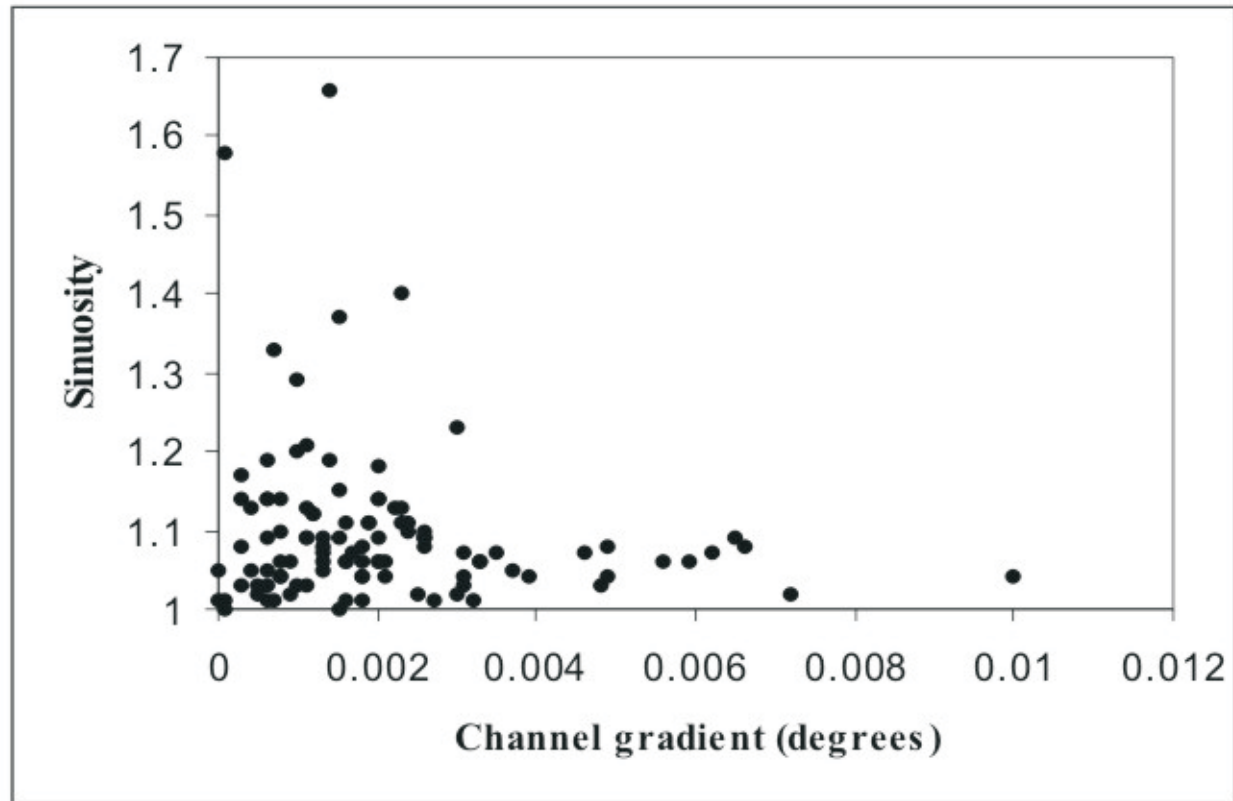
Figure 2.13: Relationship between sinuosity and gradient of channel segments mapped in the subsurface on the mid-to-outer New Jersey shelf. Sinuosity tends to decrease exponentially with increasing slope; sinuosities are generally low (see Table 2.1).

>65˚ junction angles (Figure 2.14). My results show general relationships between increasing junction angles and both increasing gradient and shortening of channel segments, both of which are consistent with modeling by Howard (1971), who also noted that larger channels tend to deflect toward the point of junction with tributaries. In the case of the northern drainage, the main thalweg indeed deflects towards the east, towards merging tributaries from the north (Figure 2.9).

Geomorphology of drainage systems

The observed variety in seismic geometries of buried channels on the New Jersey shelf suggests that latest Quaternary channelized flow occurred over a large range of spatial scales (Figure 2.3). The dominant controls on cross-sectional forms are discharge, the amount of bed-load transport and the geologic composition of the channel boundary, particularly as it relates to bank stability. I have also noted above that the observed channel morphology varies in response to variations of gradient and to tributary influences (Figures 2.13-2.14). Width and depth clearly respond to changing environmental conditions, although the rate and scale of such adjustments vary along the drainages (Figure 2.9). Previous work by Tuttle et al. (1966) has shown that older valleys are larger than young valleys, and that incisions become more box-shaped and less triangular with time, as observed seismically. They have also shown that the duration of channel existence is important, as a channel will tend to widen more quickly than it will deepen in unconsolidated Coastal Plain strata. This could lead to more typical rectangular cross-sections of main channels (Figure 2.3), which are likely the oldest features. Schumm (1993) has also suggested that considerable bank erosion takes place in cohesionless sediments, so that widening of the channel occurs while stream competence declines with time.
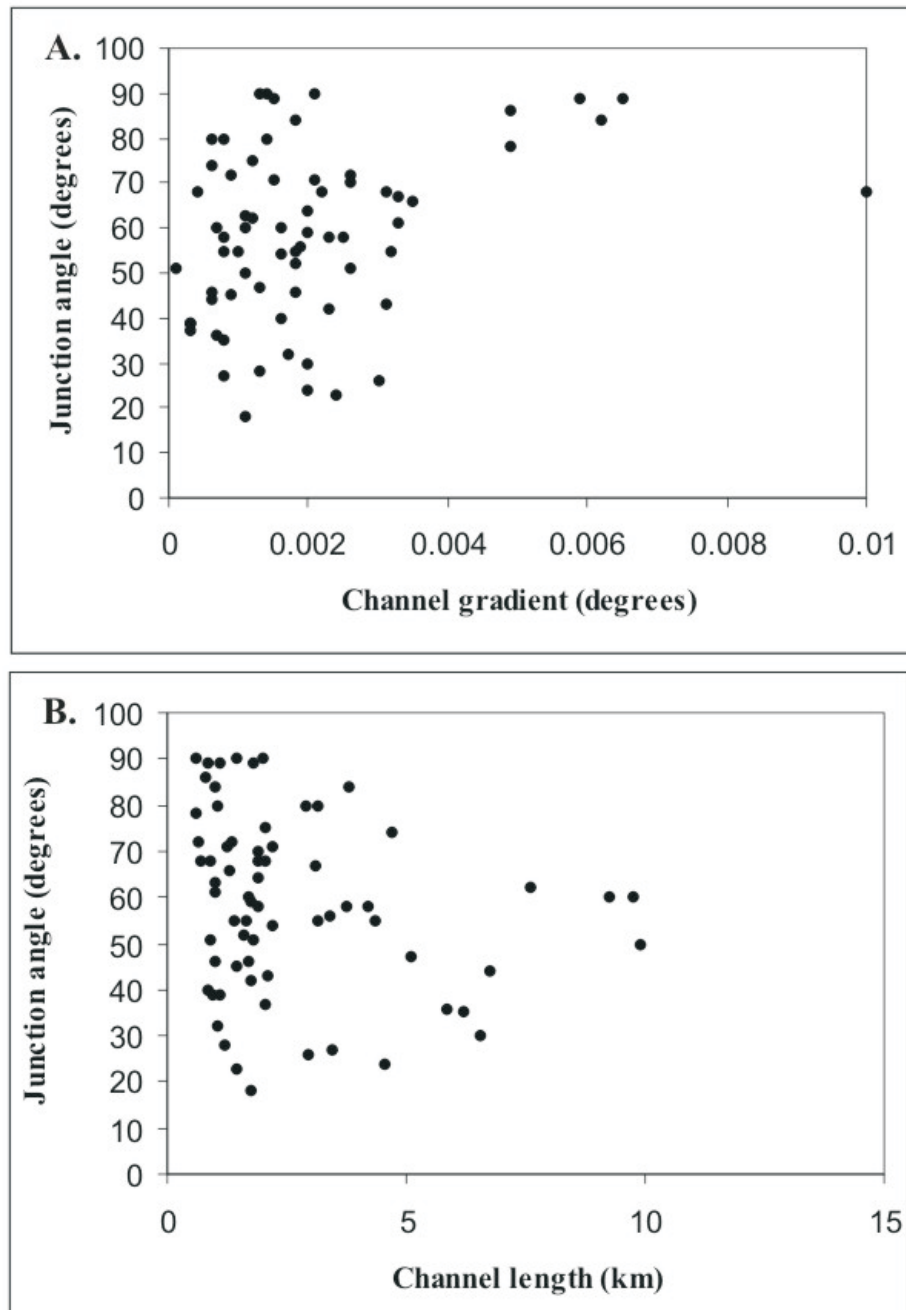
Figure 2.14: Junction angles of all tributaries (see Figure 2.9) plotted versus (A) gradient of the channels and (B) the length of each channel segment. In (A), the angles tend to increase for all the channel segment with increasing gradient. In (B), longer channel show the most consistent relationship with junction angle. There is little or no consistency at channel lengths < 3 km.

72

Width/depth ratios are generally high for the observed channels (Table 2.1), which suggests that they are bed-load channels with limited carrying capacities. I obtain higher aspect ratios for wide, shallow trunk channels (Figure 2.3), while lower ratios characterize tributary cross sections (Figure 2.3).

Sinuosities are generally very low (~1.1) for all mapped channel branches (Table 2.1, Figures 2.8, 2.9 and 2.13). Low-sinuosity channels tend to erode laterally and deposit intra-channel bars (Galloway and Hobday, 1996). These low sinuosities, combined with low slopes (<0.02º) and high width/depth ratios (Table 2.1), place these channels within a braided system classification (Figure 2.8). However, the overall morphology of the channel systems mapped beneath the New Jersey shelf does not appear braided in any way; these systems are dendritic and the thalwegs do not branch and reconnect (Figure 2.9).

Wood et al. (1993) has shown that the initial response of fluvial systems to a lowering of base level is vertical incision; in such youthful stages, river channels are typically of low sinuosity (Keller, 1972). However, there is a difference in this response for steeply and gently dipping shelves, when rivers attempt to adjust to lower base levels. Small shelf dips cause more gradual vertical incision, and more river energy is expended in lateral erosion, widening of the valley and in development of meanders (Wood et al., 1993). Shallow incised valleys are the result, characterized by high width/depth ratios and, ultimately, higher degrees of sinuosity as compared to those developed in steeper settings (e.g., type "C", Figure 2.8). New Jersey drainage networks should resemble such systems, but they do not. I speculate that the lack of sinuosity of the observed channels is a result of insufficient time to reach a state of equilibrium, perhaps because sea level transgressed too quickly after initial fluvial incision, drowning and filling these channel systems and effectively transforming them into estuaries.

Relating quantitative geomorphologic results to depositional environments

I suggest that the New Jersey channels were likely formed in a dynamic Coastal Plain setting landward of, but proximal to, the shoreline. Because these paleo-drainages formed within ~50 km of a very low-gradient shelf edge, they may even have been within the influence of tides during the LGM, and most certainly were quickly so influenced during the ensuing transgression. Accordingly, both tidal and fluvial forces must be considered when interpreting the channel paleo-hydrology and backfilling history. Therefore, I consider the two likeliest paleoenvironmental scenarios: marginal marine and fluvial hydrographic regimes.

Estimated paleo-flow values for the seismically mapped systems (Figure 2.9, Table 2.2) are consistent with medium-sized tidal creeks and estuaries of the modern Atlantic Coastal Plain (*e.g.,* Friedrichs, 1995). This is an environment where driving forces for sand–gravel transport are fairly low, at least within the upper reaches of these drainage systems. The mean paleo-flow estimates, 1.0-1.5 m/s, are within expected limits for tidal creeks of the sizes that the observed channels display, <2 km wide and <25 m deep (Figure 2.9). Lower values within this range compare well with flow conditions in modern tidal environments, and thus do not contraindicate a marginal marine paleoenvironment for the observed channel systems. Furthermore, estimated boundary shear stresses are high enough to transport particles up to several millimeters in diameter, which matches grain-sizes of a recently recovered channel-fill (Alexander et al., 2003; Nielson et al., 2003; Nordfjord et al., 2003).

Under a fluvial (non-tidal) assumption, paleo-flow estimates (Table 2.2) yield values too high for a lowland Coastal Plain setting. For example, U.S. Geological Survey records indicate typical peak-flows (1-yr recurrence interval) for the modern Delaware and Hudson rivers of 2000 m^3/s and 1500 m^3/s, respectively. This suggests that upland-

74

rivers will yield flow velocities slightly higher than 1.5 m/s, which is not expected for a gently dipping Coastal Plain drainage system. The estimated values (Table 2.2) therefore justify a marginal marine system instead. However, as previously noted, estimated paleo-flows are highly dependent on which power-law relationships are used, leading to some uncertainty in my retrodicted values. Boundary shear stresses calculated for fluvial systems are large enough to move sediment grains up to 15 mm in diameter; grains of this size are generally too coarse to be transported by small, non-tidal Coastal Plain rivers due to their low hydraulic gradients and competence.

However, if high flows prevailed during fluvial entrenchment, as could have been the case for short time periods when these channel systems were not in equilibrium, e.g., during meltwater pulses (see Uchupi et al., 2001; Fulthorpe and Austin, 2004), then transport of gravel as bedload may have been possible. This again implies quick transitions between formation, filling and final drowning of observed drainage systems.

Timing of the formation and filling of the New Jersey channels

The shallow preserved stratigraphy of the New Jersey continental shelf is geologically complex, a result of the onset of fairly high amplitude, rapid sea level changes during the Quaternary and abrupt spatial and temporal changes in environmental conditions during the last glacio-eustatic cycle (~120 ka). The full range of environments that exist in onshore and nearshore areas today (e.g., river valleys, marshes, estuaries, tidal creeks) were all likely to have been exposed subaerially for varying periods during the last lowstand half-cycle of eustatic sea level. Since the LGM ~20-22 ka, the New Jersey shelf has been progressively submerged. The modern seafloor does not reflect the shallow geology just beneath it (Austin et al., 1996; Goff et al., 1999).

75

Based on biostratigraphic results from a vibracore collected within channel fill sediments in ~76 m water depth (Figure 2.9), Buck et al. (1999) inferred a marginal-marine to inner-to-middle-shelf depositional environment during channel infilling. Another recent core within the focus area (Site 3, Figure 2.1) has found an iron-rich, oxidized thin sand layer corresponding to a seismic channel flank (Gulick et al., 2003; Nordfjord et al., 2003), confirming that channels mapped on the outer New Jersey shelf formed subaerially. These results, combined with prior inferences from geomorphologic and paleo-flow analyses presented in this paper, lead us to propose the following hypothesis for timing of formation and filling of the New Jersey buried channels (Figure 2.15).

(1) Fluvial incision would have begun as a response to rapid sea level fall, most likely associated with Wisconsinan glacial advance prior to the LGM (Figure 2.15A). However, channels could have been incised at any time during such subaerial exposure, and this could also have occurred post-LGM. For example, Fulthorpe and Austin (2004) have hypothesized that similar channels just to the south of the focus area formed just after major outflows (jökulhlaups) from breached glacial lakes in southern New England (*i.e.*, after ~14 kyr).

(2) Rapid erosion then occurred along low sinuosity channels. Flume studies by Pelletier (2003) demonstrate that fluvial erosion in a developing system is concentrated well upslope of base-level. Dendritic drainages on the New Jersey outer shelf may therefore have developed when the shoreline was seaward of the 90 m isobath (Figure 2.15A), the deepest point at which I have mapped these channels. Talling (1998), referring to a concept of erosion of a coastal prism put forward by Posamentier et al. (1992), has suggested that the inflection point of a coastal wedge is where fluvial entrenchment will begins as the shoreline regresses. Therefore, the shape of the paleo-

76
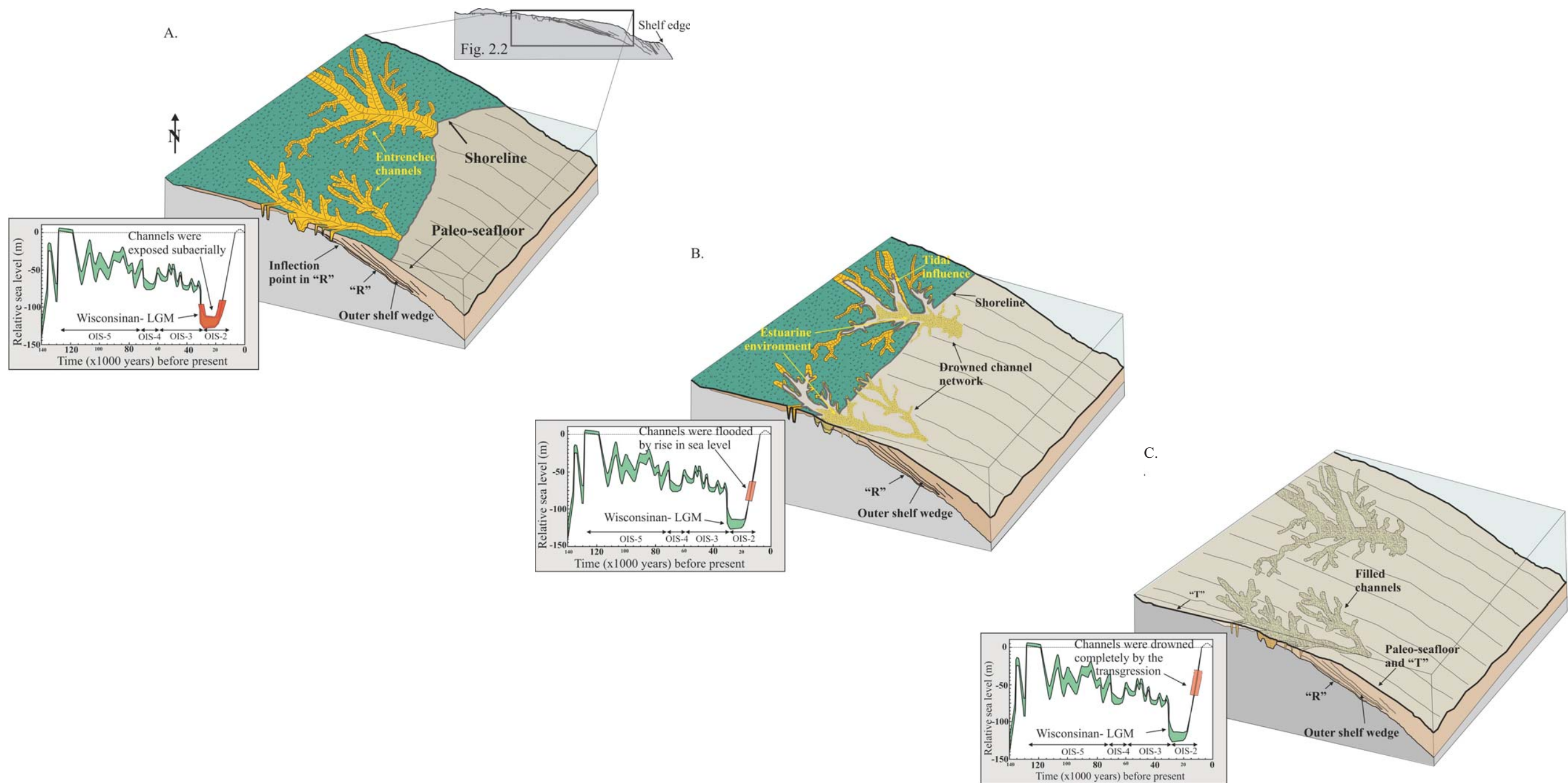
Figure 2.15: Model for the formation of buried channel networks on the outer New Jersey shelf. (A) Dendritic channel networks were incised during exposure of the shelf prior to and during the last glacial maximum. The shoreline was likely further basinward when these fluvial channels were entrenched. Record of the last glacio-eustatic cycle shows the possible emergence of the "Channels" horizon, based on present depths of shallowly buried channels on the New Jersey shelf (Lambeck and Chappel, 2001). (B) Rising sea-level flooded channel systems filling them with marginal marine environmental strata. In ~80 m water depth, the age of this fill is ~12-13 ka (Buck et al., 1999). (C) The channels eventually were submerged completely when sea level continued to rise. A transgressive ravinement truncated the channels and the sand sheet capped the fill; "T" is the resultant flat-lying surface in Figures 2.2, 2.10 and 2.14.

77

seafloor would primarily determine the pattern and depth of incision. Gulick et al. (2003) has documented such an inflection point in the underlying "R" reflector, marking a transition from a sub-horizontal reflector <9 m beneath the modern seafloor to eastward-dipping, ~0.5° farther seaward (Figure 2.15A). Based on this geometry, and the existence of an adjacent offlapping wedge deposited to the east, they have interpreted "R" as a paleo-seafloor and the inflection point as a seaward-migrating shelf-edge during sea level fall, ~35-22 ka (Figure 2.15, inset). Incision of "R" may have led to deposition of the outer shelf wedge seaward of the inflection. The resultant lobe of sediments in turn generated topography susceptible to channel incision and deposition of a second sediment wedge even farther seaward during the LGM (Butcher, 1990; Gulick et al., 2003).

(3) After the LGM, relative sea level began to rise, and incised valleys on the exposed shelf flooded, apparently with insufficient time to reach equilibrium, forming tidal rivers and estuaries (Figure 2.15B). Fluvial, non-marine sediments trapped in these estuaries were prevented from reaching the shelf edge. Since fluvial sediment supply on the New Jersey continental shelf has been commonly less than the rate of creation of accommodation space during sea-level rise, I believe that a drowned-valley estuary was generated at the seaward end of each incised valley (Figure 2.15B). As sea level continued to transgress the shelf, the incised valley estuarine fills were truncated by the retreating shoreface, producing the transgressive ravinement surface, reflector "T" or its equivalent (Figure 2.15C).

Comparing the New Jersey drainage systems with other shelf settings

The eustatic sea-level fall which accompanied the LGM resulted in the formation of incised valleys on continental shelves all over the world; subsequent marine flooding during the Holocene sea-level rise likely converted them all into estuaries, if accommodation space still remained. The channel systems that I have studied on the New

Jersey shelf may be typical of those produced in similar settings; i.e., on a gently dipping outer shelf with minimal subsidence and tectonically quiescent. Investigations of late Pleistocene-Holocene incised river valleys on other continental margins, for example the Mobile and the Trinity/Sabine incised valleys of the Mississippi-Alabama and east Texas shelf, respectively (Thomas and Anderson, 1994; Bartek et al., 2004), underscore the widespread importance of this study. In particular, the eastern part of the Mobile incised valley shows similarities to the incised valleys on the outer New Jersey shelf. However, the Mobile system is deeper and wider, likely due to slightly higher sediment supply. Other examples include the Cretaceous incised valleys observed in outcrop studies in the Viking Formation, Alberta (Posamentier and Allen, 1993) and the lowermost Pennsylvanian fluvial channels observed in subsurface log data in the Anadarko Basin (Bowen and Weimer, 2004). More generally, the quantitative seismic geomorphology methodology presented here provides a valuable procedure for gaining insight into the hydrographic regimes associated with the paleoenvironments prevailing when incised valleys were active, thereby creating a unique link among depositional architecture, modern processes, and the ancient rock record.

CONCLUSIONS & FUTURE WORK

My quantitative geomorphological study, based on high resolution seismic mapping of buried incised valley systems, seeks to link the hydrological properties of stratal surfaces of these valleys and their fills to specific mechanisms of their formation and evolution. This method involves applying empirically derived hydraulic equations for modern rivers and estuaries to estimate former discharges on the basis of preserved and seismically observable paleo-channel geometric parameters, such as width, depth, and cross-sectional area.

The New Jersey channels were likely formed originally as fluvial drainages, as evidenced by erosion into older Pleistocene strata and chaotic seismic units consistently observed at the bases of channel fills which I interpret as probable gravel lags. Stream junction angles are also consistent with a dendritic fluvial system. However, channel morphologies may have been subsequently and relatively quickly modified and partially overprinted by erosion and deposition imparted by tidal currents and waves. I have therefore estimated paleo-flow values using both fluvial and tidal assumptions. Mean paleo-flows under the tidal assumption fall within expectations for modern tidal creeks with the same channel sizes observed seismically. Estimated tidal shear stresses are sufficient to initiate sediment transport of coarse sand and fine gravel as bedload. The upper range of mean paleo-flow velocities under the fluvial assumption is generally considered too high for the presumed low hydraulic gradients of mapped channel systems on the New Jersey outer shelf. Retrodicted fluvial discharge and boundary shear stresses would have been sufficient to transport gravel as bedload, generally too coarse-grained to be transported by modern, sluggish Coastal Plain rivers. This may indicate either that flows were quite high when these systems were initially incised, perhaps due to the drop in sea level during the LGM, or that tidal energy modified the channel geometry and preserved fill deposits during subsequent transgression.

The high width/depth ratios combined with low sinuosities and slopes of the shallowly buried channels on the New Jersey outer shelf are consistent with braided, bed-load dominated river channels. However, because the seismically mapped channels do not appear braided in any way, I conclude that they did not have time to reach their preferred high sinuosity equilibrium state (e.g., type "C" in Figure 2.8). Relative sea level rise must have reduced the regional hydraulic gradient and transport competency of the observed paleo-drainages, which with the onset of tidal influences would have initiated

channel backfilling. Fluvial processes were rapidly replaced by tidal and estuarine processes prior to burial.

Future seismic and drilling investigations on the New Jersey continental shelf must further explore and sample filling facies within these incised channels; such facies provide much more detail concerning backfilling and drowning processes. Additional core information is crucial, in order to test my hypotheses with enhanced chronostratigraphic constraints, along with supplemental paleoenvironmental and paleo-bathymetric data.

Chapter 3: Seismic facies of incised valley-fills, New Jersey continental shelf: implications for erosion and preservation processes acting during latest Pleistocene/Holocene transgression

INTRODUCTION

Buried, dendritic, incised valley systems are common features of the Quaternary stratigraphy preserved on many continental shelves (e.g., Foyle and Oertel, 1997; Duncan et al., 2000; Warren and Bartek, 2002; Anderson et al., 2004). Formed originally by fluvial incision, they provide evidence of paleo-flow conditions during lowstands of relative sea-level (Nordfjord et al., 2005). Such valleys are also important because their geometry as coastal depressions provide accommodation space for lowstand and early transgressive sediments deposited in shelf environments (Vail et al., 1987; Van Wagoner et al., 1988; Posamentier and Allen, 1993), and also protect these sediments from removal by subsequent transgressive ravinement erosion (Swift and Thorne, 1991a, b). Consequently, remnants of valley-fill sediments are key elements for unraveling processes that create and preserve continental-margin sequence stratigraphy (Posamentier et al., 1988; Thorne, 1994).

Conceptual models have been introduced to explain the responses of the morphology and general sediment facies distribution of estuaries (Dalrymple et al., 1992; Zaitlin et al., 1994) to environmental forcing; e.g., drowning as a result of rising sea level, fluctuations in sediment supply and attendant physiographic changes. These models provide a basis for comparison of estuarine valley systems in different parts of the world. They divide valley-fills into: (1) a landward zone, dominated by riverine sedimentation (e.g., bayhead deltas or straight tidal and fluvial channels), (2) a seaward zone, dominated

by wave and/or tidal processes (e.g., estuary mouth complex), and (3) an intermediate zone of mixed energy (e.g., muddy central basin deposits).

An idealized valley-fill succession resulting from steady sea-level rise and continuous sediment supply will incorporate at least three transgressive surfaces within and external to the estuarine bay. The *bay flooding surface* forms by initial flooding (Nummedal and Swift, 1987), and separates underlying fluvial deposits from overlying basal estuarine/tidal deposits. Ensuing erosion by tidal currents in inlets or channels creates a *tidal ravinement* surface (sensu Zaitlin et al., 1994), which erodes underlying deposits confined within the seaward part of the incised valley system (Allen, 1991). At the same time as the tidal ravinement forms in or near the mouth of the paleovalley, a bayhead channel diastem is produced locally in the inner part of the estuary by progradation of a bayhead delta (e.g., Ashley and Sheridan, 1994). Finally, a more extensive *wave ravinement surface* is produced by landward retreat of the shoreface (Swift 1968) that marks the top of the estuarine deposits. This surface may remove by wave erosion a significant portion of the flood-tidal delta deposits and possibly some central basin facies (Ashley and Sheridan, 1994). All of these transgressive surfaces are diachronous, and could become amalgamated with a preserved sequence boundary associated with the transgression. These ravinements are all bounding parasequences (Swift et al., 1991); however, they are mainly produced by autocyclic processes controlled by the preexisting topography.

Over the last decade applications of very high-resolution seismic profiling methods to shelf environments (e.g., Reynaud et al., 1999; Duncan et al., 2000) provide new insights into 3D geometries of incised-valley fill deposits in the shallow subsurface. Geometry and juxtaposition of the seismic facies units which fill these valleys are keys to how these valleys responded geologically to transgression. This Chapter summarizes

sequence stratigraphic analyses of dense 2D and pseudo-3D deep-towed chirp seismic (1-4 kHz and 1-15 kHz) profiles collected over preserved valley-fill sequences now shallowly buried beneath the middle and outer New Jersey shelf (Figure 3.1). Incised valleys off New Jersey, previously recognized using more sparse and lower frequency seismic data (e.g., Davies et al., 1992; Austin et al., 1996), are believed to have formed as riverine systems during shelf exposure accompanying the Last Glacial Maximum (LGM) at ~22 ka, then subsequently filled and modified during early stages of the latest Pleistocene/Holocene transgression ~15-12 ka (Davies et al., 1992; Duncan et al., 2000; Nordfjord et al., 2005).

The New Jersey shelf (Figure 3.1) today is quiescent, receiving little sediment. Therefore, this shelf constitutes an excellent setting to study erosion and preservation of sedimentary strata in a range of accommodation-dominated marginal-marine environments. Subsidence on this margin has been very low throughout the Neogene and Quaternary (Greenlee et al., 1988). Therefore, eustatic change has been the prevalent sedimentologic force during formation, filling and modification of the valley examined in this paper. Although incised valley-fills on the continental shelf comprise only a small portion of this continental margin's deposits, they are likely to be the only preserved geological record of the early stages of the most recent sea-level rise.

Using the new data, I describe and map the 3D distribution of seismic facies within New Jersey incised valley systems (Figure 3.1). Detailed facies mapping enhances existing sequence stratigraphic models of incised valley fills. Next, I compare these seismic facies with a tripartite zonation models developed for wave- and tide-dominated estuaries (Dalrymple et al., 1992; Allen and Posamentier, 1993; Zaitlin et al., 1994). Finally, I compare my observed facies architecture to that of other selected incised valley systems, both recent and ancient, in order to determine the extent to which my

Figure 3.1: Location of deep-towed chirp seismic profiles (solid lines) collected in 2001 aboard R/V Endeavor (EN359), superimposed on NOAA's bathymetry merged with STRATAFORM swath mapping (Goff et al. 1999) of the New Jersey middle and outer continental shelf. My interpretation of part of these profiles is shown. Location of the area of study is identified on a 3-D image (inset, upper left) of the New York bight region, which is from NOAA's Ocean Explorer (http://oceanexplorer.noaa.gov/). The inset to the right enlarges the mapped dendritic incised valley systems (visual differences between the enlarged and original version results from pixel size and resolution) (Nordfjord et al., 2005); locations of figures presented later are indicated. Sites 1-3 identify sites that were cored with the DOSECC AHC-800 drilling system aboard R/V Knorr (KN168) in fall 2002. Contours are in meter below present sea-level.
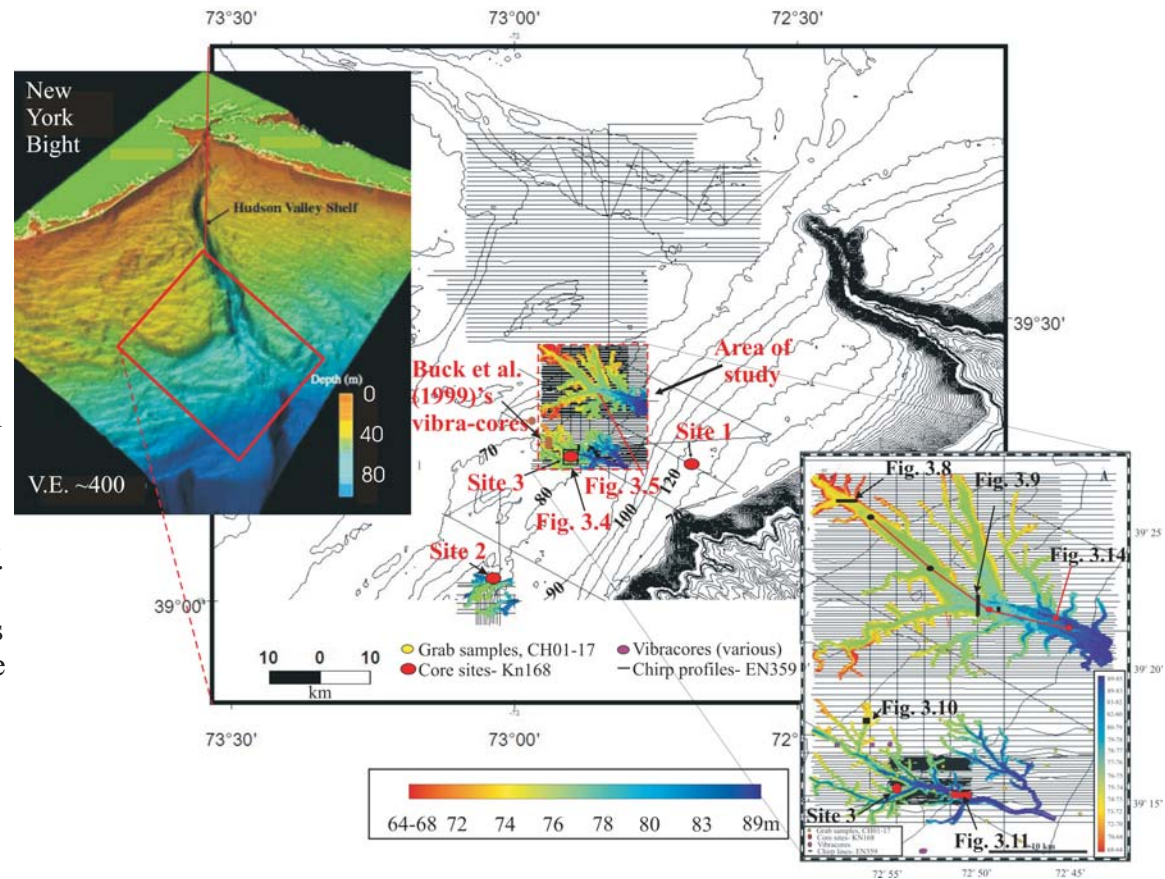
85

evolutionary model for the New Jersey outer shelf can be generally applied.

GEOLOGICAL SETTING

General physiography

The New Jersey outer shelf is part of the east coast U.S. margin (Figure 3.1), a mature, passive continental platform presently characterized by low subsidence rates and negligible alluvial sediment influx (Milliman and Emery, 1968; Greenlee et al., 1988; Duncan et al., 2000). This part of the shelf is 120-150 km wide and very gently sloping seaward (<0.001°) (Figure 3.1). The modern hydrodynamic regime includes a tidal range of 1-2 m, mean significant wave height of ~1 m (e.g., Carey et al., 1998) and generally southwest-directed currents (e.g., Vincent et al., 1981). Periglacial conditions in a storm-dominated environment have prevailed on this shelf since the Last Glacial Maximum (LGM) ~22 ka.

Latest Pleistocene-Holocene stratigraphy of the New Jersey shelf

Late Quaternary seismic stratigraphic horizons and intervening sequences beneath the New Jersey middle-outer continental shelf have been summarized by Duncan et al. (2000), Nordfjord et al. (2005) and Gulick et al. (2005), and include (Figure 3.2):

(1) R- horizon and (2) Outer-shelf sediment veneer and shelf-edge wedges: The R-reflector, recognized throughout this region, was originally interpreted as a subaerial exposure surface formed during the last lowstand (Milliman et al., 1990; Sheridan et al., 2000). Duncan et al. (2000) re-interpreted the R-horizon as a combined subaerial and marine unconformity that formed diachronously across a sediment-starved shelf. Based on sparse chronological control, R-horizon formed from 47-33 ka (Duncan et al., 2000;

86
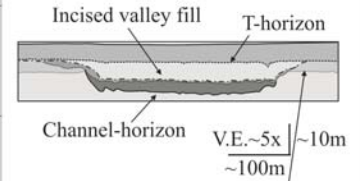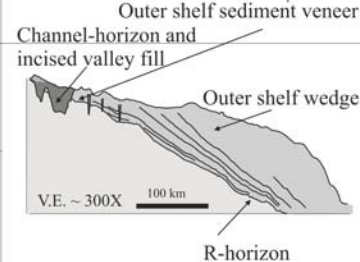
Stratigraphic Horizons/ Depositional Units	Characteristics	Stratigraphic and Depositional Interpretation	Age Constaints	References	Schematic Cross-Sections
(6) Holocene sand sheet	Oblique-to-flow sand ridges, modified by later erosion	Shelfal deposition and erosion during transgression and highstand	Last transgression, <10 ka	Goff et al., 1999; Duncan et al., 2000; Goff et al., 2004	
(5) T-horizon	Variable amplitude, caps and truncates channels	Transgressive, ravinement, formed by shore-face erosion	~ 12-10 ka	Duncan et al., 2000; Goff et al., 2005; Nordfjord et al, 2005	
(4) Incised valley fills	Basal chaotic seismic facies, overlain by more transparent facies	Backfill during the last transgression, drowned river estuary	~15-12 ka	Davies et al., 1992; Buck et al., 1999; Duncan et al., 2000; Nordfjord et al., 2005	
(3) Channel-horizon	Dendritic, box-to v-shaped incisions	Incisions during shelfal exposure associated with last lowstand	~25-15 ka	Davies et al., 1992; Buck et al., 1999; Duncan et al., 2000; Nordfjord et al., 2005;	
(2) Outer shelf wedge and sediment veneer	Muddy, laminated, wedge-shaped, downlapping	Marine, progradational delta	~33-22 ka	Milliman et al., 1990; Davies et al., 1992; Sheridan et al., 2000; Gulick et al., 2005	
(1) R-horizon	Prominent, regional reflector, base of outer shelf wedge	Subaerial and marine uncon-formity, diachronous	~47-33 ka	Milliman et al., 1990; Davies et al., 1992; Sheridan et al., 2000; Gulick et al., 2005	

Figure 3.2:   Principal late Quaternary seismic stratigraphic horizons and intervening sequences beneath the outer New Jersey shelf (modified from Duncan et al. 2000).

Alexander et al., 2003; Gulick et al., 2005). On the outer shelf, the R-horizon is sequentially overlain by an outer-shelf sediment veneer and two regressive sediment wedges (i.e., formed during a sea level fall), the outer-shelf and deep-shelf wedge (Gulick et al., 2005) These seaward prograding wedges were deposited ~33-22 ka (Figure 3.2; Alexander et al., 2003; Gulick et al., 2005).

(3) Channels-horizon, defining incised valley systems and (4) related incised valley fills: Davies et al. (1992) identified the Channels-horizon as a complex incision surface that eroded the outer-shelf wedge and the R-horizon (Figure 3.2). Duncan et al. (2000) mapped these incisions over a wider area (>5000 km^2). A vibracore through ~3 m of preserved incised valley-fill sediments sampled multiple inner-to-middle shelf to marginal-marine benthic foraminifera faunal intervals, implying at least three subtle (<10 m?) base-level fluctuations within that incised valley (Buck et al., 1999). An AMS ^{14}C age of 12,300 ± 450 yrs was also derived from this fill (Lagoe et al., 1997; Buck et al., 1999), consistent with the hypothesis that this valley was incised sometime during the last lowstand (~25-15.7 ka) and then filled during the subsequent transgression (Davies et al., 1992).

(5) T-horizon: Duncan et al. (2000) identified another, shallower variable-amplitude seismic reflection, which they named the T-horizon, that always truncates the Channel-horizon where both can be observed (Figure 3.2). Where it is observed, the T-horizon is sub-parallel to the seafloor, capping incised valley fills. Duncan et al. (2000) interpreted this reflector as a ravinement surface, formed as a result of progressive shoreface erosion during the Holocene transgression.

(6) Post-T sand sheet: The surficial sand sheet has been deposited upon the wave ravinement surface, T-horizon, in a landward migrating shoreface environment (Goff et al., 1999). This unit is composed largely of oblique sand ridges, formed first at the

shoreface and then modified during transgression through mid-shelf water depths by continued reworking (Figure 3.2; Swift et al. 1972; Goff et al., 2005). Analyses of swath bathymetry, backscatter, grab samples and chirp seismic data on the outer New Jersey shelf all suggest that sand ridges in outer-shelf water depths are now moribund, although erosion has significantly modified the surficial sand sheet since its initial formation (Goff et al., 2005).

METHODOLOGY

Data

High-resolution, 1-4 kHz and 1-15 kHz seismic reflection records were obtained using a deep-towed, chirp sonar aboard R/V *Endeavor* in 2001. The seismic profiles used for this study were collected at profile spacings ranging from 50 to 400 m (typically 200 m) over a region of ~600 km^2 (Figure 3.1). The data provide vertical resolution of ~10 cm, horizontal resolution of ~2 m and image to depths up to 30 m sub-seafloor. Processing steps included (1) application of time varying gain to compensate for spherical divergence, (2) smoothing the seafloor at 75 trace (~35 m) intervals, (3) predictive deconvolution to reduce short-period multiples and remove the source signature, (4) application of a 1-3.5 kHz bandpass filter to the 1-4 kHz data to reduce noise, (5) zeroing returns prior to the seafloor arrival to remove ringing in the water column, and (6) numerically shifting each record to the correct seafloor arrival time based on measurements of direct-wave, ghost and seafloor reflections, along with the local tidal record. Accurate ship positioning of ~1-2 m was obtained by differential global positioning system (DGPS), and chirp fish location relative to the ship was determined by a short-baseline acoustic positioning system. Because the chirp system was towed 10-15

89

m off the seafloor, ghost reflections (fish-seasurface-fish) generally do not interfere with primary reflections in the upper 15-20 m sub-seafloor.

Depths (below mean sea level) to mapped acoustic reflectors and thicknesses of inferred intervening sedimentary units were determined using an assumed average compressional-wave velocity of 1500 m/s in water and 1750 m/s in the sediments. This sediment velocity is consistent with recent velocity measurements at the seafloor on the New Jersey outer shelf (Goff et al., 2004).

Lithostratigraphic analysis

Three sites were drilled in this area in 2002 (Figure 3.1) using the DOSECC AHC-800 coring system (Nielson et al., 2003) deployed from R/V *Knorr*. A total of ~26 m of core was collected, with ~80% average recovery for all sites. Site 3 was the only site located within one of the mapped incised valleys (Figure 3.1). Penetration at this site was 7.5 m sub-seafloor, through part of the incised valley fill, valley flank and the R- horizon (Figure 3.3). Physical properties measurements, i.e., saturated bulk density, compressional wave velocity, and magnetic susceptibility of the cored sediments, were obtained on whole-round, 1.5 m long sections using a GeoTek multisensor core logger (MST). These physical properties data facilitated correlation of the seismic data with cored lithology. Sampling of these cores provided material for grain size analysis and chronostratigraphy. Alexander et al. (2005) are attempting to unravel patterns of deposition and erosion using detailed analyses of sediment grain size and composition, radiocarbon age determinations and foraminiferal micropaleontology.

Interpretation of depositional environments from seismic data requires correlating the character of the seismic reflections with sampled sedimentary facies. To do this, I generated synthetic seismograms from the Multi Sensor Track (MST) sonic and density
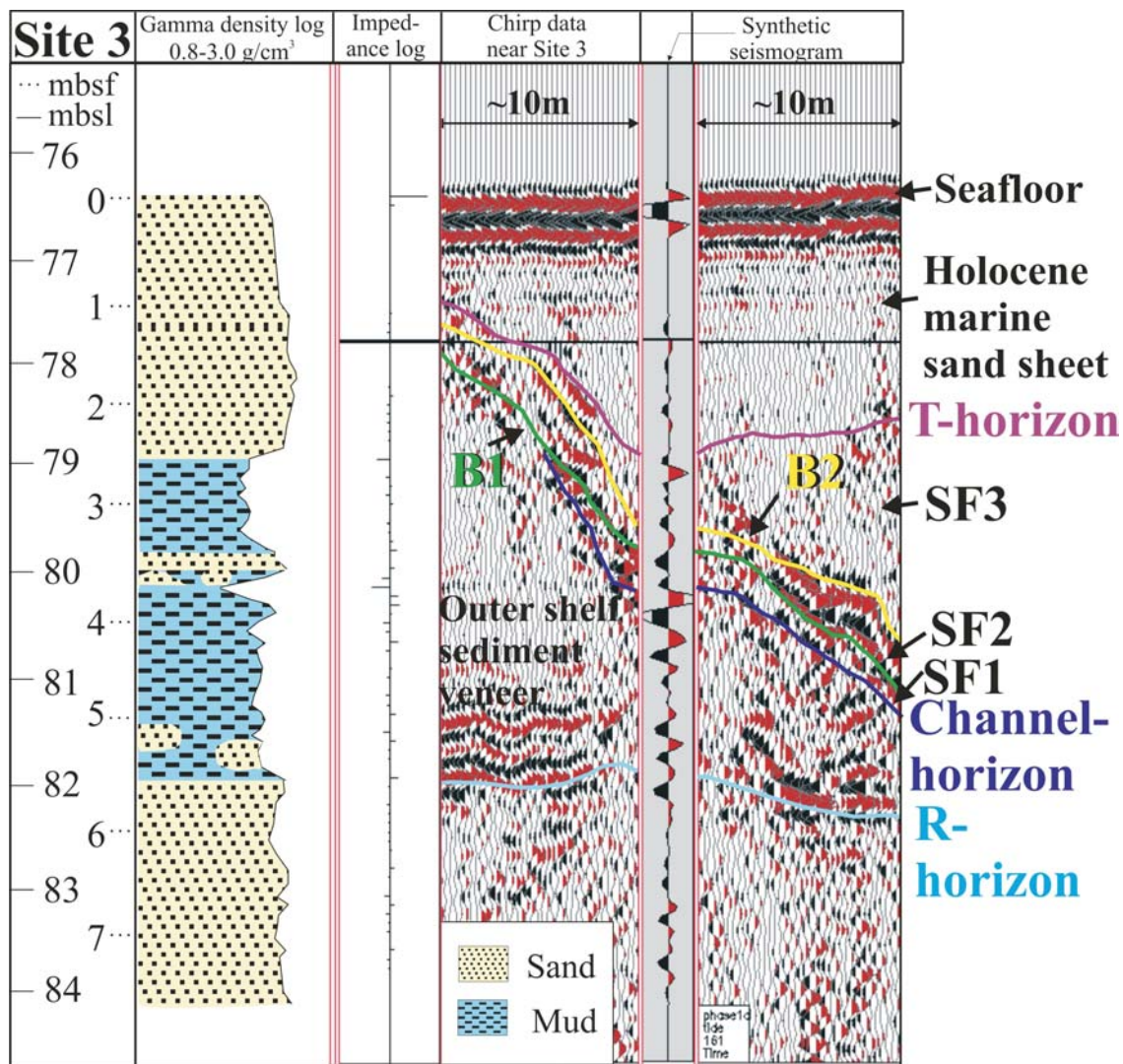
Figure 3.3: Synthetic seismogram generated for the Site 3 core (Figure 3.1), including depth below sea-level (mbsl-meters below sea-level) and seafloor (mbsf-meters below seafloor), lithologic description and a gamma density log of cores collected aboard R/V Knorr in 2002. The seismogram can be used to tie the seismic facies units directly to lithologic data at the well location. Sand occurs to ~2.5 mbsf, where it is underlain by a clay section. The clay interval extends to ~3.55 mbsf, where I observe a thin (~10 cm), iron rich sandy layer overlying a thin (~15 cm) mud layer with abundant sand lenses. The upper clay interval correlates to my interpreted facies SF2 and SF3. SF3 correlates with the upper stiff clay section. SF2 is the lower less stiff, muddy section. The oxidized thin layer overlying homogenous clay is tied to SF1.

91

core logs (Figure 3.3) to produce a vertical acoustic impedance profile which, when convolved with a seismic (Ricker) wavelet, creates such a seismogram (Sheriff, 1995). I then used a representative seismic trace at the core location and compared it with the synthetic. Where observed and modeled seismic reflections look similar (Figure 3.3), I assume that the seismic facies can be mapped into the cored lithostratigraphy. I use these correlations to interpret incised valley-fill facies elsewhere.

Seismic stratigraphic analysis

I have analyzed groups of reflections to differentiate external form, configuration, continuity, amplitude and frequency (Figure 3.4). I use the observed variations of seismic character, when placed within the context of sampled sedimentary sequences to classify distinct seismic facies, which I then relate to lithology by using the Site 3 core-log-seismic integration results (Figure 3.3). Finally the spatial association of these seismic facies units within the mapped area (e.g., Figure 3.5) allows us to interpret depositional environments and formative processes. I have mapped four seismic facies units (SF1-SF4) within the incised valley fills. I have also identified five seismic horizons throughout the survey area. These include the previously identified Channel-horizon and T-horizon (Figure 3.2), and three new incised valley-fill horizons, which I identify as B1, B2 and B3.

Chirp sonar profiles in both frequency ranges, 1-4 kHz and 1-15 kHz, were used to interpret the chirp data. The 1-15 kHz data more clearly imaged the main stratigraphic boundaries, while the 1-4 kHz data were more useful for interpretation of seismic facies and intervening sequence geometries (Figure 3.4).

I have interpreted incised valley fill units by identifying and mapping the extent of key seismic boundaries. Previous work, using multichannel seismic and boomer
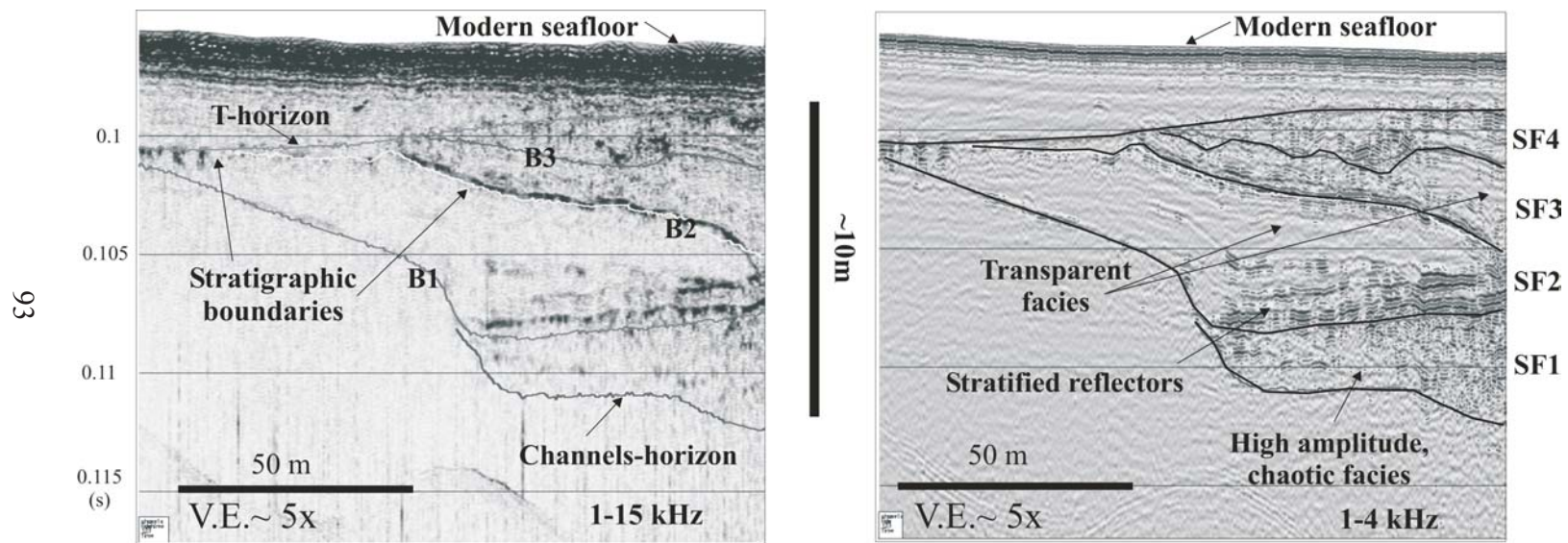
Figure 3.4:   Representative co-located chirp images at 1-15 kHz (left panel) and 1-4 kHz (right panel). The 1-15 kHz data were used as a guide for interpreting significant seismic boundaries (see text), while the 1-4 kHz data provided more detail of the seismic facies (see text). See Figure 3.1 for location.

seismic data collected on both the U.S. Atlantic continental shelf (Ashley and Sheridan, 1994; Belknap and Kraft, 1994; Foyle and Oertel, 1997) and from the Gulf of Mexico shelf (Smyth, 1988; Siringan and Anderson, 1993; Thomas and Anderson, 1994; Bartek et al., 2004), has established typical seismic facies characteristics for late Quaternary and modern valley-fill environments. Most of these studies conclude that the presence of chaotic seismic facies indicates fluvial fill, and that this facies often lies upon the sequence boundary representing the fluvial incision at or near the relevant lowstand of relative sea-level. Thomas and Anderson (1994), Foyle and Oertel (1997) and Bartek et al. (2004) all recognize transgressive facies within their valley systems as fluvial drainages evolved into estuarine bays, comprising muddy central basin deposits, estuary mouth complexes and bayhead deltas. These studies provide useful analogs for recognizing seismic facies in the New Jersey paleo-valleys, which are also late Quaternary in age.

SEISMIC FACIES

Based on stratigraphic superposition and observed geometries of both intervening seismic facies (Figure 3.6) and bounding surfaces (Figure 3.7), I have recognized four main fill units within New Jersey incised valleys (Figures 3.4 and 3.5). The northern dendritic valley system is larger and wider (Figures 3.8 and 3.9) than the system just to the south (Figures 3.10 and 3.11). The northern drainage also shows a more systematic facies zonation (Figures 3.8 and 3.9).

Seismic Facies Units

Seismic facies characteristics (i.e., continuity, amplitude, frequency and spacing
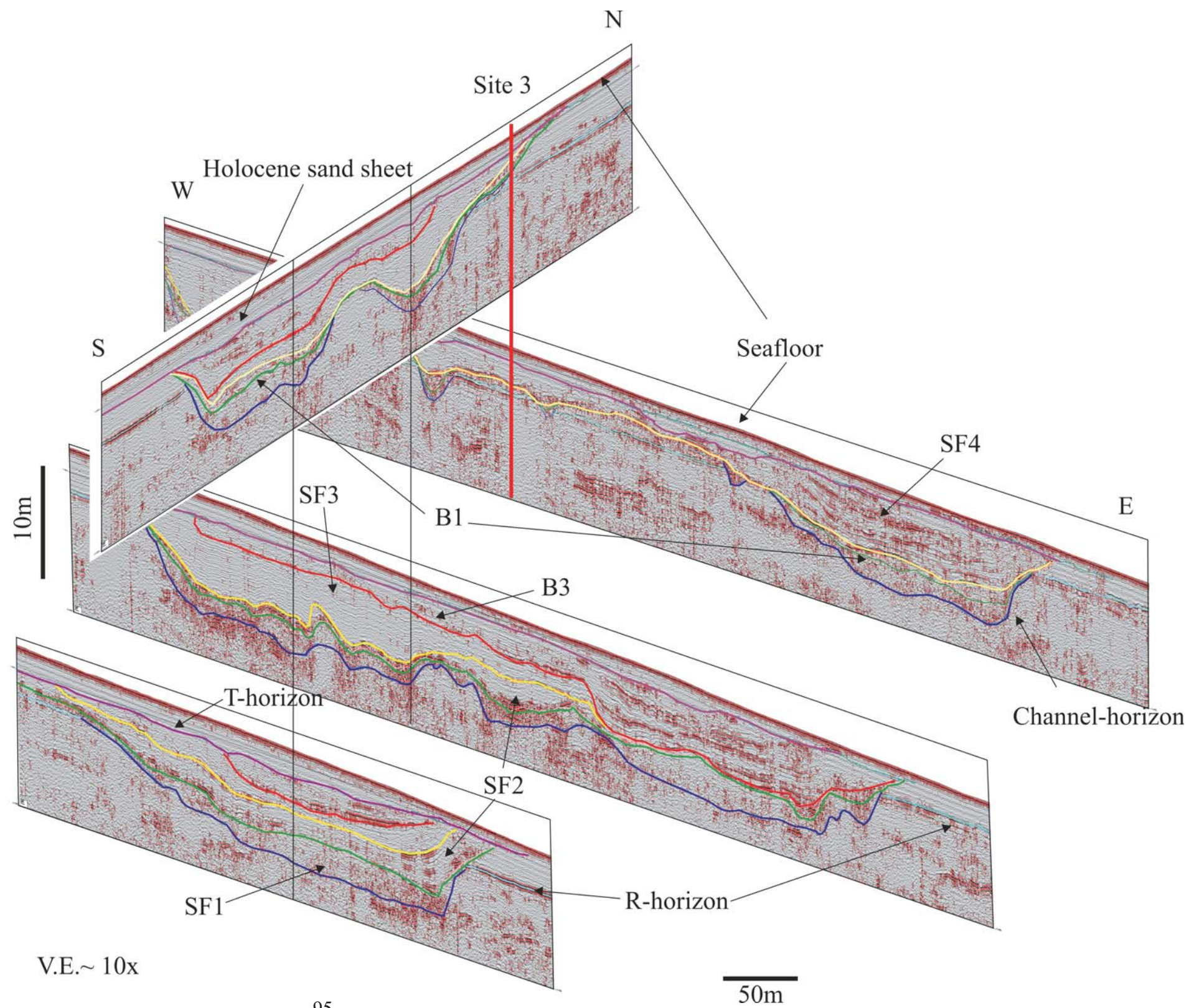
Figure 3.5: Fence diagram of chirp seismic data in the vicinity of Site 3 showing the distribution of interpreted seismic sequence boundaries and facies. Four main seismic facies units (SF1-SF4) have been recognized, along with five seismic stratigraphic boundaries (Channel-horizon, T-horizon [see Figure 3.2] and valley-fill horizons B1-B3 [see Figure 3.7]). See Figure 3.1 for location.

95
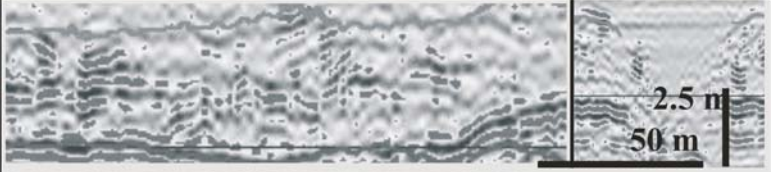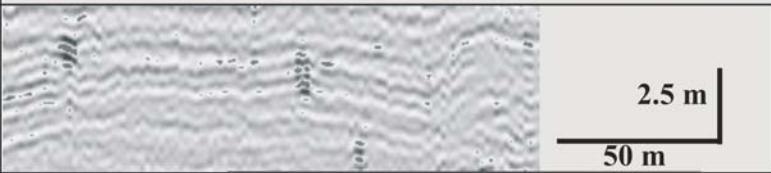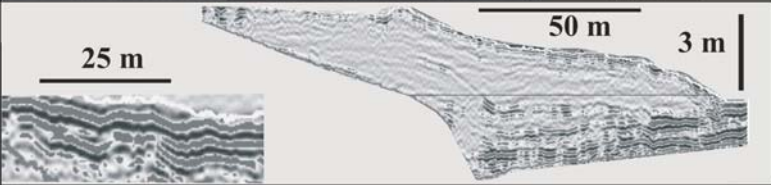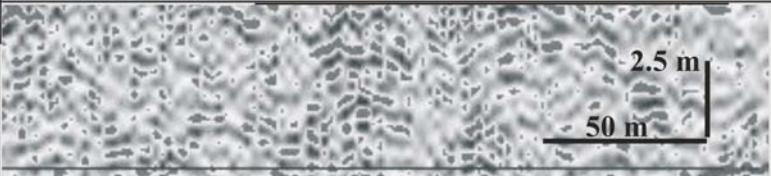
Principal internal reflector characteristics	Amplitude	Geometry	Sedimentary facies interpretation	Seismic facies	
Small parallel, tangential clinoforms, sub-horizontal	Variable, high to low	Wedging out landward (see Figs. 3.12D & 3.18)	Estuary-mouth deposits (Zaitlin et al. 1994)	2.5 m 50 m	SF4
Low frequency, sub-horizontal	Low	Wedging out seaward (see Fig. 3.12C)	Estuary central basin/bay (Allen 1991; Dalrymple et al. 1992)	2.5 m 50 m	SF3
Fairly continuous, stratified, sub-horizontal and "into the valley" dipping reflectors	Variable	Sub-planar in axial plain, bars/clinoforms on flanks (See Fig. 3.12B)	Estuarine coastal plain facies (Allen and Posamentier 1993)	50 m 3 m 25 m	SF2
Discontinuous, chaotic	Variable, but mostly high	Concave upward (confined byChannel-horizon, see Fig. 3.8)	Fluvial lag deposits (Thomas and Anderson 1994)	2.5 m 50 m	SF1

Figure 3.6:   Seismic facies associated with New Jersey shelf incised valley fills, based on internal configurations of reflectors, their amplitude and shape, combined with geometry and superposition of observed stratigraphic units. Interpretations based upon selected studies are also shown.

Seismic bound-aries	Surface charac-teristics	Interpretation	References	Seismic Horizons
T-horizon	Valley capping horizon, base of marine sand sheet	Wave ravinement	Swift, 1968; Zaitlin et al., 1994; Duncan et al., 2000	
B3	Above: SF4 Below: SF3	Tidal ravinement (sensu Zaitlin et al., 1994)	Allen, 1991; Allen and Posamentier, 1993; Zaitlin et al., 1994	
B2	Above : SF3 Below : SF2	Intermediate Flooding surface	Thomas and Anderson, 1994	
B1	Above : SF2 Below : SF1	Bay flooding/ transgressive surface	Nummedal and Swift, 1987; Zaitlin et al., 1994	
Channel-horizon	Below: Pleistocene clay Above: SF1	Fluvial incision	Davies et al,. 1992; Zaitlin et al., 1994; Duncan et al., 2000	

Figure 3.7:   Seismic boundaries observed within New Jersey incised valley fills, based on characteristics, amplitude and seismic facies above and below.
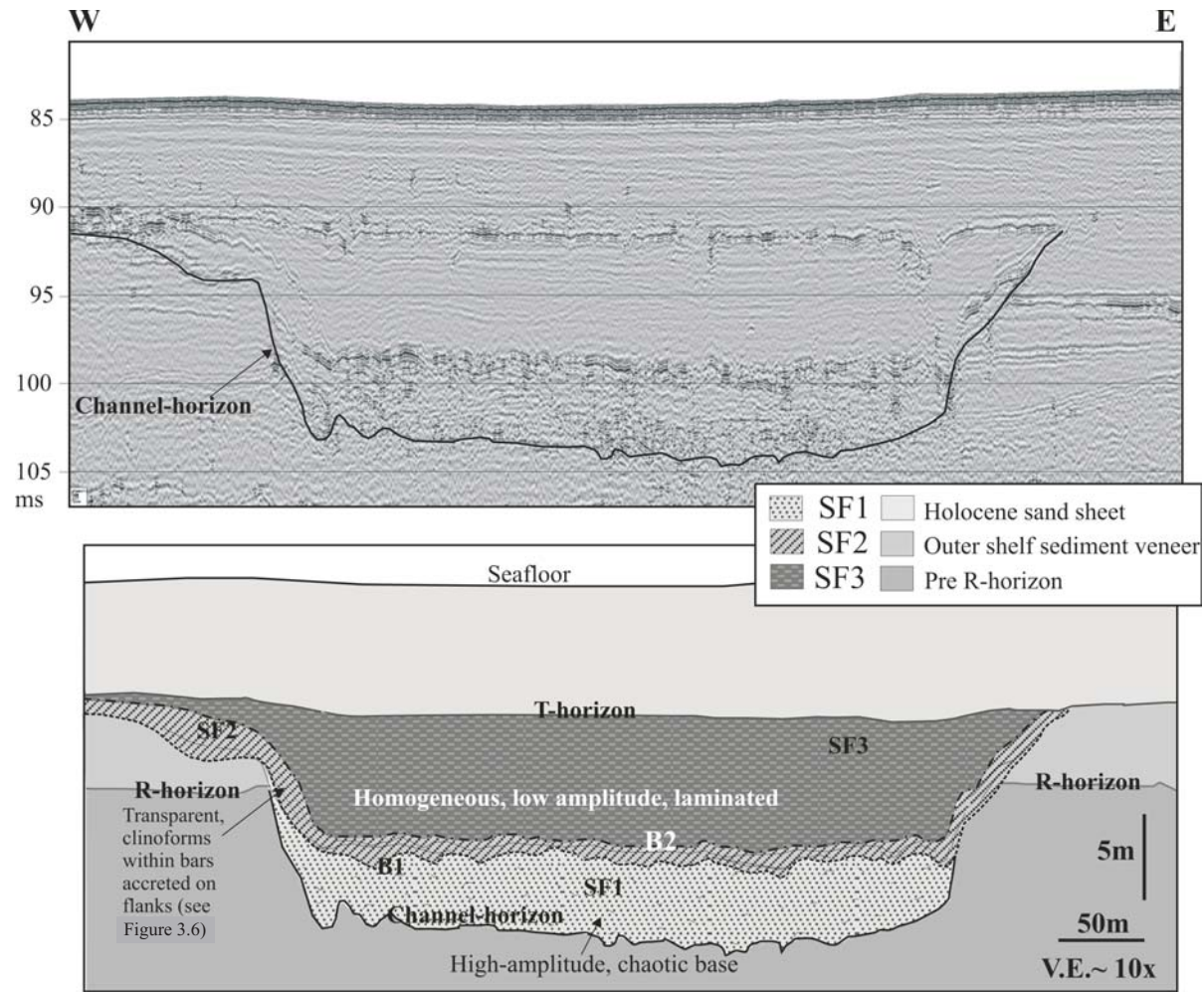
Figure 3.8: A seismic cross-section (top panel) and interpretation (bottom panel) within the landward part of the northern incised valley system, showing the stratigraphy and geometry of seismic facies units SF1-SF3, and stratal boundaries Channel-horizon, B1, B2 and T-horizon. Facies SF4 and boundary B3 are absent in this section. See Figure 3.1 for location.
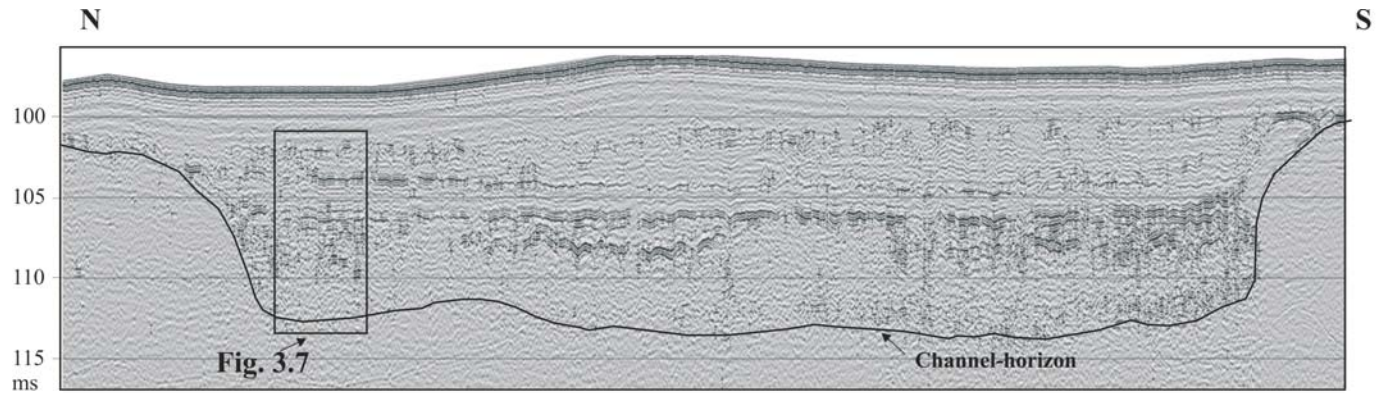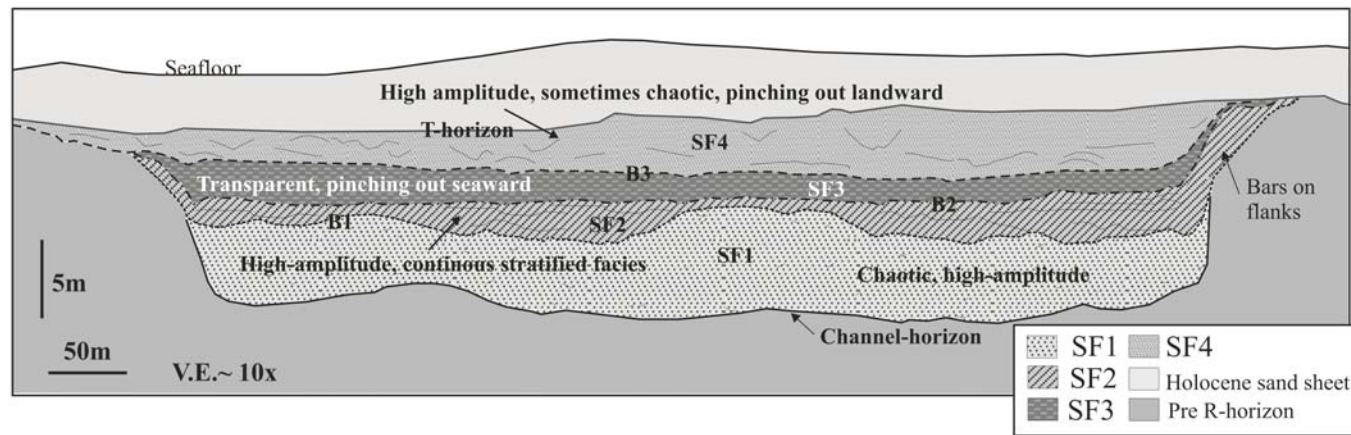
Figure 3.9: A seismic cross-section (top panel) and interpretation (bottom panel) within the seaward part of the northern incised valley system, showing the stratigraphy and geometry of seismic facies units SF1-SF4, and stratal boundaries Channel-horizon, B1-3 and T-horizon. See Figure 3.1 for location.
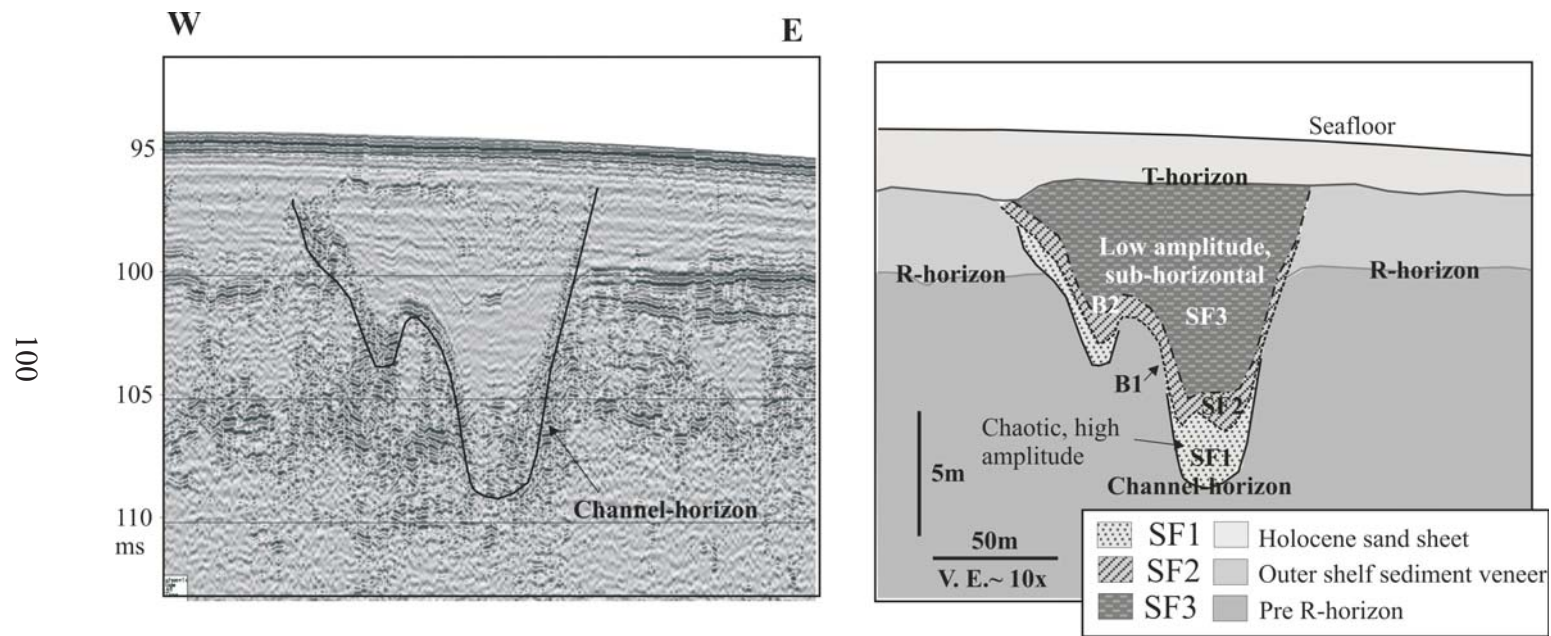
Figure 3.10: A seismic cross-section (top panel) and interpretation (bottom panel) within the landward part of the southern incised valley system, showing the stratigraphy and geometry of seismic facies units SF1-SF3, and stratal boundaries Channel-horizon, B1, B2 and T-horizon. Facies SF4 and boundary B3 are absent. See Figure 3.1 for location.
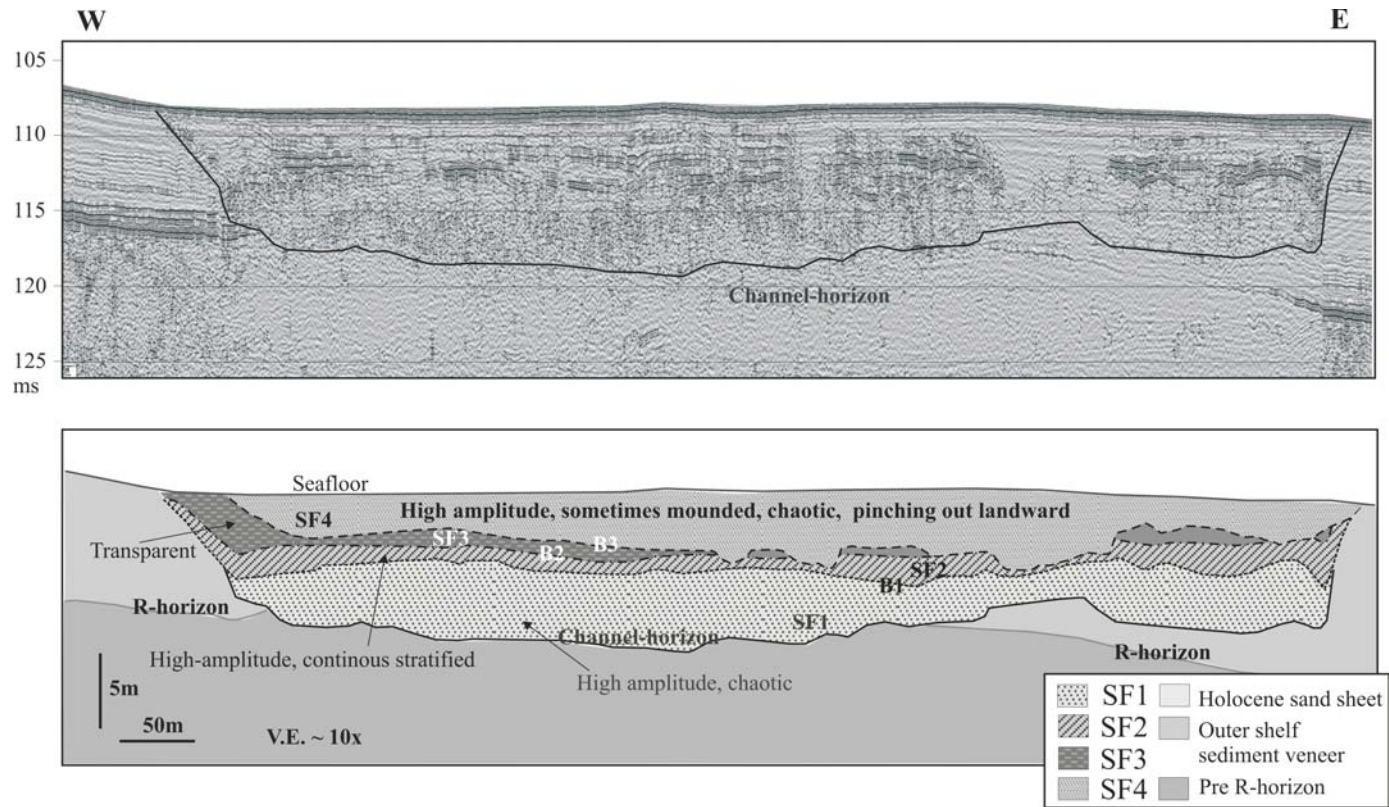
Figure 3.11: A seismic cross-section (top panel) and interpretation (bottom panel) within the seaward part of the southern incised valley system, showing the stratigraphy and geometry of seismic facies units SF1-SF4, and stratal boundaries Channel-horizon and B1-3. SF3 is nearly absent in this cross-section, truncated by B3. T-horizon is not present in this section. See Figure 3.1 for location.

of subbottom reflections), combined with geometry and superposition of observed stratigraphic units, define the observed seismic stratigraphy within New Jersey incised valleys (Mitchum et al., 1977a; Mitchum and Vail, 1977; Sangree and Widmier, 1977). I recognize four seismic facies units (SF1-4; Figure 3.6) and five seismic-stratigraphic boundaries (T-horizon, Channel-horizon, B1-B3; Figure 3.7) within these fills (Figures 3.8-3.11). I use the differing reflectivity patterns of these facies, along with other evidence, to infer seismic facies distribution (Foyle and Oertel 1997; Anderson and Fillon 2004). Transparent units reflect insignificant changes in velocity or density and are likely to be homogeneous (Figure 3.3). Acoustically laminated units suggest interbedded grain sizes. Such inferences are supported by the comparison of sparse cores on the New Jersey shelf with 2D and 3D seismic data (Buck et al. 1999; Goff et al., 1999; Duncan et al., 2000; Nordfjord et al., 2002; Gulick et al., 2003; Alexander et al., 2005; Figure 3.3).

Seismic Facies 1 (SF1): SF1 (Figure 3.6) exhibits chaotic and high amplitude reflections near the base of observed incisions formed by the Channel-horizon, and is generally ~1-3 m thick (Figures 3.8-3.11). Its base, the Channel-horizon, is often difficult to distinguish, presumably because there is not everywhere a prominent acoustic impedance contrast between the eroded base of these valleys and underlying material.

Internal seismic characteristics exhibit variations between landward and seaward valley cross-sections. The thickness of SF1 is generally greater seaward (Figures 3.9 and 3.11) than landward (Figures 3.8 and 3.10). Seaward profiles tend to exhibit higher acoustic amplitude than landward profiles. Where high amplitude reflections appear in landward sections, they tend to be present toward the base of SF1 (e.g., Figure 3.8). The local seismic configuration of SF1 also varies significantly, with patches of high-amplitude diffractions adjacent to low amplitude zones (Figure 3.8). High amplitude reflections occur most frequently toward the lowest point of incision (Figure 3.9).

102

The SF1 facies generally exhibits higher and more chaotic amplitude reflections in the southern (Figures 3.10 and 3.11) than in the larger northern system (Figures 3.8 and 3.9). The sediment into which the southern drainage is incised shows a more patchy, chaotic and occasionally high amplitude seismic character, which makes it difficult to define the base of the valley system.

The isopach map for SF1 as mapped in the northern incised valley system (Figure 3.12A), shows consistently greater thicknesses in the center of the valley. The middle segment of the main trunk channel displays the thickest SF1, whereas tributaries generally do contain only small amounts of this facies (Figure 3.12A). Overall, SF1 tends to thin landward (Figure 3.12A). SF1 thickness is more variable along the axes of the southern valley (12A), but SF1 exhibits the same general pattern of variation.

Seismic Facies 2 (SF2): SF2 (Figure 3.6) consists of a thin (<1-2 m) layer of high amplitude, parallel-continuous reflectors along the valley axis (Figures 3.8-3.11). This facies is often observed to merge with small wedges along valley flanks, with a mostly transparent acoustic response (Figures 3.6, 3.9 and 3.10).

Landward, SF2 exhibits a nearly constant thickness (~1 m) across the valleys, with ~2-3 sub-horizontal reflectors (Figures 3.8 and 3.10). The thickness of SF2 tends to be more variable in seaward sections (Figures 3.9 and 3.11), with ~2 m thick, vertically stratified segments separated by connecting thin intervals. The thicker parts of this facies tend to be located toward valley flanks.

As evidenced by the isopach map of the northern valley system (Figure 3.12B), SF2 is patchy due, in part, to transparent wedges that are variably present on the valley flanks, as well as the internal variability in thickness noted above. Flank wedges tend to be more persistent where the northern valley is wider (Figure 3.12B). Such flank wedges

103
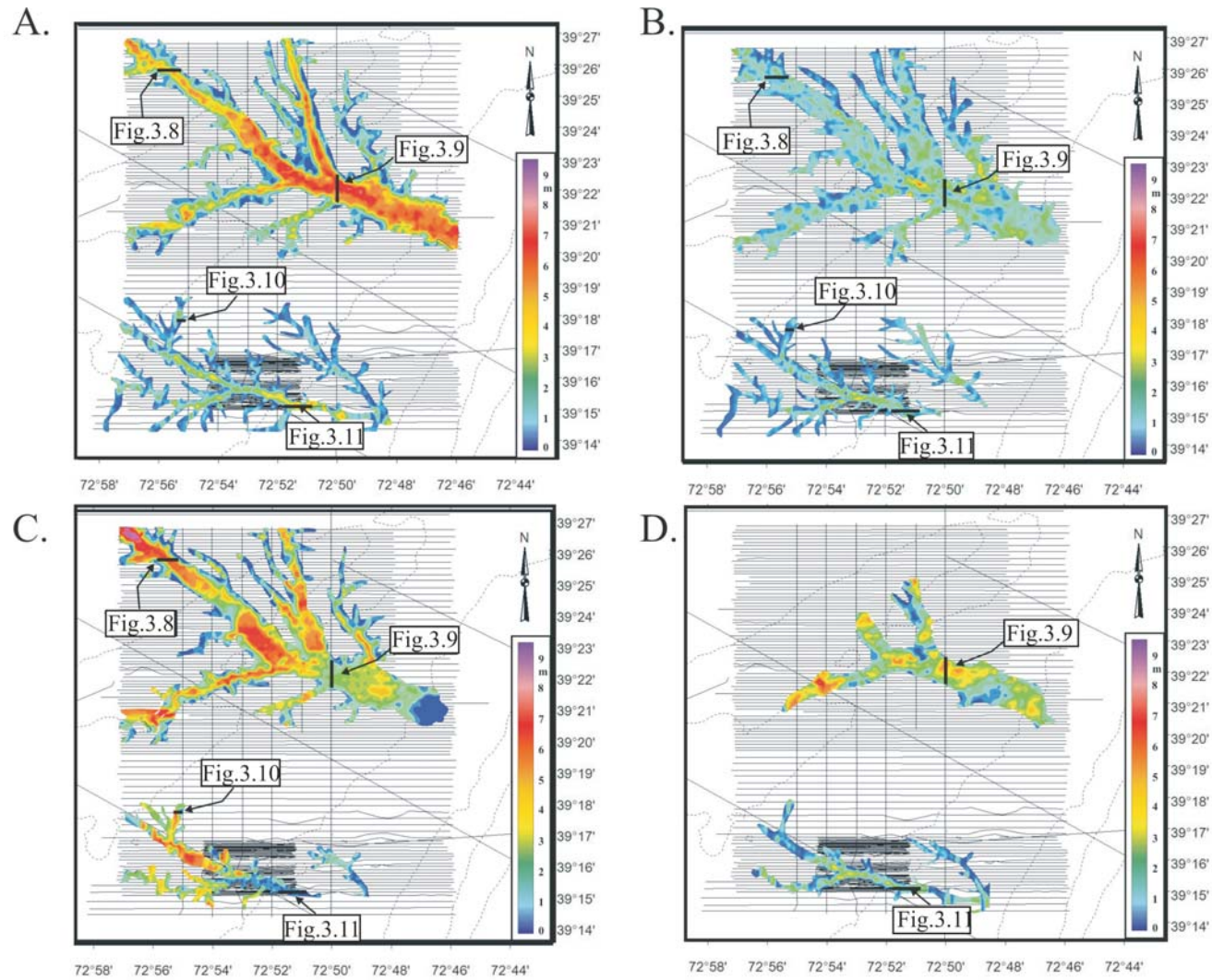
Figure 3.12: Isopach maps of seismic facies (A) SF1, (B) SF2, (C) SF3 and (D) SF4 for the northern and southern incised paleo-valley systems.

are not resolvable in the smaller southern valley system (Figure 3.12B).

Seismic Facies 3 (SF3): SF3 (Figure 3.6) is predominantly acoustically transparent, with occasional, low-amplitude sub-horizontal reflectors onlapping valley flanks (Figures 3.8-3.11). Some higher amplitude sub-horizontal reflectors are interbedded into the sequence on seaward profiles (Figure 3.9). Individual reflectors are generally not mappable from one profile to another (~200 m distance), which implies that these are very localized acoustic responses. Landward, SF3 is up to 6-7 m thick (Figures 3.8 and 3.10), while seaward it is thin (<1 m) and is occasionally absent (Figures 3.9, 3.11 and 3.12C). SF3 is patchy throughout its extent (Figure 3.12C).

Seismic Facies 4 (SF4): SF4 (Figure 3.6) is predominantly observed seaward on profiles crossing both mapped channel systems (Figures 3.9 and 3.11). SF4 subcrops beneath the upper truncation surface, T-horizon. The facies is variable in amplitude and configuration (Figures 3.9 and 3.11), and includes continuous-parallel reflectors, small truncation surfaces, wavy reflections and small clinoforms (Figure 3.6). Although in some instances SF4 resembles SF2, the two are distinguished both by the intervening SF3 and by variability within SF4 (Figures 3.9 and 3.11).

SF4 is variable but generally thick along the axis within both valley systems (Figure 3.12D), but is fairly constant in thickness across-valley in the north (Figures 3.9, 3.11 and 3.12D). The isopach map shows that SF4 is absent in smaller tributaries of the northern system (Figure 3.12D). SF4 is preserved further landward and within more tributaries of the southern valley system (Figure 3.12D)

STRATIGRAPHIC BOUNDARIES

I have recognized and mapped five seismic horizons associated with incised valley fills on the New Jersey outer shelf. Each of these surfaces has been characterized.

in depth as a function of location, truncation style and associated facies distributions above and below (Figure 3.7).

Channels-horizon: I define the basal incision as the previously identified Channel-horizon (Figure 3.7; Davies et al., 1992; Austin et al., 1996; Duncan et al., 2000). This surface is normally preserved only within the axes of paleo-valleys, where it is generally concave-upward (Figures 3.8-3.11 and 3.13A). Channel-horizon exhibits ~25 m of elevation change over a distance of ~15 km (Figure 3.1), an average seaward dip of 0.002˚. Where Channel-horizon is most prominent, I recognize it as the base of the overlying high-amplitude, chaotic SF1 unit (Figures 3.8-3.11).   Channel-horizon is, however, often difficult to identify, a result either of a low acoustic impedance contrast between SF1 and the material into which the valley has been incised or the chaotic, reflective nature of SF1. In these instances, channel-horizon is interpreted simply as the base of SF1.

B1: Horizon B1 (Figure 3.7) is more laterally extensive than Channel-horizon, and truncates or merges with Channel-horizon along valley flanks. B1 is flatter in the central parts of paleo-valleys than Channel-horizon (Figures 3.8-3.11). Along paleo-valley axes, B1 truncates SF1 and is overlain by high-amplitude, subhorizontal, continuous reflectors of SF2 (Figures 3.8-3.11). Seaward, B1 is often deeper toward paleo-valley flanks (e.g., Figure 3.9), associated with thicker overlying SF2 deposits. In both the northern and southern valley systems B1 displays irregularities that appear to be localized erosion (Figure 3.9).

The structure contour map of B1 (Figure 3.13B) indicates a generally wider cross-valley extent than that of the Channel-horizon (Figure 3.13A), particularly seaward. This suggest that B1 is the product of an erosional event that expanded the channel walls,
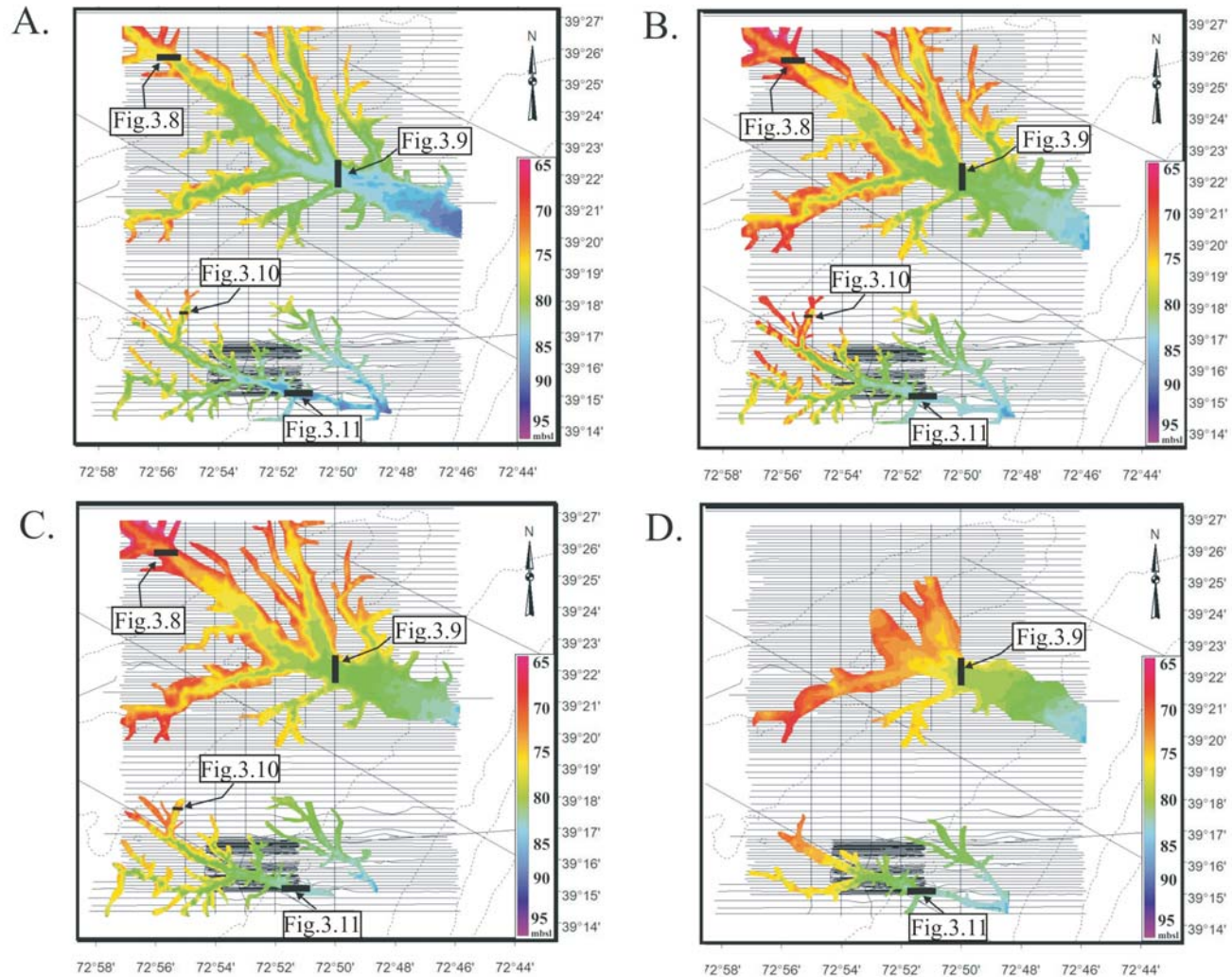
Figure 3.13: Structural contour maps of stratal boundaries (A) Channel-horizon (B) B1, (C) B2, (D) B3 for the northern and southern incised paleo-valley systems, and (E) T-horizon, which extends beyond mapped incised-valley boundaries. The T-horizon is absent where it has been truncated by seafloor erosion.

E.
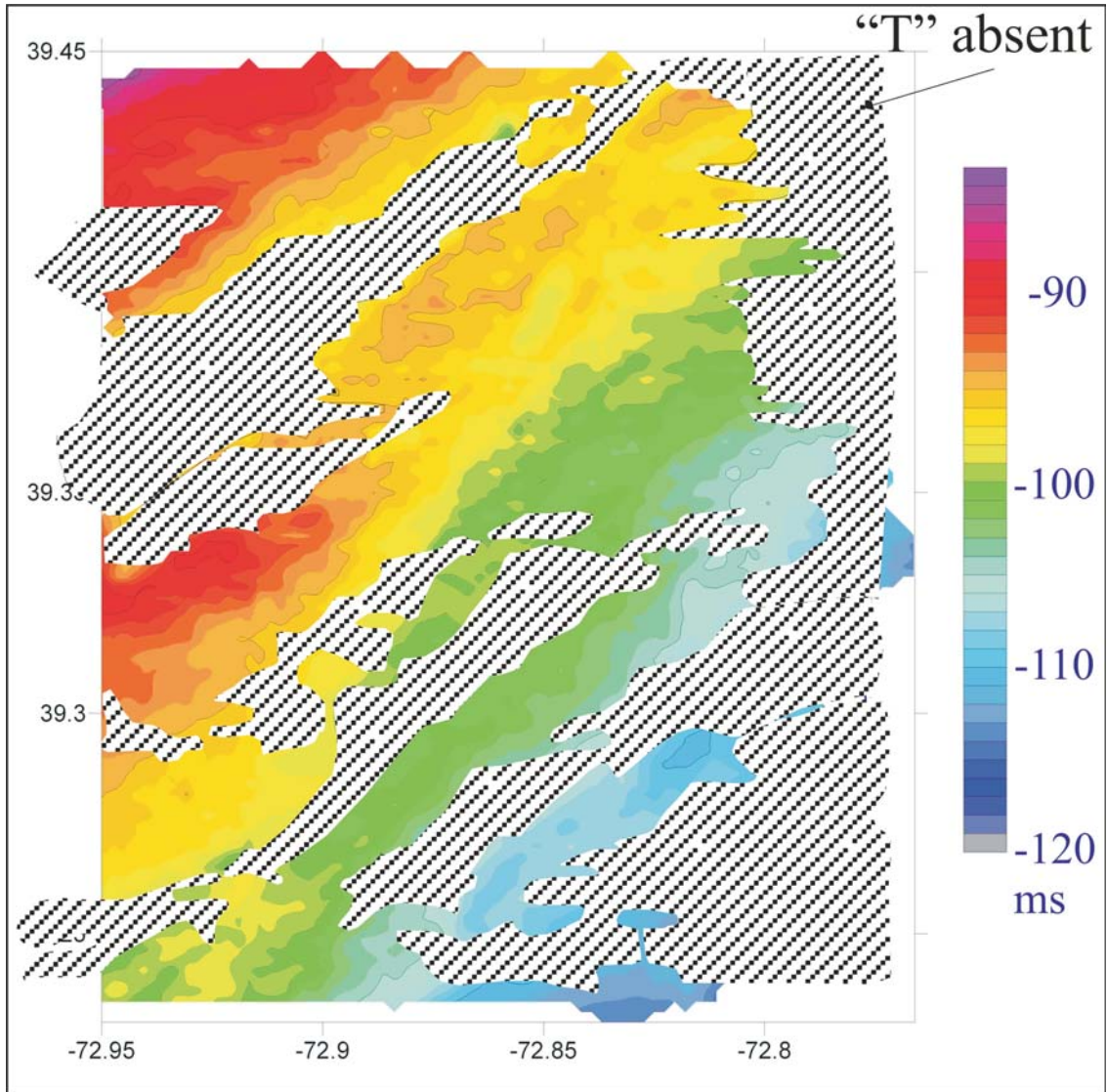
truncating the Channel-horizon.

B2: The B2 horizon (Figure 3.7) marks the boundary between facies SF2 and SF3 (Figures 4.8-4.11). Seaward, B2 is deeper toward the valley flanks (Figures 3.9 and 3.13C). B2 is onlapped by weak, subhorizontal reflectors SF3 (Figures 3.8-3.11). The structure contour map (Figure 3.13C) indicates a narrower cross-valley extent than for underlying B1 (Figure 3.13B), suggesting that the erosion that carved B2 is contained within a depression formed by B1. B2 is occasionally absent from the seaward section of the northern valley, because it is truncated there by the B3 horizon (Figure 3.11). Such truncation of B2 is more widespread in the southern paleo-valley (Figure 3.13B).

B3: The B3 horizon (Figure 3.7) is recognized only in the seaward parts of my mapped paleo-valley systems, and is absent from most smaller tributaries of both systems (Figures 3.9, 3.11 and 3.13D). B3 is the result of a series of small incisions localized within the larger incised valley defined by Channel-horizon and B1. I identify it as the boundary between by underlying facies SF3 and overlying reflectors of variable amplitude characteristic of facies SF4. In downdip portions of the northern valley system, B3 is occasionally difficult to distinguish from high-amplitude reflectors within SF3 (Figure 3.9).

T-horizon: The T-horizon (Figure 3.7) caps my valley fills (Duncan et al., 2000). I identify this boundary by truncation of reflectors below and subtle onlap above (Figures 3.8-3.10). On both boomer and chirp data, T-horizon is a reflector of moderate but highly variable amplitude (Duncan et al., 2000; Goff et al., 2005; Figures 3.8 and 3.10). Seaward a low-amplitude T-horizon truncates underlying units (Figure 3.9). Generally, I recognize T-horizon both from reflections that toplap into horizontal reflectors within SF4, and a significant upward change in facies to acoustically transparent material (Figure 3.9). Landward, T-horizon is a moderate-to-high amplitude surface within a transparent

seismic facies (Figures 3.8 and 3.10). T-horizon is everywhere a truncation surface, as it cross-cuts incised valley flanks. However, where incised valleys are not observed, the T-horizon can still be recognized as an erosional unconformity within outer shelf sediment veneer (Gulick et al., 2005). The structure contour map (Figure 3.13E) shows that T-horizon is relatively planar and occasionally absent as a result of truncation by the seafloor (Figure 3.11). These truncated regions are elongated in a NE-SW direction (Figure 3.13E) parallel to the principal bottom current direction (Vincent et al., 1981).

DISCUSSION

Stratigraphic significance of seismic facies distribution

I hypothesize that the four seismic facies (SF1-4) that make up and post-date my mapped incised valley fill represent distinct sedimentary successions (Figures 3.6 and 3.14). In this section, I attempt to tie the seismic facies to sparse available geologic data. Then, I interpret these units with respect to two conceptual models that relate facies distributions to known sedimentary processes associated with drowned river estuaries (Figure 3.15; Dalrymple et al., 1992; Zaitlin et al., 1994). The interpreted facies units and seismic-stratigraphic boundaries within the incised valleys are illustrated in Figure 3.14, an idealized dip section through the main trunk of the northern paleo-valley system (Figure 3.1).

Fluvial deposits: Facies SF1 (Figure 3.6) is composed of high-amplitude, chaotic reflections (Figures 3.8-3.11). I correlate SF1 with the thin (~ 10cm), iron rich sand layer sampled at Site 3 on an upper valley flank (Figure 3.3). I interpret SF1 as fluvial lag deposited during the lowstand associated with the LGM (Figure 3.15A). In addition to the evidence of subaerial exposure from Site 3, the chaotic, patchy seismic characteristics

110
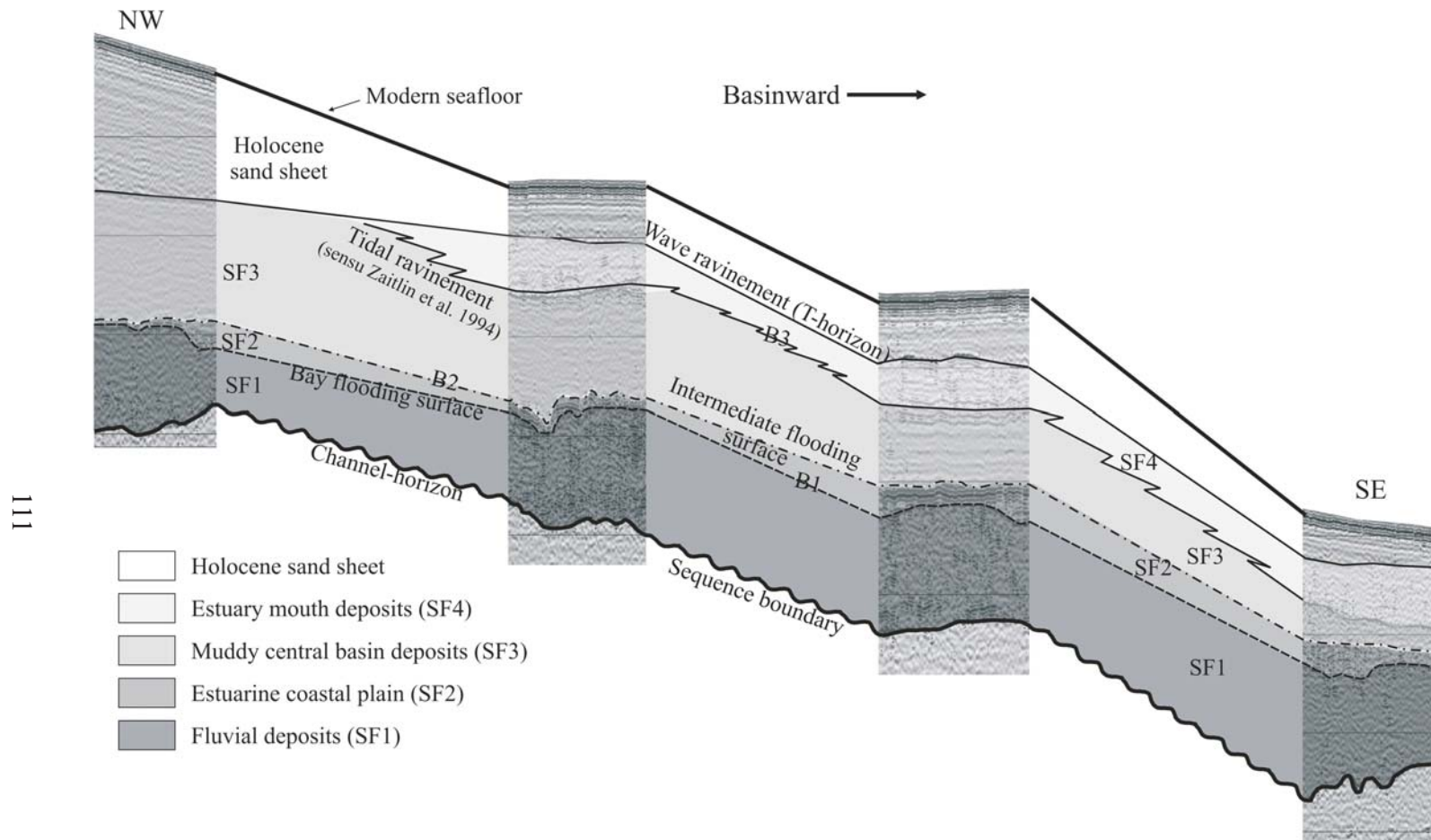
Figure 3.14: Interpreted distribution of sedimentary facies along a dip section through the trunk channel of the northern incised valley system. See Figure 3.1 for location.

(Figures 3.8-3.11) of SF1 suggest deposition under high energy conditions. Further indirect evidence of a fluvial origin for this facies is derived from a grab sample from what is interpreted as the base of an eroded channel, just south of my seismic coverage (Goff et al., 2005). This sample consisted of abundant rounded gravel and cobbles up to 6 cm in diameter, clearly indicative of a coarse-grained lag deposits. I have also employed empirically derived hydraulic equations for modern rivers and estuaries to estimate paleo-discharges, velocities and maximum shear stresses, using mapped preserved and interpolated paleo-channel geometries as a guide (Nordfjord et al., 2005). These retrodicted fluvial discharges and boundary shear stresses would have been sufficient to transport particles up to ~1.5 cm in diameter as bedload. The channel-like geometries of SF1 deposits suggest meandering to braided fluvial systems flowing to base level (Bartek et al. 2004). The SF1 facies usually lies upon the Channel-horizon (Figure 3.2), which has also been interpreted as a product of fluvial incision (Davies et al., 1992; Austin et al., 1996; Duncan et al., 2000). The distribution of fluvial strata (SF1; Figure 3.6) within my incised paleo-valleys suggest that they are preserved only when the fluvial erosion surface, Channel-horizon, and the first fill boundary, B1, are separated in space.

Estuarine coastal plain/aggradational deposits: I suggest that facies SF2 (Figure 3.6) was deposited as transgression began, backfilling the incised fluvial valleys. Based on Site 3 facies SF2 correlates with muddy sediments (Figure 3.3). During early transgression, a zone of fluvial aggradation and tidal influence migrated landward with the shoreline as base-level rose (Figure 3.15B; Dalrymple et al., 1992; Allen and Posamentier, 1993; Zaitlin et al., 1994). Foraminiferal and sedimentological evidence from available drill cores collected suggest the presence of an estuarine depositional sequence (Buck et al., 1999; Alexander et al., 2005).

112

Alternating bank-attached bars and some mid-channel bars within SF2 (Figures 3.6, 3.9 and 3.11) may represent estuarine/tidal point bars which developed as the existing drainages became more meandering during initial flooding (Figure 3.15B). Wedges located along the inside of incised paleo-valley flanks also suggest point bar deposits, emplaced either in an alluvial or tidal/estuarine environment (Allen and Posamentier, 1993). Allen and Posamentier (1993) have shown the existence of similar estuarine coastal plain sedimentary facies in the Gironde incised valley, France. Ashley and Renwick (1983) have also demonstrated the presence of a meandering tidal facies in part of what is today the wave-dominated estuary of the Raritan River, New Jersey. Weber et al. (2004) have also used single-channel high-resolution reflection profiles, calibrated with vibracores to show the significance of point bar deposits emplaced in either an alluvial or a tidal environment in the paleo-Charente River, France.

Central basin fill deposits: The appearance of facies SF3, sub-horizontal reflections with acoustically transparent zones, leads us to interpret this unit as central basin/bay deposits (Figures 3.6 and 3.15C). This onlapping, aggradational seismic characteristics facies suggest a low-energy, passively infilling depositional environment. The only core from Site 3 that sampled this facies shows it to be composed of a stiff clay (Figure 3.3). These presumed muddy deposits represent low-energy depositional conditions during a more advanced stage of the Holocene transgression, perhaps related to an estuarine turbidity maximum (Allen, 1991). Thomas and Anderson (1994) have demonstrated the presence of a similar seismic facies within the Trinity/Sabine incised valleys on the East Texas shelf; this Gulf of Mexico facies corresponds to stiff clay in geotechnical borings.

I observe facies SF3 to thicken toward the landward end of my seismic coverage (Figures 3.12C and 3.14). I hypothesize that this is a result of variation in settling rates of

fine-grained sediments of the central bay, perhaps as a function of quantity of riverine input and proximity to the shoreline (Allen, 1991). In particular, low fluvial discharge from the continent and higher wave and current activity seaward would shift the turbidity maximum and associated settling of fine-grained sediments landward (Allen, 1991). However, to preserve such an asymmetry in a clearly transgressive environment, I must also postulate some sort of change in conditions associated with valley infilling. I identify two possibilities: (1) that sea level rise did not occur at a constant rate (Buck et al., 1999), and that (2) along-strike changes in valley morphology has an important effect on local sedimentation rates within the drainage system.

The asymmetric distribution of SF3 suggests either pauses or perhaps even small retreats in the transgression, which is consistent with the foraminiferal analysis of Buck et al. (1999) A non-uniform transgression would produce thicker or thinner units of fill along valley-strike.

If shoreline advanced steadily across this region, then local valley geometry must have played the defining role in controlling the sedimentological impact of wave and tidal currents. In particular, I speculate that the wider mouth of the flooding valley would have experienced wave orbital currents during transgression, while the narrower parts of valleys farther landward did not. As a consequence, SF3 is less prominent seaward as it is finer-grained, while coarse-grained SF4 is more prominent there.

Estuary mouth complex: I suggest that seismic facies SF4 (Figures 3.6, 3.9, 3.11 and 3.12D) reflects complex deposition within a wave-dominated estuary (Figure 3.15C), a dynamic environment represented by frequent lateral variations in sedimentary facies, ranging from tidal inlets to washovers, flood-tidal deltas and barrier beaches (Dalrymple et al., 1992; Zaitlin et al., 1994). I do not have any samples from SF4; my suggested paleoenvironment for this facies is based solely on seismic characteristics (Figure 3.6).

114

The common presence of mounded facies (Figure 3.11) within SF4 suggests a longitudinal section through multiple lobes of a flood-tidal delta (Anderson et al., 1992), above the presumed muddy central basin fill represented by SF3 (Figure 3.15C). Updip basin fill facies occur at the same travel-time (Figure 3.14). Individual high amplitude, sub-horizontal to gently dipping reflections (Figures 3.6, 3.9 and 3.11) within SF4 may represent migrating sand waves, sourced either by longshore drift across the paleo-estuary mouth or by reversing tidal flows within a paleo-estuary entrance (e.g., Foyle and Oertel, 1997). SF4 pinches out landward (Figures 3.12D and 3.14), which may indicate either a pause in the transgression, causing a thicker estuary mouth complex to be deposited proximal to a stillstand shoreline, or that changes in along-strike valley morphology control depositional rates of fine- versus coarse-grained sediments. Wave orbital energy will be more important in wider parts of the valley system, which should inhibit fine-grained deposition (SF3) while enhancing coarse grained deposition (SF4).

Since I do not have any samples from SF4, I can use studies from similar environments to infer the lithologic character of this seismic facies. For example, Siringan and Anderson (1993) have sampled the upper part of a flood-tidal delta from a tidal inlet/delta complex off Bolivar Peninsula in Texas. That complex consists of clay and fine sand inter-laminae to inter-beds. The presence of high-amplitude, stratified reflectors (Figure 3.11) within SF4 could be correlated to such inter-laminae or –beds of clay and sand. Marine sands deposited in deep incisions within estuarine mud have also been observed within the James microtidal barrier estuary, located along the transgressive coast of New South Wales, Australia; these have also been interpreted by Nichol (1991) to be estuary mouth sediments.
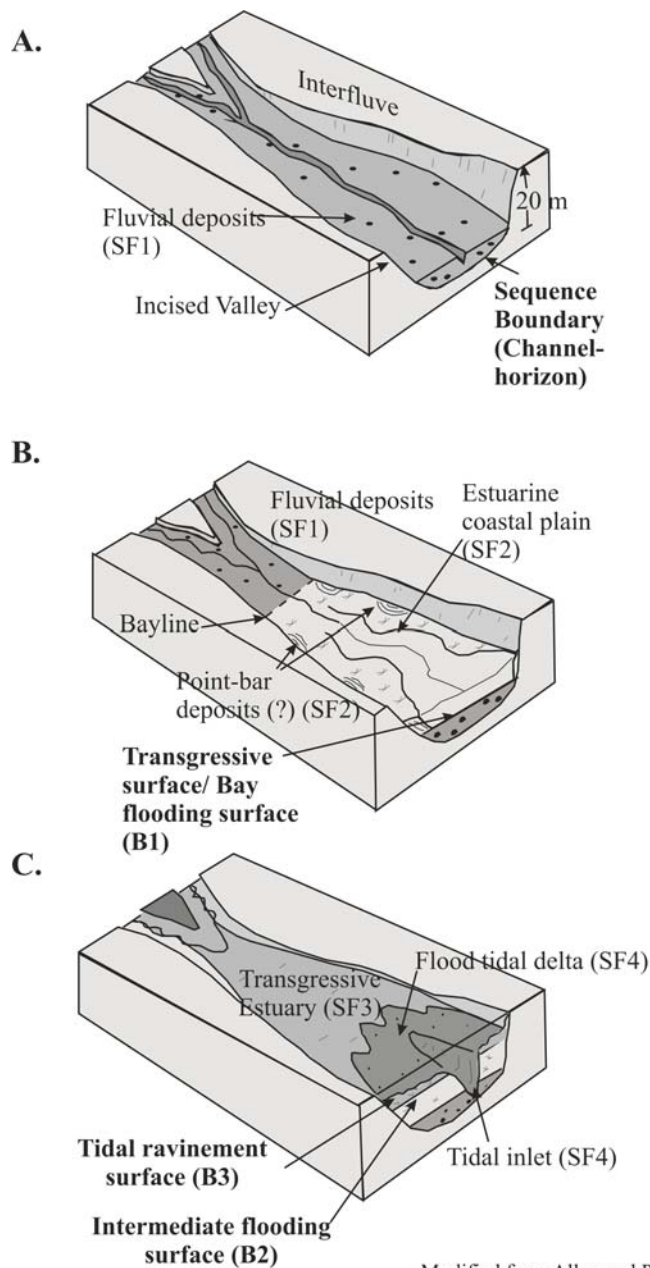
Figure 3.15: Schematic representations of the evolution of New Jersey outer shelf incised paleo-valley systems, including their stratigraphic boundaries and sedimentary facies. (A) fluvial systems, with preserved channel lags; (B) aggradational system starting to be back-filled; (C) passive infilling stage, with developed central basin muds and estuary mouth complexes. Not shown is the formation of the transgressive wave ravinement (T-horizon), which likely reworked and selectively removed portions of these fill deposits.

116

Holocene surficial sand sheet: Much of the modern New Jersey shelf is overlain by a thin, patchy veneer of Holocene shelf sands (Swift et al. 1980; Goff et al. 1999, 2004). This marine facies is interpreted as the uppermost part of the transgressive to highstand system tracts (Swift and Thorne, 1991a). The marine facies unit is largely seismically transparent, with occasional subtle, sub-horizontal internal reflections and a mounded geometry (Figure 3.11). I consider these deposits analogous to the sheet-like geometries of shallow marine clastics deposited by wave transport processes in the Gulf of Mexico (Tye and Moslow, 1993). Sand bodies lying on the transgressive wave ravinement surface, the T-horizon (Figure 3.8), have likely been formed as shoreface deposits, later modified by reworking in outer shelf depths (Goff et al., 1999; 2004; 2005).

Intra-fill sequence stratigraphic framework

The lack of accommodation space on the New Jersey outer shelf during the Holocene transgression did not allow significant vertical separation of the LGM/lowstand surface from subsequent bounding stratigraphic surfaces associated with ensuing inundation (Figure 3.14). Within the incised paleo-valleys, however, surfaces can be mapped which separate the valley-fill facies successions previously described: fluvial, estuarine and tidal delta/inlet (Figures 3.6 and 3.14). Within these filled incisions, high-frequency sea-level events associated with the last transgression have been preserved (Buck et al., 1999). My seismic horizons are spatially localized within the paleo-valleys (Figure 3.13), so they must have been produced by localized processes, such as tidal channel migration/switching, inlet scour and/or wave-base erosion. I suggest that any seismic horizon traceable throughout the mapped valley-fill complexes is related to

relative sea-level changes, particularly the interpreted lowstand incision surface, Channel-horizon, and the wave ravinement surface, T-horizon.

Seismic boundaries observed within the incised paleo-valley fill are all representative of fluvial incision during coastal plain exposure and/or subsequent flooding erosive events associated with the Holocene transgression. The hierarchy and geometry of flooding surfaces reflects the landward translation of valley-fill facies during sea-level rise. These boundaries represented composite surfaces, where younger stratal boundaries merge with subjacent horizons in both cross-valley (Figures 3.8-3.11) and dip directions (Figure 3.14). Although the relationship between two successive facies may appear conformable, minor erosion and a time discontinuity are probably both associated with any flooding surface/seismic boundary.

Channels-horizon: sequence boundary-lowstand/LGM fluvial incision surface: The Channel-horizon (Figure 3.7) has long been interpreted as a fluvial incision surface (Davies et al., 1992; Duncan et al., 2000). I also interpret these incised paleo-valleys as fluvial in origin (Figure 3.15A), based on their systematic incision into underlying Pleistocene strata, chaotic seismic fill (SF1) at their bases (Figure 3.14), which may be indicative of non-marine, coarse-grained lag (Austin et al., 2001; Goff et al., 2005), and a dendritic plan-view geometry with junction angles that are consistent with a riverine origin (Figure 3.1; Nordfjord et al. 2005). The Channel-horizon correlates at Site 3 to a transition from clay below to an iron-rich sand layer above suggesting subaerial exposure within a terrestrial (coastal plain) environment (Figure 3.3).

B1: bay flooding surface: I interpret B1 (Figure 3.7) as a bay flooding surface (Nummedal and Swift, 1987), the surface that separates fluvial (SF1) from paralic facies: marsh and estuarine coastal plain (SF2), estuarine (SF3) and/or tidal delta/inlets (SF4). Bay flooding surfaces, also known as estuarine transgressive or tidal flooding surfaces

(Allen and Posamentier 1993), are cut within estuarine or tidal river settings. The leading edge of the bay flooding surface, the landward limit of tidal influence, is defined by the bayline (Figure 3.15B; Posamentier et al., 1988; Anderson et al., 1992). The bayline is cut by wave and/or tidal-current scour and is also the landward limit of transgressive estuarine deposits. This low-relief (>0.002°) surface (Figure 3.14) is the estuarine equivalent of the wave ravinement (T-horizon, Figure 3.14) that develops seaward, on the open-ocean coast under higher wave-energy conditions (Dalrymple et al., 1992; Zaitlin et al., 1994). However, the development of B1 is confined to coastal embayments, and is absent on non-embayed, or headland-fronted, coasts. B1 is also equivalent to the transgressive surface in the idealized sequence stratigraphic model of a wave-dominated estuary (Zaitlin et al., 1994). Erosion associated with the bay flooding surface may modify all parts of the preexisting fluvial erosion surface. However, off New Jersey the Channel-horizon, fluvial incision surface is preserved and is not modified by B1 within the axis of mapped paleo-valleys (Figure 3.14).

My seismic data show that B1 may truncate the subjacent fluvial erosion surfaces, Channel-horizon, along the paleo-valley flanks (Figures 3.8-3.11). Basal sequence boundaries are composite surfaces created by different physical processes. Modification/erosion by the bay flooding surface of the fluvial lag deposits (SF1) is generally less severe than that associated with the tidal ravinement (sensu Zaitlin et al., 1994), B3, of the central basin (SF3) or the transitional (SF2) facies (e.g., Figure 3.11).

B2: intermediate flooding surface: I interpret B2 (Figure 3.7) as another subtle flooding surface within the estuarine sequence (Figures 3.14 and 3.15C). I suggest that this seismic boundary was created by superimposing muddy central basin deposits of facies SF3 over estuarine coastal plain deposits of facies SF2. This intermediate flooding surface between the bay flooding surface and tidal ravinement (sensu Zaitlin et al., 1994)

119

can be traced downdip until it is truncated by or merges with B3 (Figure 3.14). A similar surface has been reported from the Gulf of Mexico by Thomas and Anderson (1994).

B3: tidal ravinement surface (sensu Zaitlin et al., 1994): I interpret horizon B3 (Figure 3.7) as a tidal ravinement surface (Figures 3.14 and 3.15C), formed as a result of both landward and lateral migration of the estuary mouth during transgression. B3 is preserved as a moderate-relief erosional surface within the paleo-estuary bay (Figures 3.9 and 3.11). At paleo-estuary margins, the tidal ravinement surface (sensu Zaitlin et al. 1994) shoals and is generally truncated by the wave ravinement surface, T-horizon (Figures 3.6 and 3.14). Therefore, the erosion related to the formation of the tidal ravinement surface (sensu Zaitlin et al., 1994) is principally confined to the central axis of the drainage basin (Figures 3.9, 3.11 and 3.13D).

B3 is typically associated with overlying barrier/flood-tidal-delta complexes within wave-dominated estuaries, facies SF4 (Figure 3.14; Zaitlin et al., 1994). As this tidal ravinement surface (sensu Zaitlin et al., 1994) in bay mouth settings migrates laterally and landward, its trailing edges are buried by downlapping estuary-mouth sands of SF4, that also prograde landward and across-estuary (Figures 3.9, 3.11 and 3.14; Colman et al., 1990; Fletcher et al., 1992); this process serves to preserve an equilibrium tidal-scour trench cross-sectional area. Downlapping sands are sourced by littoral drift from the estuary-mouth margins and probably from the adjacent coastline, and are reworked by shore-orthogonal, reversing tidal-currents at the bay mouth (Ludwick, 1972). B3, the tidal ravinement surface (sensu Zaitlin et al., 1994), is distinguishable from the stratigraphically higher wave ravinement T-horizon by larger local gradients in cross section (Figures 3.9 and 3.11), and by its absence outside the immediate vicinity of paleo-estuary mouths (Figure 3.13D).

120

Allen and Posamentier (1993) have recognized a tidal ravinement surface in the Gironde River estuary, France, particularly where inner-estuary deposits were eroded and overlain by thick, estuary mouth tidal-inlet sands. Lericolais et al. (2001) used chirp sonar data to highlight the significance of this tidal ravinement seaward of Allen and Posamentier's (1993) study area. The Gironde River valley incisions are deeper and wider than the New Jersey outer shelf valleys, which may be explained by the fact that they are connected directly with the main terrestrial drainage system of the modern Gironde estuary (Lericolais et al., 2001). Nevertheless, both incised paleo-valley systems exhibit well-developed tidal- and wave-ravinement surfaces.

T-horizon: transgressive wave ravinement surface: The T-horizon (Figure 3.7) was first interpreted by Duncan et al. (2000) as the seismic expression of a transgressive ravinement surface. I refine their interpretation to identify the T-horizon as a wave ravinement surface (Figure 3.14), formed by erosional shoreface retreat during rising sea level (Swift 1968; Nummedal and Swift, 1987). The T-horizon therefore represents the first regional marine flooding event across the submerging continental shelf. This boundary also marks the top of both estuarine deposits within the incised paleo-valley fills (SF3 and/or SF4) and the regressive outer shelf sediment veneer outside these valleys (Gulick et al., 2005). The T-horizon also forms the base of the marine sand sheet (Figure 3.7). The T-horizon truncated and likely excavated parts of the underlying paleo-valley successions during its formation, but it has also since been truncated in part by late transgression to early highstand erosion (Figures 3.11 and 3.13E, Goff et al., 2005).

Siringan and Anderson (1993), seismically and with cores, have documented inner-shelf sediments overlain by a wave ravinement surface marked by a transgressive lag in the Bolivar Road, Gulf of Mexico, tidal inlet, along the east Texas coast. The lag consisted of large and mixed shell fragments, calcareous nodules and other granule-size

to pebble-size lithic fragments. Posamentier (2002) also recorded shell lag deposits associated with the transgressive ravinement surface in a study of sand ridges offshore Java. At Site 3, the T-horizon is not associated with a lag deposit. However, large areas of the New Jersey shelf which have been eroded down to or below the T-horizon horizon are covered by a shell hash layer, which shows up as bright returns on backscatter images (Goff et al., 2004; 2005). Goff et al. (2005) infer that these deposits are remnants of the T-horizon, and a contributor to the impedance contrast which gives rise to its seismic expression.

Wave- versus tide-dominated models for incised valley deposition

Dalrymple et al. (1992) and Zaitlin et al. (1994) have presented conceptual models of wave- and tide-dominated estuarine deposits that describe the stratigraphic arrangement of facies produced during a transgressive-regressive cycle (Figures 3.16 and 3.17). In these models, the incised-valley system is divided into three segments: (1) an inner, river-dominated zone, (2) a relatively low-energy, central zone where river flow is countered by flood-tidal energy, and (3) an outer, marine zone dominated by waves and/or tides (Figure 3.16). The difference between the wave- and tide-dominated estuarine end-members is primarily reflected in the distribution of sand bodies at the mouth of the estuary (Figures 3.16 and 3.17). The wave-dominated estuary contains a barrier beach and tidal inlet complex at its mouth (Figure 3.16), whereas the tide-dominated estuary (Figure 3.17) is fronted by intertidal sand bars that grade to mud flats and peripheral salt marshes in an up-estuary direction. The tide-dominated model does not exhibit as pronounced a tripartite distribution of lithofacies (i.e., coarse-fine-coarse) as the wave-dominated model does. In the wave-dominated model, coarse-grained sediments are deposited at the head of the estuary by the river, forming a bayhead-delta (Dalrymple et al., 1992). In contrast, tidal energy penetrates further headward than wave

energy in the tide-dominated estuaries, and the bayhead delta and muddy central basin deposits are not present in the river-dominated portion of these estuaries. Instead, the inner/landward zone consist of tidal meanders and inner straight fluvial/tidal channels (Dalrymple et al., 1992).

These sequence stratigraphic models (Figures 3.16 and 3.17) both assume a constant energy setting throughout the relative sea-level cycle, and a tidal excursion within the incised valleys during late lowstand-early transgression. Recent Holocene studies coupled with ancient outcrop studies, however, suggest that depositional energy is more complicated, a function of coastal bathymetry, shelf width, tidal resonance and sea level behavior, and thus can change at any time during the relative sea-level cycle (Yoshida et al. 2005).

My fluvial SF1 facies (Figure 3.18) is consistent with wave- and tide-dominated models (Figures 3.16 and 3.17), which records the early incision stage with a remnant fluvial lag (Figure 3.15A). My SF2 facies corresponds to the tidal-fluvial facies of the tide-dominated estuary model (Figures 3.17 and 3.18), which accumulated as the inner, straight paleo-valleys were flooded by seawater. Antecedent topography of these valleys on a very gently dipping shelf created increased accommodation space, which likely caused a tidal amplification and therefore promoted tide-dominated facies early in the valley fill sequence (Figure 3.17).

My interpretation of the buried incised valley fill facies SF3 and SF4 and intervening stratal boundary B3 on the New Jersey shelf (Figure 3.18) is largely consistent with the tripartite zonation of wave-dominated estuaries (Figure 3.16; Dalrymple et al., 1992; Zaitlin et al., 1994). Their zonation corresponds with the general pattern of net bedload transport. Coarse sediments supplied by marine processes, my SF4 facies, accumulate primarily in the seaward portions of the mapped valley systems, while

123

Shelf/Ramp ← → Incised-valley system (IVS) → Non-incised Fluvial System →

← Marine → Segment 1 Outer IVS | Segment 2 Middle IVS | Segment 3 Inner IVS | ← Fluvial →

Maximum Flooding Surface

Wave Ravine-ment Surface (T-horizon)

Transgressive Surface (B1) (Bay flooding surface)

Sequence Boundary (Channels-horizon)

Tidal Ravinement Surface (B3)

124

Facies:

Transgressive systems

Wave-dominated:
- Barrier/Inlet (SF4)
- Central Basin (SF3)
- Bayhead Delta

Lowstand systems
- Fluvial (SF1)
- Marine
- Shoreline

Highstand systems
- TST/HST Marine
- Fluvial
- Shoreline
- TST Fluvial

Modified from Dalrymple et al. (1992) and Zaitlin et al. (1994)

Figure 3.16: Schematic model of a wave-dominated, incised valley estuary (after Dalrymple et al. 1992; Zaitlin et al. 1994), showing its infill by landward progradation of flood-tidal delta deposits and the seaward progradation of fluvial-estuarine delta (i.e., bayhead delta) deposits.
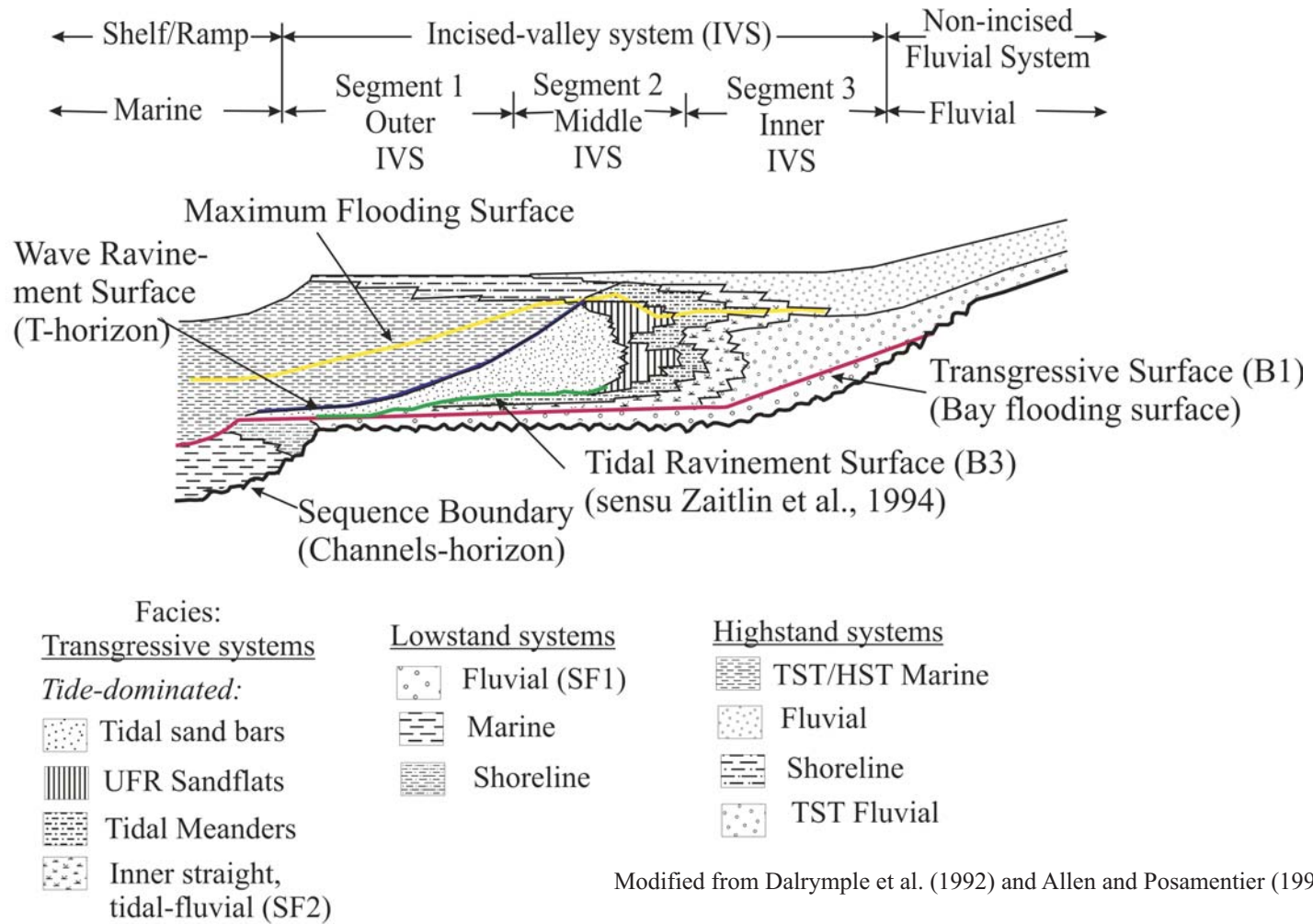
Figure 3.17: Schematic model of a tide-dominated incised valley estuary (after Dalrymple et al. 1992; Allen and Posamentier 1993), which differs from the Zaitlin et al. (1994) model (Figure 3.16) in the distribution of sand bodies at the mouth. The inner estuary consists of muddy and sandy point bars and tidal flats, while the outer estuary consists of elongated sandy tidal sand bars.

finer-grained sediments, my SF3, accumulate landward. As discussed above, whether this asymmetry is caused by a stillstand in the shoreline, the geometry of the valley system (wider valleys seaward, narrower landward), or some other unconsidered factor, has yet to be determined. However, depositional conditions clearly changed through space and time; the seaward parts of these systems were influenced by marine processes, while landward parts were dominated by tidal processes.

Unlike the idealized depositional morphologies described in the wave-dominated (Figure 3.16) model (Dalrymple et al., 1992; Zaitlin et al., 1994), I do not find convincing seismic evidence for the presence of bayhead delta morphologies within what I interpret as aggradational riverine deposits (SF2; Figure 3.18). If present, bayhead delta deposits would be evident as subtle, high-amplitude, low-angle clinoforms, dipping in a seaward direction with interspersed distributaries (Anderson et al., 1992). Instead, my SF2 facies is more consistent with the inner, straight tidal/fluvial channel zone of the tide-dominated model (Figure 3.17). I interpret the alternating wedges observed within SF2 along valley flanks (Figures 3.8 and 3.12B) as tidal point bars deposited in an estuarine coastal plain setting, an aggradational phase initiated as these valleys began to experience back-filling and meandering of tidal creeks. The evident lack of a bayhead delta in my data may also be a result of continuing minor fluvial (coarse-grained?) sediment input during initial transgression (Honig and Boyd, 1992). The incised valleys on the New Jersey outer shelf do not appear to be linked to any modern terrestrial rivers like the Hudson or Delaware, and so perhaps river sediment supply was not significant during transgression. Therefore, a bayhead delta may be present landward of my seismic coverage, although I appear to have imaged almost the entire systems on the outer shelf (Figure 3.1).

Due to their location near the lowstand shoreline and today's shelf break, the incised valley systems that I have mapped were certainly filled and drowned during the

early stages of the Holocene transgression. Radiocarbon analyses of benthic foraminifera from one vibracore of an incised valley flank in my study area constrain the age of this fill to AMS ^{14}C 12.3 ± 0.45 ka (Lagoe et al., 1997; Buck et al., 1999). By contrast, valleys that incise the landward edge of continental shelves, such as the Gironde estuary (Allen and Posamentier, 1993) and Shoalhaven and Lake Macquarie, Australia (Roy, 1994; Umitsu et al., 2001), are also often subjected to late transgressive to highstand sedimentation. Such sedimentation could take the form of prograding bayhead delta (at sea-level stillstand) or increased fluvial sediment input (overwhelming the sea-level rise) (Reynaud et al., 1999). Since my study area was completely submerged by ~12 ka, I assume that the highstand system tract facies, a regressional/progradational bayhead delta, was either never deposited or not preserved. Instead, the wave ravinement surface, T-horizon, is observed over much of my study area (Figures 3.8 and 3.13E).

As noted above, the widespread presence of estuarine coastal plain facies SF2 (Figure 3.12B) and a lack of evidence for bayhead deltas in the fill stratigraphy suggest early tide-domination for New Jersey outer shelf incised paleo-valleys (e.g., Fletcher et al., 1992). These estuaries have sufficient tidal prism to maintain tidal currents against both longshore and cross-shore, wave-driven littoral sediment transport (Cooper, 2002). The shape of valley systems being flooded may control the nature of the facies developed in that estuary, particularly during early infilling (Dalrymple et al., 1992). I speculate that, as a result of the funnel shaped valley that I observe off New Jersey (Figure 3.1), incoming/flood tides were progressively compressed into smaller cross-sectional areas, thereby amplifying tidal height and speeding up flood-tidal currents. This may explain the early presence of a more tidally influenced facies SF2 (Figures 3.8-3.11 and 3.12B). If I compare SF2 with tide-dominated incised valley fill models (Figure 3.17), then this transitional facies, with possible point-bars may correspond with tidal meanders of inner

127
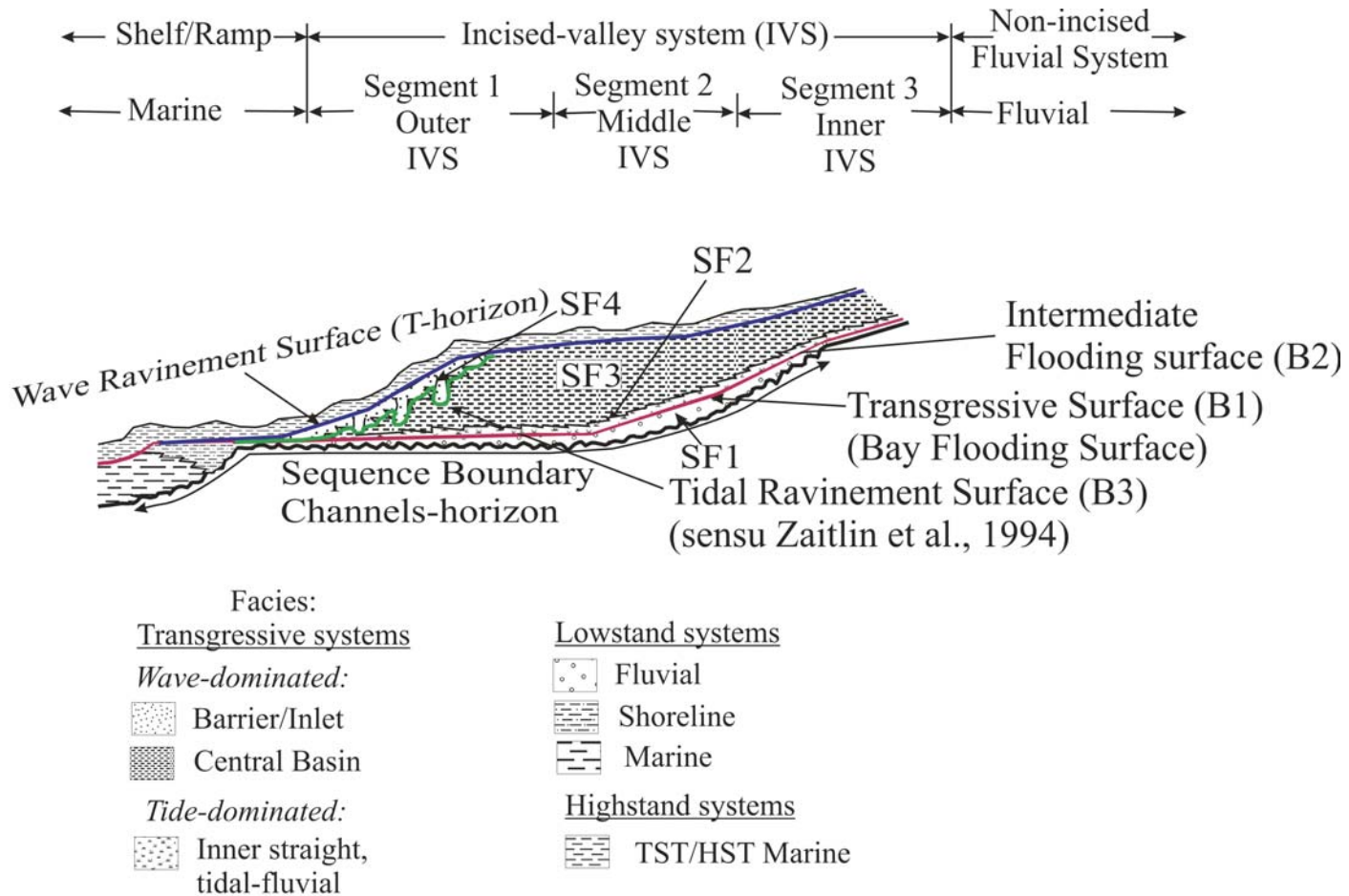
Figure 3.18: Our interpreted stratigraphic record of New Jersey outer shelf incised valleys, showing sedimentary facies from both the tide-dominated (SF2-inner straight tidal-fluvial) and wave-dominated settings (SF3 and SF4- central basin mud and estuary mouth complex).

128

straight fluvial/tidal facies (Figure 3.15B).

As transgression of the New Jersey shelf continued and the antecedent fluvial geomorphology was further modified, early tide-dominated valleys were likely transformed into wave-dominated systems (Figure 3.16) (e.g., Fletcher et al., 1992). The shoreline became more proximal to these incised valleys, with a consequent dissipation of tidal currents (due to increasing cross-sectional area), and the intermediate flooding surface (B2) could have been formed and overlain by central basin deposits (SF3) as wave influence increased. Tides distributed sediment along paleo-shoreface, forming the tidal ravinement (sensu Zaitlin et al., 1994; B3) and associated overlying flood-tidal deltas, tidal inlets and washovers deposits (SF4; Figure 3.14).

Reynaud et al's. (1999) interpretation of the Neogene incised valley system at the Southern Celtic shelf margin does not recognize the existence of significant amounts of estuary mouth (such as my SF4 facies may represent) or open-marine deposits. Instead, that valley fill is interpreted to consist almost entirely of fluvial-estuarine and estuarine central-basin sediments. Reynaud et al. (1999) and this paper show that transgressive facies will dominate the fill, if the rate of relative sea-level rise exceeds that of sediment flux.

Comparisons with other incised valley system studies

East Coast United States. The Beach Haven tributary channel, on the New Jersey inner shelf (Ashley and Sheridan, 1994), displays size and geometry similar to the outer shelf incised valleys described in this paper. The Beach Haven system represents a drowned river estuary eventually filled and buried during the Holocene transgression. The valley fill consists of 1 m of pebbly sand overlain by 3-4 m of organic clay (Ashley and Sheridan, 1994). The authors suggest that the pebbly sand was deposited fluvially

when the shoreline was farther seaward; these deposits likely correlate with my SF1 facies (Figure 3.6). The organic clay was deposited as sea-level continued to rise and the valley became a drowned river estuary (Ashley and Sheridan, 1994). I relate these sediments to my SF3 facies (Figure 3.6).

Foyle and Oertel (1997) have also identified transgressive paleo-valley-fill successions on the Virginia inner shelf. These fluvially incised valleys were modified during subsequent marine transgression, as dendritic riverine drainage basins evolved to become estuaries. The fill of these valleys is punctuated by a bay flooding surface, and both tidal and wave ravinements. However, valley fills were dominated by estuary mouth deposits of the outer zone (Figure 3.16; Dalrymple et al., 1992; Zaitlin et al., 1994) that overlie a high-relief tidal ravinement surface (Figure 3.16). Fluvial deposits are only locally preserved above the fluvial erosion surface, in contrast to significant SF1 thickness throughout my mapped survey area (Figure 3.12A). Aggradation of lowstand fluvial deposits may not have occurred in Virginia inner shelf fluvial valleys during the latest Pleistocene. Instead, higher relief fluvial channels, incising the emerging shelf during regression and lowstand, would have bypassed fluvial sediments downdip, towards the paleo-shoreline near the modern shelf-break.

Gulf of Mexico. Incised valleys offshore Mobile, Alabama (Bartek et al., 2004) are morphologically and stratigraphically similar to New Jersey incised paleo-valleys. Two valleys were cut during stream rejuvenation associated with subaerial exposure during the LGM, through headward (knickpoint) erosion of coastal streams initiated at the shelf edge, by way of a mid-shelf or topographic break. Nordfjord et al. (2005) have shown similar formative mechanism for the New Jersey valleys. The rapid rate of sea-level fall on both shelves (Figure 3.1) resulted in multiple incised valleys in both locations, as individual drainage systems were not able to keep pace with the falling sea-

level (Wood et al., 1993). However, the vertical facies stacking pattern off Alabama differs from the stacking patterns preserved off New Jersey, particularly in preservation of a well-developed, prograding bayhead-delta facies. Mapped incised valley systems off Alabama are also larger and closer to the shoreline today than my New Jersey systems, as they may be connected with the Mobile River (Bartek et al., 2004).

Studies of fill units mapped within the Trinity/Sabine incised-valley systems off Texas have recognized three landward-stepping parasequences, consisting of paired upper-bay and flood-tidal delta/tidal-inlet facies (Thomas and Anderson 1994). These parasequences are bounded by flooding surfaces (which possibly correlate with my B2 surface), formed when sea-level rise flooded antecedent fluvial terraces along the valley, increasing accommodation space (Rodriguez et al., 2004). The New Jersey paleo-valleys do not show any evidence of fluvial terraces; however, their fill consists of seismic facies similar to those characterizing valley fills on the gently dipping, low subsidence, wide east Texas shelf (Thomas and Anderson, 1994). Fluvial lags, central basin, flood-tidal delta and tidal inlet deposits there all correspond to my SF1, SF3 and SF4 facies, respectively (Figure 3.6).

One ancient analog. The Pennsylvanian Morrow Formation in eastern Colorado and Kansas (Krystinik, 1989) is an ancient setting that shows similarities with New Jersey paleo-valleys. Morrow Formation fills are interpreted to incised valley deposits. The valleys were cut during glacially-induced eustatic sea-level drops, and then gradually filled with sediment as base level rose during interglacial transgressions.

CONCLUSIONS

Incised paleo-valleys along passive margins commonly develop during lowstands (Vail, 1987; Van Wagoner et al., 1987, 1988). The New Jersey coastal plain incised

valley systems documented here are the product of a single sea-level cycle that incorporates lowstand and transgressive system tracts. The valley fill occupies incisions that were likely cut during the Last Glacial Maximum. New Jersey outer shelf estuaries resulted from drowning of these river valleys during ensuing sea level rise; their stratigraphic organization reflects successive migration of depositional environments during transgression. From oldest to youngest, recognized seismic facies can be interpreted as fluvial lags (SF1), estuarine mixed sand and muds (SF2), estuary central bay muds (SF3) and redistributed estuary mouth sands (SF4). Estuary filling occurred within a framework of ongoing relative sea-level rise. The dominant sediment supply was from marine sources, the product of continued reworking and redistribution by tides and waves. The resulting stratigraphy was composed largely of transgressive facies, i.e., central basin (SF3), flood-tidal delta and tidal inlet (SF4), bounded by flooding (B1 and B2) and ravinement (B3 and T-horizon) surfaces. I suggest two possibilities to explain downdip changes in the thickness of the finer grained SF3 and coarser grained SF4 units: (1) that the transgressive migration of the seashore across this region did not occur uniformly, but rather with pauses or even transitory regressions that affected total accumulation of these units as a function of proximity to the shoreline, or (2) that the resultant partition between fine (SF3) and coarse (SF4) grained sediments in the valley fill is strongly influenced by valley morphology, with wave forces favoring coarse-grained deposition in the wider valley portions of these systems.

Evidence from the fill stratigraphy of New Jersey shelf incised paleo-valleys suggests a transition from tide-dominated to wave-dominated with time. New Jersey incised valleys did not receive significant fluvial sediment supply during transgression, so bayheads are absent. Instead, sands in the upper fill units of New Jersey valleys were derived by longshore transport and headland erosion.

132

Chapter 4: The formation of the transgressive ravinement surface on New Jersey mid-outer continental shelf: implications for margin erosion and deposition

INTRODUCTION

Transgressive deposits on continental shelves are of interest in both academic and applied research (Cattaneo and Steel, 2003). These deposits are particularly interesting within the context of recently developed sequence stratigraphic concepts (Swift and Thornea, 1991; Posamentier, 2002), because of their often sand-rich composition and variable stratigraphic expression, including backstepping shoreline/deltaic deposits, transgressive lag deposits and offlapping shelf wedge or the "healing phase" deposits (Swift and Thorne, 1991a; Posamentier and Allen, 1993; Galloway and Hobday, 1996). Transgressive sands are commonly more mature both texturally and mineralogically than regressive sands, and therefore in many cases also make excellent hydrocarbon reservoirs (e.g., Snedden and Dalrymple, 1999; Posamentier, 2002). Unfortunately, these transgressive sediments are also difficult to study, because they are commonly very thin over generally flat coastal plains/exposed shelves, usually as a result of a rapidly transgressing shoreline.

Although maximum flooding or near-maximum flooding conditions exist today on most continental margins globally, surprisingly few high-resolution seismic profiles are available to resolve the depositional geometry of patchy Holocene transgressive deposits on continental shelves. One prominent exception is the continental shelf off New Jersey (Figure 4.1), where the shallow stratigraphy has been studied extensively for more than 30 years (e.g., Emery and Uchupi, 1984; Knebel and Spiker, 1977; Swift et al., 1980; Milliman et al., 1990; Davies et al., 1992; Goff et al., 1999; Duncan et al., 2000;

Fulthorpe and Austin, 2004; Gulick et al., 2005; Nordfjord et al., 2005). These studies have provided insights into spatial and temporal variations of latest Pleistocene-Holocene sediment deposition, erosion and transport caused by variations in both supply and accommodation space. Interpretations based on very high-resolution seismic data of the shallow sub-seafloor, coupled with samples of transgressive deposits of the last sea-level cycle, are most informative because of my detailed knowledge of eustatic sea-level behavior during the last ~50 kyr (Fairbanks et al., 1989; Bard et al., 1990; Lambeck and Chappell, 2001). I also have estimates of shoreface location on the New Jersey shelf during the Holocene transgression, as well as knowledge about bottom current direction and magnitude since the Last Glacial Maximum (LGM; Dillon and Oldale, 1978; Duncan et al., 2000; Butman et al., 2003).

The New Jersey continental shelf is wide, exhibits low-relief physiography, and is tectonically quiescent with a long-term, low sediment supply regime. Stratigraphic studies of this and similar margins indicate that such high-energy, sediment-starved shelves are the site of active transport of sediment seaward (Swift and Thorne, 1991). In general, both sediment supply and hydrodynamic regime dominate the formation of internal geometry of surficial shelf depositional sequences on very short time intervals (decades to millennia), even during cycles that are primarily driven by sea-level oscillations (Thorne and Swift, 1991). Sediment starvation, coupled with high-frequency eustatic fluctuations associated with glacial events, have created laterally-variable lowstand and transgressive deposits and composite erosional surfaces on the New Jersey continental shelf that can only be mapped with three-dimensional, high-resolution seismic control. Fortunately, the New Jersey shelf has been the site of both modern, high-resolution seismic data acquisition and precisely-positioned sediment cores to ground-truth those images.

My goal in this Chapter is to identify key markers in the shallow sedimentary record of the New Jersey shelf that tell us about the interplay of erosional and depositional processes during the Holocene transgression. I use a suite of ultra-high resolution chirp reflection data (1-4 and 1-15 kHz), swath bathymetry, grab samples and short cores (Figure 4.1) on the mid-outer New Jersey shelf to map an important regional stratigraphic horizon, interpreted as the Holocene transgressive ravinement surface, and the overlying surficial sand sheet on what is today a storm-dominated margin. I examine the significance of the ravinement, previously named the T-horizon (Duncan et al., 2000) and its complex with respect to the Holocene transgression, in order to demonstrate how the complex geometry of T influences both the depositional architecture of overlying sediments and the locus of marine erosion during the Holocene sea-level rise.

GEOLOGICAL SETTING OF THE T-HORIZON AND THE SURFICIAL TRANSGRESSIVE SEDIMENTS

My study area is located between the Mid-shelf (~50 m depth) and Franklin (~100 m depth) scarps on the New Jersey shelf (Figure 4.1). These two scarps have previously been interpreted as drowned Holocene paleo-shorelines (e.g., Dillon and Oldale, 1978). However, the mid-shelf scarp, which has been named variously the Fortune shore (Veatch and Smith, 1939), the Tiger scarp (Knebel and Spiker, 1977) and the mid-shelf shore (Swift et al., 1972; Goff et al., 1999), has recently been re-interpreted as the seaward edge of a depositional lobe generated subaerially as massive outpourings from collapsed glacial lakes along the Hudson River ~17-14 kyr, associated with retreat of the Laurentide ice sheet (Uchupi et al., 2001; Donnelly et al., 2005). Duncan (2001), while concurring that the mid-shelf scarp represents a depositional front, has disputed the timing of its formation, based upon interpretations of high-resolution chirp seismic data

135

(Figure 4.1). Duncan (2001) has proposed that the surficial wedge is instead a prograding clinoform that postdates the interpreted transgressive ravinement, the T-horizon, and so must have been deposited in a marine setting ~10-8 ka, after the postulated glacial lake collapses. This depocenter lies south of the Hudson Shelf Valley, a broad swale in the seafloor that bisects the Mid-Atlantic Bight and extends from the mouth of the modern Hudson River to the head of Hudson Canyon (Figure 4.1; Butman et al., 2003). The Hudson Shelf Valley has been interpreted as a partially-filled extension of the Hudson River valley cut during one or more episodes of shelf exposure during lowered sea level (Freeland et al., 1981). Such a swale would prevent debris from glacial lake collapse from reaching the vicinity of the mid-shelf scarp (Figure 4.1).

Three primary horizons bound the latest Pleistocene-Holocene stratigraphy of the New Jersey shelf: the R-horizon, the Channels-horizon, which incises the R-horizon, and the T-horizon, which truncates all other material and forms the base of the surficial sand sheet (Davies et al., 1992; Duncan et al., 2000; Duncan, 2001; Goff et al., 2005; Nordfjord et al., 2005). The R-horizon (Figure 4.2A) is a regionally recognized, generally high-amplitude reflection that forms the base of the outer shelf wedge (Milliman et al., 1990). The origin of this surface is complex, but its age (~40 kyr) makes it considerably older than the latest sea-level regression associated with the LGM. The outer shelf wedge is a series of offlapping strata deposited on the R-horizon, presumably as a late Wisconsinan regressive deposit (Gulick et al., 2005). The Channels-horizon (Figure 4.2B) delineates an incised valley system that erodes both the outer shelf wedge and in places the R-horizon (Davies et al., 1992; Austin et al., 1996; Duncan et al., 2000; Nordfjord et al., 2005). Ages of channel-fill sediments of ~12.5 kyr (Buck et al., 1999) indicate that these channels were likely carved during the LGM lowstand and then filled as the shoreline migrated across this region during the ensuing Holocene transgression.

The T-horizon (Figure 4.2B) caps channel-fill strata, truncates the Channels-horizon (Duncan et al., 2000; Goff et al., 2005; Nordfjord et al., in revisions) and forms the base of the surficial sand sheet (Goff et al., 1999). Duncan et al. (2000) interpret the T-horizon as the transgressive ravinement associated with Holocene sea-level rise. A core through the surficial sand sheet has penetrated 23 cm to a muddy, sandy shell hash layer, which Goff et al. (2005) hypothesize represents lag associated with ravinement erosion. Currents that erode the substrate during the formation of such a ravinement act as winnowing agents, resulting in deposition of such lag deposits across this erosional surface (Galloway and Hobday, 1996; Nummedal and Swift, 1987; Posamentier, 2002).

Oblique sand ridge morphology, a variably thick veneer of well-sorted sand, and an assemblage of recognizable marine fauna typify modern siliciclastic, sediment starved shelfal surfaces around the world (Anderson et al., 1996; Berne et al., 1998; Goff et al., 1999; Tesson et al., 2000). The New Jersey surficial sand sheet has been deposited upon the T-horizon in response to Holocene transgression and post-transgressive processes (Goff et al., 1999; Duncan et al., 2000). The Holocene sand sheet has likely been winnowed from underlying, fluvial substrata during landward migration of the shoreface in response to rising sea-level (Swift and Thorne, 1991). That sheet, composed largely of oblique sand ridges, originally formed at the shoreface and has since been modified by continued reworking (Figure 4.2A; Swift et al., 1972; Snedden and Dalrymple, 1999; Goff et al., 1999). Analyses of swath bathymetry, backscatter, grab samples and chirp seismic data on the outer New Jersey shelf all suggest that sand ridges in water depths of >50m are moribund (Goff et al., 1999). However, localized erosion, resulting in the formation of ribbon-floored swales and scour pits (Figure 4.1), has significantly modified the surficial sand sheet since its deposition, at least through mid-shelf water depths (Goff et al., 1999, 2005).

Goff et al. (2005) document post-transgressive marine erosion on the outer New Jersey shelf. The timing of erosion is constrained by truncation at the seafloor of the transgressive ravinement surface, the T-horizon, and truncation of moribund sand ridges along erosional swales oriented parallel to the primary direction of modern bottom flow (approximately southwest) and oblique to the strike of the ridges (Figure 4.1; Galloway and Hobday, 1996, p. 177). Goff et al. (2005) infer that this erosion postdates passage of the shoreface and the evolution of bedforms that evolved in the near-shore environment during transgression. Depths of erosion reported from their study range from a few meters to >10 m; the seafloor within eroded areas is often marked by "ribbon" morphology (Figures 4.1, 4.2A and C). Goff et al. (2005) suggest that significant modification of the seabed at greater water depths has continued to take place through bottom current-driven erosion.

DATA AND METHODS

A suite of ultra-high resolution, deep-towed chirp seismic reflection profiles and samples from shallow drilling were acquired on the New Jersey shelf in 2001 and 2002. The chirp seismic data were collected aboard the R/V *Endeavor* (cruise EN359) over a broad region of the middle and outer shelf south of the Hudson Shelf Valley and Canyon (Figure 4.1). Track line spacing varied from 50 m to 1 km, and the towfish was flown at ~10 m above the seafloor. The 1-4 and 1-15 kHz chirp source resulted in vertical resolution of ~10 cm, a lateral trace spacing of ~0.5 m, and imaging of surficial strata to depths of up to ~30 m (Figures 4.2 and 4.3). Seismic data presented here have been deconvolved with the source wavelet and tidal static effects have been removed (Luhurbudi et al., 1998).

Bathymetric data for the outer New Jersey shelf are available from two primary

sources. A multibeam bathymetry and backscatter survey was conducted on the middle and outer New Jersey shelf in 1996 (Figure 4.1; Goff et al., 1999). This survey employed a 95 kHz, Simrad EM1000 multibeam system mounted on the CHS *Creed*. These data have been combined with archive data available from the National Geophysical Data Center (Figure 4.1).

Sample and sedimentary age constraints, though sparse, are available from a variety of sources. Grab samples and short cores were collected on the R/V *Cape Henlopen* in 2001, within the multibeam survey area (Figure 4.1). These provide geologic information on surface and near-surface sediments. Archival sediment cores and age dates can be found in a number of published sources (Knebel and Spiker, 1977; Knebel et al.,1979; Buck et al., 1999). In 2002, cores have been collected using the Automatic Heave Compensated-800 system (http://www.dosecc.org) aboard the R/V *Knorr* (Nielson et al., 2003). Three sites were sampled to a maximum penetration of ~13 mbsf (Figure 4.1).

Using the chirp data, I have analyzed groups of reflections to differentiate external form, configuration, continuity, amplitude and frequency, and sequence boundaries have been identified from reflector terminations. For example, I identify the T-horizon by truncation of reflectors below and subtle onlap above (Figures 4.2 and 4.3). Observations of the T-horizon are facilitated below sand ridges and above channel fills (e.g., Figure 4.2A). Based upon profile interpretation, I have generated a structure contour map for the T-horizon (Figure 4.4), and isopach maps for sediments between the R- and the T-horizons (Figure 4.5) and for the surficial sand sheet above the T-horizon (Figure 4.6).Bathymetric data for the outer New Jersey shelf are available from two primary sources. A multibeam bathymetry and backscatter survey was conducted on the middle and outer New Jersey shelf in 1996 (Figure 4.1; Goff et al., 1999). This survey

139
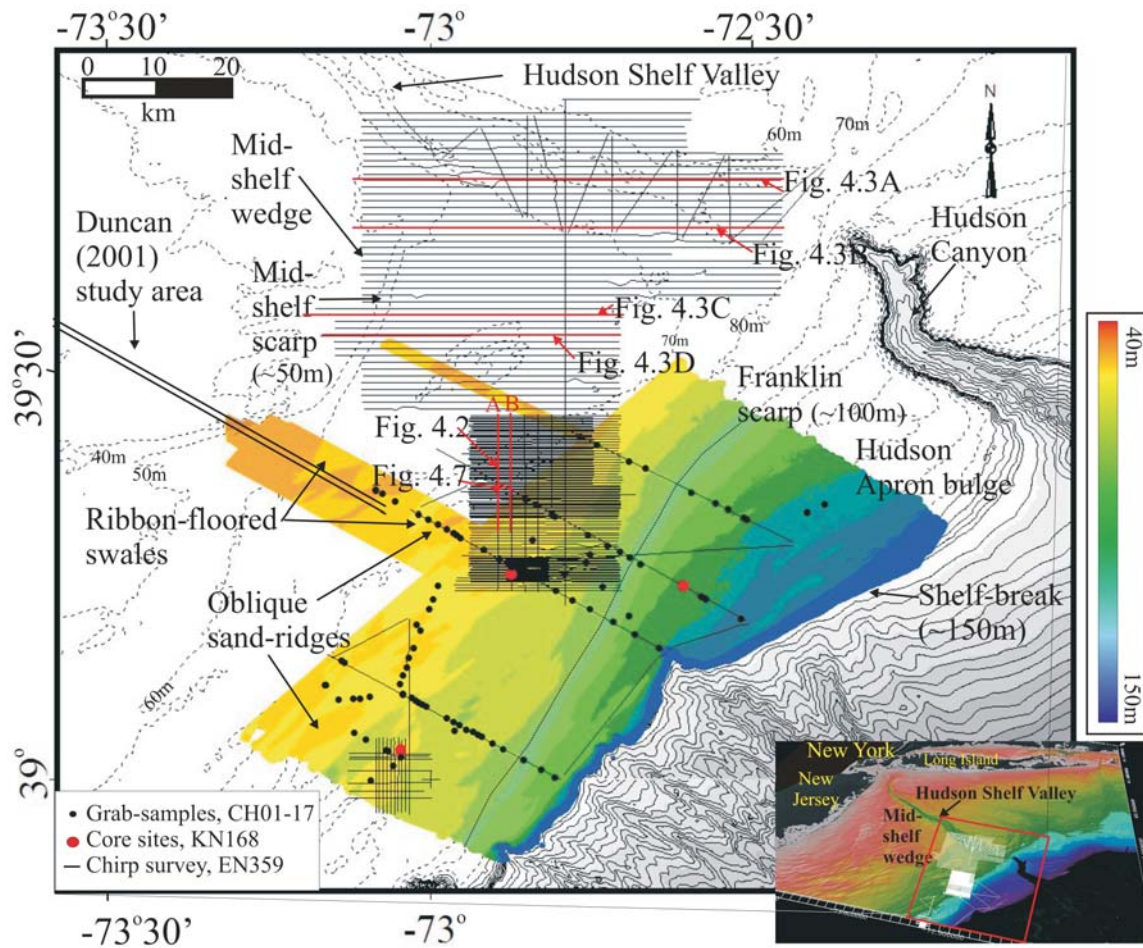
Figure 4.1: Locations of deep-towed, chirp sonar seismic reflection profiles collected aboard R/V Endeavor during cruise EN359, superimposed on annotated multibeam (color contoured; Goff et al., 1996) and NOAA bathymetry (line contoured in m) of the New Jersey middle and outer continental shelf. Inset locates the study area within a 3-D rendering of the Mid-Atlantic Bight. Locations of grab samples (CH01-17) and AHC-800 (KN168) core sites are identified, as are locations of Figures 4.2, 4.3 and 4.7.

employed a 95 kHz, Simrad EM1000 multibeam system mounted on the CHS *Creed.* These data have been combined with archive data available from the National Geophysical Data Center (Figure 4.1).

SEISMIC OBSERVATIONS OF T-HORIZON AND HOLOCENE SAND SHEET:

The T-horizon is observed regionally as a variable but generally moderate-amplitude reflector (Figure 4.2A; Duncan et al., 2000). The T-horizon truncates shallowly buried channel systems (Figure 4.2A; Duncan et al., 2000; Nordfjord et al, in revision) and underlies the surficial sand sheet and the Holocene mid-shelf wedge (Figures 4.2B and 4.3B; Goff et al., 1999; Duncan et al., 2000). Between the mid-shelf scarp at ~50 m water depth and the Franklin scarp at ~100 m, the T-horizon is undulatory but mostly subparallel to the modern seafloor (Figures 4.2B and 4.4). At the mid-shelf scarp (Figures 4.1 and 4.4), a ~15 m topographic step is also observed on the T-horizon between 37 m and 52 m water depth, with slopes approaching 2˚ (Figures 4.3C and 4.4). This is much steeper than the slope (~0.12˚) of the same step in the T-horizon noted by Duncan (2001) along a crossing of the scarp further south (Figure 4.1). In several places, the T-horizon appears to outcrop or is truncated at the seafloor, exposing underlying uppermost Pleistocene sediments (Figures 4.2B and 4.3A). Available samples constrain the age of the T-horizon landward of the ~90 m isobath to between that of outer-shelf channel-fill muds, AMS ^{14}C 12.3 ± 0.45 kyr (Buck et al. 1999), and that of many ^{14}C dates of <10 kyr from the surficial sand sheet on the outer shelf (Figure 4.5; Knebel and Spiker, 1977; Alexander et al., 2003).

The mid-shelf wedge is a lobate sediment deposit on the shelf south of the Hudson Shelf Valley in ~30-50 m water depth (Figure 4.1), which I can observe both on
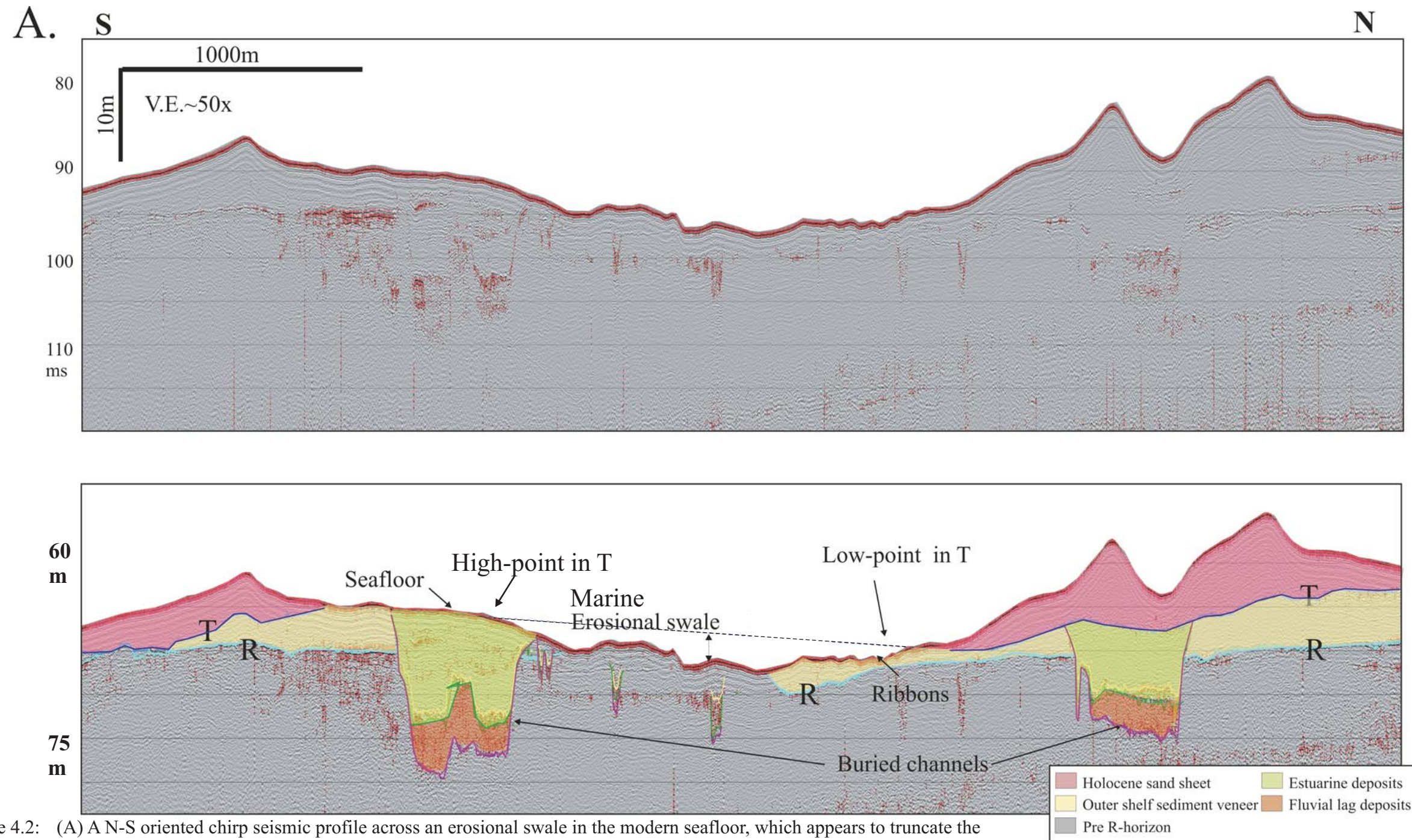
Figure 4.2: (A) A N-S oriented chirp seismic profile across an erosional swale in the modern seafloor, which appears to truncate the interpreted transgressive ravinement surface (horizon T). Ribbon-floored morphology is observed within this swale, above a low-point in the T-horizon. Shallow subsurface channels that truncate the R-horizon are interpreted as fluvial (Davies et al., 1992; Duncan et al., 2000; Nordfjord et al., 2000, submitted); their fills consist of estuarine sediments overlying fluvial lags (Nordfjord et al., submitted).(B) A profile parallel to A , but located ~1 km east of A. A younger asymmetrical incision is observed, which we interpret as a possible tidal inlet filled by remnant back-barrier/lagoon strata. The moderate amplitude T-horizon is truncated on both sides of the depression created by post-transgressive erosion. The ravinement, T, and the seafloor are also truncating the underlying, box-shaped channels, which are associated with fluvial incision at or near the LGM (Davies et al., 1992; Duncan et al., 2000; Nordfjord et al., 2005). These channels were subsequently infilled in an estuarine setting during Holocene sea-level rise (Buck et al., 1999; Nordfjord et al., in revision). For locations, see Figure 4.1.

B.

S

N

80

90

100

110
ms

60
m

1000m

V.E.~50x

10m

Seafloor

Local high in T

Marine erosional (post-transgressive) swale

T

R

T

R

75
m

Back-barrier lagoonal deposits?

Strike-oriented incision (Tidal inlet?)

Buried channels

Holocene sand sheet	Estuarine deposits
Outer shelf sediment veneer	Fluvial lag deposits
Pre R-horizon	

143
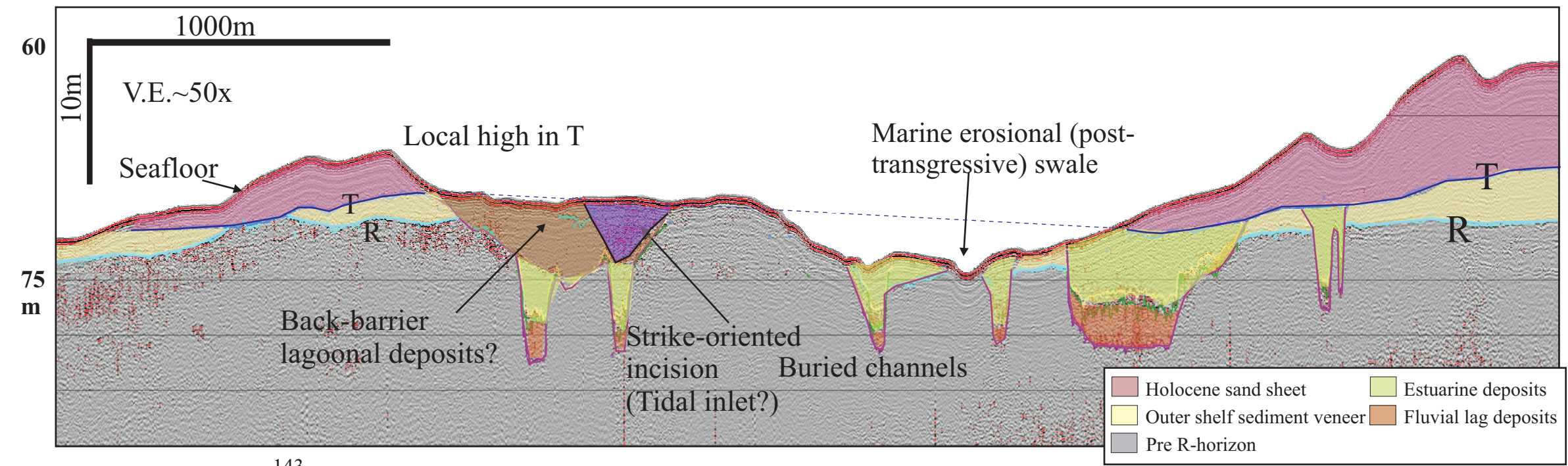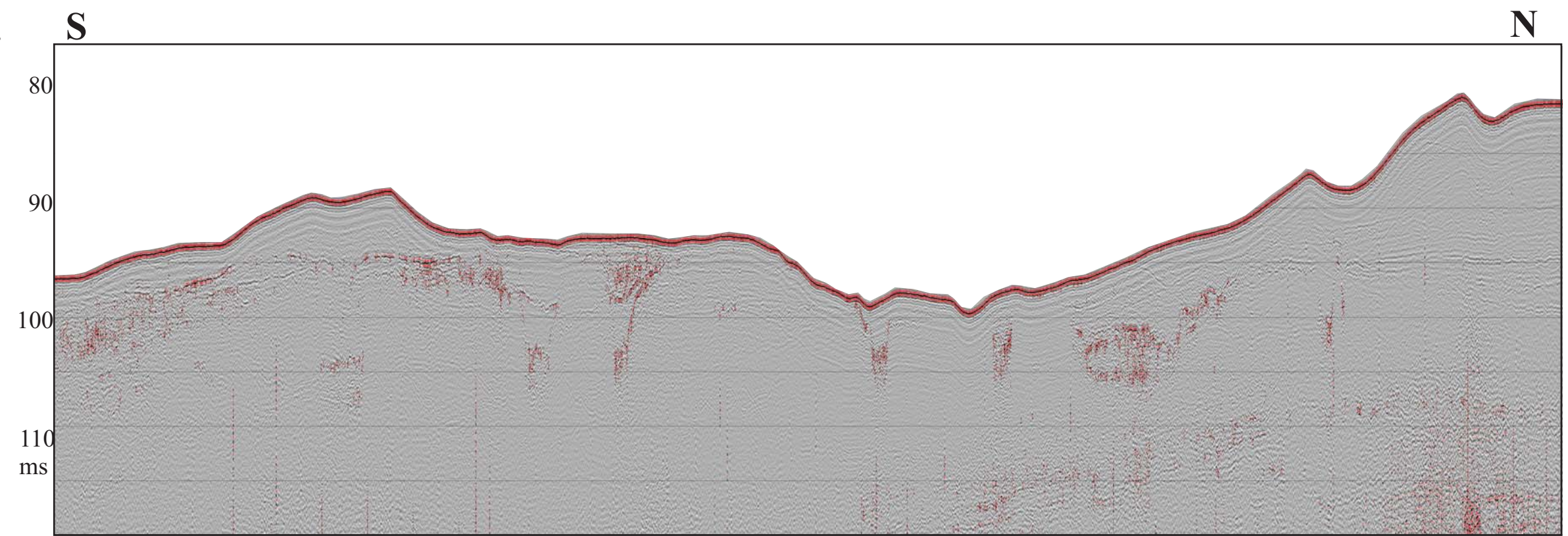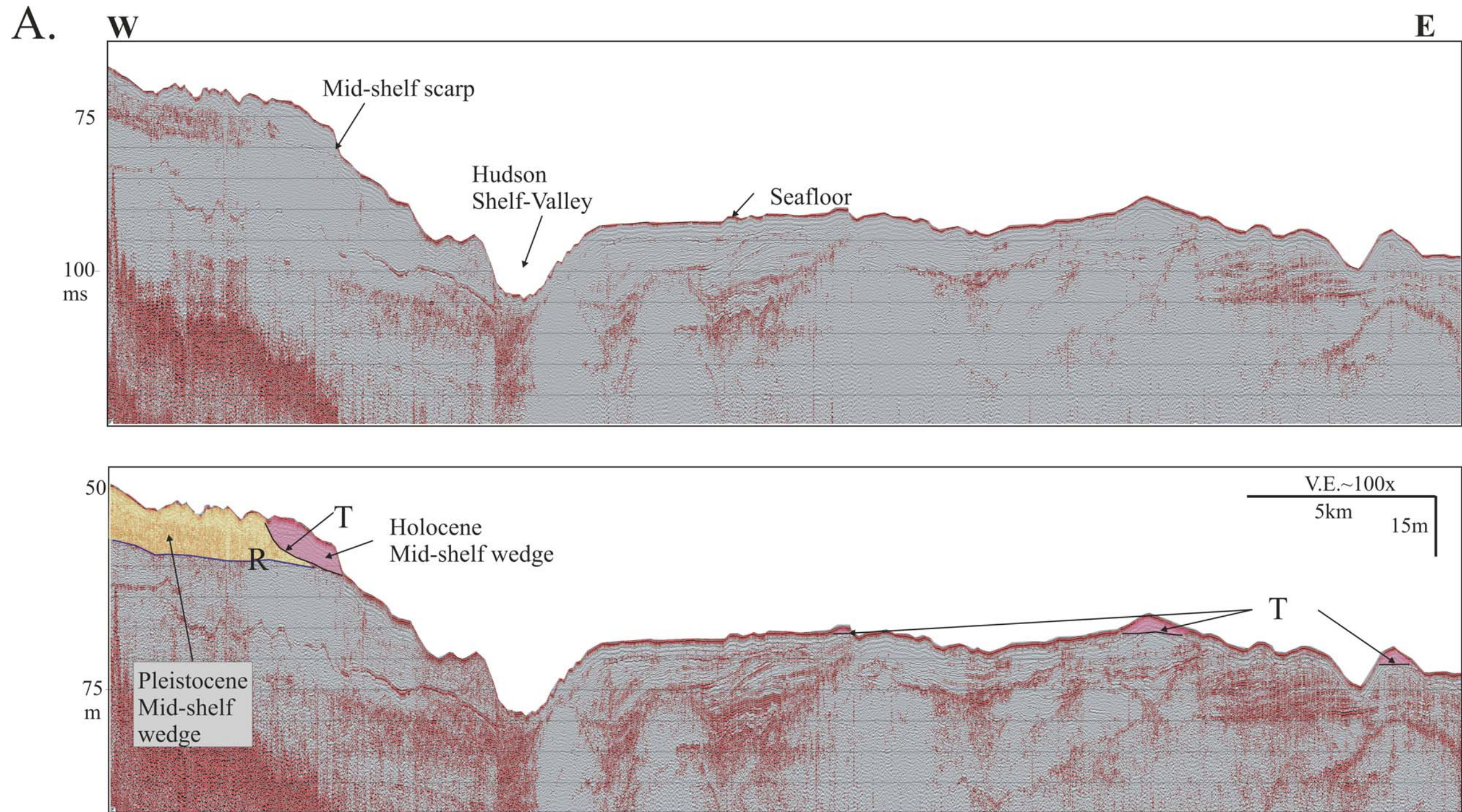
Figure 4.3: Chirp seismic profiles crossing the mid-shelf scarp and extending seaward. All these cross-sections image the latest Pleistocene mid-shelf wedge. However, only profiles A and B show the smaller Holocene mid-shelf wedge; these profiles also display how the T-horizon is truncated by erosion at or near the modern seafloor. On profiles C and D, the T-horizon truncates incisions within the latest Pleistocene mid-shelf wedge. Incisions observed in C and D are assumed to be LGM-related fluvial incisions (Duncan et al., 2000; Nordfjord et al., 2005), later filled with estuarine deposits and subsequently drowned during the Holocene transgression (Nordfjord et al., in revision). On C, it is evident from truncation of underlying channels that the mid-shelf scarp was formed by post-transgressive erosion of the T-horizon. On all profiles, the T-horizon forms the base of surficial sand ridges (Goff et al., 1999). See location in Figure 4.1.

B.

146

D.

W   E

Mid-shelf scarp

Seafloor

75

100
ms

T truncates
underlying
channel

V.E.~100x

5km

15m

50

R

Sand ridges

T

Marine
Erosional swale

Pleistocene
Mid-shelf
wedge

75
m

147
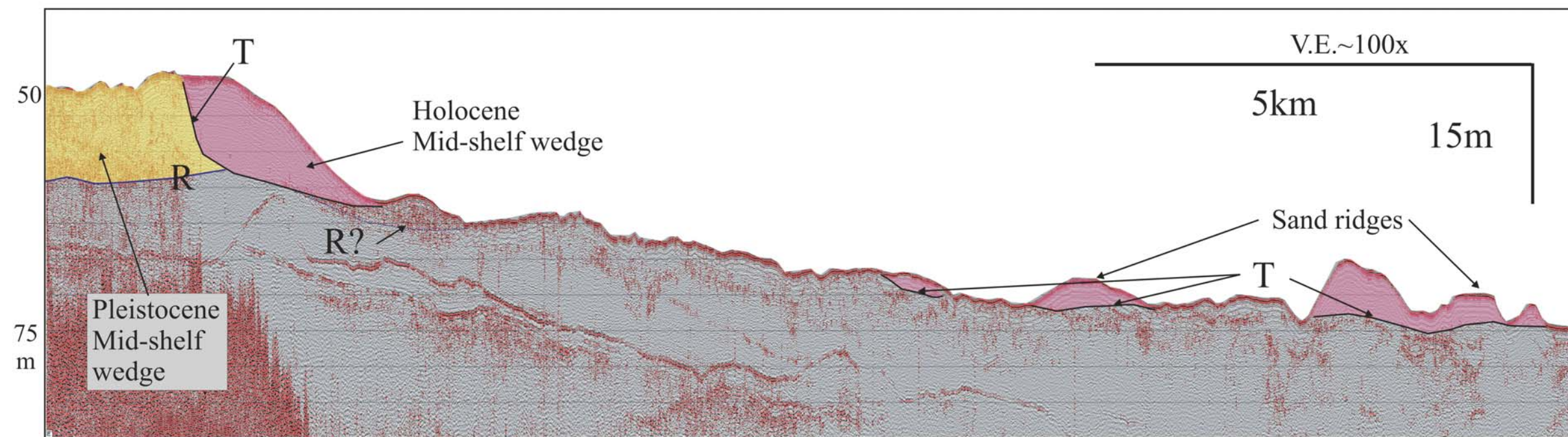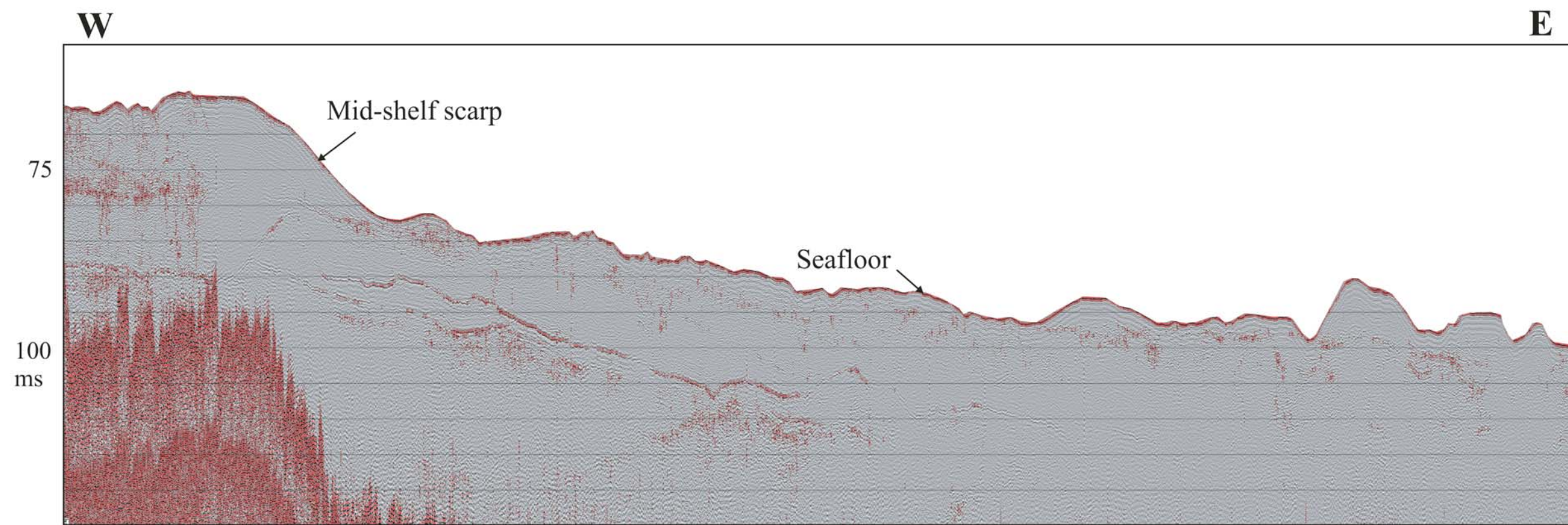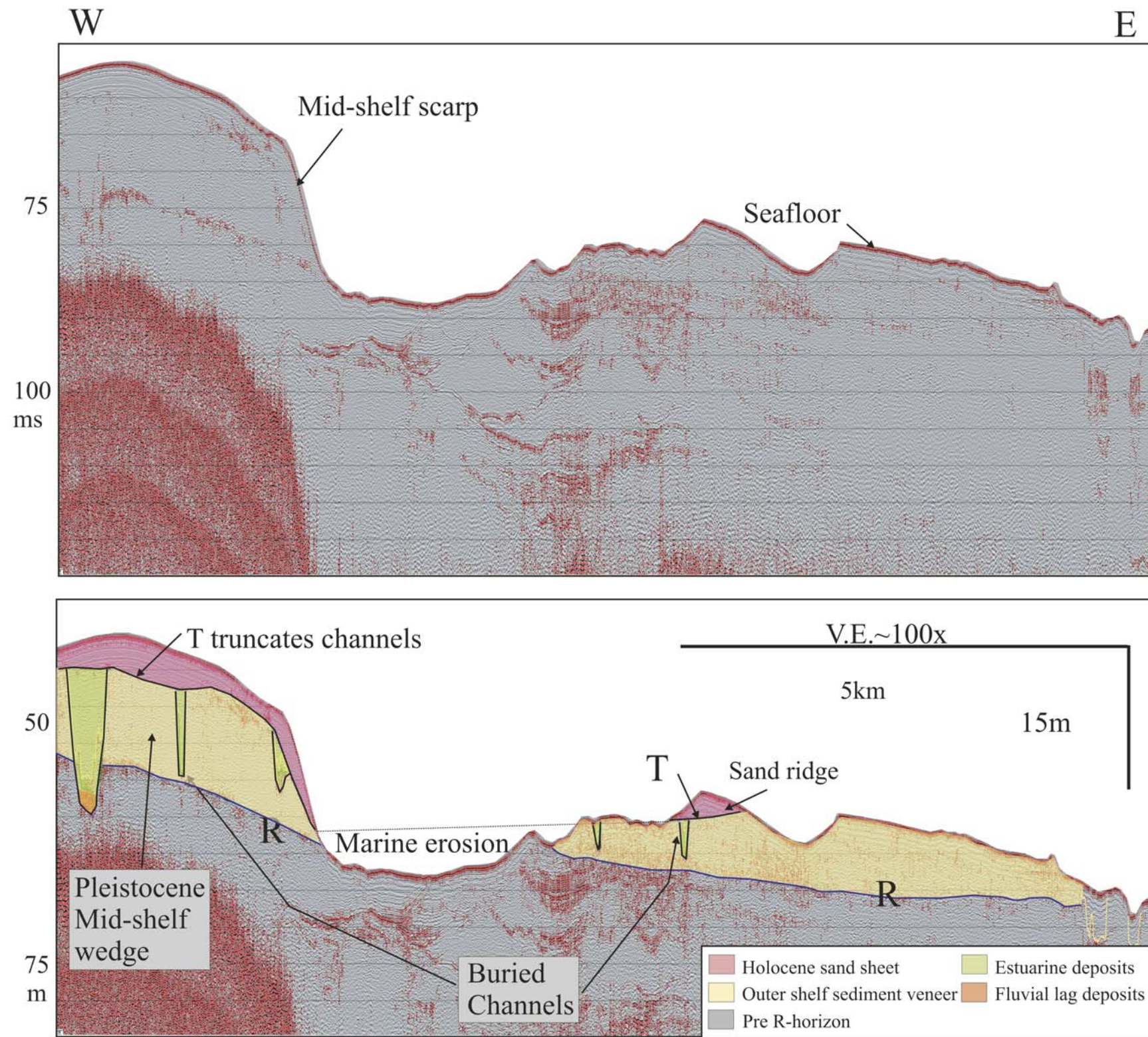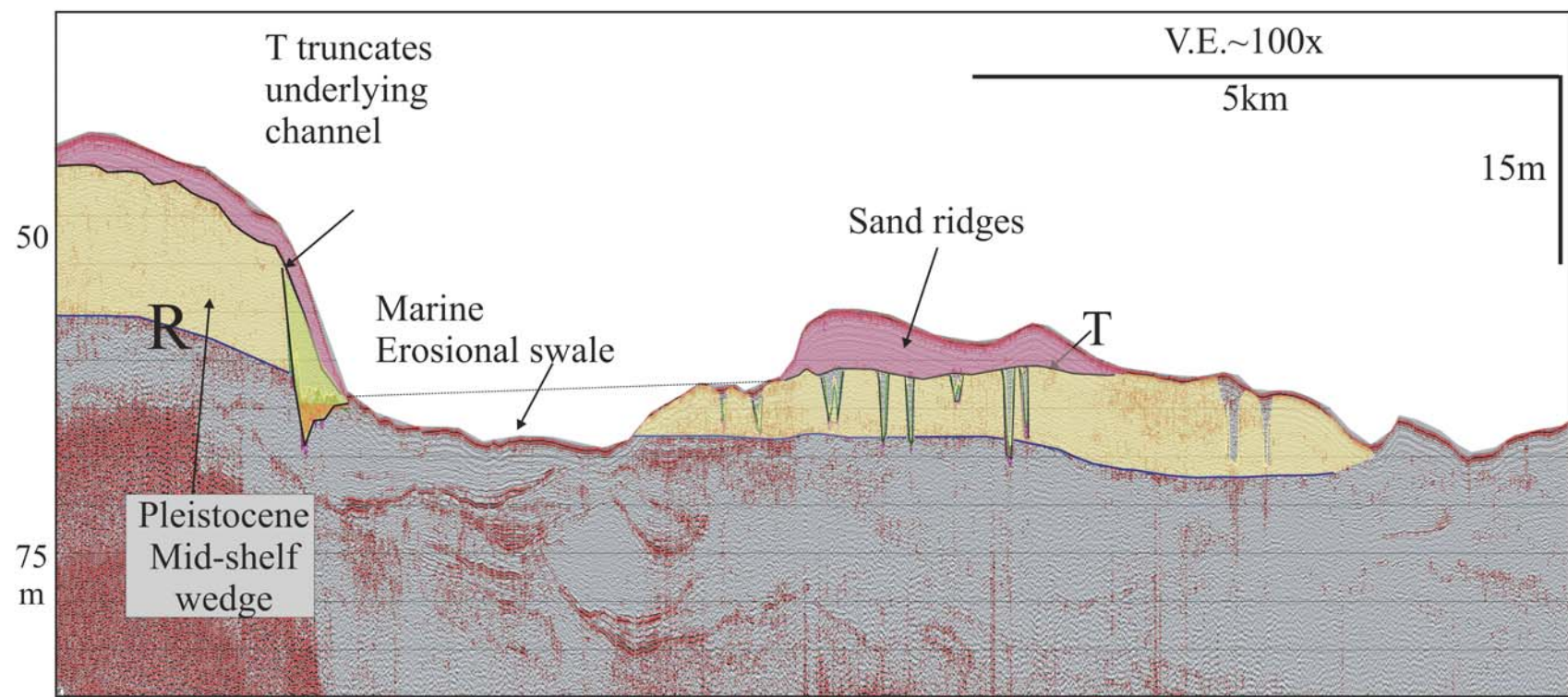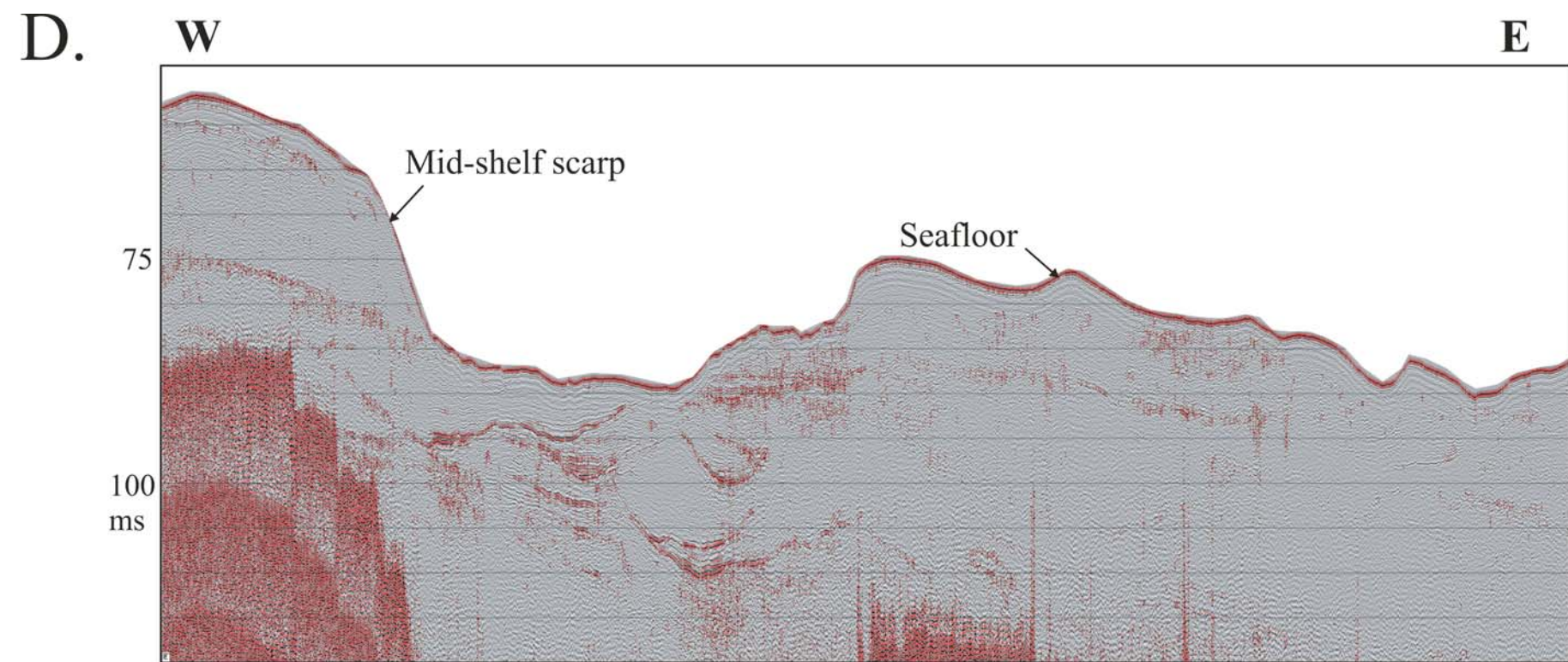
can be divided into at least two parts; the T-horizon separates a smaller, overlying Holocene component from a thicker, underlying uppermost Pleistocene component (Figure 4.3A). An isopach map of the unit between the older (~40 kyr) R-horizon and the younger (<10-12.3 kyr) T-horizon shows ~15 m of sediments within the mid-shelf wedge (Figure 4.5, #4) and >30 m of sediments within the outer-shelf wedge (Figure 4.5, #5; Milliman et al., 1990; Gulick et al., 2005). Sediments cored from the mid-shelf wedge landward of the mid-shelf scarp by Knebel et al (1979) are partitioned into a younger, Holocene-age sand unit with ^{14}C dates <8 kyr, and a lower muddy unit with ^{14}C dates >28 kyr (Figure 4.6). Although Knebel et al (1979) did not observe the T-horizon on their lower-resolution seismic data, I can reasonably assume that the boundary between their Holocene sands and Pleistocene muds represents this transgressive ravinement, and that the muds in turn represent the unit I have since identified as the Pleistocene mid-shelf wedge (Figures 4.3C and 4.5). The smaller Holocene mid-shelf wedge is significant only in the northeast (Figures 4.3B and 4.6) and southwest (as reported by Duncan, 2001) ends of the mid-shelf scarp. This Holocene wedge has an aggradational (i.e., vertical stacking pattern) rather than retrogradational (i.e., landward progradational) seismic characteristic (Figure 4.3B), which infers sufficient sediment supply. The steeper parts (~2°) of the scarp do not exhibit a Holocene wedge (Figure 4.3C and D); these steeper declivities are coincident with a region of intense recent/modern erosion evidenced by outcropping of subsurface reflections (Figure 4.4, #1; Figure 4.3C and D). This area of focused erosion is ~8 km wide, >15 km long, ribbon-floored and oriented NNE-SSW (Figure 4.6). Both the T-horizon and the R-horizon outcrop along both flanks of this depression (Figure 4.3C and D).

Although largely obscured by a post-transgressive erosional swale (Figure 4.4; Goff et al., 2005), there is seismic evidence for a topographic low in the T-horizon just

multibeam bathymetry data and on the chirp seismic profiles (Figures 4.1 and 4.3B). Seismic cross-sections show that the wedge seaward of the mid-shelf scarp (Figure 4.3C and D). The T-horizon outcrops along either side of the erosional swale in the seafloor, but it is clear on these two profiles that the outcrop of the T-horizon at the landward (western) edge is deeper than the outcrop at the seaward (eastern) edge (Figure 4.3D). Recent marine erosion is spatially coincident with this relief in the transgressive ravinement surface (Figure 4.3D).

Another significant topographic low/high association in the T-horizon is observed at ~70 m water depth, which is not associated with any scarp (Figure 4.2A and B). This low is coincident with a post-transgressive erosional swale (Figure 4.4) which truncates the T-horizon (Figure 4.2C). Seaward (south) of this topographic low (Figure 4.4), I observe a wedge-like succession cut by a ~1500-m-long, strike-oriented incision (Figures 4.2B, 4.4 and 4.7). This incision is stratigraphically younger than the dendritic channel system (Nordfjord et al., in revision), and has a more asymmetrical geometry than the box-shaped dentritic channels in this region (Figure 4.7; Nordfjord et al., 2005). I also observe packages of lateral accretion within its fill (Figure 4.7).

Other interesting geomorphologic features revealed by the isopach map of the surficial sand sheet (Figure 4.6) are (1) a lobe-like sediment unit on the northern side of the Hudson Shelf Valley, (2) several clusters of ENE-WSW trending, presumably relict, oblique-to-flow ridges located adjacent to areas of modern erosional swales, and (3) a field of five parallel sand ridges located in the eastern side of the mouth of the Hudson Shelf Valley in 70-80 m water depth, proximal to the Hudson Canyon (Figure 4.6). These low width/depth ratio ridges have also been recognized by Butman et al. (2003) on high-resolution multibeam bathymetry of this area.

149
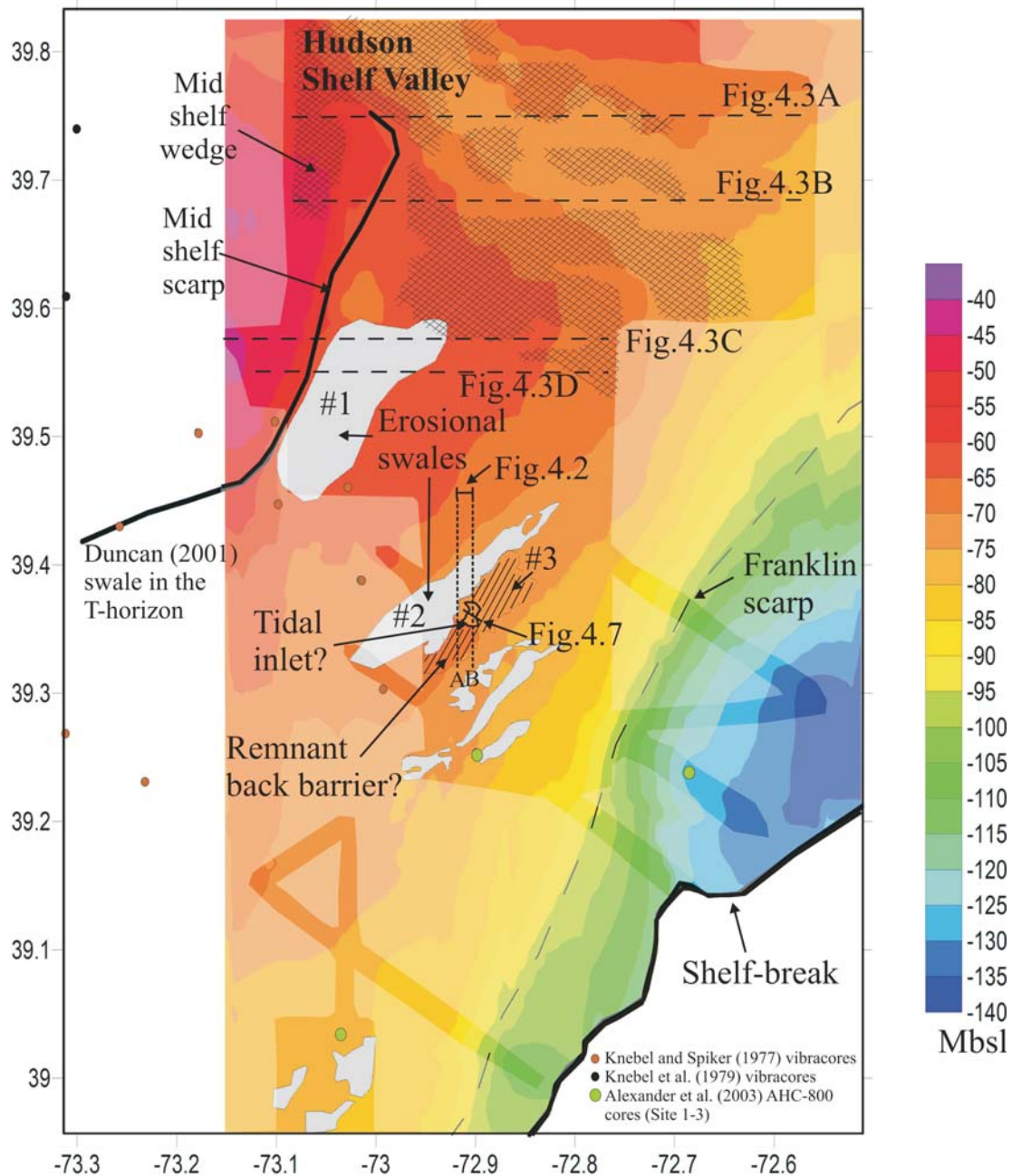
Figure 4.4: Structure contour map of the T-horizon, in m below sea level. White areas outline ribbon-floored swales formed by erosion (Figure 4.2A-B and 4.3C-D). Cross-hatching in the northern part of the survey area, where line spacing is ~1 km, represents areas where T is either excavated by post-transgressive erosion (e.g., Figure 4.3A, Figure 4.3C) or is non-identifiable due to its proximity to the prominent seafloor reflection. Light shaded areas mark interpolation outside of survey limits (darker shades). Depths to the T-horizon were determined using an assumed average compressional-wave velocity of 1500 m/s.
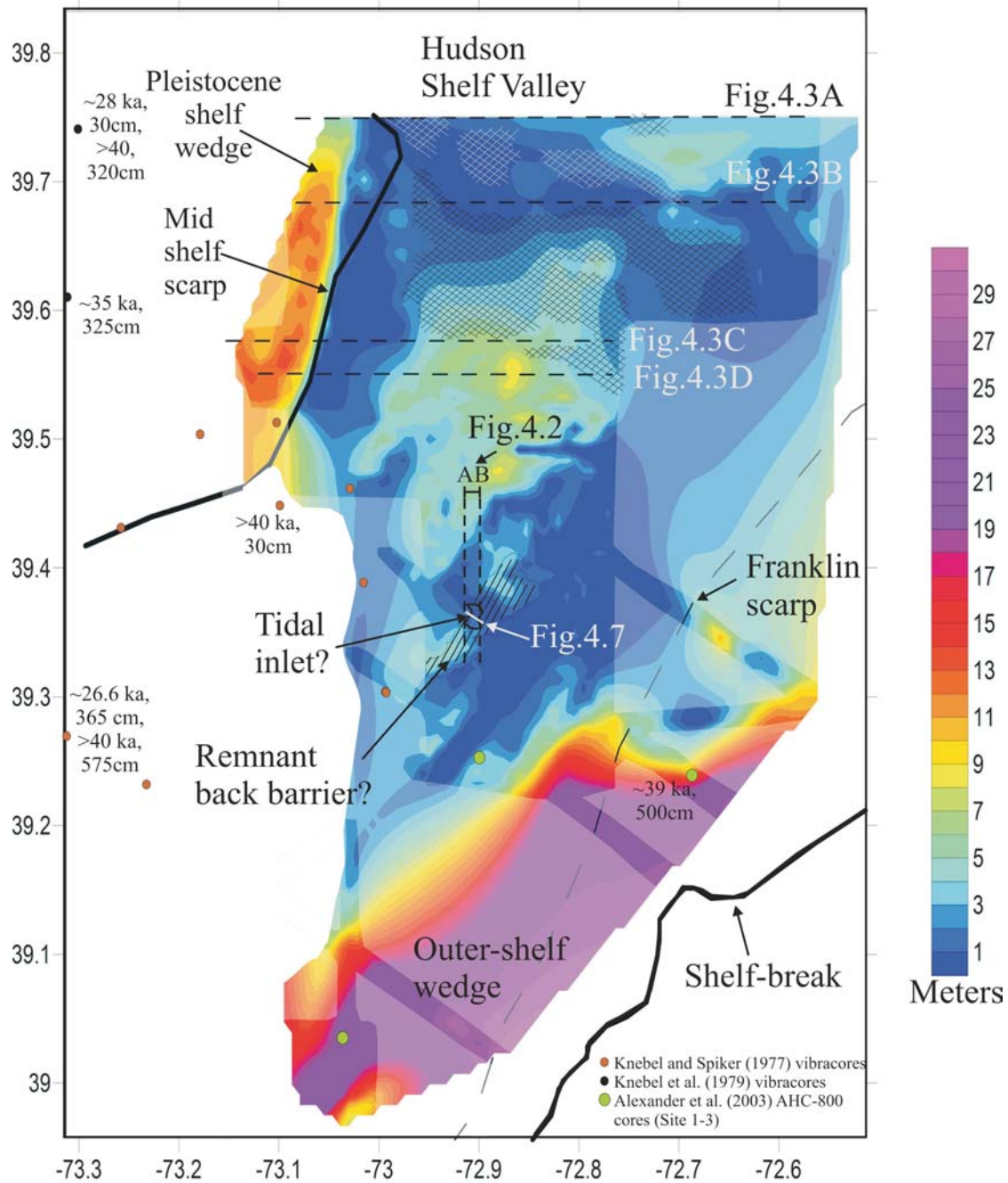
Figure 4.5: Isopach map of uppermost Pleistocene sediments between the R- and T-horizons. Sediment unit landward of the mid-shelf scarp (Knebel et al., 1979; Duncan, 2001) is >15 m thick, whereas the outer/deep-shelf wedges (Milliman, 1990; Davies et al., 1992; Gulick et al., 2005) display thicknesses of >30 m.

151
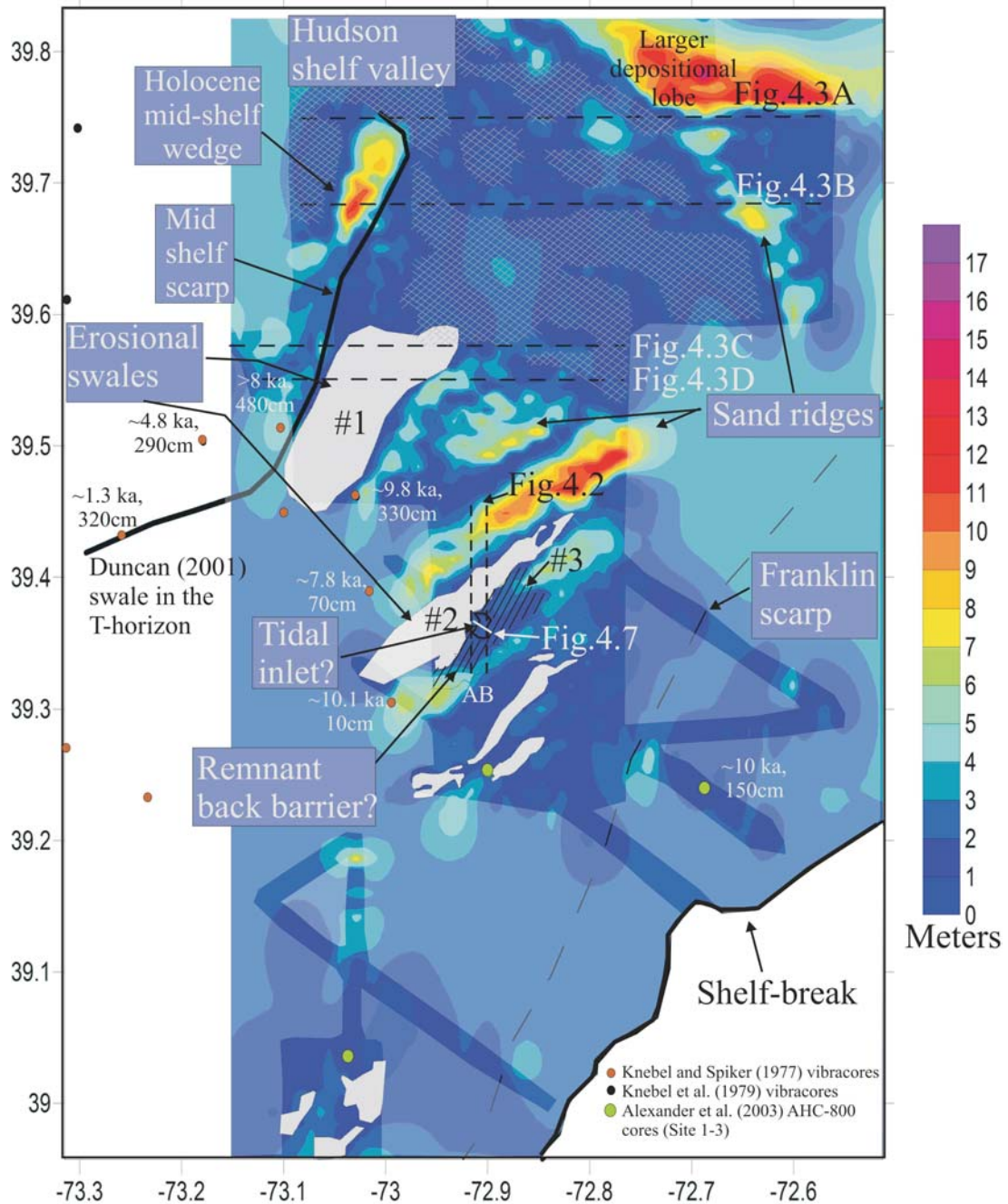
Figure 4.6: Isopach map of the Holocene sand sheet lying above the T-horizon. Large, SW-NE oriented sand ridges are evident between the mid-shelf and Franklin scarps. A small Holocene depositional wedge is present at the north end of the mid-shelf scarp (see also Figure 4.3B), while a larger depositional lobe is observed on the north flank of the Hudson Shelf Valley.

152

DISCUSSION

Topographic lows in the T-horizon: evidence of remnant lagoonal/back barrier geomorphology

The interpreted transgressive ravinement surface, horizon T, records the shoreline migration across the outer and mid-shelf before deposition of the overlying surficial sand sheet. The T-horizon is not a simple seaward dipping ramp; rather, I observe two ~NE-SW strike-oriented swales in the topography of T (Figure 4.4, #1 and #2), and a ~10+-m step in T coincident with the mid-shelf scarp (Figure 4.3C and D). The depression in T at 70 m water depth (Figure 4.4, #2) exposes possible lagoonal/back barrier stratigraphy and related morphology (Figures 4.2B and 4.7). No regional antecedent topography is evident, so this topographic high, superimposed on interpreted back-barrier lagoonal deposits (Nordfjord et al., in revision) suggests either a stillstand or slowing of sea-level rise during the Holocene transgression. I interpret the NE-SW high in the T-horizon seaward of this depression (Figure 4.4, #3) as a truncated late Pleistocene/Holocene transgressive barrier (Figures 4.2B and 4.7). This wedge-shaped, transparent unit resembles a truncated shore-zone system composed of back-barrier and tidal inlet fill facies (Figure 4.7; Duke, 1990; Galloway and Hobday, 1996; Morton et al., 2000). Arguments for a tidal origin of the observed channel within this topographic high are: (1) the ~1500 m strike-linear geometry of this channel system (Figures 4.4 [#3] and 4.7), (2) its younger stratigraphic age than mapped dendritic networks, formed during the LGM lowstand, and filled with estuarine deposits dated at AMS ~13-12 ka (Figure 4.2B; Buck et al., 1999; Nordfjord et al., 2005) and (3) asymmetric seismic geometries and lateral accretion characteristics similar to previously studied tidal inlets preserved in Gulf of Mexico stratigraphic sections (Tye and Moslow, 1993). I interpret sediments incised by

153

NW   SE

Modern seafloor

Lateral accretion

Dendritic channel networks

Tidal inlet?

Back barrier lagoonal sediments?

50m

5m   V.E.~10x

100

110
ms

154
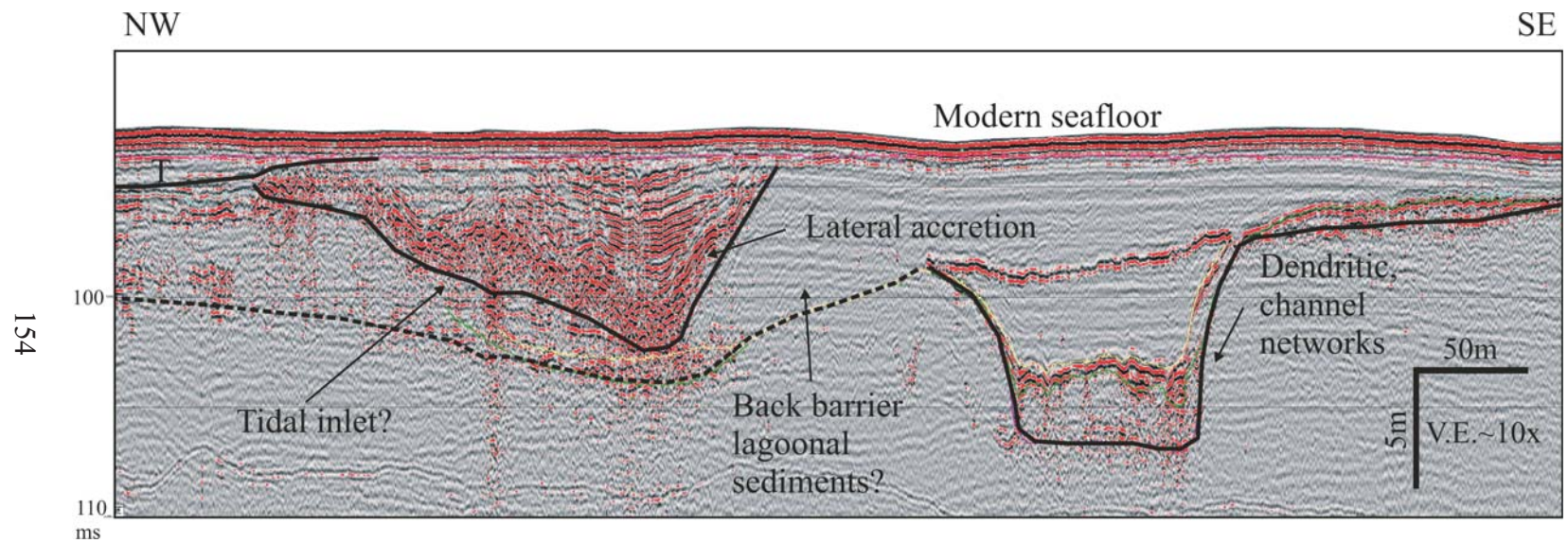
Figure 4.7:   Chirp seismic section showing two generations of incisions in the shallow subsurface on the outer New Jersey shelf. The deeper incision can be traced for several kilometers and is a dip-oriented feature (Nordfjord et al., 2005), while the upper, more asymmetrical incision is a 1.5 km long strike-oriented feature on the outer shelf. See location in Figure 4.1.

this inlet as lagoonal deposits of a backstepping barrier system. Local preservation of this back-barrier complex occurred either as a result of acceleration in sea-level rise after the short stillstand or additional accommodation space provided by subsidence of underlying initial topography; the NW-SE dendritic channel systems previously carved and filled (Nordfjord et al., 2005).

My data do not reveal remnant back-barrier stratigraphy at the depression in T at 50 m water depth, at the base of the mid-shelf scarp (Figure 4.4, #1). However, Duncan (2001) observed both a shallow swale in the T-horizon at the base of the mid-shelf scarp to the south and also a lenticular unit and incisions just below T within this swale. She interpreted this geomorphology as a lagoonal/ back-barrier deposit with possible tidal inlets. The Duncan (2001) survey area, which is south of a landward bend in the mid-shelf scarp (Figure 4.1) and thus in the lee of prevailing SE-directed long-shore currents, probably was not subjected to the intensity of erosion apparent in my study area, either during transgression or afterwards. Therefore, LGM-related and transgressive stratigraphy there is better preserved.

Formation of the mid-shelf scarp and potential remnant back-barrier strata

The ~10+-m step in the T-horizon coincident with the mid-shelf scarp (Figures 4.3C and 4.4) establishes the seaward edge of the Pleistocene mid-shelf wedge (Figure 4.5). I hypothesize that the Pleistocene wedge is responsible for the existence of at least this part of the mid-shelf scarp, the presence of the overlying Holocene mid-shelf wedge (Figure 4.3B) and the intermittent preservation of remnant back-barrier morphology and stratigraphy near the base of the scarp. The mid-shelf scarp (Figure 4.3D) and possible lagoonal deposits at its base were probably formed during a pause in shoreface retreat caused by the vertical relief of the Pleistocene mid-shelf wedge (Figures 4.3C and 4.4).

155

This slope is steeper than the 0.12° slope of the step in the T-horizon noted by Duncan (2001) further south. These slope changes of the scarp along strike suggest that the scarp may be genetically tied to antecedent topography created by the preexisting wedge. Such antecedent topographic relief probably slowed down the shoreface retreat, regardless of the prevailing rate of eustatic sea-level rise.

Locally stagnant rates of shoreface retreat would accentuate formation and preservation of back-barrier/ lagoonal morphology and result in the locally higher relief of the transgressive ravinement as I observe. As transgression proceeded and the shoreline moved landward of the mid-shelf wedge, the shore-face resumed a rapid horizontal landward translation across the low-gradient coastal plain.

Transgressive mid-shelf wedge deposits

The Holocene mid-shelf wedge was probably deposited in front of the Pleistocene shelf wedge subaqueously after ca. 11.5 ka, directly above the transgressive ravinement surface as the shoreline migrated landward (Figures 4.3A and B, 4.6). Shell samples from cores into this Holocene wedge exhibit radiocarbon ages ~8 kyr and younger (Figure 4.4; Knebel and Spiker, 1977; Knebel et al., 1979). Such Holocene mid-shelf wedge deposits represent the healing phase sedimentation of Posamentier and Allen (1993) or the offlapping transgressive wedge of Swift and Thorne (1991a, b). Continuing transgression of the middle shelf (landward) shed sediments seaward across the mid-shelf scarp and reestablished a more gentle longitudinal profile into deeper waters characterized by lower wave energy. However, as the shelf underwent post-transgressive open-shelf erosion following mid-shelf deposition, the depositional front of the subaqueous transgressive sediment lobe was itself modified and locally removed (Figures 4.3D and 4.6).

Uchupi et al. (2001) have speculated that the mid-shelf wedge represents a subaerial deposit associated with massive outflows from breached meltwater lakes to the north that were known to have occurred between ~17 and 14 kyr, during glacial retreat. However, along the Barnegat Corridor where it crosses the scarp (Figure 4.1), Duncan (2001) concluded that the outer part of the wedge instead consists of a prograding sequence that lies above the "T" horizon. She postulated that the mid-shelf wedge must have been deposited in the marine environment, perhaps ~11-10 ka or later based on known eustatic sea level curves, and therefore could not have been associated with such meltwater events. Based on my seismic interpretation and age constraints (Knebel and Spiker, 1977; Knebel et al., 1979), the mid-shelf sediment wedge consists of an older (latest Pleistocene) wedge deposited prior to 28 kyr and a minor younger, transgressional, offlapping wedge deposited in the early Holocene, ~10 ka (Figure 4.3B). My chirp seismic data reveal ~15 m deep incisions within the mid-shelf wedge (Figure 4.3C and D), which have been interpreted to have formed during the LGM, ~25-16 ka (Duncan et al. 2000). Such incisions suggest that most of the sediments that constitute the mid-shelf wedge was not deposited between ~17 and 14 kyr, as suggested by Uchupi et al. (2001), but instead were deposited earlier, before the LGM.

Shelf current reworking of mid-outer shelf sediments

Truncation of stratal horizons at the seafloor provides direct evidence for recent erosion in the marine setting, after the shoreface has transgressed through this region. Two prominent areas have been observed in the study area to have undergone significant marine erosion: (1) seaward of the mid-shelf scarp (Figure 4.3D) and (2) landward of the interpreted paleo back-barrier located in ~70 m water depth (Figure 4.2B; Figure 4.4, #3; Figure 4.7). Both of these erosional swales coincide with depressions in the T-horizon

landward of topographic highs in that horizon (stippled lines; Figures 4.2A and 4.3D). These depressions in the T-horizon appear susceptible to localized, SW-striking bottom flow, exposing underlying deposits (Figures 4.2B and 4.3C). Reasons for such localized erosion may be: (1) that intepreted lagoonal/back-barrier sediments exposed within these swales are more susceptible to erosion, or (2) that the uneven topography focuses modern bottom currents capable of causing erosion. Radiocarbon dates from Knebel and Spiker (1977) of >40 kyr from sediments within the northern swale (Figure 4.4) support my interpretation that modern marine erosion is exposing older sediments in these topographic lows.

Following deposition of the Holocene mid-shelf wedge and transgression across the middle shelf at ~8.5 ka, water depth has continued to increase to the present. The hydrodynamic regime has also changed on the mid-outer continental shelf; wave-current activity has decreased and advective bottom currents have increased. The transgressive sand sheet, initially formed nearshore and composed of sand ridge and swale geomorphology, is now being reworked by those currents. I attribute observed NNE-SSW orientation and morphology of the northern ribbon-floored erosional swale to perturbation of generally SW-directed currents by the seaward edge of the mid-shelf wedge (Figures 4.3C, D and 4.6, #1; Goff et al., 2005). Continuing cannibalization and reworking of lowstand fluvial and transgressive shore-zone deposits by shelf currents have modified the modern middle and outer shelf seascape. Wave- and tide-dominated shelves worldwide are similar in this respect; regardless of sediment supply during the LGM, preexisting shoreface retreat-derived deposits have been reworked into shelf sand ridges and sand has been widely distributed to blanket underlying lowstand sedimentary features (Swift and Field, 1981; Dalrymple and Hoogendoorn, 1997; Berne et al., 1998). These sediments continue to be reworked by shelf currents to the Present.

158

Evolution model of the transgressive strata (Figure 4.8)

I present a model for the latest Pleistocene and Holocene evolution of the New Jersey middle and outer shelf to explain available seismic and geologic observations (Figure 4.8). The most recent stratigraphy of the wide, passive margin off New Jersey has been shaped primarily by erosional events as a consequence of low sediment supply, low subsidence and relative sea-level fluctuations. During Phase I, fluvial incisions formed when the entire shelf was exposed during the last lowstand (Figure 4.8; Davies et al., 1992; Duncan et al., 2000; Nordfjord et al., 2005). During Phase I and II, these fluvial networks were converted into passively infilling estuaries with the approach of the landward-retreating shoreline (Figure 4.8A and B; Nordfjord et al., in revision). During late lowstand/early transgression (Phase II) shoreface retreat occurred and the base of the shoreface migrated landward (Figure 4.8B; Bruun, 1962; Swift, 1968). Preexisting deposits were truncated by wave action, creating a ravinement surface, the T-horizon (Figure 4.8B; Duncan et al., 2000; Goff et al., 2005; Nordfjord et al., in revision). Coeval flooded incised channel deposits were preserved both below the T-horizon and above it, as (Figure 4.8B; Nummedal and Swift, 1987). During the stage II, a deceleration in the relative sea level likely happened, as evidenced by remnant back-barrier deposits at depth of ~70 mbsl (Figure 4.8B). Also, landward shoreface retreat slowed down in places during Phase III, focusing ravinement along the seaward edge of the wedge. This deceleration of the shoreface retreat during Phase III was due in part or in whole to the inherited physiography of the latest Pleistocene shelf sediment wedge, which in turn steepened its slope to create a lagoonal/beach barrier geomorphology (Figure 4.8C). The ravinement of the Pleistocene wedge formed the underlying foundation for the modern-day mid-shelf scarp. During Phase IV, as sea level finally rose across the scarp, the

159
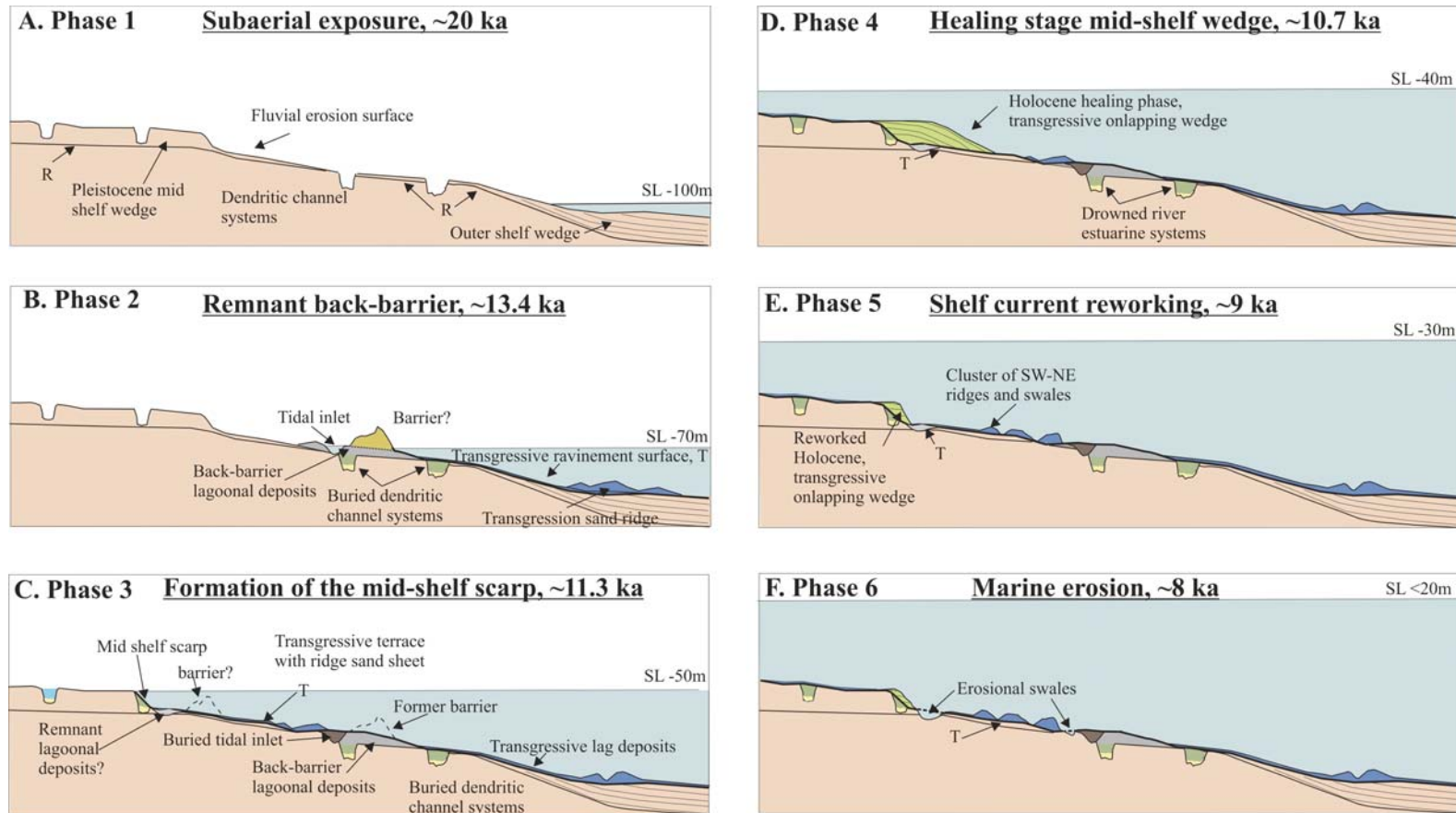
Figure 4.8: Evolutionary model for the sediment formation and preservation during the Holocene transgression. Phase 1 begins during shelf exposure with formation of incisions at ~20 ka, while phase 6 represents the most recent modifications of the outer shelf.

Holocene mid-shelf wedge (Figures 4.3B and 4.6) was in turn constructed from eroded shoreface sediments (Figure 4.8D). During Phase V, powerful storm flows swept southward across the depositional lobe, which consequently removed sediments from the mid-shelf wedge and truncated its base (Figure 4.8E; Swift and Freeland, 1978). As the water column deepened over shelf sand ridges and the shoreline receded, ridges evolved (Swift and Thorne, 1991a; Goff et al., 1999; Snedden et al., 1999). During Phase VI, successive erosion of outer-shelf sediments and significant modification of the seabed has evidently continued to take place through bottom current-driven erosion (Figures 4.2A, 4.3D and 4.8F), perhaps by undercutting of surface-armored seabeds (Goff et al., 2005).

The largest change in strike of the east coast margin occurs at the head of the Hudson Canyon, ~50 km north of my study area (Figure 4.1). Its proximity to the canyon and the presence of SW-directed currents likely concentrates shelf-edge flows on the southern side of the Hudson Shelf Valley, where most of the recent, deeper reworking of sediments has occurred (Figure 4.6). However, the dynamics of shoreline displacement and the resulting architecture and thickness of transgressive deposits are strongly dependent on the rate of sediment influx relative to the rate of sea-level change, shelf gradient (or, more generally, basin physiography) and spatial distribution of energy. The physiography of the terrestrial surface preceding transgression has the greatest influence on the nature of the transgressive coastal system. I speculate that topography associated with incised valleys and pre-existing sediment lobes both may have been important factors in influencing the ravinement trajectory and the generation of paleo-barriers, which in turn controlled the preservation potential of lowstand to early transgressive deposits. Paralic fluvial and estuarine deposits are preserved only in fragmented fashion below the ravinement surface (Nordfjord et al., in revision), typical of low-gradient shelf settings that undergo a stepwise retreat of the coast, thereby allowing barrier drowning

161

and cannibalization during intervals of accelerated relative sea-level rise. The transgressive ravinement surface, T-horizon, morphology dominates New Jersey seafloor bathymetry today (Figure 4.1 compared with Figure 4.4), but I have shown in this Chapter that stratigraphers must also consider the formation of ridge and swale features which have been modified by open-marine erosion when investigating the maximum flooding surface.

CONCLUSIONS

On the New Jersey middle and outer shelf, the transgressive ravinement is not a simple seaward inclined ramp. Rather, its morphology is influenced by both the deposition and erosion of overlying post-transgressive strata and preservation of underlying, mainly lowstand and early transgressive strata. Two strike-oriented depressions at ~50 m and ~70 m water depths and a scarp characterize the ravinement surface. I interpret these depressions as remnant lagoonal/back barrier geomorphologies, associated with preserved back-barrier stratigraphy below the ravinement. Deposition of these shelf strike-parallel, lenticular facies likely created zones more susceptible for modern marine erosion. I propose that these depressions represent periods of a deceleration or even a pause in shoreface retreat during the Holocene transgression. The seaward trough is controlled by eustatic fluctuations and the trough adjacent to the base of the mid-shelf wedge is related to the local wedge physiography. The preexisting Pleistocene mid-shelf wedge/lobe likely forced shoreface retreat to slow down along its seaward front. This change in shoreface retreat rate resulted in steepening of the T-horizon slope due to the concentrated erosion along this edge. This slow down may also have encouraged the formation and preservation of a lagoonal/back barrier geomorphology and associated facies even without a decrease in relative sea level rise.

162

The modern mid-shelf scarp, which has been a type locality of a paleo-shoreline (Veatch and Smith, 1939; Swift et al., 1980), appears to be a product of the inherited underlying mid-shelf wedge and reworking of the sediment front by shelf currents (Figure 4.3C and D). The mid-shelf scarp has provided accommodation space for the formation of the small Holocene component of the mid-shelf wedge, as the topographic step in the T-horizon at ~40-50 m water depth served to concentrate shoreface-derived sediment in to a transgressive offlapping shelf wedge during sea level rise. This Holocene wedge-shaped unit properly belongs in the transgressive system tract, because it lies beneath the maximum flooding surface (i.e., the modern seafloor), above the ravinement surface (i.e., the T-horizon), and because it was deposited during the Holocene transgression. In contrast, the Pleistocene mid-shelf sediment wedge is a product of regressive deposition during a forced sea-level fall prior to the LGM. My study does not support Uchupi et al. (2001)'s and Donnelly et al. (2005)'s speculations that the mid-shelf wedge could be a subaerial deposit associated with massive meltwater outflows from breached glacial lakes between ~17 and 13 kyr.

Significant modification of the seabed by powerful storm flows sweeping southwestward across the outer shelf, as observed in two ribbon-floored swales that truncated predated stratigraphic surfaces, has evidently continued to take place. These erosional swales are associated with topographic lows in the transgressive ravinement surface. The underlying morphology of the T-horizon appears to continue to focus marine, bottom-flow erosion on this part of the New Jersey shelf.

Chapter 5: Speculative chronologic synthesis

The overall goal of this study has been to interpret observed seismic stratigraphy across the New Jersey continental shelf in the context of a relatively well-known eustatic sea-level cycle and associated glaciation/deglaciation during the last ~120 ka. Therefore, this last chapter constitutes a brief chronological, but speculative summary over events interpreted in the subsurface for this margin.

Glacial processes can impact the stratigraphy of continental margin sediments in a variety of ways. The most obvious of these are through direct glacial erosion and sedimentation and deposition of sediment from the ice sheet itself or from icebergs. However, a number of indirect glacial influences on stratigraphy are more difficult to recognize from the stratigraphic record. For example, the weight of a large continental ice sheet can depress the crust beneath it by hundreds of meters and produce an uplifted peripheral bulge around its margins, affecting regional drainage and sedimentation patterns. Glaciers will also increase sediment supply, both by direct sediment transport from the glacier by meltwater, and from glacial and proglacial sediments eroded and transported by rivers. These processes may significantly impact sediment supply in both time and space. Furthermore, glacial-isostatic effects and blockage of existing rivers by ice and/or glacial deposits can influence drainage patterns, thereby either increasing or decreasing sediment flux.

The Hudson River drainage basin, which has been the principal source of sediment for the New Jersey shelf throughout the Pleistocene (Poag and Sevon, 1989), was influenced by ice through much of the last glacial cycle. Thus, continental glaciation had a significant impact on this shelf, despite its being beyond the direct influence of the ice itself. Some of these indirect effects during the most recent deglaciation have been

discussed (e.g. Milliman et al., 1990; Davies et al., 1992; Uchupi et al., 2001; Fulthorpe and Austin, 2004; Donnelly et al., 2005), but the impact of earlier glacial events has only been recognized in sediments from the upper slope (Savrda et al., 2001; McHugh and Olson, 2002).

Even without accounting for sediments that were deposited on the slope and rise, or subsequently eroded, sediment supply on the shelf was significantly greater than of present during OIS 4 and 3, ca. 70-35 ka. It is likely that at least part of the St. Lawrence drainage basin must have been captured by the Hudson River during parts of OIS 5 and throughout OIS 4 through 2, as it was earlier during the late Pleistocene (Teller, 1987). This could account for increased sediment supply during OIS 4 and 3. The waxing and waning of small ice caps in the northern Appalachians is another possible source of additional sediment.

Heavy precipitation, combined with a change in vegetation from forest to tundra in uplands during glacial stages, could result in increased erosion. Church and Ryder (1972) have noted that tundra climates are characterized by flashy, surficial drainage favoring increased rates of erosion. These drainage conditions, combined with an abundance of unconsolidated, recently deposited glacial sediments with limited vegetation cover, combined to give enhanced sediment supply during glacial times.

The paleo-drainage system from the New Jersey Highlands across the Piedmont and Coastal Plain of New Jersey throughout the late Pleistocene carried sediments from the Appalachians directly to the continental shelf (Turner, 2004). Transport may have been through the ancestral Hudson River system or through smaller, parallel river systems. According to Turner (2004), regardless of the river system that transported these sediments, the system did so in a manner that was direct and swift. The pristine nature of

the majority of hornblende grains analyzed suggests a freshly weathered and proximal source.

A striking aspect of the New Jersey late Pleistocene stratigraphy is the presence of numerous interpreted subaerial erosion surfaces in a relatively thin section. Futhermore, there are large differences in elevation between lowstand and highstand coastal deposits. Also noteworthy is the predominance of transgressive and lowstand deposits and limited highstand deposition. Modeling suggests that this is characteristic of high-amplitude, high-frequency eustatic fluctuations, because the HST forms during times when sea level is still rising, but sediment supply is sufficient to allow progradation (Steckler et al., 1993; Carey et al., 1999). High rates of sea level rise tend to limit the length of time during which progradation can occur. Furthermore, subsequent subaerial erosion during sea level fall tends to reduce preservation of highstand deposits. This must have occurred, probably multiple times, offshore New Jersey.

Unlike the Miocene, which was characterized by the progradation of thick, highstand deltas onto the shelf (Fulthorpe et al., 2000), the Quaternary section on the New Jersey shelf is marked by truncated highstands, lowstand shorelines that are detached from underlying highstands, and sequences that are thin and discontinuous across most of the shelf. These characteristics are suggestive of forced regressions, driven by relative sea-level fall rather than sediment supply (Posamentier et al., 1992).

PALEO HUDSON DRAINAGE AND THE R-HORIZON

Knebel et al. (1979) mapped a buried, north-south trending, flat bottomed, 2-17 km wide and 3-15 m deep valley in the R-horizon using high-resolution single-channel seismic profiles. Their paleo-Hudson valley has been used as evidence that the ancestral Hudson River migrated across the shelf at times of lowered sea level, and did not always

166

flow along the trend of the shelf valley on the modern seafloor (Freeland et al., 1981; Swift et al., 1980). The modern River Hudson follows a path tightly controlled by the hard crystalline rocks of the Palisades Sill and Manhattan Schist (Maguire et al., 1999), but on the Coastal Plain during a lowstand of sea level during OIS 6, it would have been unconfined (Carey et al., 2005).

Carey et al. (2005) investigated the drainage evolution of the Hudson River during the last glacio-eustatic cycle. Their deepest truncation surface, traced across much of the shelf on the Uniboom™ seismic data, is a prominent angular unconformity. This surface trends in the same N-S direction as the Knebel et al. (1979) paleo-drainage and is likely associated with the sea-level fall during the OIS 6, ca. 140-120 ka (Figure 5.1A and 5.2).

Carey et al. (2005) inferred that their overlying sequence boundary II formed during the OIS 4 lowstand (~70–75 ka; Figures 5.1B and 5.2). This paleo-Hudson river valley and parts of the diachronous R-horizon are probably approximately coeval. However, the portion of the R-horizon that underlies the Davies et al. (1992) "S" horizon is perhaps a remnant of the older part of the time-transgressive R-horizon; sediments deposited within the "S"-"R" interval protected the underlying surface from erosion.

Numerous valleys incise the base of Carey et al. (2005)'s Sequence III, the largest of which is the prominent Paleo-Hudson valley described by Knebel et al. (1979). The great depth of incision of the valley, up to 35 m, and its widening and shallowing in the seaward direction, are both suggestive of a fluvial system. This valley trends more eastward than the valley in the underlying Sequence III. Radiocarbon dates within Sequence III are consistent with an OIS 3 age, with the incision likely occurring during the 45–50 ka lowstand followed by filling of valleys with sediment during the last interstadial, OIS 3 (~35 ka; Figure 5.2; Carey et al., 2005). Uchupi et al. (2001)
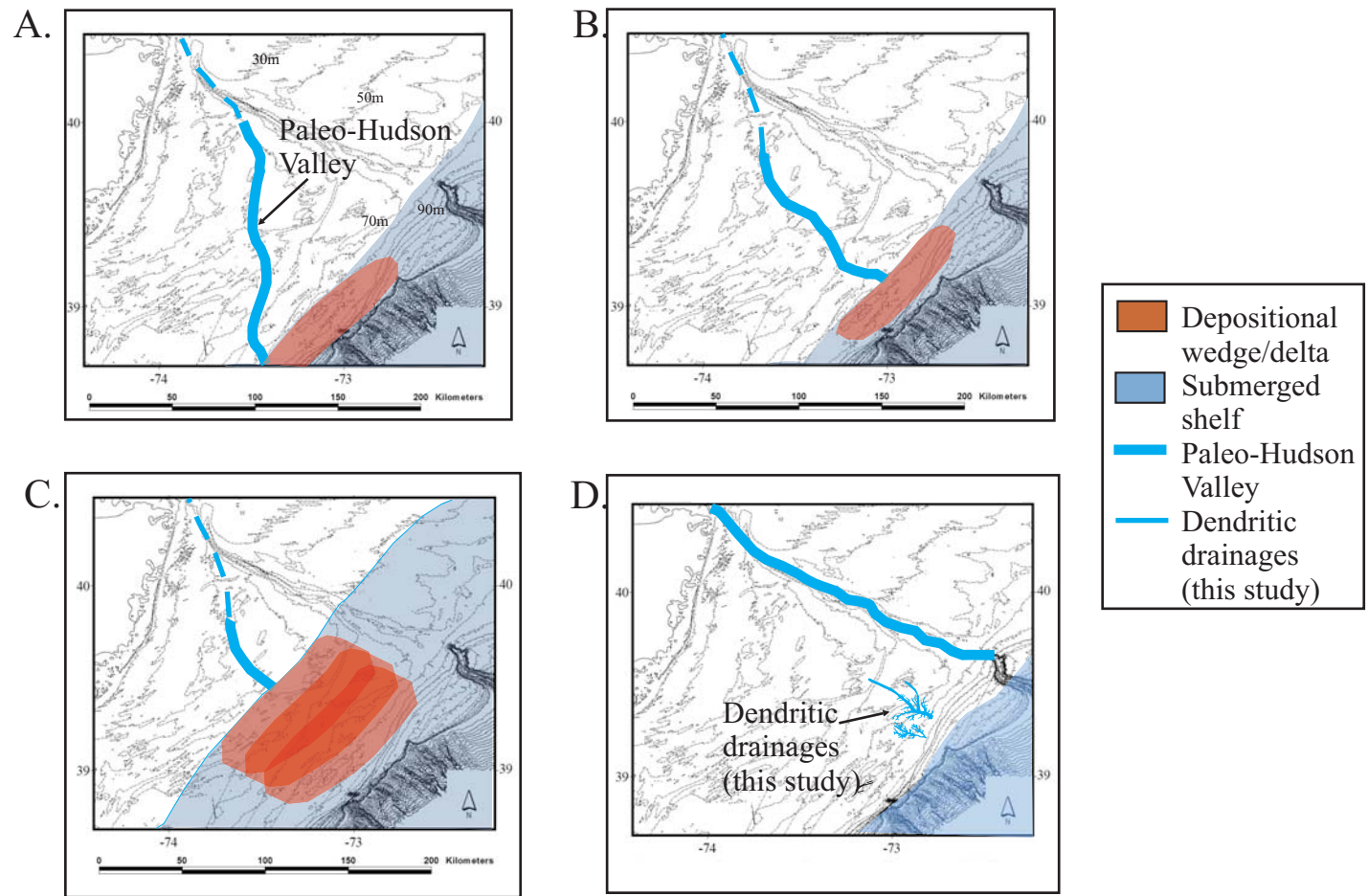
Figure 5.1: Paleogeographic maps for (A) Oxygen Isotope stage 4 lowstand, ~70 ka. Position of Paleo-Hudson Valley is modified from Carey et al. (2005); (B) Oxygen Isotope stage 3 lowstand, ~ 50 ka. Deflection of Paleo-Hudson Valley observed by Carey et al. (2005); (C) Oxygen Isotope stage 3 depositional delta-lobes, including Pleistocene mid-shelf wedge and parts of outer shelf wedge, ~ 45-28 ka and (D) Oxygen Isotope stage 2 lowstand, ~20 ka, with Hudson Shelf Valley crossing the modern shelf to the head of Hudson Canyon.

postulated that the ancestral Hudson River system was actually carved by drainage of Lake Hackensack and Hudson Lake through Raritan Bay, ca. 18 ka. However, the age of surficial sediments in the shelf area mapped by Knebel and Spiker (1977) precludes such a young age for the ancestral valley.

Carey et al. (2005) documented a complex ancestral Hudson valley fill for their Sequence III. This sequence has a tripartite division, which may correlate to that predicted by the Dalrymple et al. (1992) model for estuarine fills. The lowest part consisted of high amplitude, gently dipping, parallel reflections that could result from fluvial point bars or progradation of a bayhead delta into an estuary. The central, nearly reflection-free facies resembles that in muddy valley fills observed in late Pleistocene–Holocene deposits from the inner shelf of New Jersey (Ashley and Sheridan, 1994). Predominantly muddy sediments typically fill the central basin of wave-dominated estuaries (Dalrymple et al., 1992). The more chaotic, multiply-incised, upper fill is suggestive of migrating tidal channels of the baymouth as tidal influence increases. This upper fill appears the most transgressive in nature (Carey et al., 2005).

The R horizon (Figure 5.2) was modified during the complicated sea-level oscillation associated with OIS 3 that preceded the LGM. These base-level fluctuations probably resulted in a series of forced regressive lobes (Figure 5.1C). The Pleistocene mid-shelf wedge could have been deposited as a wave-dominated delta early in this interval, ~45-50 ka, when the shoreline was approximately 40 m below modern sea-level (Figure 5.2). However, in areas with no or little sedimentation, modification of the R-horizon occurred as the shoreline swept landward and seaward, likely making the R-horizon a diachronous, integrated regressive/marine surface.

The ancestral Hudson River, which trended across the shelf to the south through OIS 3 and 4, apparently did not re-incise the shelf during OIS 2, suggesting that during

169

the last glaciation, drainage was likely via the modern Hudson Shelf Valley (Figure 5.1D). The change in course of the Hudson River may have been related to the advance of ice into the region. As the ice sheet depressed the crust immediately in front of it and created a peripheral bulge to the south, the reduction in gradient of the Hudson may have allowed it to be captured by other smaller drainage systems located within the foredeep. The valley was further incised by the drainage of various glacial lakes, ~13 ka (Uchupi et al., 2001; Donnelly et al., 2005). Reworking occurred by marine processes during ensuing Holocene transgression, creating the modern Hudson Shelf Valley observed today (Nordfjord et al., in prep.).

CATASTROPHIC OUTBURST EVENTS

Uchupi et al. (2001) proposed that late Wisconsinan deposition and erosion on the shelf and slope from New Jersey to southern New England were a consequence of the catastrophic drainage of glacial lakes behind terminal moraine systems, the huge volume of water stored beneath the Laurentide ice sheet, and subsequent erosion of the lake sediments by flash floods. They postulated that the morphology of the shelf seaward of the late Wisconsinan terminal moraines was dominated by a series of lobes aligned parallel to Hudson and Block Island valleys (Figure 5.3). The lobes appeared to be superimposed one upon another. Uchupi et al. (2001) postulated that this lobate morphology, the wavy terrain in the vicinity of the mouth of the Hudson Shelf Valley, coarse clasts on the mid-shelf and abundance of land mammal remains on the shelf were all the creations of this episodic massive flooding of the shelf. They postulated that two major episodes of catastrophic draining occurred, one at 17 to 15 ka, creating the shelf features east of the Hudson Shelf Valley and the Hudson Apron, and a second at 14 to 12 ka creating the sediment lobes, including the mid-shelf wedge, on either side of the

170
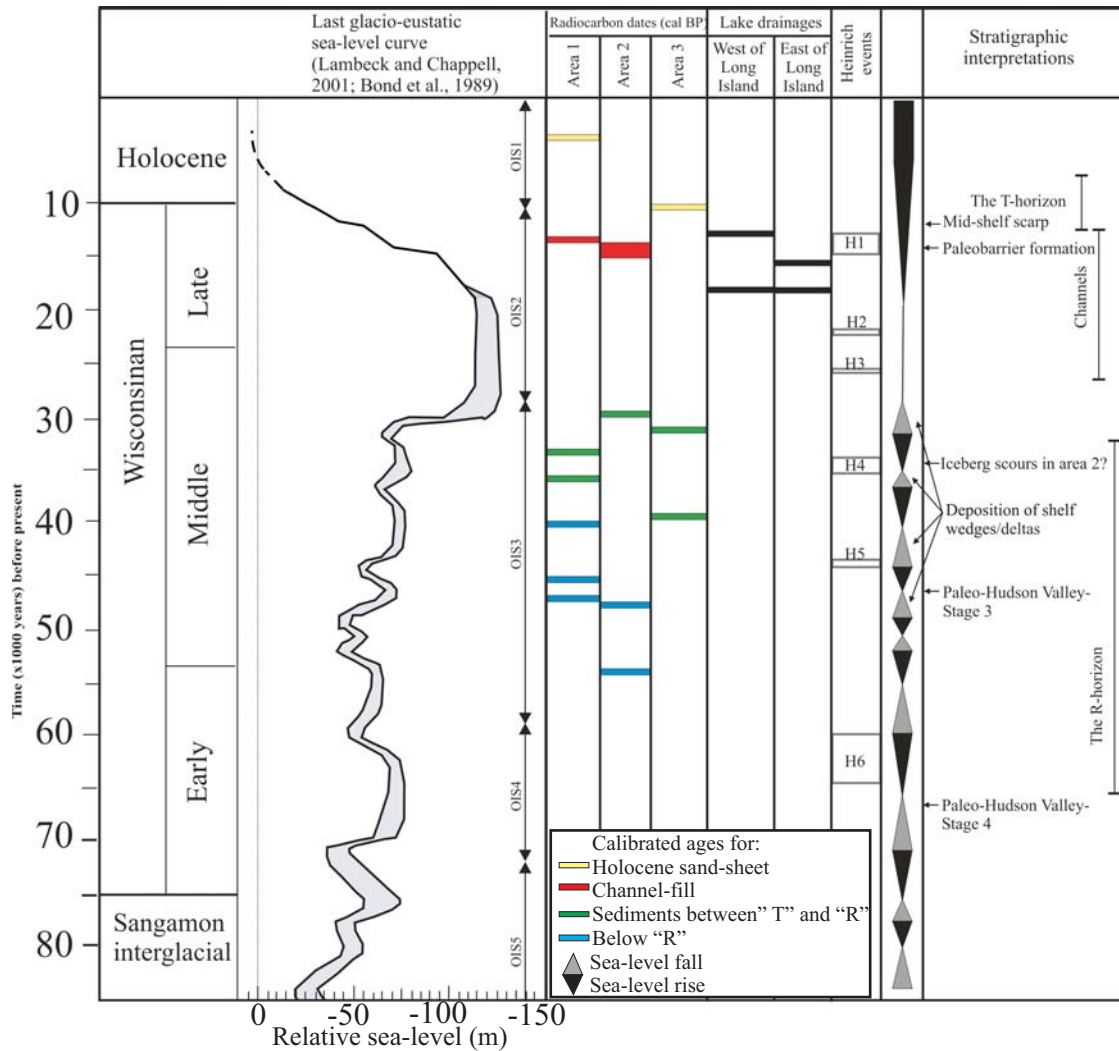
Figure 5.2: Summary of depositional and erosional events observed in the sub-
surface ascribed to the last glacio-eustatic cycle. The regressive portion
of the sea-level curve is from Lambeck and Chappell (2001) and the
Holocene transgression is from Bard et al. (1990). Radiocarbon dates are
from Lagoe et al. (1994) and Alexander et al. (2003), lake drainage
constraints are from Uchupi et al. (2001) and Donnelly et al. (2005), and
Heinrich events are from Cronin (1999). Column with triangles displays
regressions (grey) and transgressions (black).

171
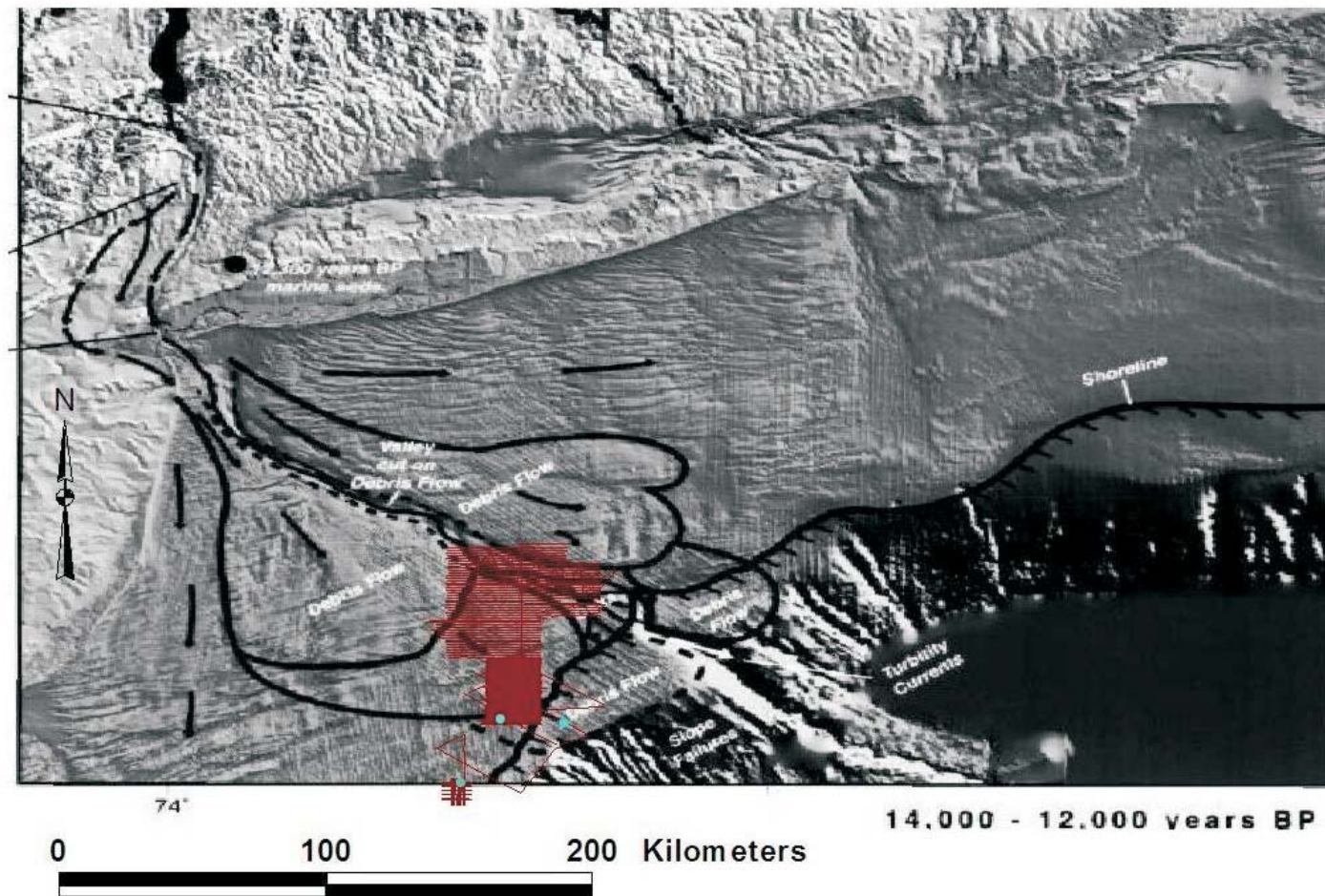
Figure 5.3:   Morphology of the Mid-Atlantic Bight interpreted by Uchupi et al. (2001) showing lobes inferred to be a result of catastrophic glacial lake drainages that occurred ~13 ka (Donnelly et al., 2005) and ~18 ka (Dineen et al., 1988; Uchupi et al., 2001). Purple lines represent Chirp track lines used in this study.

Hudson Shelf Valley (Figure 5.4 and 5.5).

The ice front stayed at its southern terminus about 2 kyr. As it retreated northward, about 18 kyr BP, it formed the end, interlobate and recessional moraines outlining the peripheries of the Great South Channel, Cape Cod, Narrangansett-Buzzards Bay, Connecticut Valley and Hudson-Champlain lobes (Sirkin, 1991). By 12 kyr BP, the Laurentide ice front was located along the northwest side of the modern St. Lawrence River (Figure 5.1; Hughes et al., 1985; Hughes, 1987; Uchupi et al., 1996; Kaplan, 1999). This recession was disrupted by the 13 kyr BP Port Huron Readvance/Delmar Stadial in northern New York and the 11.9-11.8 kyr BP, Little-Bethelehem Readvance in northern New Hampshire and Vermont. These stadials are older than the Younger Dryas cooling event which took place 11-10.5 kyr BP (Fairbanks, 1989).

The lakes appeared to have drained sequentially from east to west, with the lake in Nantucket Sound off southern New England draining as early as 17 ka, the one in Block Island Sound 16 ka, the one in Long Island Sound 15.5 ka and the lake system in Hudson Valley 12 ka. Uchupi et al. (2001) have proposed that these catastrophic floods which were responsible for the creation of much of the topography and shallow stratigraphy of the shelf from New Jersey to south of Nantucket Island. Initially, these outbursts probably exceeded the capacity of what few valleys were present on the shelf, and waters spread out over the shelf's surface. With time, however, as flows dissipated, they became channeled and incised sediments of the Hudson Shelf and Block Island valleys. These channels then served as passageways for later flows.

Donnelly et al. (2005) also found evidence of a catastrophic meltwater discharge through the Hudson Valley between 13,280 and 13,050 year BP, constrained by ^{14}C-dated samples (Figure 5.5). They suggest that Glacial Lake Iroquois breached its ice dam and then flowed into Glacial Lake Vermont and Glacial Lake Albany, breaching their

173
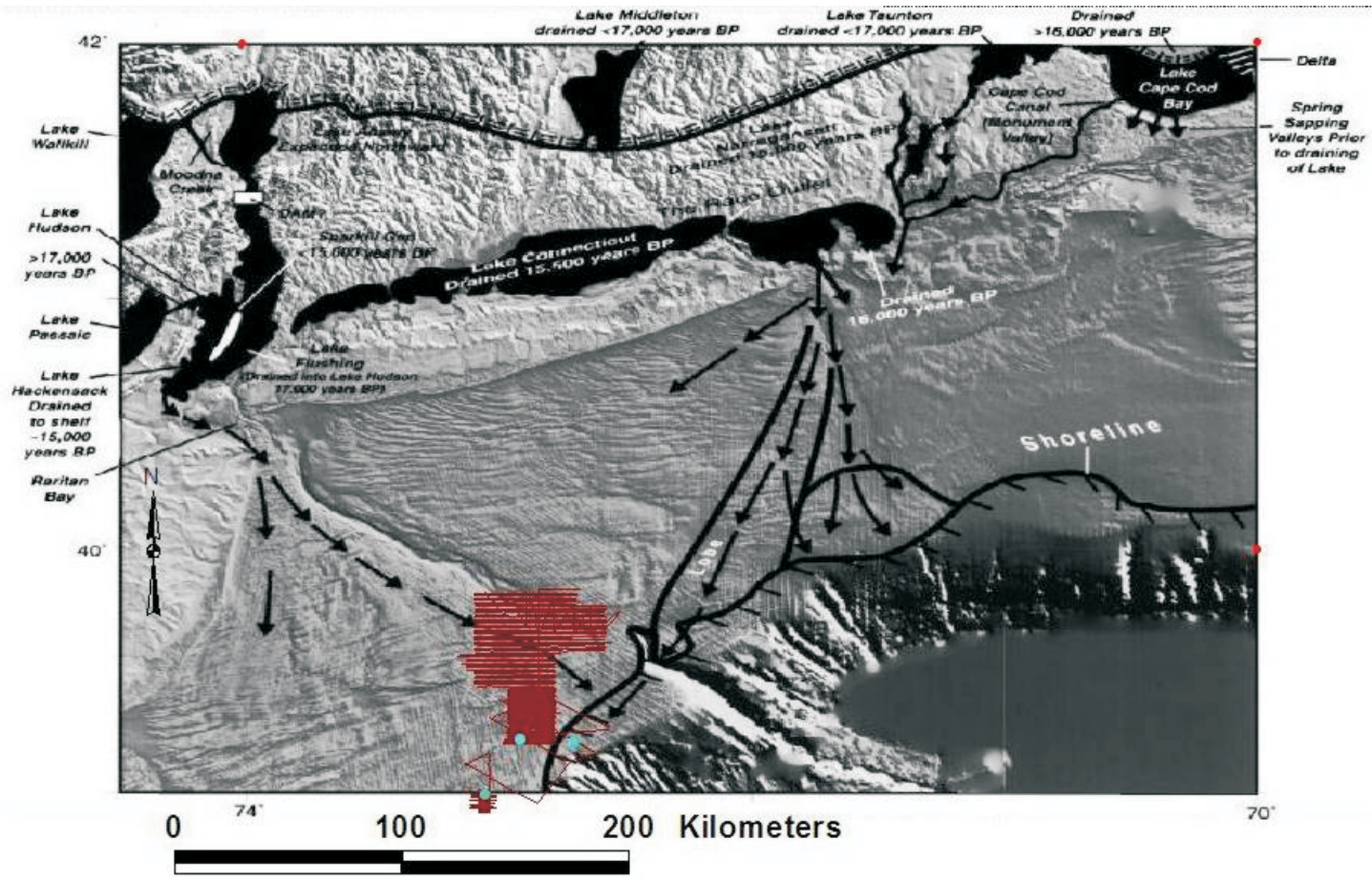
Figure 5.4: Paleogeographic map 17-15 ka, including the shoreline position at 17 ka (Uchupi et al., 2001). Purple lines represent Chirp track lines used in this study.
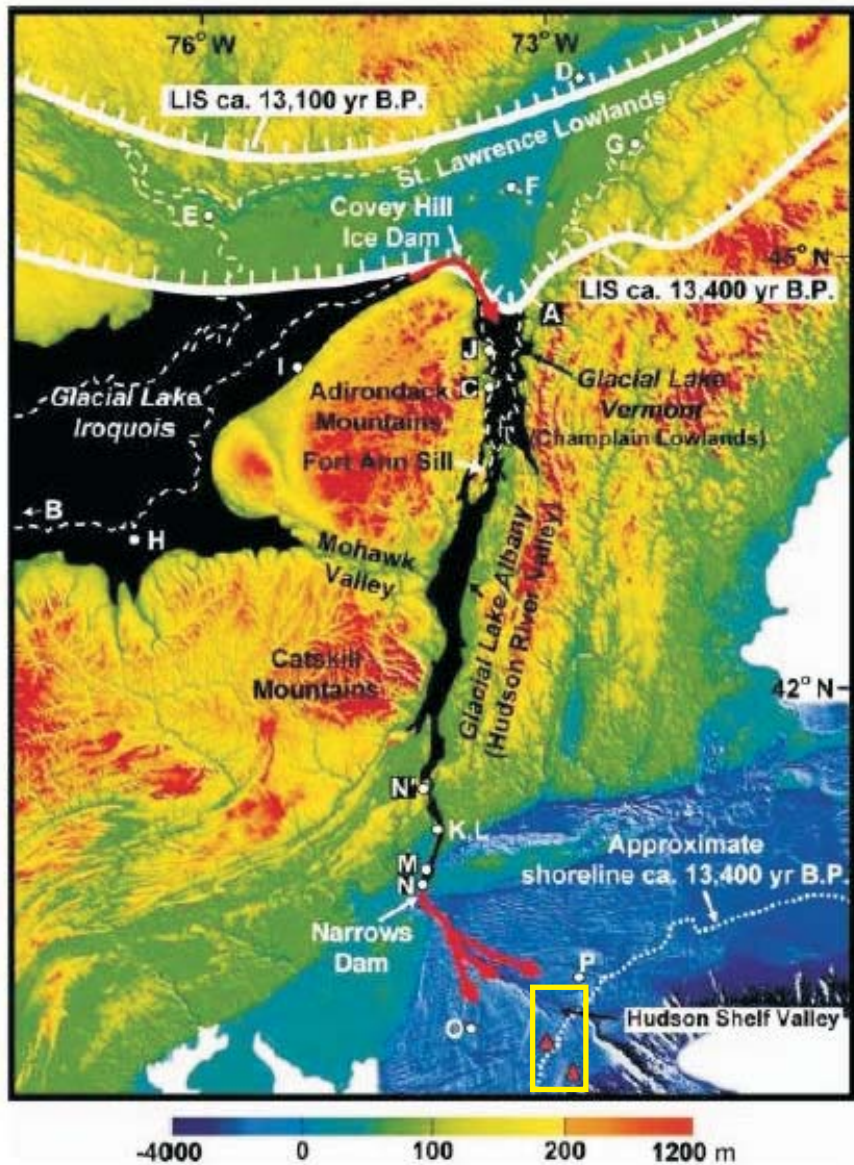
Figure 5.5: Relief map of northeast U.S. margin and southern Canada including bathymetric data from continental shelf and slope. Locations A-P correspond to sites referred to in Donnelly et al. (2005), where ^{14}C and stratigraphic ages provide constraints on timing of meltwater release from Glacial Lake Iroquois down Hudson Valley. Black -approximate extent of glacial lakes ca. 13.4 kyr B.P. Solid white lines southern margin of Laurentide Ice Sheet (LIS) ca. 13.4 and 13.1 kyr B.P. Red arrows - path of meltwater during Hudson Valley jokulhlaup. Yellow box- my study area. Red triangles - locations of glacial erratics inferred to have been transported to outer shelf during jokulhlaup (Uchupi et al., 2001). Hudson Shelf Valley is cut across shelf lobes and likely was cut during aqueous flow conditions following initial pulse of water and sediment to shelf.

175

terminal moraine dams. This massive outwash event is believed to have been large enough to reduce thermohaline circulation in the North Atlantic Ocean (Donnelly et al., 2005).

Fulthorpe and Austin (2004) addressed this question of glacial dam breaching. They identified deep (up to 10 m) incisions on the New Jersey shelf which they interpreted might have been cut by flood events following such breaching. These incisions can be traced for up to 10 km along the shelf and are >40 m wide (Figure 5.6). Fulthorpe and Austin (2004) proposed that episodic flooding, which occurred between 19-12 ka, is the best scenario to explain the creation and subsequent infilling of these channels. Catastrophic drainage of Lake Albany, associated with breaching of glacial Lake Iroquois ca. 13 kyr BP (Donnelly et al., 2005), could have caused a glacial surge capable of cutting the exposed continental shelf and creating the deep incisions identified by Fulthorpe and Austin (2004), but is too young to have formed these incisions, as dates from a recently collected core within an overlying fluvial channel yield dates of ~14 ka (Alexander et al., 2003). However, this outburst event may have provided a direct transport mechanism for moving freshly eroded sediments from the New Jersey Highlands and more northern source areas such as the Adirondack and Catskill Mountains to the study area on the New Jersey shelf (Turner, 2005). In fact, this later lake drainage may be responsible for erosion of the NW-SE trending Hudson Shelf Valley, the sediment lobes north of the Hudson Shelf Valley (Figure 5.3) and the glacial sediments recognized in cores from the New Jersey slope and rise (Savrda et al., 2001; McHugh and Olson, 2002). If catastrophic erosion and redeposition following breaching of glacial lake dams to the north generated Fulthorpe and Austin (2004)'s incisions, then catastrophic drainage of Lake Hackensack at 18 ka (Dineen et al., 1988) could have provided the causative mechanism. Fulthorpe and Austin (2004) overlying transparent

176
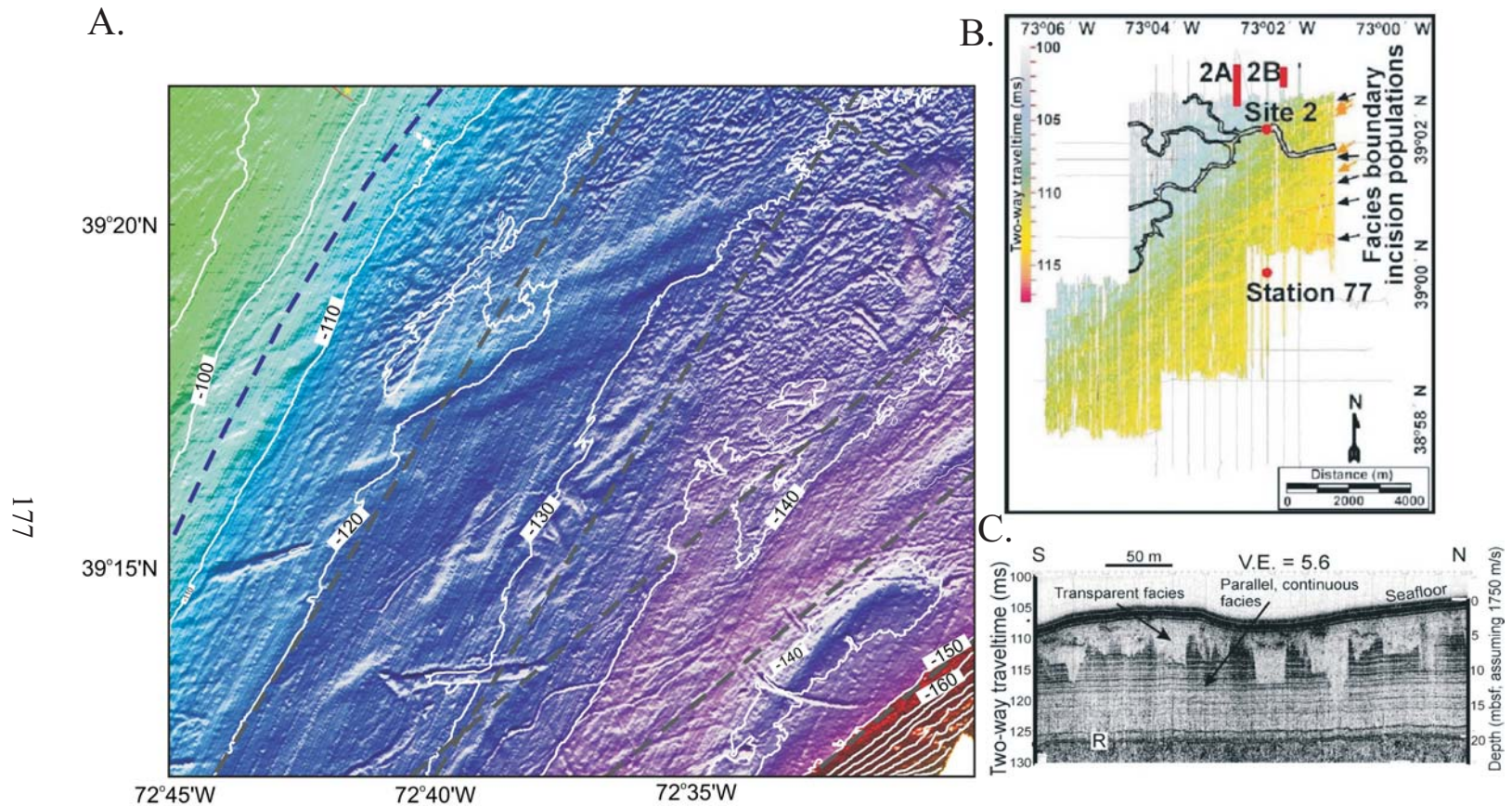
Figure 5.6: (A) Multibeam bathymetry data from the outer New Jersey shelf illustrating iceberg scours (Duncan et al., 2001). (B) Map of facies boundary interpreted by Fulthorpe and Austin (2004) to have been generated by catastrophic erosion and redeposition associated with glacial lake outwash events. (C) A chirp seismic profile illustrating the flat bottomed, steep-sided incisions mapped in (B).

facies, with the presence of stratified blocks and a mud clast in a mixed matrix from a surficial sample (Figure 5.6C; Sommerfield, 2003; Fulthorpe and Austin, 2004) also suggests a rapid, catastrophic deposition, which may be tied to the ca. 18 ka Lake Hackensack outburst. Other episodic floodings at ~16-18 ka that are thought to have occurred on the eastern side of the Long Island (Figure 5.2; Uchupi et al., 2001) are unlikely to have been the mechanism for the observed steep-sided incisions to the south as there is no evidence for these incisions in sediments northeast of their mapped area. In addition, meltwater would have had to cross the Hudson shelf valley drainage (Figure 5.1D), which probably existed at the time, and there is no evidence for that.

ICEBERG SCOURS

Fulthorpe and Austin (2004) northeast and east-northeast trending incisions do not show any morphologic similarities with other features created from catastrophic flooding, such as the Channeled Scabland known to have formed by outwash from Glacial Lake Missoula (O'Conner and Baker, 1992; Fulthorpe and Austin, 2004). An alternative interpretation could be these incisions are buried iceberg scours produced in consolidated clay, based on their morphologic similarity to iceberg scours within exposed upper Pleistocene sediments on the outer shelf of New Jersey to the NE (Figure 5.6; Duncan et al., 2001). Duncan et al. (2001) observed that in water depths >110 m, the modern sea floor is marked by long narrow grooves that have a generally NE-SW orientation. The grooves are typically 100 m wide, a few meters deep, and 1-2 km in length, consistent with the Fulthorpe and Austin (2004)'s incisions. In addition, the two populations of these incisions trending in NE and E-NE directions and show similar cross-cutting characteristics.

178

I speculate that the Fulthorpe and Austin (2004) "keel marks" correspond to the Heinrich event 4 (i.e., H4), one of six Heinrich episodes of anomalously high ice-rafting in the North Atlantic, which occurred at irregular intervals throughout the late Pleistocene (Figure 5.2). The layers (H6-H1) have been identified for this time range in northern Atlantic marine sediment deposits. Heinrich layer H6 is 65-60 ka, H5 at 44.0 ka, H4 is 33.2-35.1 ka, H3 at 26.0 ka, H2 at 22.0 ka, and H1 is 15-13 ka (Cronin, 1999).

FLUVIAL ENTRENCHMENT SURFACE AND HOLOCENE TRANSGRESSION

The dendritic nature of my mapped shelf drainages (Figure 2.9) and the ~100 km distance from the Laurentide ice front at the LGM (Figure 3.1) rule out chaotic deposition during a catastrophic glacial flood event, or jökulhlaup. I agree with earlier interpretations by Davies et al. (1992) and Duncan et al. (2000), which inferred "Channels" to be a subarial incision surface developed across the shelf between ca. 25 ka and 16 ka. The observed dendritic patterns of channels observed strongly imply a fluvially derived morphology, likely formed by watershed runoff processes (Nordfjord et al, 2005). While we have not yet sampled high acoustic amplitude material at the base of "Channels" fill, I speculate that it represents coarse-grained sediment, perhaps fluvial lag deposits (Figure 3.11). I also agree with Duncan et al. (2000)'s statement that "Channels" is the clear candidate for the Wisconsinan maximum lowstand surface in the shelf corridor.

The shoreline transgressed the New Jersey shelf between ca. 16 ka and 10 ka (Figure 5.2). Disregarding regional variations from the global sea-level curve, and subsequent erosion on the shelf, the shoreline moved to the Franklin "paleo-shore" (~100 m isobath) ca. 15.7 ka, then to the mid-shelf scarp ca 10.5 ka, a distance of ~50 km (Figure 4.4). The most recent transgression erased all bathymetric evidence of features

179

older than ca. 15.7 ka from the New Jersey mid-shelf corridor. Distinctive geologic features, like filled fluvial incisions buried just a few meters below the seafloor, are morphologically undetectable, even on high-resolution swath sonar bathymetry maps (Figure 4.1; Evans et al., 2000).

References

Abrahams, A.D., 1984. Channel Networks: A Geomorphological Perspective. Water Resources Research, 20(2): 161-168.

Alexander, C., Christensen, B., 2005. Paleochannel incision and infill on the New Jersey shelf: timing, character and depositional environment, GSA.

Alexander, C., Sommerfield, C., Austin, J. A., Jr., Christensen, B., Fulthorpe, C., S., Goff, J., Gulick, S. P. S., Nordfjord, S., Nielson, D., Schock, S., 2003. Sedimentology and age control of Late Quaternary New Jersey shelf deposits, Eos Trans. AGU. Fall Meeting Suppl., San Francisco.

Allen, G.P., 1991. Sedimentary processes and facies in the Gironde estuary: a recent model for macrotidal estuarine systems. In: D.G. Smith, Reinson, G. E., Zaitlin, B. A., Rahmani, R. A. (Editor), Clastic Tidal Sedimentology. Canadian Society of Petroleum Geologists, pp. 29-40.

Allen, G.P., Posamentier, H. W., 1993. Sequence stratigraphy and facies model of an incised valley fill: the Gironde Estuary, France. Journal of Sedimentary Petrology, 63: 378-391.

Anderson, J.B., Abdulah, K., Sarzalejo, S., Siringan, F., Thomas, M. A., 1996. Late Quaternary sedimentation and high-resolution sequence stratigraphy of the east Texas shelf. In: M. De Batist, Jacobs, P. (Editor), Geology of Siliciclastic Shelf Seas. Geological Society Special Publication, pp. 95-124.

Anderson, J.B., Fillon, R. H., 2004a. Late Quaternary Stratigraphic Evolution of the Northern Gulf of Mexico Margin. Special publication, No. 79. SEPM, Tulsa, 311 pp.

Anderson, J.B., Molnia, B. F., 1989. Glacial-Marine Sedimentation. Short Course in Geology, Volume 9, 125 pp.

Anderson, J.B., Rodriguez, A., Abdulah, K., Fillon, R. H., Banfield, L., McKeowen, H., Wellner, J., 2004b. Late Quaternary stratigraphic evolution of the Northern Gulf of Mexico margin: A synthesis. In: J.B. Anderson, Fillon, R. H. (Editor), Late Quaternary stratigraphic evolution of the Northern Gulf of Mexico margin. SEPM, Tulsa, pp. 1-24.

Anderson, J.B., Thomas, M. A., Siringan, F. P., Smith, W. C., 1992. Quaternary evolution of the East Texas Coast and continental shelf. In: C.H. Fletcher, III, Wehmiller, J. F. (Editor), Quaternary coasts of the United States: Marine and lacustrine systems. SEPM, Tulsa, pp. 253-265.

Ashley, G.M., Renwick, W. H., 1983. Channel morphology and processes at the riverine-estuarine transition, the Raritan River, New Jersey. In: J.D. Collison, Lewin, J. (Editor), Modern and Ancient Fluvial Systems. International Association of Sedimentologists, pp. 207-218.

Ashley, G.M., Sheridan, R. E., 1994. Depositional model for valley fills on a passive continental margin. In: R.W. Dalrymple, Boyd, R., Zaitlin, B. A. (Editor), Incised-valley systems: Origin and sedimentary sequences. SEPM Special Publication, pp. 285-301.

Austin, J.A., Jr., Fulthorpe, C. S., Mountain, G. S., Orange, D. L., Field, M. E., 1996. Continental-margin seismic stratigraphy: Assessing the preservation potential of heterogeneous geological processes operating on continental shelves and slopes. Oceanography, 9(3): 173-177.

Austin, J.A., Jr., Goff, J., and Olson, H., 2000. Geophysical and Geological Reconnaissance for the ONR Geoclutter Program, University of Texas Institute for Geophysics.

Baker, V.R., 1974. Paleohydraulic interpretation of Quaternary alluvium near Golden, Colorado. Quaternary Research, 4: 95-112.

Barber, D.C., Dyke, A., Hillaire-Marcel, C., Jennings, A. E., Andrews, J. T., Kerwin, M. W., Bilodeau, G., McNeely, R., Southon, J. Morehead, M. D., Gagnon, J. M., 1999. Forcing of the cold event of 8,200 years ago by catastrophic drainage of Laurentide lakes. Nature, 400: 344-348.

Bard, E., Hamelin, B., Fairbanks, R. G., and Zindler, A., 1990. Calibration of the 14C timescale over the past 30,000 years using mass spectrometric U-Th ages from Barbados corals. Nature, 345: 405-409.

Bartek, L.R., Cabote, B. S., Young, T., Schroeder, W., 2004. Sequence stratigraphy of a continental margin subjected to low-energy and low-sediment-supply environmental boundary conditions: Late Pleistocene-Holocene deposition off shore Alabama, U.S.A. Late Quaternary Stratigraphic Evolution of the Northern Gulf of Mexico Margin, Special Publication No. 79. SEPM, Tulsa, 85-109 pp.

Bartek, L.R., Wellner, R. W., 1995. Do equilibrium conditions exist during sediment transport studies on continental margins? An example from the East China Sea. Geo-Marine Letters, 15: 23-29.

Beard, J.H., Sangree, J. B., Smith, L. A., 1982. Quaternary chronology, paleoclimate, depositional sequences, and eustatic cycles. AAPG Bulletin, 66: 158-169.

Belknap, D.F., Kraft, J. C., 1981. Preservation potential of transgressive coastal lithosomes on the U.S. Atlantic shelf. In: C.A. Nittrouer (Editor), Sedimentary Dynamics of Continental Shelves, Developments in Sedimentology.

Belknap, D.F., Kraft, J. C., 1985. Influence of antecedent geology on stratigraphic preservation potential and evolution of Delaware's barrier system. Marine Geology, 63: 235-262.

Berne, S., Lericolais, G., Marsset, T., Bourillet, J. F., and De Batist, M., 1998. Erosional offshore sand ridges and lowstand shorefaces: Examples from tide- and wave-dominated environment of France. Journal of Sedimentary Research, 68(4): 540-555.

Blum, M.D., Tornqvist, T. E., 2000. Fluvial responses to climate and sea-level change: a review and look forward. Sedimentology, 47(s1): 2-39.

Boyd, R., Suter, J., Penland, S., 1989. Relation of sequence stratigraphy to modern sedimentary environments. Geology, 17: 926-929.

Bradley, H.C., Mears, A.I., 1980. Calculations of flows needed to transport coarse fraction of Boulder Creek alluvium at Boulder, Colorado. GSA Bulletin, 91: 1056-1090.

Broecker, W.S., Kennett, J. P., Flower, B. P., Teller, J. T., Trumbore, S., Bonani, G., Wolfli, W., 1989. The routing of meltwater from the Laurentide ice-sheet during younger Dryas cold episode. Nature, 341: 318-321.

Bruun, P., 1962. Sea-level rise as a cause of shore erosion. In: A.S.o.C. Engineers (Editor), Journal of Waterways Harbour Division, pp. 117-130.

Buck, K.F., Olson, H. C., Austin, J. A., Jr., 1999. Paleoenvironmental evidence for Latest Pleistocene sea level fluctuations on the New Jersey outer continental shelf: combining high-resolution sequence stratigraphy and foraminiferal analysis. Marine Geology, 154: 287-304.

Butcher, S.W., 1989. The nickpoint concept and its implications regarding onlap to the stratigraphic record. In: T.A. Cross (Editor), Quantitative Dynamic Stratigraphy. Prentice Hall, Englewood Cliffs, New Jersey, pp. 375-385.

Butman, B., Noble, M. and Folger, D.W., 1979. Long-term observations of bottom current and bottom sediment movement on the Mid-Atlantic continental shelf. Journal of Geophysical Research, 84(C3): 1187-1205.

Butman, B., Middleton, T. J., Thieler, E. R., Schwab, W. C., 2003. Topography, shaded relief, and backscatter intensity of the Hudson Shelf Valley, offshore of New York. 03-372, USGS, Woods Hole, MA.

Carey, J.S., Sheridan, R.E. and Ashley, G.M., 1998. Late Quaternary sequence stratigraphy of a slowly subsiding passive margin, New Jersey continental shelf. American Association of Petroleum Geologists Bulletin, 82(5A): 773-791.

Carey, J.S., Sheridan, R. E., Ashley, G. M., Uptegrove, J., 2005. Glacially-influenced late Pleistocene stratigraphy of a passive margin: New Jersey's Record of the North American ice sheet. Marine Geology, 218(1-4): 155-173.

Carey, J.S., Swift, D.J.P., Steckler, M., Reed, C.W., Niedoroda, A., 1999. High resolution sequence stratigraphic modeling: 2. Effects of sedimentation processes. In: J.W. Harbaugh, Watney, W.L., Rankey, E.C., Slingerland, R., Goldstein, R.H., Franseen, E.K. (Editor), Numerical Experiments in Stratigraphy: Recent Advances in Stratigraphic and Sedimentologic Computer Simulations. SEPM, pp. 151– 164.

Cattaneo, A., Steel, R. J., 2003. Transgressive deposits: a review of their variability. Earth-Science Reviews, 62: 187-228.

Catuneanu, O., 2002. Sequence stratigraphy of clastic systems: concepts, merits and pitfalls. Journal of African Earth Science, 35: 1-43.

Church, M., Ryder, J.M., 1972. Paraglacial sedimentation: a consideration of fluvial processes conditioned by glaciation. GSA Bulletin, 83: 3059–3072.

Colman, S.M., Halka, J. P., Hobbs, C. H., III, Mixon, R. B., Foster, D. S., 1990. Ancient channels of the Susquehanna River beneath Chesapeake Bay and Delmarva Peninsula. Bulletin Geological Society of America, 102: 1268-1279.

Cooper, J.A.G., 2002. The role of extreme floods in estuary-coastal behaviour: contrasts between river- and tide-dominated microtidal estuaries. Sedimentary Geology, 150: 123-137.

Costa, J.E., 1983. Paleohydraulic reconstruction of flash-flood peaks from boulder deposits in the Colorado Front Range. Bulletin of Geological Society of America, 94: 986-1004.

Dalrymple, R.W., Boyd, R., Zaitlin, B. A., 1994. History, of research, types and internal organization of incised-valley systems: introduction to the volume. In: R.W. Dalrymple, Boyd, R., and Zaitlin, B. A. (Editor), Incised-Valley Systems: Origin and Sedimentary Sequences. SEPM, pp. 3-10.

Dalrymple, R.W., Hoogendoorn, E. L., 1997. Erosion and deposition on migrating shoreface-attached ridges, Sable Island, Eastern Canada. Geoscience Canada, 24(1): 27-35.

Dalrymple, R.W., Zaitlin, B. A., Boyd, R., 1992. Estuarine facies models: conceptual basis and stratigraphic implications. Journal of Sedimentary Petrology, 62: 1130-1146.

Dansgaard, W., White, J. W., and Johnson, S. J., 1989. The abrupt termination of the Yonger Dryas climate event. Nature, 339: 532-534.

Davies, T.A., Austin, J. A., Jr., 1997. High-resolution 3D seismic reflection and coring techniques applied to late Quaternary deposits on the New Jersey shelf. Marine Geology, 143: 137-149.

Davies, T.A., Austin, J. A., Jr., Lagoe, M. B., Milliman, J. D., 1992. Late Quaternary sedimentation off New Jersey: New results using 3-D seismic profiles and cores. Marine Geology, 108: 323-343.

Demarest, J.M., Biggs, R. B, Kraft, J. C., 1981. Time-stratigraphic aspects of a formation: Interpretation of surficial Pleistocene deposits by analogy with Holocene paralic deposits, southeastern Delaware. Geololy, 9: 360-365.

Demarest, J.M., Kraft, J. C., 1987. Stratigraphic record of Quaternary Sea Levels: Implications for more Ancient Strata. In: D. Nummedal, Pilkey, O. H., Howard, J. D. (Editor), Sea Level Fluctuation and Coastal Evolution. SEPM, Tulsa, pp. 223-239.

Demarest, J.M., Leatherman, S. P., 1985. Mainland influence on coastal transgression: Delmarva Peninsula. Marine Geology, 63: 19-33.

Dillon, W.P. and Oldale, R.N., 1978. Late Quaternary sea level curve: Reinterpretation based on glacio-tectonic influence. Geology, 6: 56-60.

Donnelly, J.P., Driscoll, N. W., Uchupi, E., Keigwin, L. D., Schwab, W. C.,Thieler, E. R. Swift, Stephen A., 2005. Catastrophic meltwater discharge down the Hudson Valley; a potential trigger for the intra-Allerod cold period. Geology, 33(2): 89-92.

Duke, W.L., 1990. Geostrophic circulation of shallow marine turbidity currents? The dilemma of paleoflow patterns in storm-influenced prograding shoreline system. Journal of Sedimentary petrology, 60(6): 870-883.

Duncan, C.S., 2001. Latest Quaternary Stratigraphy and Seafloor Morphology of the New Jersey Continental Shelf. Ph.d. Dissertation Thesis, University of Texas at Austin, Austin, 226 pp.

Duncan, C.S., Goff, J. A., Austin, J. A., Jr., 2000. Tracking the last sea-level cycle: seafloor morphology and shallow stratigraphy of the latest Quaternary New Jersey middle continental shelf. Marine Geology, 170: 395-421.

Dury, G.H., 1976. Discharge prediction, present and former, from channel dimensions. Journal of Hydrology, 30: 219-245.

Dury, G.H., 1985. Attainable standards of accuracy in the retrodiction of palaeodischarge from channel dimensions. Earth Surface Processes and Landforms, 10: 205-213.

Emery, D., Myers, K. J., 1996. Sequence Stratigraphy. Blackwell Science Ltd, Oxford, England, 297 pp.

Emery, K.O., Uchupi, E., 1972. Western North Atlantic Ocean: topography, rocks, structure, water, life and sediments. Memoir, v. 17, 532 pp.

Emery, K.O., Uchupi, E., 1984. The Geology of the Atlantic Ocean. Springer, New York, 1050 pp.

Etheridge, F.G., Wood, L. J., Schumm, S. A., 1998. Cyclic variables controlling fluvial sequence development: problems and perspectives. In: K.W. Shanley, McCabe, P. J. (Editor), Relative Role of Eustasy, Climate and Tectonism in Continental Rocks. SEPM, pp. 17-29.

Evans, R.L., Law, L. K., Louis, B. St., and Cheesman, S., 2000. Buried paleo-channels on the New Jersey continental margin: channel porosity structures from electromagnetic surveying. Marine Geology, 170: 381-394.

Fairbanks, R.G., 1989. A 17,000-year glacio-eustatic sea level record: influence of glacial melting rates on the Younger Dryas event and deep-ocean circulation. Nature(342): 637-642.

Fischer, A.G., 1961. Stratigraphic record of transgressing seas in light of sedimentation in the Atlantic coast of New Jersey. AAPG Bulletin, 45: 1656-1666.

FitzGerald, D.M., Kulp, M., Penland, S., Flocks, J., Kindinger, J., 2004. Morphologic and stratigraphic evolution of muddy ebb-tidal deltas along a subsiding coast: Barataria Bay, Mississippi River delta. Sedimentology, 51: 1-22.

Fletcher, C.H., III., Knebel, H. J., Kraft, J. C., 1992. Holocene evolution of an estuarine coast and tidal wetlands. Geological Society of America Bulletin, 102(3): 283-297.

Foyle, A.M., Oertel, G. F., 1997. Transgressive systems tract development and incised-valley fills within a Quaternary estuary-shelf system: Virginia inner shelf, USA. Marine Geology, 137: 227-249.

Freeland, G.L., Stanley, D.J., Swift, D.J.P. and Lambert, D.N., 1981. The Hudson Shelf Valley: its role in shelf sediment transport. Marine Geology, 42: 399-427.

Friedrichs, C.T., 1995. Stability, shear stress and equilibrium cross-sectional geometry of sheltered tidal sections. Journal of Coastal Research, 11(4): 1062-1074.

Fulthorpe, C.S., Austin, J. A., Jr., 2004. Shallowly buried, enigmatic seismic stratigraphy on the New Jersey outer shelf: Evidence for latest Pleistocene catastrophic erosion? Geology, 32(12): 1013-1016.

Gallagher, C., 2002. The morphology and paleohydrology of a submerged glaciofluvial channel emerging from Waterford Harbour onto the nearshore continental shelf of the Celtic Sea. Irish Geography, 35(2): 111-132.

Galloway, W.E., 1981. Depositional architecture of Cenozoic Gulf Coastal plain fluvial systems. SEPM Special publication, 31: 127-155.

Galloway, W.E., 1989. Genetic sequences in basin analyis I: architecture and genesis of flooding-surface bounded depositional sequences. American Association of Petroleum Geologists Bulletin, 73: 125-142.

Galloway, W.E., and Hobday, D. K., 1996. Terrigenous Clastic Depositional Systems. Springer-Verlag, New York, 423 pp.

Galloway, W.E., Sylvia, D. A., 2002. The many Faces of Erosion: Theory Meets Data in Sequence Stratigraphic analysis, 22nd Annual Gulf Coast Section SEPM Foundation Bob F. Perkins Conference.

Gary, M., McCafee, R., 1974. Glossary of Geology. America Geological Institute, Falls Church, Virginia, 805 pp.

Genesous, B., Tesson, M., 1996. Sequence Stratigraphy, seismic profiles, and cores of Pleistocene deposits on the Rhone continental shelf. Sedimentary Geology, 105: 183-190.

Goff, J.A., Austin, J. A., Jr., Gulick, S., Nordfjord, S., Christensen, B., Sommerfield, C., Olson, H., Alexander, C., 2005. Post-Transgressive and Modern Erosion on the New Jersey Outer Shelf. Marine Geology, 216: 275-296.

Goff, J.A., Kraft, B. J., Mayer, L. A., Schock, S. G., Sommerfield, C. K., Olson, H. C., Gulick, S. P. S., Nordfjord, S., 2004a. Seabed characterization on the New Jersey middle and outer shelf: correlatability and spatial variability of seafloor properties. Marine Geology, 209: 147-172.

Goff, J.A., Nordfjord, S, 2004b. Interpolation of Fluvial Geomorphology Using Channel-Oriented Coordinate Transformation: A Case Study from the New Jersey Shelf. Mathematical Journal, 36(6): 643-658.

Goff, J.A., Swift, D. J. P.,Duncan, C. S., Mayer, L. A., Hughes-Clarke, J., 1999. High-resolution swath sonar investigation of sand ridge, dune and ribbon morphology in the offshore environment of the New Jersey margin. Marine Geology, 161: 307-337.

Greenlee, S.M., Schroeder, F.W. and Vail, P.R., 1988. Seismic stratigraphic and geohistory analysis of Tertiary strata from the continental shelf off New Jersey: calculation of eustatic fluctuations from stratigraphic data. In: R.E. Sheridan and J.A. Grow (Editors), The Atlantic continental margin: U.S. Geology of North America. Geological Society of America, pp. 437-444.

Gulick, S.P., Fulthorpe, C. S., Goff, J. A., Austin, J. A., Jr., Nordfjord, S., Sommerfield, C., Alexander, C., Christensen, B., Schock, S., Nielson, D. L., 2003. Mapping a Pre-Last Glacial Maximum Paleo-Seafloor and Shelf-Slope Sediment Wedges beneath the New Jersey Shelf, Eos Trans. AGU. Fall Meeting Suppl., San Francisco.

Gulick, S.P.S., Goff, J. A., Austin, J. A., Jr., Alexander, C. R., Nordfjord, S., Fulthorpe, C. S., 2005. Basal inflection-controlled shelf-edge wedges off New Jersey track sea-level fall. Geology, 33(5): 429-432.

Hambry, M., 1994. Glacial environments. UBC Press/Vancouver.

Hernandez-Molina, F.J., Somoza, L., and Pomar, L., 1994. Late Pleistocene-Holocene sediments on the Spanish continental shelves: Model for very high resolution sequence stratigraphy. Marine Geology, 120: 129-174.

Hey, R.D., Thorne, C. R., 1986. Stable channels with mobile gravel beds. Journal of Hydraulic Engineering, 112: 671-689.

Hine, A.C., Snyder, S. W., 1985. Coastal lithosome preservation: Evidence from the shoreface and inner continental shelf off Bogue Banks, North Carolina. Marine Geology, 63: 307-330.

Honig, C., Boyd, R., 1992. Estuarine sedimentation on the Eastern Shore of Nova Scotia. Journal of Sedimentary Petrology, 62.

Horton, R.E., 1945. Erosional development of streams and their drainage basins: hydrophysical approach to quantitative geomorphology. Bulletin of Geological Society of America, 56: 275-370.

Howard, A.D., 1971. Optimal Angles of Steam Junction: Geometric, Stability to Capture, and Minimum Power Criteria. Water Resources Research, 7(4): 863-873.

Hughes, T., 1987. Ice dynamics and deglaciation models when ice sheet collapsed. In: W.F. Ruddiman, Wright, H.E., Jr. (Editor), North America and Adjacent Oceans During the Last Deglaciation. Geological Society of America, pp. 183-220.

Hughes, T., Borns Jr. H.W., Fastook, J.L., Hyland, M.R., Kite, J.S., and Lowell, T.V., 1985. Models of glacial reconstruction and deglaciation applied to Maritime Canada and New England. In: H.W.J. Borns, LaSalle, P., Thompson, W.B. (Editor), Late Pleistocene History of Northeastern New England and Adjacent Quebec. Geological Society of America, pp. 139-150.

Imbrie, J., Hays, J. D., Martinson, D. G., McIntyre, A., Mix, A. C., Morley,J. J. Pisias, N. G., Prell, W. L., and Shackleton, N. J., 1982. The orbital theory of Pleistocene climate: support from revised chronology of the marine D18O record. In: A.L.e.a. Berger (Editor), Milankovitch and Climate, Part 1, pp. 269-305.

Jarrett, J.T., 1976. Tidal prism-inlet area relationships. 3, U.S. Army Coastal Engineering Research Center, Vicksburg, MS.

Johnson, D.W., 1919. Shore processes and shoreline development, New York, 584 pp.

Kaplan, M.R., 1999. Retreat of a tide-water margin of the Laurentide ice sheet in eastern Maine between ca. 14,000 and 13,000 14C yr B.P. Geological Society of America Bulletin, 111: 620-632.

Keller, E.A., 1972. Development of alluvial stream channels: a five-stage model. Geological Society of America Bulletin, 83: 1531-1536.

Kidwell, S.M., 1993. Influence of subsidence on the anatomy of marine siliciclastic sequences and on distribution of shell and bones. Journal of Society London, 150: 165-167.

Kindinger, J.L., 1988. Seismic stratigraphy of the Mississippi-Alabama shelf and upper continental slope. Marine Geology, 83: 79-84.

Knebel, H.J., Wood, S.A. and Spiker, E.C., 1979. Hudson River: Evidence for extensive migration on the exposed continental shelf during Pleistocene time. Geology, 7: 254-258.

Knebel, H.J., and Spiker, E., 1977. Thickness and Age of Surficial Sand Sheet, Baltimore Canyon Trough Area. AAPG Bulletin, 61(6): 861-871.

Knighton, D., 1998. Fluvial forms and processes: A new perspective. Arnold publishers, London.

Krystinik, L.F., 1989. Morrow Formation facies geometries and reservoir quality in compound valley fills, central state line area, Colorado and Kansas. AAPG Bulletin, 73(3): 375.

Lagoe, M.B., Davies, T. A., Austin, J. A., Jr., Olson, H. C., 1997. Foraminiferal constraints on very high-resolution seismic stratigraphy and Late Quaternary glacial history, New Jersey continental shelf. Palaios, 12: 249-266.

Lambeck, K., Chappell, J., 2001. Sea Level Change Through the Last Glacial Cycle. Science, 292: 679-686.

Leopold, L.B., Maddock, T., 1953. The hydraulic geometry of stream channels and some physiographic implications. U. S. Geological Survey Professional Paper, 252: 56.

Leopold, L.B., Wolman, M. G., Miller, J. P., 1964. Fluvial processes in geomorphology. W. H. Freeman and Co., San Francisco and London, 522 pp.

Lericolais, G., Auffret, J., Bourillet, J., 2003. The Quaternary Channel River: seismic stratigraphy of its palaeo-valleys and deeps. Journal of Quaternary Science, 18(3-4): 245-260.

Lericolais, G., Berne, S., Fenies, H., 2001. Seaward pinching out and internal stratigraphy of the Gironde incised valley on the shelf (Bay of Biscay). Marine Geology, 175: 183-197.

Liu, J.P., Milliman, J. D., Gao, S., 2002. The Shandong mud wedge and post-glacial sediment accumulation in the Yellow Sea. Geo-Marine Letters, 21: 212-218.

Lobo, F.J., Sanchez, R., Gonzales, R., Dias, J. M. A., Hernandez-Molina, F. J., Fernandez-Salas, L. M., Diaz del Rio, V., Mendes, I., 2004. Contrasting styles of the Holocene highstand sedimentation and sediment dispersal systems in the northern shelf of the Gulf of Cadiz. Continental Shelf Research, 24: 461-482.

Ludwick, J.C., 1972. Migration of Tidal Sand Waves in Chesapeake Bay Entrance. In: D.J.P. Swift, Duane, D. B., Pilkey, O. H. (Editor), Shelf Sediment Transport: Process and Pattern. Dowden, Hutchinson & Ross, Stroudsburg, Pennsylvania, pp. 377-410.

Luhurbudi, E.C., Pulliam, J., Austin, J. A., Jr., Saustrup, S., and Stoffa, P. L., 1998. Removal of diurnal tidal effects from an ultra-high-resolution 3-D marine seismic survey on the continental shelf offshore New Jersey. Geophysics, 63(3): 1036-1040.

Maguire, T.J., Sheridan, R.E., Volkert, R.A., Feigenson, M.D., and Patino, L.C., 1999. Continuation of Appalachian Piedmont under New Jersey Coastal Plain. Geol. Soc. Amer. Bull, Special Paper, vol. 330: 27.

McClennen, C.E., 1973. Nature and origin of New Jersey continental shelf ridges and depressions. Ph.D. Thesis, University of Rhode Island, Providence, Rhode Island, 94 pp.

McHugh, C.M.G., Olson, H.C., 2002. Pleistocene chronology of continental margin sedimentation: new insights into traditional models, New Jersey. Marine Geology, 186: 389– 411.

Miall, A.D., 1991. Stratigraphic sequences and their chronostratigraphic correlation. Journal of Sedimentary Research, 61: 497-505.

Miall, A.D., 1992. Exxon global cycle chart; an event for every occasion? Geology, 20(9): 787-790.

Miller, K.G., Mountain, G. S., Christie-Blick, N., Austin, J. A., Jr., 1995. ODP Drilling Proposal 348A-revised, Department of Geological Science.

Miller, M.C., McCave, I. N., Komar, P. D., 1977. Threshold of sediment motion under unidirectional currents. Sedimentology, 24: 507-527.

Milliman, J.D., Emery, K. O., 1968. Sea-levels during the past 35 ky. Science, 162: 1121-1123.

Milliman, J.D., Jiezao, Z., Anchun, L., Ewing, J. I., 1990. Late Quaternary sedimentation on the outer and middle New Jersey continental shelf: Results of to local deglaciation. Journal of Geology, 98: 966-976.

Mitchum, R.M. and Vail, P.R., 1977. Seismic stratigraphy and global changes of sea level, part 7: Seismic stratigraphy interpretation procedure. In: C.E. Payton (Editor), Seismic Stratigraphy-Applications to Hydrocarbon Exploration, pp. 135-143.

Mitchum, R.M., Vail, P.R. and Sangree, J.B., 1977a. Seismic stratigraphy and global changes of sea level, part 6: stratigraphic interpretation of seismic reflection patterns in depositional sequences. In: C.E. Payton (Editor), Seismic Stratigraphy-Applications to Hydrocarbon Exploration, pp. 117-133.

Mitchum, R.M., Vail, P.R. and Thompson, S., 1977b. Seismic stratigraphy and global changes of sea level, part 2: The depositional sequence as a basic unit for stratigraphic analysis. American Association of Petroleum Geologists Memoir, 26: 99-133.

Mitchum, R.M., Van Wagoner, J. C., 1991. High-frequency sequences and their stacking patterns: sequence stratigraphic evidence of high-frequency eustatic cycles. Sedimentary Geology, 70: 131-160.

Morrison, R.B., 1991. Introduction. In: R.B. Morrison (Editor), The Geology of North America, Vol. K-2, Quaternary Nonglacial Geology: Conterminous U.S. Geological Society of America, Boulder, Colorado, pp. 1-12.

Morton, R.A., Paine, J. G., and Blum, M. D., 2000. Response of stable bay-margin and barrier-island systems to Holocene sea-level highstand, western Gulf of Mexico. Journal of Sedimentary Research, 70(3): 478-490.

Nichol, S.L., 1991. Zonation and sedimentology of estuarine facies in an incised valley, wave dominated, microtidal setting, New South Wales, Australia. In: D.G. Smith, Reinson, G. E., Zaitlin, B. A. and Rahmani, R. A. (Editor), Clastic Tidal Sedimentology. Canadian Society of Petroleum Geologists, pp. 41-58.

Nichol, S.L., Boyd, R., Penland, S., 1994. Stratigraphic response of wave-dominated estuaries to different relative sea-level and sediment supply histories: Quaternary case studies from Nova Scotia, Louisiana and eastern Australia. In: R.W. Dalrymple, Boyd, R., and Zaitlin, B. A. (Editor), Incised-valley systems: Origin and Sedimentary Sequences, pp. 265-283.

Nichol, S.L., Boyd, R., Penland, S., 1996. Sequence stratigraphy of a coastal-plain incised valley estuary: Lake Calcasieu, Louosiana. Journal of Sedimentary Research, 66(4): 847-857.

Nichols, M.M., Biggs, R. B., 1985. Estuaries. In: R.A. Davis (Editor), Coastal Sedimentary Environments. Springer-Verlag, New York, pp. 77-186.

Nichols, M.N., Johnson, G. H., Peebles, P. C., 1991. Modern sediments and facies model for a microcoastal plain estuary, the James estuary, Virginia. Journal of Sedimentary Petrology, 61: 883-899.

Nielson, D.L., Pardey, M., Austin, J. A., Jr., Goff, J., Alexander, C., Christensen, B. A., Gulick, S. P. S., Fulthorpe, C. S., Nordfjord, S., Sommerfield, C., Venherm, C., 2003. Active Heave-compensated Coring on the New Jersey Shelf, Eos Trans. AGU. Fall Meeting Suppl., San Francisco.

Nittrouer, C.A., and Kravitz, J. H., 1995. Integrated Continental Margin Research to Benefit Ocean and Earth Sciences. Eos, Transactions, American Geophysical Union, 76(12): 121,124,126.

Nittrouer, C.A., and Kravitz, J. H., 1996. Strataform: A program to study the creation and interpretation of sedimentary strata on continental margins. Oceanography, 9(3): 146-152.

Nordfjord, S., Goff, J. A., Austin, J. A., Jr., Fulthorpe, C., Gulick, S. P. S., Sommerfield, C., Alexander, C., Christensen, B., Schock, S., 2003. Geomorphologic comparisons of shallowly buried, dendritic draiange systems on the outer New

Jersey shelf with modern fluvial and estuarine analogs, Eos Trans. AGU. Fall Meeting Suppl., San Francisco.

Nordfjord, S., Goff, J. A., Austin, J. A., Jr., Gulick, S. P. S., Galloway, W. E., submitted. Seismic facies of incised valley-fills, New Jersey continental shelf: implications for erosion and preservation processes acting during late Pleistocene/Holocene transgression. Journal of Sedimentary Research.

Nordfjord, S., Goff, J. A., Austin, J. A., Jr., Sommerfield, C. K., 2005. Seismic geomorphology of buried channel systems on the New Jersey outer shelf: Assessing past environmental conditions. Marine Geology, 214(4): 339-364.

Nummedal, D., Swift, D. J. P., 1987. Transgressive stratigraphy at sequence-bounding unconformities: some principles derived from Holocene and Cretaceous examples. In: D. Nummedal, Pilkey, O. H., Howard, J. D. (Editor), Sea Level Fluctuation and Coastal Evolution. SEPM, Tulsa, pp. 241-260.

Oertel, G.F., 1987. Backbarrier and shoreface controls on inlet channel orientation. In: A.S.o.C.E. Waterways Division (Editor), Coastal Sediments, pp. 2022-2029.

Payton, C.E. (Editor), 1977. Seismic stratigraphy- applications to hydrocarbon exploration, 26. American Association of Petroleum Geologists Memoir, Tulsa, Oklahoma, 516 pp.

Pelletier, J.D., 2003. Drainage basin evolution in the Rainfall Erosion Facility: dependence on initial conditions. Geomorphology, 53: 183-196.

Peltier, W.R., 1998. Postglacial variations in the level of the sea: implications for climate dynamics and solid-earth geophysics. Reviews of Geophysics, 36(4): 603-689.

Poag, C.W., 1992. U.S. Middle Atlantic Continental Rise: Provenance, Dispersal, and Deposition of Jurassic to Quaternary Sediments. In: C.W. Poag, de Graciansky, P,C. (Editor), Geologic Evolution of Atlantic Continental Rises. Van Nostrand Reinhold, New York, pp. 100-156.

Poag, C.W., Sevon, W.D., 1989. A record of Appalachian denudation in postrift Mesozoic and Cenozoic sedimentary deposits of the U.S. middle Atlantic continental margin. Geomorphology, 2: 119– 157.

Posamentier, H.W., 2002. Ancient shelf ridges- A potentially significant component of the transgressive system tract: A case study from offshore northwest Java. AAPG Bulletin, 86(1): 75-106.

Posamentier, H.W., Allen, G. P., 1993a. Variability of the sequence stratigraphic model: effects of local basin factors. Sedimentary Geology, 86: 91-109.

Posamentier, H.W., Allen, H. W., James, D. P., Tesson, M., 1992. Forced regression in a sequence stratigraphic framework: Concepts, examples, and sequence stratigraphic significance. AAPG Bulletin, 76: 1687-1709.

Posamentier, H.W., Jervey, M. T., Vail, P. R., 1988a. Eustatic controls on clastic deposition I- conceptual framework. In: C.K. Wilgus, Hastings, B. S., Kendall, C. G., Posementier, H. W., Ross, C. A.,Van Wagoner, J. C. (Editor), Sea-Level Changes- an integrated approach. Society of Economic Paleontologists and Minerologists Special Publication 42, pp. 110-124.

Posamentier, H.W., Kolla, V., 2003. Seismic geomorphology and stratigraphy of depositional elements in deep-water settings. Journal of Sedimentary Research, 73(3): 367-388.

Posamentier, H.W., Vail, P. R., 1988b. Sequence stratigraphy; sequences and systems tract development. In: D.P. James and D.A. Leckie (Editors), Sequences, stratigraphy, sedimentology; surface and subsurface. Canadian Society of Petroleum Geologists Memoir, Calgary, pp. 571-572.

Posamentier, H.W., Weimer, P., 1993b. Siliciclastic sequence stratigraphy and petroleum geology-where to from here? AAPG Bulletin, 77: 731-742.

Pratson, L.F., Ryan, W. B. F., 1994. Submarine Canyon initiation by downslope-eroding sediment flows: Evidence in late Cenozoic strata on the New Jersey continental slope. Geological Society of America Bulletin, 106: 395-412.

Rabineau, M., Berne, S., Ledrezen, E., Lericolais, G., Marsset, T., and Rotunno, M., 1998. 3D architecture of lowstand and transgressive Quaternary sand bodies on the outer shelf of the Gulf of Lion, France. Marine and Petroleum Geology, 15: 439-452.

Reynaud, J., Tessier, B., Auffret, J., Berne, S., De Batist, M., Marsset, T., Walker, P., 2003. The offshore Quaternary sediment bodies of the English Channel and its Western Approaches. Journal of Quaternary Science, 18(3-4): 361-371.

Reynaud, J., Tessier, B., Proust, J., Dalrymple, R., Bourillet, J. and De Batist, M., Lericolais, G., Berne, S., Marsett, T., 1999. Architecture and Sequence Stratigraphy of a Late Neogene Incised Valley at the Shelf Margin, Southern Celtic Sea. Journal of Sedimentary Research, 69(2): 351-364.

Riggs, S.R., Belknap, D. F., 1988. Upper Cenozioc processes and environments of continental margin sedimentation: eastern United States. In: R.E. Sheridan, Grow, J. A. (Editor), The Geology of North America, Vol. I-2, The Atlantic Continental Margin: Conterminous U. S. USGS, Boulder, Colorado, pp. 131-176.

Rinaldo, A., Fagherazzi, S., Lanzoni, S., Marani, M., 1999. Landscape-forming discharges and studies in empirical geomorphic relationships. Water Resources Research, 35(12): 3919-3929.

Rodriguez, A.B., Anderson, J. B., Siringan, F. P., Taviani, M., 2004. Holocene evolution of the east Texas coast and inner continental shelf; along-strike variability in coastal retreat rates. Journal of Sedimentary Research, 74(3): 405-421.

Rosgen, D.L., 1994. A classification of natural rivers. Catena, 22: 169-199.

Rotnicki, K., 1983. Modelling past discharges of meandering rivers. In: K.J. Gregory (Editor), Background to Paleohydrology. Wiley, Chichester, pp. 321-354.

Rouse, H., 1946. Elementary Mechanics of Fluids. Dover Publications, Inc., New York, 376 pp.

Roy, P.S., 1994. Holocene estuarine evolution: stratigraphic studies from Southern Australia. In: R.W. Dalrymple, Boyd, R., Zaitlin, B. A. (Editor), Incised valley systems: origin and sedimentary sequences. SEPM, Tulsa, pp. 241-263.

Sanders, J.E., Kumar, N., 1975. Evidence of shoreface retreat and in-place "drowning" during Holocene submergence of barriers, shelf off Fire Island, New York. GSA Bulletin, 86: 65-76.

Sangree, J.B., Widmier, J. M., 1977. Seismic Stratigraphy and Global Changes in Sea Level, Part 9: Seismic Interpretation of Clastic Depositional Facies. In: C.E. Payton (Editor), Seismic Stratigraphy - applications to hydrocarbon exploration. AAPG, Tulsa, pp. 165-184.

Savrda, C.E., Krawinkel, H., McCarthy, F.M.G., McHugh, C.M.G., and Olson, H.C., Mountain, G., 2001. Ichnofabrics of a Pleistocene slope succession, New Jersey Margin: relations to climate and sea-level dynamics. Palaeogeogr. Palaeoclimatol. Palaeoecol., 117: 141– 161.

Schumm, S.A., 1963. A tentative classification of alluvial river channels. U. S. Geological Survey Circular, 477.

Schumm, S.A., 1968. River adjustment to altered hydrologic regimen, Murrumbidgee River and paleochannels. U. S. Geological Survey Professional Paper, 598: 1-65.

Schumm, S.A., 1993. River response to base-level change: implications for sequence stratigraphy. Journal of Geology, 101: 279-294.

Sejrup, H.P., Haflidason, H., Aarseth, I., King, E., Forsberg, C. F., Long, D., and Rokoengen, K., 1994. Late Weichselian glaciation history of the northern North Sea. Boreas, 23: 1-13.

Shanley, K.W., McCabe, P. J., 1994. Perspective on the Sequence Stratigraphy of Continental Strata. AAPG Bulletin, 78(4): 544-568.

Sheridan, R.E., Ashley, G. M., Miller, K. G., Waldner, J. S., Hall, D. W., Uptegrove, J., 2000. Offshore-onshore correlation of upper Pleistocene strata, New Jersey Coastal Plain to continental shelf and slope. Sedimentary Geology, 134: 197-207.

Shields, A., 1936. Anwendung der Ahnlichsmechanik und der Turbulenzforschung auf die Geschiebebewegung. Mitteil Preuss Versuch Aust Wasserbau Schiffbau Berlin, 26.

Siringan, F.P., Anderson, J. B., 1993. Seismic facies, architecture, and evolution of the Bolivar Roads tidel inlet/delta complex, east Texas Gulf Coast. Journal of Sedimentary Petrology, 63(5): 794-808.

Sirkin, L., 1991. Stratigraphy of the Long Island platform. Journal of Coastal Research, 11: 218-227.

Smyth, W.C., Anderson, J. B., Thomas, M. A., 1988. Seismic facies analysis of entrenched valley-fill: a case study in the Galveston Bay area. GCAGS Trans., 38: 385-394.

Snedden, J.W., Kreisa, R.D., Tillman, R.W., Culver, S.J. and Schweller, W.J., 1999. An expanded model for modern shelf sand ridge genesis and evolution on the New Jersey Atlantic shelf. Society of Economic Minerologists and Paleontologists Special Publication 64: 147-163.

Snedden, J.W., Dalrymple, R. W., 1999. Modern shelf sand ridges: from historical perspective to a unified hydrodynamic and evolutionary model. In: K.M. Bergman, Snedden, J.W. (Editor), Isolated Shallow Marine Sand Bodies: Sequence Stratigraphic Analysis and Sedimentologic Interpretation. SEPM, pp. 13-28.

Stamp, L.D., 1921. On cycles of sedimentation in the Eocene strata of the Anglo-Franco-Belgian Basin. Geological Magnetism, 58: 108-114.

Steckler, M.S., Reynolds, D.J., Coakley, B.J., Swift, B.A., Jarrard, and R., 1993. Modelling passive margin sequence stratigraphy. In: H.W. Posamentier, Summerhayes, C.P., Haq, B.U., Allen, G.P. (Editor), Sequence Stratigraphy and Facies. SEPM, pp. 19– 41.

Sternberg, R.W., 1972. Predicting Initial Motion and Bedload Transport of Sediment Particles in the Shallow Marine Environment. In: D.J.P. Swift, Duane, D. B. and Pilkey, D. H. (Editor), Shelf Sediment Transport: Process and Pattern. Dowder, Hutchinson and Ross, Inc., Stroudsburg.

Suter, J.R., Berryhill, H. L., Jr., 1985. Late Quaternary Shelf-Margin Deltas, Northwest Gulf of Mexico. AAPG Bulletin, 69(1): 77-91.

Swift, D.J.P., 1968. Coastal erosion and transgressive stratigraphy. Journal of Geology, 76: 444-456.

Swift, D.J.P., Kofoed, J.W., Saulsbury, F.P. and Sears, P., 1972. Holocene evolution of the shelf surface, central and southern Atlantic shelf of North America. In: D.J.P. Swift, D.B. Duane and O.H. Pilkey (Editors), Shelf Sediment Transport: Process and Pattern. Dowden, Hutchinson and Ross, Stroudsburg, Pa, pp. 499-574.

Swift, D.J.P., 1975. Barrier-island genesis: evidence from the central Atlantic shelf, eastern U.S.A. Sedimentary Geology, 14: 1-43.

Swift, D.J.P. and Freeland, G.L., 1978. Current lineations and sand waves on the inner shelf, Middle Atlantic Bight of North America. Journal of Sedimentary Petrology, 48: 1257-1266.

Swift, D.J.P. and Field, M.E., 1981. Evolution of a classic sand ridge field: Maryland sector, North American inner shelf. Sedimentology, 28: 461-482.

Swift, D.J.P., 1983a. Continental Shelf Sedimentation. In: B. Johns (Editor), Physical oceanography of coastal and shelf seas. elsevier oceanography series, pp. 311-350.

Swift, D.J.P., 1983b. Coastal Sedimentation. In: B. Johns (Editor), Physical oceanography of coastal and shelf seas. Elsevier publication series, pp. 255-310.

Swift, D.J.P., Moir, R., Freeland, G. L., 1980. Quaternary rivers on the New Jersey shelf: relation of seafloor to buried valleys. Geology, 8: 276-280.

Swift, D.J.P., Thorne, J. A., 1991a. Sedimenation on continental margins,VI: a regime model from depositional sequences, their component systems tracts, and bounding surfaces. In: D .J. P. Swift, Oertel, G. F., Tillman, R. W., Thorne, J.A. (Editor), Shelf sand and sandstone bodies: Geometry, facies and sequence stratigraphy. Special publication int. ass. Sediment.

Swift, D.J.P., Thorne, J. A., 1991b. Sedimentation on continental margins; I, A general model for shelf sedimentation. In: D.J.P. Swift, Oertel, G. F., Tillman, R. W., Thorne, J. A. (Editor), Shelf sand and sandstone bodies: Geometry, facies and sequence stratigraphy. Special Publications of the International Association of Sedimentologists, pp. 3-31.

Talling, P.J., 1998. How and where do incised valleys form if sea level remains above the shelf edge? Geology, 26(1): 87-90.

197

Teller, J.T., 1987. Proglacial lakes and the southern margin of the Laurentide ice sheet. In: W.F. Ruddiman and H.E. Wright (Editors), North America and Adjacent Oceans During the Last Deglaciation. GSA, Boulder, Colorado, pp. 39-69.

Tesson, M., Posamentier, H.W. and Gensous, B., 2000. Stratigraphic organization of late Pleistocene deposits of the western part of the Golfe du Lion shelf (Languedoc shelf), western Mediterranean sea, using high-resolution seismic and core data. American Association of Petroleum Geologists Bulletin, 84(1): 119-150.

Thomas, M.A., Anderson, J. B., 1994. Sea-level controls on the facies architecture of the Trinity/Sabine incised-valley system, Texas Continental shelf. In: R. Boyd, Zaitlin, B. A., Dalrymple, R. (Editor), Incised-valley systems: Origin and sedimentary sequences. SEPM, Tulsa, pp. 63-82.

Thorne, J.A. and Swift, D.J.P., 1991. Sedimentation on continental margins, VI: a regime model for depositional sequences, their component systems tracts, and bounding surfaces. In: D.J.P. Swift, G.F. Oertel, R.W. Tillman and J.A. Thorne (Editors), Shelf sand and sandstone bodies: Geometry, facies and sequence stratigraphy. Special Publications of the International Association of Sedimentologists, pp. 189-255.

Thorne, J.A., 1994. Constraints on riverine valley incision and response to sea-level change based on fluid mechanics. In: R.W. Dalrymple, Boyd, R., Zaitlin, B. A. (Editor), Incised valley systems: Origin and Sedimentary Sequences. SEPM, Tulsa, pp. 29-43.

Turner, R.J., 2005. Provenance and depositional history of late Pleistocene New Jersey shelf sediments, Georgia State University, 113 pp.

Tuttle, S.D., Milling, M. E., Rusnak, R. S., 1966. Comparisons of stream sizes (discharge) with valley sizes and shapes. Geological Society of America Special Paper, 101: 225.

Tye, R.S., Moslow, T. F., 1993. Tidal inlet reservoirs: insight from modern examples. In: E.G. Rhodes, Moslow, T. F. (Editor), Marine clastic reservoirs. Springer-Verlag, New York, pp. 77-99.

Uchupi, E., Giese, G.S., Aubrey, D.G. and Kim, D.J., 1996. The late Quaternary construction of Cape Cod, Massachusetts. Geological Society of America Special Paper 309.

Uchupi, E., Driscoll, N., Ballard, R. D., and Bolmer, S. T., 2001. Drainage of Late Wisconsin glacial lakes and the morphology and late Quaternary stratigraphy of the New Jersey- southern New England continental shelf and slope. Marine Geology, 172: 117-145.

Umitsu, M., Buman, M., Kawase, K., Woodroffe, C. D., 2001. Holocene palaeoecology and formation of the Shoalhaven River deltaic-estuarine plains, southeast Australia. The Holocene, 11(4): 407-418.

Vail, P.R., 1987. Seismic Stratigraphy Interpretation Using Sequence Stratigraphy Part I: Seismic stratigraphy interpretation procedure. In: A.W. Bally (Editor), Atlas of Seismic Stratigraphy: AAPG Studies in Geology. AAPG, Tulsa, pp. 1-10.

Vail, P.R., Mitchum, R. M., Thompson, S., 1977a. Seismic stratigraphy and global changes of sea level, Part 3: Relative changes of sea level from coastal onlap. In: AAPG (Editor), seismic Stratigraphy. AAPG, pp. 63-81.

Vail, P.R., Mitchum, R. M.,Thompson, S., 1977b. Seismic stratigraphy and global changes of sea level, part 4: Global cycles and relative changes in sea level. In: C.E. Payton (Editor), Seismic stratigraphy- Applications to Hydrocarbon Exploration: AAPG Memoir 26. AAPG, pp. 83-98.

Vail, P.R., Todd, R. G., Sangree, J. B., 1977c. Seismic stratigraphy and global changes of sea level, Part 5: Chronostratigraphic significance of seismic reflections, Seismic Stratigraphy. AAPG.

Van Wagoner, J.C., 1995. Overview of sequence stratigraphy of foreland basin deposits: terminology, summary of papers, and glossary of sequence stratigraphy. In: J.C. Van Wagoner, Bertram, G. T. (Editor), Sequence Stratigraphy of Foreland Basin Deposits. AAPG.

Van Wagoner, J.C., Mitchum, R. M., Jr., Campion, K. M., Rahmanian, V. D., 1990. Siliciclastic sequence stratigraphy in well logs, cores and outcrops. AAPG Methods Explor, Series 7: 55.

Van Wagoner, J.C., Posamentier, H. W., Mitchum, R. M., Jr., Vail, P. R., Sarg, J. F., Loutit, T. S., Hardenbol, J., 1988. An overview of the fundamentals of sequence stratigraphy and key definitions. In: C.K. Wilgus, Hastings, B. S., Kendall, C., Posamentier, H. W., Ross, C. A., Van Wagoner, J. C. (Editor), Sea-Level Changes- An integrated Approach. SEPM, Tulsa, Oklahoma, pp. 39-45.

VanWagoner, J.C., Mitchum, R. M.,Posementier, H. W., Vail, P. R., 1987. Key definitions of sequence stratigraphy. In: A.W. Bally (Editor), Atlas of Seismic Stratigraphy. AAPG Studies in Geology, pp. 11-14.

Veatch, A.C., Smith, P. A., 1939. Atlantic submarine valleys of the United States and the Congo submarine valley. Geological Society of America Special Paper, 7: 1-87.

Vincent, C.E., Swift, D. J. P.,and Hillard, B., 1981. Sediment transport in the New York Bight, North American Atlantic Shelf. Marine Geology, 42: 369-398.

Walsh, D.R., 2004. Anthropogenic influences on the morphology of the tidal River and Estuary: 1877-1987, University of Delaware, Lewis, 90 pp.

Warren, J.D., Bartek, L. R., III, 2002. The Sequence Stratigraphy of the East China Sea: Where are the Incised Valleys? 22nd Annual Gulf Coast Section SEPM Foundation Bob F. Perkins Research Conference. SEPM.

Weber, N., Chaumillon, B., Tesson, M., Garlan, T., 2004. Architecture and morphology of the outer segment of a mixed tide and wave-dominated-incised valley, revealed by HR seismic reflection profiling: the paleo-Charente River, France. Marine Geology, 207: 17-38.

Weimer, R.J., 1992. Developments in sequence stratigraphy: foreland and cratonic basins. AAPG Bulletin, 76: 965-982.

Williams, G.P., 1978. Bank-full discharge of rivers. Water Resources Research, 16: 1141-1154.

Williams, G.P., 1983. Paleohydrological methods and some examples from Swedish fluvial environments. I. Cobble and boulder deposits. Geografiska Annaler, 65A(3-4): 227-243.

Wood, L.J., Ethridge, E G., Schumm, S. A. (Editor), 1993. An experimental study of the influence of subaqueous shelf angles on coastal plain and shelf deposits. Siliciclastic Sequence Stratigraphy: Recent Developments and Applications, 85. AAPG, 381-391.

Yoo, D., Park, S., 2000. High-resolution seismic study as a tool for sequence stratigraphy evidence of high-frequency sea-level changes: Latest Pleistocene-Holocene example from the Korea strait. Journal of Sedimentary Research, 70(2): 296-309.

Yoo, D.G., Lee, C. W., Kim, S. P., Jin, J. H., Kim, J.K., Han, H. C., 2002. Late Quaternary transgressive and highstand systems tracts in the northern East China mid-shelf. Marine Geology, 187: 313-328.

Yoshida, S., Steel, R., Dalrymple, R., MacEachern, J., 2005. Facies Change between Wave/Storm- and Tide/Current-Generated Deposits within a Relative Sea Level Cycle: Outcrop examples from the Cretaceous Western Interior Seaway in North America- A Review, IGCP475 Delta conference.

Zaitlin, B.A., Dalrymple, R. W., Boyd, R., 1994. The stratigraphic organization of incised-valley systems associated with relative sea-level change. In: R.W. Dalrymple, Boyd, R., Zaitlin, B. A. (Editor), Incised-Valley Systems: Origin and Sedimentary Sequences. SEPM, pp. 45-60.

Vita

Sylvia Nordfjord was born in Haugesund, Norway on January 25, 1976 to Marie Dybdahl Ugland and Sigve Nordfjord. After graduating from Vardafjell High School in 1995, she worked full-time in a kindergarten and part-time as a dance teacher in ballet, for so to travel as a backpacker in South-East Asia for 3 months. In 1996 she attended the Norwegian University of Science and Technology, NTNU, in Trondheim, Norway, where she majored in Petroleum Geological Engineering at the department of Applied Earth Sciences. As a part of her Bachelor of Science education she attended University of Texas at Austin through a reciprocal exchange program for two-long-session semester, fall 1999 and spring 2000, where she took mainly graduate courses while taking this exchange year at UT. She graduated in December, 2000, and as a part of the program a thesis was done in collaboration with the oil company, Norsk Agip A/S, in Stavanger, Norway. The thesis was entitled; "The Smørbukk Field: A study of pressure regimes and the attempt to identify possible flow barriers." She also completed an internship with Norsk Agip, in the summer of 2000, where she worked in the Reservoir Geology area. She entered The University of Texas at Austin as a graduate student in the spring of 2001 to pursue a Ph.D. degree in Geological Sciences. During spring semester 2001 she worked as a Graduate Research Assistant at the Bureau of Economic Geology in Austin, working on stratigraphic analysis of two of the major basins in Southern Mexico. Sylvia is presently studying the late Quaternary stratigraphy and geological history of the United States continental margin off New Jersey at the Institute of Geophysics, research that is a part of the Office of Naval Research STRATAFORM initiative, and also is of primary

interest for the ONR-sponsored "geoclutter" program. Her supervisor at the Institute is Dr. James A. Austin, Jr. She has also participated in numerous field expeditions, including two cruises off New Jersey to collect seismic and lithostratigraphic data in the summer of 2001, and her Ph.D. work has appeared, or will appear, in the journals Marine Geology and Journal of Sedimentary Research. In March 2003 she married Alejandro Escalona. Their son, Alexander Escalona, was born in August 2003 and their daughter, Karolina Escalona, was born in July 2005.

Permanent address: 3545 North Hills Drive #B, Austin, Texas

This dissertation was typed by Sylvia Nordfjord.